Bone graft substitutes

in compromised conditions

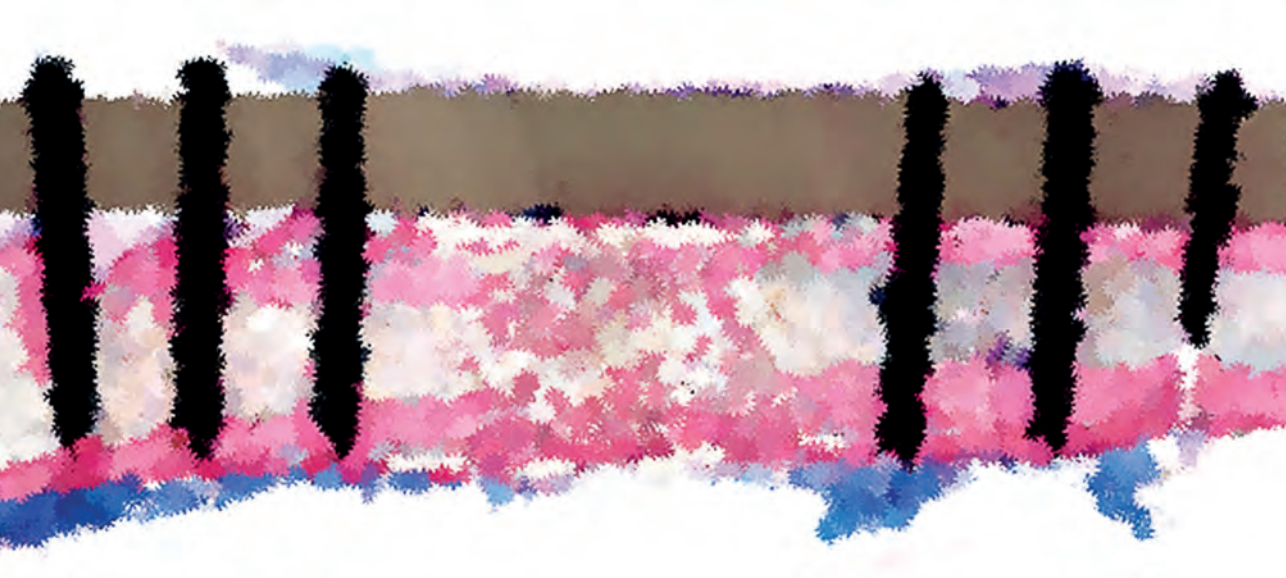

Claire van Houdt - Mauritz

Bone graft substitutes

in compromised conditions

Claire van Houdt - Mauritz

Colofon

Bone graft substitutes in compromised conditions
The work described in this thesis was performed at the Departement of Biomaterials of the Radboud University Nijmegen Medical Center, Nijmegen, The Netherlands, with summary in English and Dutch.

Cover design
Harm Mauritz

Lay-out
Stephan van Raay

Printing
Ipskamp Printing

ISBN
978-90-9034640-3

Bone graft substitutes

in compromised conditions

Proefschrift

ter verkrijging van de graad van doctor
aan de Radboud Universiteit Nijmegen
op gezag van de rector magnificus prof. dr. J.H.J.M. van Krieken,
volgens besluit van het college van decanen
in het openbaar te verdedigen op

maandag 17 mei 2021

om 10.30 uur precies

door

Claire Irma Amanda van Houdt

geboren op 10 oktober 1984

te Soest

Promotoren

prof. dr. D.J.O. Ulrich

prof. dr. J.A. Jansen

Copromotor

dr. ing. J.J.J.P. van den Beucken

Manuscriptcommissie

prof. dr. M.J.R. Edwards

prof. dr. P. Habibovic (Universiteit Maastricht)

dr. H.C. Kroese-Deutman (Rijnstate)

Paranimfen

Kassandra van Houdt

Femke van de Peppel-Mauritz

Voor mijn mannen en familie

Contents

1

CHAPTER 1

Introduction

Introduction

Bone healing

Bone tissue is continuously being turned over and possesses substantial regenerative capacity througout the adult life (Urist et al. 1954, Gianoudis et al. 2007). Most tissues in the body heal by scar formation of connective tissue, meant to immediately patch and re-establish homeostasis (Thorne et al. 2014). In contrast, bone healing results in complete and scarless healing with restored properties of bone as before or even with higher mechanical properties (Thorne et al. 2014, Gianoudis et al. 2007). The full process of bone healing is not yet understood, but studies show a complex proces with a large number of gene-regulated molecular factors combined with physiological en biomechanical principles (Thorne et al. 2014, Gianoudis et al. 2007). A disruption in this process can lead to complications, such as infections and non-union (Gianoudis et al. 2007). It has been estimated that 5-10% of all bone fractures lead to non-unions, and hence require further treatment (Gianoudis et al. 2011). Surgical intervention for bone defects can aid bone healing, for which autologous bone graft (transplantation of bone tissue from one site to another within the same individual) remains the golden standard (Van der Stok et al. 2011, Dimitriou et al. 2011).

Bone grafting is used for various indications

Bone grafting involves transplantation of autologous bone, which possesses osteogenic (by osteogenic cells), osteoconductive (guiding bone growth), and osteoinductive properties (by growth factors and/or cells) (Dimitriou et al. 2011). This surgical technique is well-described in trauma and reconstructive surgery to repair and augment damaged or diseased bone. Almost two decades ago, an estimated number of >500,000 bone grafting procedures were performed annually in the United States only, and this number easily doubles on a global basis (Greenwald et al. 2001). Despite the desirable properties, several downsides accompany the use of autologous bone, including limited availability, increased donor site morbidity, and additional surgical efforts (Dimitriou et al. 2011, Finkemeier 2002). In view of these disadvantages, multiple biological and synthetic bone substitutes have been explored over the last few decades.

Allograft and xenograft use bone from another source than the patient, with allograft derived from human donors and xenografts from other species (e.g. bovine). These graft types are an alternative for autologous bone, although immunological issues need to be considered regarding safe use (Greenwald et al. 2001). Allografts and xenografts have a long track of clinical use and already several approved products are commercially available, e.g. DBXTM by DePuy Synthes (demineralised human bone) or Bio-Oss® by Geistlich (devitalised bovine bone) (Gruskin et al. 2012, Kurien et al. 2013, Urist 1965).

Alternatively, synthetic bone grafts have emerged as an appealing modality to overcome the disadvantages of autologous and allografts. Worldwide endeavors are made to develop safe and reliable synthetic bone grafts (Van der Stok et al. 2011, Bongio et al. 2010). Commercially

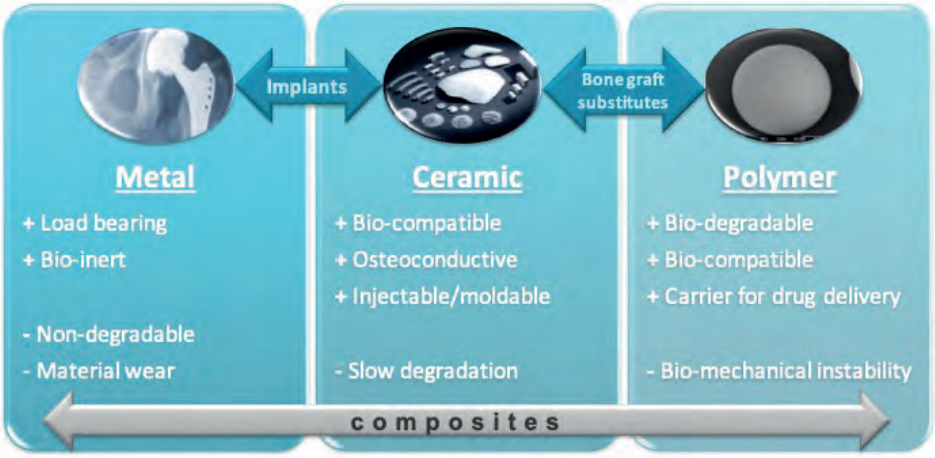

Figure 1: Benefits and drawbacks of the different materials used in bone surgery.

available synthetic bone substitutes are off-the-shelf available in various forms and shapes, adapted to the specific needs of different bone defects (Bongio et al. 2010, Van der Stok et al. 2013).

When considering a surgical intervention for bone healing next to the addition of the desired biological properties, a stable environment is mandatory to achieve uneventful bone healing (Calori et al. 2011, Giannoudis et al. 2007, Van der Stok et al. 2013). Bone grafts alone do not possess the mechanical properties to secure a stable environment under load-bearing conditions or at vital locations. Therefore, bone grafts are often combined with a stabilization method, such as pins, screws, plates, or intramedullary nails, often made out of stainless steel or alloys of cobalt, titanium or tantalum (Mantripragada et al. 2013). Titanium is a metallic material that is successfully used for a wide variety of medical applications due to its strength, low density and resistance to corrosion (Mantripragada et al. 2013, Matassi et al. 2013). With the use of advanced techniques such as selective laser sintering (SLS), tailor-made titanium implants can be generated in the form of porous scaffolds, which can provide stability and are osteoconductive (Van der Stok et al 2013, Mantripragada et al. 2013).

Bone substitutes and their different compositions

To evaluate the bone regenerative capacity of synthetic bone substitutes, one first needs to know the various types of materials and their properties that are currently used for their fabrication. Several 'off-the-shelf' synthetic bone substitutes are available for clinical bone regenerative treatments nowadays and worldwide research is done to enhance the properties of synthetic bone substitutes and improve their clinical performance. Synthetic bone substitutes can be subdivided into three main material classes, i.e. polymers, ceramics and composites (Bongio et al. 2010).

A polymer is a long molecule consisting of many small, repeating units, called monomers, joined end to end and either or not containing ramifications. Polymers of either synthetic or natural origin are intertwined in everyday life and have a wide variety of purposes. For instance, DNA as the genetic information carrier of all proteins in all flora and fauna is a natural polymer; further, multiple types of synthetic polymers find application in industrial and consumer markets, such as industrial rubbers and plastic bags. Polymer-based bone substitutes have a wide range of properties due to the versatility regarding their composition, including stiff and strong polymers (e.g. polyaryletherketones, PAEK (Kurtz 2007); polymethylmethacrylate, PMMA) and injectable and flexible polymers (e.g. hydrogels, a class of highly hydrated polymers that have overall properties similar to those of natural soft tissues) (Drury et al. 2003).

Ceramics, especially those based on calcium phosphates (CaPs), are favorable materials due to their biocompatible, bioactive and osteoconductive properties resulting from a chemical composition that shows high similarity to the mineral phase of bone (Kolk et al. 2012, Verron et al. 2012, Zhang et al. 2014). In view of optimized handling properties, CaP ceramics have become available in the form of injectable CaP cement (CPC) (Bohner 2010). First proposed in the early 80s, CPCs were designed to overcome the handling difficulties of the traditional ceramic blocks and granules (Brown et al. 1983, Bohner et al. 2005).

With the use of bone graft substitutes, one must also consider the degradation time of the material. For each material or combination of materials, different forms of degradation are applicable, resulting in different speed of degradation. Even within a material, there can be differences. For example, depending on the end-product after setting, CPCs can be classified into two main groups, i.e. brushite and apatitic CPCs. Brushite CPCs have the ability to be resorbed under physiological conditions, whereas apatitic CPCs degrade relatively slowly, limiting new bone formation (Tamimi et al. 2012). Resorption of CPC occurs either via active resorption (a cell-mediated process of osteoclasts and macrophages) or via passive resorption (based on CPC solubility) (Grossardt et al. 2010, Bohner et al. 2012, LeGeros 1993, Koerten et al. 1999). Passive resorption is mainly influenced by porosity and CPC composition, i.e. apatite being less soluble than brushite. Brushite CPCs, however, have low mechanical properties and handling can be difficult due to a fast setting time (~30 s) (Tamimi et al. 2012).

Different material properties can influence the regenerative capacity of bone defects. Therefore, the choice of material and their properties are important. Local and patient-specific conditions influence bone regenerative capacity and influence the material properties, such as degradation, as well. The relevancy of some regularly occurring local and patient-specific conditions that compromise bone healing are further addressed.

Compromising conditions, increasing life expectancy

Severe trauma, bone tumors, congenital malformation or extensive infection of bone tissue can be the cause of complex and large bone defects. Patients presenting such a defect often

need surgical intervention to stabilise or recontruct the defect. Beside the challenge to succesfully overcome these complex bone defects, the situation can be further compromised by other local and/or systemic conditions such as soft tissue defects, osteoporosis, immune system malfunction, malignancy and/or diabetes. The more we age, the more we risk to encounter co-morbidities that might affect tissue healing and with the increased life-expectancy of the world population, we can also expect an increase in the number of bone defects that need to heal under compromised conditions. We further will discuss in detail these challenging aspects of bone defect healing.

Critical sized defects

The term critical size bone defect is defined as an orthotopic intraosseous wound that does not spontaneously heal without surgical intervention (Spicer 2012). Urist concluded already in 1954 that there is no limited amount of time after which a pseudarthrosis cannot unite anymore by prolonged immobilization (Urist 1954). This suggests that even very large bone defects can spontaneously heal, but the prolongation of the immobilization sometimes expands the life time of the patient, making it a critical size defect. Urist further concluded that a new proliferative process begins after any surgical intervention and after the implantation of any type of bone graft (Urist 1954). In case of a critical size defect, bone grafting surgery can be performed to obtain bone healing and reduce recovery time. Since critical sized defects can be very large, autologous bone graft availability is often insufficient and other options need to be explored, such as allografts or synthetic bone graft substitutes.

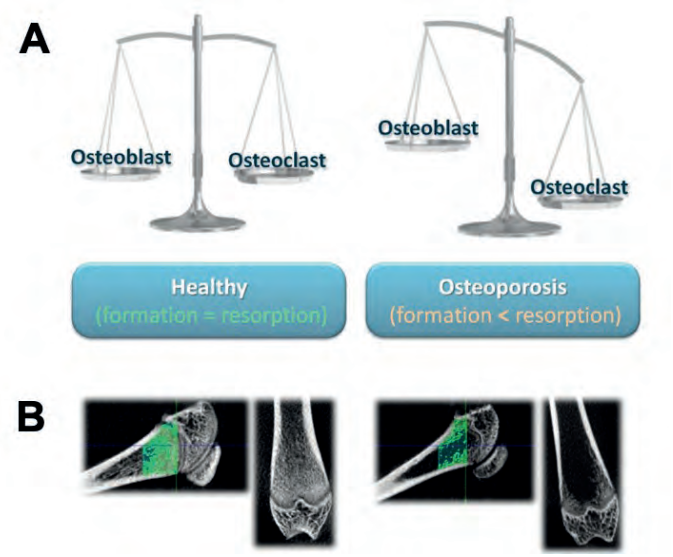

Figure 2: (A) The balance between bone formation and bone resorption in osteoporotic conditions is disturbed in favor of bone resorption. **(B)** Schematic representation of trabecular bone in the rat femoral condyle in healthy and osteoporotic conditions, showing decreased bone mass in osteoporotic conditions.

Osteoporotic conditions

Osteoporosis is a compromised condition that can interfere with bone healing and is affecting a rapidly increasing number of people. In the United States, osteoporosis affects ~10 million individuals aged >50 years, with an additional 34 million people considered to be at risk (Carmona et al. 2004). Worldwide, 9 million new osteoporosis-related fractures are estimated to occur each year (Johnell et al. 2006), two million of which occur in the United States alone (Burge et al. 2007). As osteoporosis is associated with an immense socioeconomic significance, it has been recognized as a major public health problem (Baran 2000). Osteoporosis is a complex systemic disease characterized by a decrease of bone mass and associated with (i) a decreased proliferative activity of osteoblast progenitor cells and gene expression (Meyer et al. 2001), (ii) an impaired osteoblast function (Xiao et al. 2007), (iii) a diminished osteoblast response to signalling (Kubo et al. 1999), and (iv) an imbalance between bone formation and resorption (Hollinger et al. 2008) (**Figure 2A**).

In view of the increasing number of osteoporotic patients encountered in the clinics (Fini et al. 2004) and the limitations in quantity and quality of autologous bone transplants in these patients (Fini et al. 2004), the question to what extent osteoporotic bone conditions affect the regeneration of bone defects is important from a clinical perspective. It has already been reported that patients with osteoporosis present an impaired healing process of the bone wound (Sanfilippo et al. 2003). Osteoporosis is characterized by reduced bone mineral density causing lower bone mass and deterioration of bone tissue micro-architecture (Figure 2B). This results from an imbalance in the continuous bone remodeling process, involving bone formation and resorption, and an altered variety of proteins in the bone (Fini et al. 2004). Osteoporosis is primarily observed after menopause in women, or in elderly women and men (elderly women being more affected than men in a ratio of 2:1), or secondarily by chronic predisposing medical problems. The number of elderly people is expected to significantly increase over the next 50 years as will the sex ratio of the elderly population, increasing the number of elderly women. As osteoporosis is related to age and is more prominent in women, this will increase the challenges for bone grafting in the near future, which hence causes a major clinical problem for healthcare professionals.

Main objectives and thesis outline

The main objective of this thesis was to evaluate bone regeneration using bone graft substitutes, both commercially available and novel materials, in healthy and compromised conditions using in vivo animal models. For this, we focused on evaluation of bone regeneration in osteoporotic conditions, challenged bone regeneration using defect size, and explored novel experimental bone substitute materials with appealing properties for stimulation of bone regeneration. This is further divided into the following objectives:

1. Evaluate the efficacy of two commercially available bone substitute materials, i.e. Biosilicate® and Bio-Oss®, in healthy and osteoporotic conditions at both the tissue and molecular level;

2. Evaluate the efficacy of calcium phosphate cement with porogens for healing bone defects in healthy and osteoporotic conditions;

3. Evaluate bone regeneration and material degradation by altering the PLGA porogen content in calcium phosphate cement;

4. Challenge bone regeneration by introducing demineralized bone matrix as bone substitute material into a critical sized calvarial bone defect;

5. Evaluate bone regeneration using an “enhanced” novel material by adding alendronate into calcium phosphate cement in osteoporotic conditions;

6. Evaluate bone regeneration in a critical size defect under osteoporotic conditions using an experimental bone substitute material (a self-healing hydrogel containing BP and calcium phosphate) with BMP-2.

References

1. Abushahba F, Renvert S, Polyzois I, Claffey N. Effect of grafting materials on osseointegration of dental implants surrounded by circumferential bone defects. An experimental study in the dog. Clinical oral implants research 2008;19:329-334

2. Baran DT. Osteoporosis: which current treatments reduce fracture risk? Cleve Clin J Med 2000;67(10):701-3.

3. Bohner M, Gbureck U, Barralet JE. Technological issues for the development of more efficient calcium phosphate bone cements: a critical assessment. Biomaterials 2005;26:6423-9.

4. Bohner M. Design of ceramic-based cements and putties for bone graft substitution. Eur Cell Mater. 2010;20:1-12.

5. Bohner M, Galea L, Doebelin N. Calcium phosphate bone graft substitutes: Failures and hopes. J Eur Ceram Soc 2012;32:2663-71.

6. Bowman SM, Zeind J, Gibson LJ, Hayes WC, McMahon TA. The tensile behavior of demineralized bovine cortical bone, J Biomech 1996;29: 1497-501

7. Brown WE, Chow LC. A New Calcium-Phosphate Setting Cement. J Dent Res 1983;62:672.

8. Bongio M, van den Beucken JJJP, Leeuwenburgh SCG, Jansen JA. Development of bone substitute materials: from 'biocompatible' to 'instructive'. J Mater Chem 2010;20(40):8747-59.

9. Burge R, Dawson-Hughes B, Solomon DH, Wong JB, King A, Tosteson A. Incidence and economic burden of osteoporosis-related fractures in the United States, 2005-2025. J Bone Miner Res 2007;22(3):465-75.

10. Calori GM, Mazza E, Colombo M, Ripamonti C., The use of bone-graft substitutes in large bone defects: any specific needs?, Injury 2011;42 Suppl 2: S56-63

11. Carmona RH, Beato C, Lawrence A, Moritsugu K, Noonan AS, Katz SI. Bone Health and Osteoporosis: A Report of the Surgeon General. In: McGowan JA, Raisz LG, Noonan AS, Elderkin AL, editors. Bone Health and Osteoporosis: A Report of the Surgeon General. Rockville (MD): Office of the Surgeon General (US) 2004.

12. Catanese III J, Iverson EP, Ng RK, Keaveny TM. Heterogeneity of the mechanical properties of demineralized bone, J Biomech 1999;32: 1365-9

13. Dimitriou R, Mataliotakis GI, Angoules AG, Kanakaris NK, Giannoudis PV. Complications following autologous bone graft harvesting from the iliac crest and using the RIA: a systematic review. Injury 2011;42 Suppl 2:S3-15.

14. Drury, JL, Mooney, DJ. Hydrogels for tissue engineering: scaffold design variables and applications. Biomaterials 2003;24: 4337– 4351.

15. Fini M, Giavaresi G, Torricelli P, Borsari V, Giardino R, Nicolini A, Carpi A () Osteoporosis and biomaterial osteointegration. Biomedicine & pharmacotherapy 2004;58:487-493

16. Finkemeier CG. Bone-grafting and bone-graft substitutes, J Bone Joint Surg Am 2002;84-A: 454-64

17. Giannoudis PV, Einhorn TA, Marsh D. Fracture healing: the diamond concept. Injury 2007;38 Suppl 4:S3-6.

18. Giannoudis PV, Jones E, Einhorn TA. Fracture healing and bone repair. Injury 2011;42(6): 549-550.

19. Goulet JA, Senunas LE, DeSilva GL, Greenfield ML. Autogenous iliac crest bone graft. Complications and functional assessment. Clin Orthop Relat Res 1997;(339):76-81.

20. Greenwald AS, Boden SD, Goldberg VM, Khan Y, Laurencin CT, Rosier RN. Bone-Graft Substitutes: Facts, Fictions, and Applications. J Bone Joint Surg Am 2001;83-A:98-103

21. Grossardt C, Ewald A, Grover LM, Barralet JE, Gbureck U. Passive and active in vitro resorption of calcium and magnesium phosphate cements by osteoclastic cells. Tissue Eng Part A 2010;16:3687-95.

22. Gruskin E, Doll BA, Futrell FW, Schmitz JP, Hollinger JO. Demineralized bone matrix in bone repair: history and use, Adv Drug Deliv Rev 2012;64: 1063-77

23. Hollinger JO, Onikepe AO, MacKrell J, Einhorn T, Bradica G, Lynch S, Hart CE. Accelerated fracture healing in the geriatric, osteoporotic rat with recombinant human platelet-derived growth factor-BB and an injectable beta-tricalcium phosphate/collagen matrix. J Orthop Res 2008;26(1):83-90.

24. Johnell O, Kanis JA. An estimate of the worldwide prevalence and disability associated with osteoporotic fractures. Osteoporos Int 2006;17(12):1726-33.

25. Koerten HK, van der Meulen J. Degradation of calcium phosphate ceramics. J Biomed Mater Res 1999;44:78-86.

26. Kolk A, Handschel J, Drescher W, Rothamel D, Kloss F, Blessmann M, et al. Current trends and future perspectives of bone substitute materials - from space holders to innovative biomaterials. J Maxillofac Surg 2012;40:706-18.

27. Kubo T, Shiga T, Hashimoto J, Yoshioka M, Honjo H, Urabe M, Kitajima I, Semba I, Hirasawa Y. Osteoporosis influences the late period of fracture healing in a rat model prepared by ovariectomy and low calcium diet. J Steroid Biochem 1999;68(5-6):197-202.

28. Kurien T, Pearson RG, Scammell BE. Bone graft substitutes currently available in orthopaedic practice: the evidence for their use. Bone Joint J 2013;95-B(5):583-97.

29. Kurtz SM, Devine JN. PEEK biomaterials in trauma, orthopedic, and spinal implants. Biomaterials 2007; 28(32):4845-4869.

30. LeGeros RZ. Biodegradation and bioresorption of calcium phosphate ceramics. Clin Mater 1993;14:65-88.

31. Mantripragada VP, Lecka-Czernik B, Ebraheim NA, Jayasuriya AC. An overview of recent advances in designing orthopedic and craniofacial implants, J Biomed Mater Res A 2013;101: 3349-64

32. Meyer D, Stavropolous S, Diamond B, Shane E, Green PH. Osteoporosis in a north american adult population with celiac disease. Am J Gastroenterol 2001;96(1):112-9.

33. Orsini G, Scarano A, Degidi M, Caputi S, Iezzi G, Piattelli A. Histological and ultrastructural evaluation of bone around Bio-Oss particles in sinus augmentation. Oral diseases 2007;13:586-593

34. Orsini G, Traini T, Scarano A, Degidi M, Perrotti V, Piccirilli M, Piattelli A. Maxillary sinus augmentation with Bio-Oss particles: a light, scanning, and transmission electron microscopy study in man. Journal of biomedical materials research Part B, Applied biomaterials 2005;74:448-457

35. Sanfilippo F, Bianchi AE. Osteoporosis: the effect on maxillary bone resorption and therapeutic possibilities by means of implant prostheses -a literature review and clinical considerations. Int J Periodontics Resorative Dent 2003;23:447-457

36. Spicer PP, Kretlow JD, Young S, Jansen JA, Kasper FK, Mikos AG. Evaluation of bone regeneration using the rat critical size calvarial defect. Nat Protoc 2012;7(10): 1918-29.

37. Tamimi F, Sheikh Z, Barralet J. Dicalcium phosphate cements: brushite and monetite. Acta biomaterialia 2012;8:474-87.

38. Tapety FI, Amizuka N, Uoshima K, Nomura S, Maeda T. A histological evaluation of the involvement of Bio-Oss in osteoblastic differentiation and matrix synthesis. Clinical oral implants research 2004;15:315-324

39. Thorne C, Chung KC, Gosain A, Guntner GC, Mehrara BJ (2014). Grabb and Smith's plastic surgery: Editor-in-chief, Charles H. Thorne ; editors, Kevin C. Chung, Arun Gosain, Geoffrey C. Gurtner, Babak Joseph Mehrara, J. Peter Rubin, Scott L. Spear (Seventh edition.). Philadelphia: Wolters Kluwer/Lippincott Williams & Wilkins Health.

40. Urist MR, Mazet R, Jr., McLean FC. The pathogenesis and treatment of delayed union and non-union; a survey of eighty-five ununited fractures of the shaft of the tibia and one hundred control cases with similar injuries. J Bone Joint Surg Am 1954;36-A(5):931-80; passim.

41. Urist MR. Bone: formation by autoinduction, Science 1965;150: 893-9

42. Urist MR, Silverman BF, During K, Dubuc FL, Rosenberg JM. The Bone Induction Principle, Clin Orthop Relat Res 1967;53: 243-84

43. Van der Stok J, Van Lieshout EM, El-Massoudi Y, Van Kralingen GH, Patka P. Bone substitutes in the Netherlands - a systematic literature review. Acta Biomater 2011;7(2):739-50.

44. Van der Stok J, Van der Jagt OP, Amin Yavari S, De Haas MF, Waarsing JH, Jahr H, Van Lieshout EM, Patka P, Verhaar JA, Zadpoor AA, Weinans H. Selective laser melting-produced porous titanium scaffolds regenerate bone in critical size cortical bone defects, J Orthop Res 2013;31: 792-9

45. Verron E, Bouler JM, Guicheux J. Controlling the biological function of calcium phosphate bone substitutes with drugs. Acta Biomater 2012;8:3541-51.

46. Xiao Y, Fu H, Prasadam I, Yang YC, Hollinger JO. Gene expression profiling of bone marrow stromal cells from juvenile, adult, aged and osteoporotic rats: with an emphasis on osteoporosis. Bone 2007;40(3):700-15.

47. Zhang J, Liu W, Schnitzler V, Tancret F, Bouler JM. Calcium phosphate cements for bone substitution: chemistry, handling and mechanical properties. Acta Biomater 2014;10:1035-49.

2

CHAPTER 2

Bone regeneration and gene expression in bone defect under healthy and osteoporotic bone conditions using two commercially available bone graft substitutes

van Houdt CIA, Tim CR, Crovace MC, Zanotto ED, Peitl O, Ulrich DJO, Jansen JA, Parizotto NA, Renno AC, van den Beucken JJJP.

Biomed Mater. 2015 May 8;10(3):035003

Introduction

Bone tissue is continuously being turned over and possesses substantial regenerative capacity [1,2]. Surgical intervention for bone defects can aid bone healing, for which autologous bone graft (i.e. transplantation) remains the golden standard [3,4]. However, drawbacks for this procedure are increased donor site morbidity, the limited amount and quality of autologous bone available, and a prolonged surgical time [3-7]. To overcome these disadvantages, research has focused on the development of either organic or synthetic bone substitutes to replace the need for autologous bone grafting [3,6].

Especially in compromised conditions such as infections, malignancy or increased age of the patient, bone healing is impaired and requires surgical intervention. Osteoporosis is such a compromised condition that can interfere with bone healing and is affecting a rapidly increasing number of people. In the United States, osteoporosis affects ~10 million individuals aged >50 years, with an additional 34 million people considered to be at risk [8]. Worldwide, 9 million new osteoporosis-related fractures are estimated to occur each year [9], two million of which occur in the United States alone [10]. As osteoporosis is associated with an immense socioeconomic significance, it has been recognized as a major public health problem [11]. Osteoporosis is a complex disease characterized by a decrease of bone mass and associated with (i) a decreased proliferative activity of osteoblast progenitor cells and gene expression [12], (ii) an impaired osteoblast function [13], (iii) a diminished osteoblast response to signalling [14], and (iv) an imbalance between bone formation and resorption [15].

To summarise, compromised patients such as those suffering from osteoporosis could benefit greatly from the use of bone graft substitutes with enhanced osteogenic activity. From a bone substitute material perspective, interaction of the material with bone tissue should favour bone regenerative processes for compromised patients [16,17]. Several bone substitute materials are commercially available for clinical applications nowadays. Worldwide, research is performed to enhance the properties of bone substitute materials and hence their biological performance [18]. Bio-Oss®, made from the mineral part of bovine bone, is a well-established bone substitute material and represents the major clinically-used product for dental bone regeneration [19]. It has been documented that Bio-Oss® promotes osteogenesis in vitro [20,21]. During the production process, the organic parts are removed from the bovine bone and the remaining calcium-containing bone structures are processed to slowly degradable granules [22]. Furthermore, many approaches have explored the potential of materials with a high bioactivity rate, such as bioactive glasses (BGs) and glass-ceramics (BGCs), for bone regenerative applications [23-25]. BGCs, including Biosilicate®, are synthetic silica-based bioactive materials, with the unique ability to directly bond to bone tissue, making these materials appealing for bone regeneration [25-28]. Research results indicate that upon degradation of such a silica-based material, silicon, calcium (Ca^{2+}), phosphate (PO_4^{2-}), and sodium (Na^{+}) ions are released in the physiological environment and suggest that a combination of these ions stimulates cells to form new bone tissue [29]. Biosilicate® is a novel

bone substitute glass-ceramic (crystalline) material and there are various studies underlining its suitability for bone replacement and potential to facilitate new bone formation [30-32]. For example, Granito et al. [30,31] investigated the effects of Biosilicate® with 2 different particle size distributions (180–212 µm and 300–355 µm) on bone healing in a tibial bone defect model in rats. At 20 days after implantation they observed that bone defects filled with particles of Biosilicate® (180–212 µm in diameter) showed a higher amount of newly formed bone in the area of the callus and improved biomechanical properties compared to (empty) control animals and to animals treated with original 45S5 Bioglass®. Furthermore, molecular biology studies have shown that a solution containing Ca, P and Si ions stimulates gene expression (of amongst other growth-related genes, cell adhesion receptor genes, and matrix metalloproteinase genes) in osteoblasts [33].

Pre-clinical testing of newly developed bone substitute materials is generally done using healthy animals. In view of the heterogeneity of patients that require bone regenerative treatment, these studies do not provide information on bone substitute material performance in compromised bone conditions, such as in osteoporotic bone. In view of the lack of knowledge on the performance of clinically available bone substitute materials in different bone conditions, we aimed at comparatively using a rat femoral condyle bone defect model for rats that had either or not undergone ovariectomy to induce an osteoporotic bone condition [34]. Within the created bone defects in healthy and osteoporotic bone, we used Biosilicate® or Bio-Oss® and evaluated the biological performance of these bone substitute materials as well as their effects on in vivo gene expression. Additionally, we evaluated the in vitro cellular response to these bone substitute materials.

Materials and Methods

Materials

Biosilicate® (fully crystallized bioactive glass ceramic of the quaternary Na_2O-CaO-SiO_2-P_2O_5 system, containing weight percentages of respectively 23.75%, 23.75%, 48.5% and 4%) was provided by Vitreous Materials Laboratory, Department of Materials Engineering, Federal University of São Carlos (São Carlos, São Paulo, Brazil) [35]. Bio-Oss® was purchased from Geistlich Pharma AG (Wolhusen, Switzerland). The materials used were in the form of dense particles (size: 0.25-1 mm).

In vitro biological response to Biosilicate® and Bio-Oss®

Cell culture

Cryo-preserved rat bone marrow stromal cells (BMSC) were employed in this study. BMSCs were grown in Minimum Essential Medium (MEM-α; Gibco BRL, Life Technologies, Breda, the Netherlands) supplemented with 10% foetal bovine serum (FBS; Gibco), and penicillin/streptomycin (100 units/ml; Gibco). All tissue culture procedures were performed under strict aseptic conditions in a biological safety cabinet. BMSCs were grown in sterile, vented, tissue culture flasks (75 cm2; Greiner Bio-one, Utrecht, the Netherlands) in a humidified incubator at 37°C in 5% carbon dioxide (CO2), 95% air. The cells were expanded for five passages using standard tissue culture techniques.

Pre-incubation of Biosilicate® particles and cell seeding

Prior to cell seeding, Biosilicate® (0.025 grams) was placed in 24-well ThinCert™ cell culture inserts (Greiner Bio-one) and incubated in tissue culture growth medium supplemented with 25 mM HEPES (Sigma-Aldrich, Zwijndrecht, Netherlands) and 10% FBS (Gibco) at 37°C, 5% CO_2 for at least 48 hours, in order to decrease the pH of the medium to allow for cell culture. After this period, the medium was discarded. This pre-incubation of Biosilicate® is needed, because the ion exchange reaction which are known to occur at the surface of bioactive glasses in physiological environment can lead to an increase of media pH with cytotoxic effects [36]. Bio-Oss® particles (0.025 grams) were also placed in 24-well ThinCert™ cell culture inserts (Greiner Bio-one), but without the need of pre-incubation. Subsequently, BMSCs were seeded in direct contact with the particles at a density of 20.000 cells/insert. Cell culture medium was changed every 2-3 days, and the cells were cultured for up to 28 days.

Determination of cell metabolic activity

Cell metabolic activity was evaluated using AlamarBlue® (Invitrogen, Life Technologies, Breda, the Netherlands) according to the manufacturer's instructions. Briefly, AlamarBlue® (1 ml) was added directly to BMSCs in cell culture media (n=8) and the plate was incubated for 4 hours at 37°C in a cell culture incubator. Subsequently, 200 µl of each sample was transferred to a 96 well plate (in duplicates). Finally, the plate was read in a spectrophotometer (Bio-Tek Instruments, Winooski, United States) at 570 nm.

Cell proliferation

Cell proliferation was determined by quantifying the amount of DNA (QuantiFluor® dsDNA quantitation kit; Promega, Leiden, the Netherlands). After 7, 14 and 28 days of culture, BMSCs were washed with PBS (n=8), homogenized in ultrapure water (1 ml), frozen, and thawed twice before analysis. Then, the DNA sample (100 µl) or standard was incubated with working solution (100 µl) in the dark for 10 minutes. Finally, the samples were read in a spectrophotometer (Bio-Tek Instruments) at 530 nm.

ALP activity

The specific activity of alkaline phosphatase (ALP) was assayed by the use of an ALP activity assay (Sigma). Briefly, 80 µl sample (n=8) or standard (serial dilutions of 4-nitrophenol at the concentrations of 0–25 nM) and 20 µl buffer solution (0.5 M 2-amino-2-methyl-1-propanol) were added into a 96-well plate. Then, a substrate solution (p-nitrophenyl phosphate; 100 µl) was added to all the wells and subsequently the mixture was incubated at 37°C for 1 hour. The reaction was stopped by adding of 0.3M NaOH (100 µl), and the ALP activity was measured in a spectrophotometer (Bio-Tek Instruments) at 405 nm with subsequent normalization for DNA content.

Calcium content

After 7, 14, and 28 days of culture, the amount of deposited calcium by BMSCs (n=8) was quantified using the ortho-cresolphthalein complexone method (Sigma). Briefly, cell layers were washed twice with PBS, and then incubated in 0.5 N acetic acid (1 ml) on a shaking platform overnight. For analyses, a sample (10 µl) or standard was incubated with work reagent (300 µl) in a 96-well plate at room temperature for 10 minutes. The standards (0 - 100 mg/ml) were generated by serial dilutions of a $CaCl_2$ stock solution. Finally, the plate was read in a spectrophotometer reader (Bio-Tek Instruments) at 570 nm. Negative control reactions with particles (Biosilicate® and Bio-Oss®) without cells were also included in each assay and it was used to normalize deposition calcium data.

Scanning electron microscopy (SEM)

On days 7, 14 and 28 days post-seeding, biomaterial particles with attached cells were washed twice with PBS and fixed for 10 minutes using glutaraldehyde (2% in 0.1 M cacodylate buffer). Subsequently, the samples were washed with 0.1 M cacodylate buffer (pH 7.4) and dehydrated in graded series of ethanol. Finally, samples were dried with tetramethylsilane (Sigma), sputter coated with gold and examined using a scanning electron microscope (JEOL 6310, Nieuw-Vennep, the Netherlands).

RNA isolation

Total RNA was isolated from the cells using TRIzol reagent (Invitrogen) (n=5 per group) according to the manufacturer's instructions. In brief, after removing the culture medium, TRIzol reagent (1 ml) was added to each well. The cell extract was mixed vigorously with chloroform (0.2 ml) and centrifuged at 12,000 g for 15 minutes at 4°C. The aqueous phase

of the sample was collected and mixed with 100% isopropanol (0.5 ml). After incubation at room temperature for 10 minutes, the extract was centrifuged and then washed with 75% ethanol. Successively, the RNA pellet was dissolved in RNase-free water and concentration and purity were determined using the NanoDrop (ND-2000; Thermo Scientific, Waltham, MA USA). RNA samples with an A260/A280 ratio <1.8 were excluded.

Real-time PCR

Total RNA (1 µg) was applied as template for cDNA synthesis using the iScript cDNA synthesis kit (Bio-Rad, Veenendaal, the Netherlands) following the manufacturer's instructions. The cDNA samples were subjected to quantitative real time polymerase chain reaction (qRT-PCR) using a BIORAD CFX96 real-time system.

Oligonucleotide primers were designed for RPS18 (NM_181374.2), Runx-2 (NM_053470.2), alkaline phosphatase (ALP) (J03572.1), Osteocalcin (OC) (NM_013414.1) (**Table 1**) using Primer Express Software 2.0 (Applied Biosystems, Foster City, USA). All real-time primers were initially tested against standards and a standard curve was generated.

The optimized PCR conditions were: initial denaturation at 94°C for 10 minutes, followed by 40 cycles consisting of denaturation at 94°C for 15 seconds, annealing at 60°C for 1 minute, and extension at 72°C for 45 seconds, with a final extension step at 72°C for 2 minutes. Negative control reactions with no template (deionised water) were also included in each run. For each gene, all samples were amplified simultaneously in duplicate in one assay run. Analysis of relative gene expression was performed using the 2-ΔΔCT method. RPS18 was used as a housekeeping gene to normalize expression data.

Animal experiment

Animal model and validation

For this experiment, 36 mature female Wistar rats were used (weight ~250 g; Charles River Nederland B.V., Leiden, The Netherlands). A 1-week acclimatization period was maintained in standard housing (i.e. 2 rats per box). All rats received two surgical procedures during the course of the experiment: the first surgery was a bilateral ovariectomy (OVX; 19 rats) to induce an osteoporotic bone condition or a sham operation (SHAM; 17 rats) for a healthy bone condition; in the second surgery, bone defects were created in both femoral condyles (bilateral) of all animals, which were left empty as control or filled with Biosilicate® or Bio-Oss®. Access to food and bottled water was maintained ad libitum. All experiments were in accordance with institutional, national and international guidelines for animal care and the Dutch law concerning animal welfare. The studies were reviewed and approved in advance by the Experimental Animal Committee of the Radboud University (RUDEC 2013-187).

Surgery to induce osteoporotic condition

Nineteen animals received an ovariectomy (OVX) through two separate incisions in the lateral abdominal wall [34]. The remaining seventeen rats received a sham surgery (SHAM) using an identical surgical approach as for the other animals without removal of the ovaries. Pre-operatively, pain medication was provided 15 minutes before surgery by injecting Carprofen (5 mg/kg; Rimadyl®, Pfizer Animal Health, New York, USA). Anaesthesia was induced and maintained by isoflurane inhalation (2-5%; Rhodia Organique Fine Limited). The back area was shaved and disinfected with a povidone iodine solution. The animal was placed on an electric heating mat in prone position to prevent hypothermia. A dorsal midline incision (~2 cm) caudal to the posterior border of the ribs was created to enter the abdominal cavity. The ovary was located in a fat pad and gently pulled outside the abdominal cavity. A single ligature was placed around the fallopian tube using a surgical polyester suture (Terylene® 2.0 undyed, Serag-Wiessner GmbH & Co, Naila, Germany). The ovary was removed by cutting above the ligated area and after haemostasis the tuba was returned into the abdomen. The abdominal muscles were closed with continuous absorbable sutures (Vicryl® 4.0, Ethicon, Amersfoort, the Netherlands) after which the skin was sutured with multiple single absorbable sutures (Vicryl® 4.0, Ethicon). The procedure was repeated for the contro-lateral ovary using the same incision design. Postoperative pain medication for a minimum of 2 days was provided by injection of Carprofen every 24 hours and Buprenorfine (0.02 mg/kg; Temgesic®, Reckitt Benckiser Health Care Limited) every 12 hours. To ensure progression toward an osteoporotic bone condition, the OVX group received a low calcium diet of pellets containing 0.01% calcium and 0.77% phosphorous (Ssniff Spezialdiäten GmbH, Soest, Germany) for six weeks, whereas the SHAM group received no dietary restrictions.

Surgery for femoral bone defect and material implantation

Six weeks after OVX or SHAM surgery, a bone defect was created in both femoral condyles of each animal. Anaesthesia and pain medication were administered as described for the first operation. Both hind limbs of the rats were shaved and disinfected with povidone iodine. The rats were immobilized in supine position on a heating mat. A longitudinal incision through skin and muscle was made on the medial surface of the knee in flexed position. After exposure of the medial side of the distal femoral condyle the knee capsule was incised. By extension of the knee, luxation of the patella laterally was possible. When a clear view of the femoral side of the knee joint was established, a defect longitudinal to the length of the femur (Ø 2.5 mm by 6 mm in depth) was created. To create the defect, a dental drill (Elcomed 9927 SPS; W&H Dentalwerk Burmoos GmbH, Burmoos, Austria) with a series of increasing bur diameters were used at a speed of maximum 5000 rpm and a constant cooling using saline. The defect was either left empty as control or filled with Biosilicate® or Bio-Oss®. The muscular layer and skin were closed with single resorbable sutures (Vicryl® 4.0 Ethicon). After implant surgery, both experimental groups (SHAM and OVX) had free access to normal pellet food and water. The animals were housed per pair under the same conditions. In the initial postoperative period, the intake of water and food was monitored as well as the weight of the animals. In addition, the animals were observed for signs of pain, infection and proper

activity and weighed again postoperatively once a week to identify significant weight loss (>20%) compared to preoperative body weight of each rat.

Validation of osteoporotic condition by ELISA for serum TRAP analysis

The osteoporotic condition by OVX was evaluated by a serum analysis for TRAP enzyme activity performed with the RatTRAPTM Assay kit (Immunodiagnostic Systems GmbH, Frankfurt am Main) at the end of the experiment, 4 weeks after implantation surgery.

Retrieval of specimens

The femurs were retrieved 4 weeks after implantation surgery. The femurs used for gene expression of both osteoporotic (n≥6) and healthy conditions (n≥5) were placed on ice for transport and immediately processed for RNA isolation. The femurs needed for histology of both osteoporotic (n≥5) and healthy conditions (n≥4) were immediately fixed in 10% formaldehyde for 24 hours, and then dehydrated in 70% ethanol. After dehydration, one femur of each group was scanned by micro-CT, then all femurs for histology were embedded in polymethylmethacrylate (pMMA), prepared by mixing methylmethacrylate (600 ml; Acros Organics BVBA, Geel, Belgium) with dibutyl phthalate (60 ml; Merck KGaA, Darmstadt, Germany) and Perkadox 16 (1.25 g; AkzoNobel, Amersfoort, The Netherlands).

Micro-CT

A desktop micro-CT system (Skyscan-1072, TomoNT version 3N.5, Skyscan®, Kontich, Belgium) was used for 3D imaging. The specimens were placed with the long axis of the implant perpendicular to the scanning beam, after which a high resolution scan was performed. 3D reconstruction and imaging processing was performed using NRecon V1.4 and CTvox v2.7 (Skyscan®), respectively.

Histology

After polymerization, thin sections (~10-15 µm) in perpendicular to the longitudinal direction, were prepared using a diamond blade microtome (Leica® Microsystems SP 1600, Nussloch, Germany). A minimum of three sections of each specimen were stained with methylene blue and basic fuchsine and examined using light microscopy (Leica® Microsystems AG, Wetzlar, Germany).

Histomorphometry

Using an imaging microscope (Axio Imager Microscope Z1, Carl Zeiss Micro Imaging GmbH, Göttingen, Germany), the pMMA-embedded histological sections were digitalized (5x magnification). Quantitative analysis of the digitalized images was performed using ImageJ software (Java® ImageJ 1.47, Image processing and analysis in Java). Within a circular region of interest (ROI) with an equal diameter (2.5 mm) to the created bone defects, the amount of newly formed bone was determined. Vital bone could be distinguished by the pink colour and distinctive cell morphology including a nucleus, allowing to be easily discerned from other tissues as wells as from Biosilicate® and Bio-Oss® particles. The maturity of bone was

differentiated by morphology, as mature trabecular bone is formed in lamellae, whereas newly formed bone has a more woven structure. Detection of different cell types could be performed as osteocytes are trapped within the lacunae of bone, osteoblasts are arranged in rows with basophilic eccentric nuclei and osteoclasts are relatively larger and multinucleated cells.

In vivo gene-expression

For RNA isolation, the femurs were dissected and the bone defect area was trephined (inner diameter of 2.5 mm) using drilling equipment (Weiss Machine WMD20LV, Jiangsu Province, China). The retrieved tissues were placed in sterilized microtubes (1.5 ml) and frozen at -80°C until analysis. To facilitate processing of multiple samples, the Bullet Blender (Next Advance, New York, United States) was used with centrifuge technology that homogenizes tissue by bead disruption of the tissue. The bone sample was added to a pre-chilled microtube containing the beads recommended by the manufacturer for RNA isolation (~50 µl stainless steel blend, 6 x 3.2 mm stainless steel) followed by the addition of TRIzol reagent (600 µl; Invitrogen). The bone was homogenized in the Bullet Blender (Next Advance) centrifuge (kept in a cold room at 4°C) for 5 minutes, then the solubilised bone extract was isolated by centrifugation for 15 seconds at 8.600 rpm at room temperature and the solution was transferred to a new microtube. Then, the RNA protocol was performed using TRIzol reagent according to the manufacturer's instructions.

The cDNA and real time PCR procedures were performed as described above for in vitro experimental work. In addition to the primers used for in vitro experimental work, primers for osteoprotegerin (OPG; NM_012870.2) and RANKL (AF187319.1; **Table 1**) were used.

Table 1: Primers and the expected PCR product size at indicated annealing temperatures for each gene analyzed. RPS18: ribosomal protein S18; Runx-2: runt-related transcription factor 2; ALP: alkaline phosphatase; OC: Osteocalcin; RANKL receptor activator of nuclear factor kappa-B ligand; OPG: Osteoprotegerin.

Gene	Forward primer	Reverse primer	Annealing temperature
RPS18	GTGATCCCCGAGAAGTTC	AATGGCAGTGATAGCGAA	60 °C
Runx-2	TTATGTGTGCCTCCAACCTGTGT	GGTTTCTTTCCCCCTCAATTTGT	60 °C
ALP	AACTACATCCCCCACGTCATG	CCCAGGCACAGTGGTCAAG	60 °C
OC	ACGAGCTAGCGGACCACATT	CCCTAAACGGTGGTGCCATA	60 °C
RANKL	CCGTTTGCTCACCTCACCAT	TGGTACCAAGAGGACAGACTGACTT	60 °C
OPG	GATATTGCCCCCAACGTTCA	AGGGCGCATAGTCAGTAGACACT	60 °C

Statistical analysis

Data are presented as mean with SDs. Statistical analysis of quantitative data was performed using one-way analysis of variance (ANOVA) with a Tukey post-hoc test. GraphPad Software (PRISM; La Jolla CA, USA) was used to carry out the statistics analysis. For a comparison between both conditions and for the analysis of the serum TRAP enzyme, a one-tailed student t-test was used. Values of $p<0.05$ were considered statistically significant.

Results

In vitro biological response of Biosilicate® and Bio-Oss®

The metabolic activity of rat bone marrow stromal cells (BMSCs) seeded on the materials and control samples showed a temporal evolution during the culture period. On days 7, 14 and 28, the cell metabolic activity was significantly higher for controls (on tissue culture plastic) compared to either Biosilicate® or Bio-Oss® ($p<0.001$; **Figure 1 (a)**). Furthermore, the cell metabolic activity of rat BMSCs on Biosilicate® was significantly increased compared to Bio-Oss® on both day 7 and 28 ($p<0.001$; **Figure 1 (a)**). For cell proliferation (**Figure 1 (b)**), controls showed significantly increased DNA-content values ($p<0.001$) compared to both Biosilicate® and Bio-Oss® at each time point. As a marker for early osteogenic differentiation, ALP-activity showed a peak for both Biosilicate® and Bio-Oss® on day 14 (Figure 1 (c)), whereas a continuous increase in ALP-activity was observed for controls. BMSCs cultured on Biosilicate® showed a significantly increased ALP-activity compared to controls at day 14 ($p<0.001$) and compared to Bio-Oss® at 28 days ($p<0.05$). As a marker for late osteogenic differentiation, extracellular calcium deposition (Figure 1 (d)) on both Biosilicate® and Bio-Oss® was significantly higher ($p<0.001$) compared to controls at all time points. Further, cells in contact with Biosilicate® deposited more calcium by day 14 and 28 compared to Bio-Oss® ($p<0.001$). Morphologically, SEM analysis showed that rat BMSCs were successfully grown on Biosilicate® and Bio-Oss® particles at all time points (data not shown).

Real time PCR

Figure 2 (a-b) represents the gene expression data of rat BMSCs cultured on Biosilicate®,

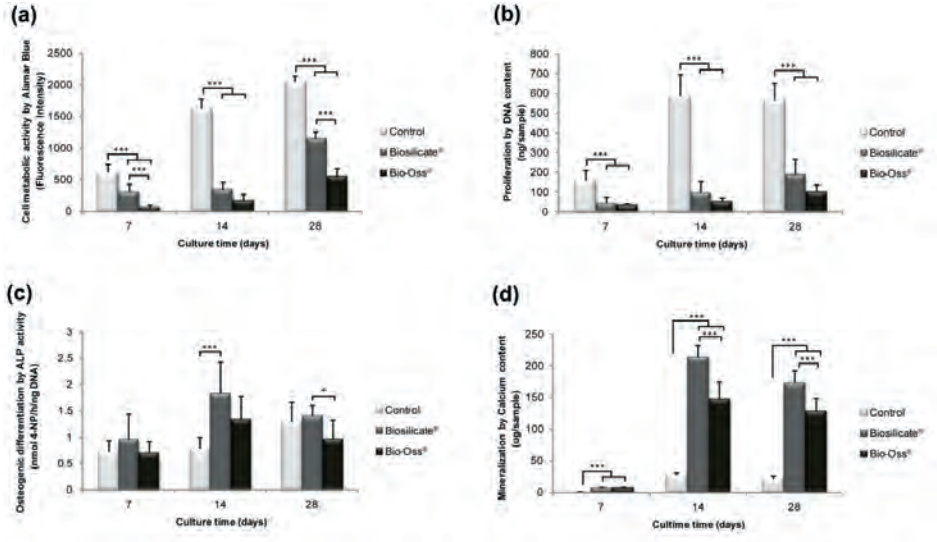

Figure 1 (a-d): In vitro biological response analysis (mean ±SD; n=8); **(a)** Cell metabolic activity. **(b)** DNA content (cell proliferation). **(c)** ALP-activity (as a marker of early differentiation). **(d)** Calcium content (as a marker of late differentiation); * $p< 0.05$, *** $p< 0.001$

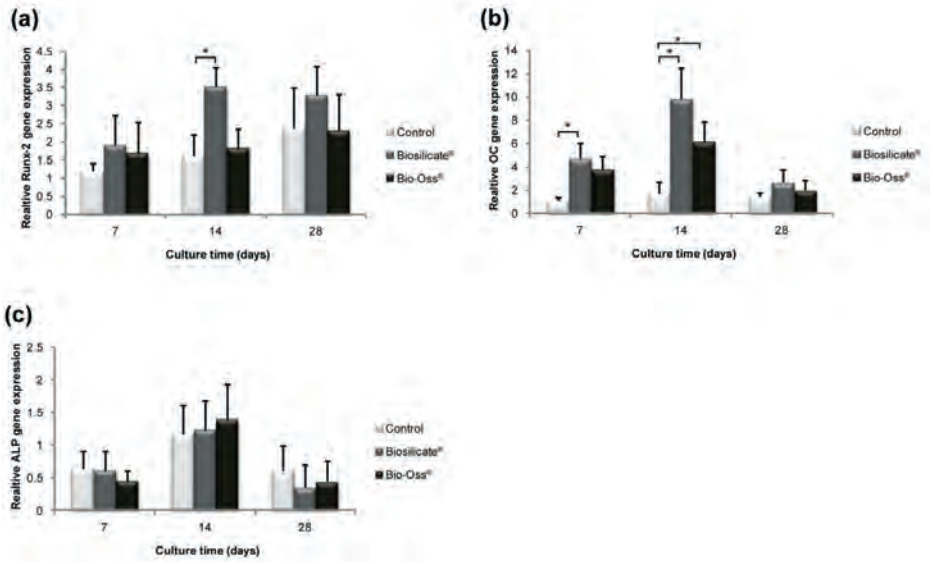

Figure 2 (a-c): In vitro results of the relative quantification of gene expression levels from BMSCs (n=8), mean ±SD; **(a)** Runx-2 gene-expression **(b)** OC gene-expression **(c)** ALP gene-expression; * p<0.05

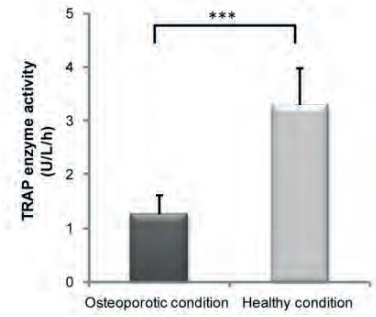

Figure 3: Serum TRAP enzyme activity (mean ±SD) in rats with osteoporotic and healthy bone condition (n=5); *** p<0.001

Bio-Oss®, and tissue culture plastic controls after culture for 7, 14 and 28 days. Significantly increased Runx-2 expression **(Figure 2 (a)**; p<0.05) was observed for rat BMSCs cultured on Biosilicate® compared to controls after 14 days. For rat BMSCs cultured on Biosilicate® and Bio-Oss®, the expression of OC **(Figure 2 (b)**) was significantly increased compared to controls after 7 and 14 days (p<0.05) and 28 days (p<0.05), respectively. Similar ALP gene expression levels were observed for all experimental groups **(Figure 2 (c)**).

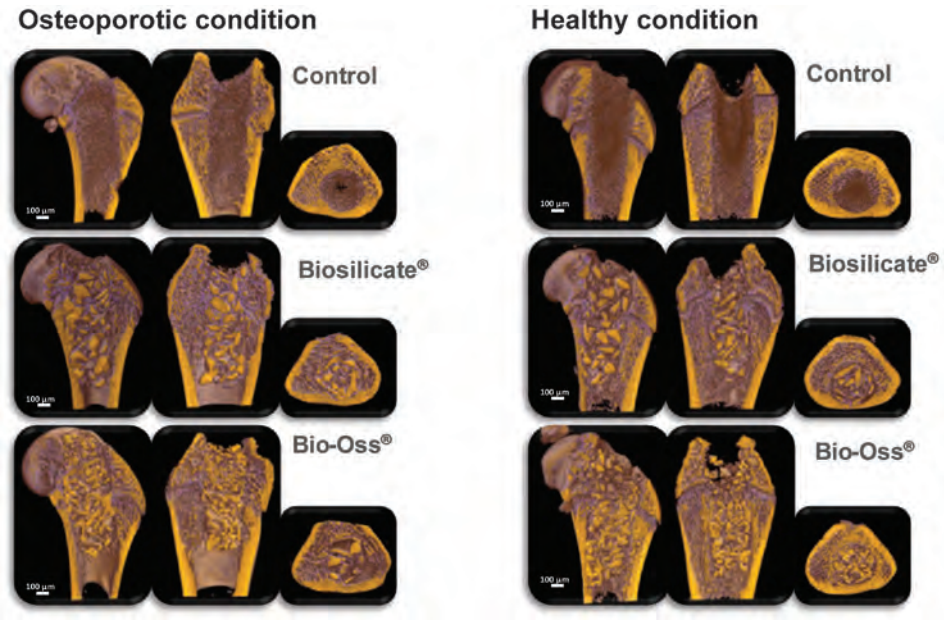

Figure 4: Representative 3D-reconstructions of the defect area obtained via ex vivo micro-CT

Animal experiment

Animal model and validation

Validation of the osteoporotic condition in this study was performed by a serum TRAP ELISA analysis. Our data showed that rats with osteoporotic bone condition had significantly decreased serum TRAP enzyme activity ($p<0.0001$) compared to healthy rats (**Figure 3**). Clinical observations after OVX and bone defect surgery showed that SHAM surgery led to euthanisation of one rat, due to >20% weight loss in the first week postoperatively related to intestinal problems. Upon implantation surgery, two rats (one OVX, one SHAM) were euthanized due to fracture of the femur during the drilling of the bone defect. All remaining rats recovered without clinical signs of complications and remained healthy during course of the experiment.

Micro-CT

An overview of 3D reconstructed bone defects from ex vivo micro-CT is presented in **Figure 4**, showing sagittal, frontal and transverse planes through the defect area for each experimental group after 4 weeks of implantation. The images provide information on the amount and space between trabecular bone as well as the distribution of and space between the particles.

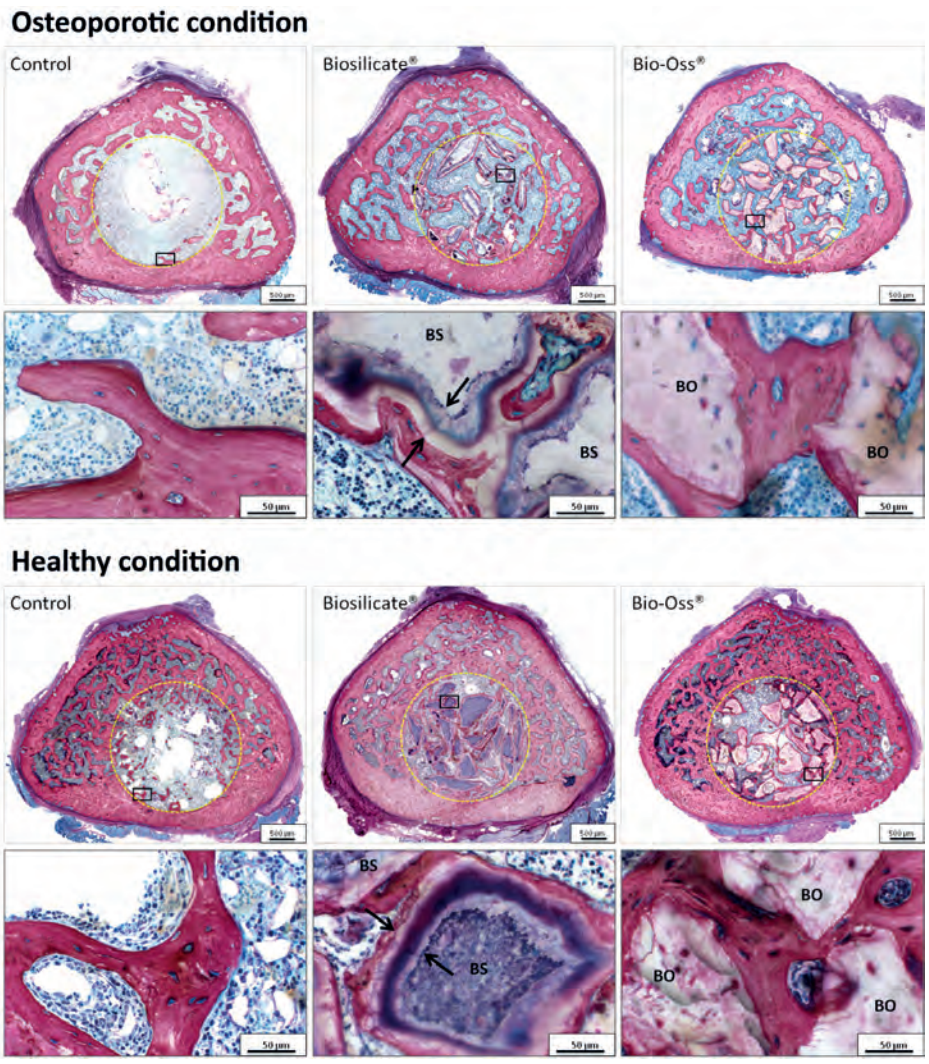

Figure 5: Images of histological slides of osteoporotic and healthy conditions with detailed images (black box), yellow circle= ROI (equal to defect of 2.5 mm), BS= Biosilicate® particles, BO= Bio-Oss® particles; arrows indicate the Biosilicate® silica-layer

Histology

Representative histological images at 4 weeks after implantation for each of the experimental groups are presented in **Figure 5**. Histological differences were observed between osteoporotic and healthy bone conditions regarding the amount and spacing of the trabecular bone outside the ROI. The space between the trabeculae was filled with bone marrow. The empty defects clearly showed that bone regeneration starts at the edges of

the defect, growing inwards. The circumference of Biosilicate® and Bio-Oss® particles was mostly covered with newly formed bone, all the way to the centre of the defect. This shows the osteoconductive properties of both Biosilicate® and Bio-Oss®, as this was never reached by the empty defects in the osteoporotic conditions. Our histological images clearly showed a gel-like layer to be present on the Biosilicate® particles implanted in both conditions (black arrows in **Figure 5**).

Histomorphometry

Quantitative histomorphometry showed material new bone formation around the Biosilicate® and Bio-Oss® particles with remnant amounts for both osteoporotic and healthy conditions compared to empty controls (**Table 2** & **Figure 6 (a-c)**). Osteoporotic conditions lead to bone formation (means with SDs) of respectively 5±8%, 11±4% and 15±5% for the empty control, Biosilicate® and Bio-Oss®, compared to respectively 20±9%, 14±5% and 16±4% in healthy conditions. For the empty defects, a significant difference ($p<0.05$) for bone formation was seen between the osteoporotic and healthy conditions, again underlining the systemic effect of OVX surgery.

Table 2: Percentages (mean ±SD) of new bone formation within the ROI of osteoporotic (n≥5) and healthy conditions (n≥4); significant difference compared to the osteoporotic control group; * $p<0.05$, ** $p<0.01$

	Control		Biosilicate®		Bio-Oss®	
	Mean	SD	mean	SD	mean	SD
Osteoporotic condition	5	± 8	11	± 4	15*	± 5
Healthy condition	20**	± 9	14	± 5	16	± 4

Real time PCR

To progress in the understanding of the mechanisms by which the process of bone healing is influenced in the presence of Biosilicate® and Bio-Oss®, an evaluation of gene expression for bone formation-related genes was performed. Expressions of the selected osteogenic genes in osteoporotic and healthy conditions are shown in **Figure 7 (a-e)**, measured at 4 weeks after implantation of Biosilicate® and Bio-Oss®. The relative gene expression showed that in osteoporotic conditions, Biosilicate® increases Runx-2, ALP, OC, OPG and RANKL expression. Bio-Oss® did not up-regulate either of the selected genes in osteoporotic conditions compared to controls. In healthy conditions, Biosilicate® demonstrated an up-regulation of Runx-2, ALP, OC and RANKL, while Bio-Oss® up-regulated only Runx-2, ALP and RANKL gene expression. Between the materials significantly more expression of Runx-2 and RANKL was seen for Biosilicate® in osteoporotic conditions and of OC and RANKL in healthy conditions.

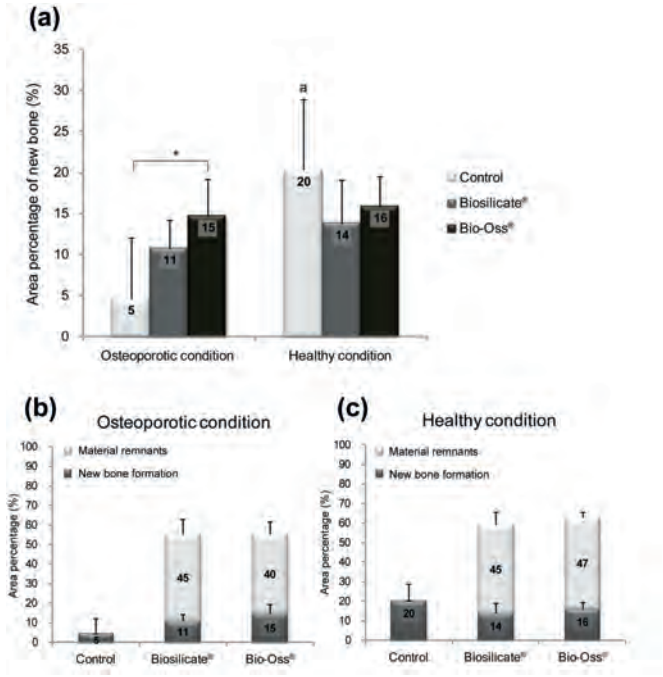

Figure 6 (a-c): (a) Percentage (mean ±SD) of new bone formation and material remnants within ROI of osteoporotic (n≥5) and healthy conditions (n≥6) **(b)** new bone formation with addition of material remnants within ROI of osteoporotic and **(c)** healthy conditions; * $p<0.05$, a $p<0.01$

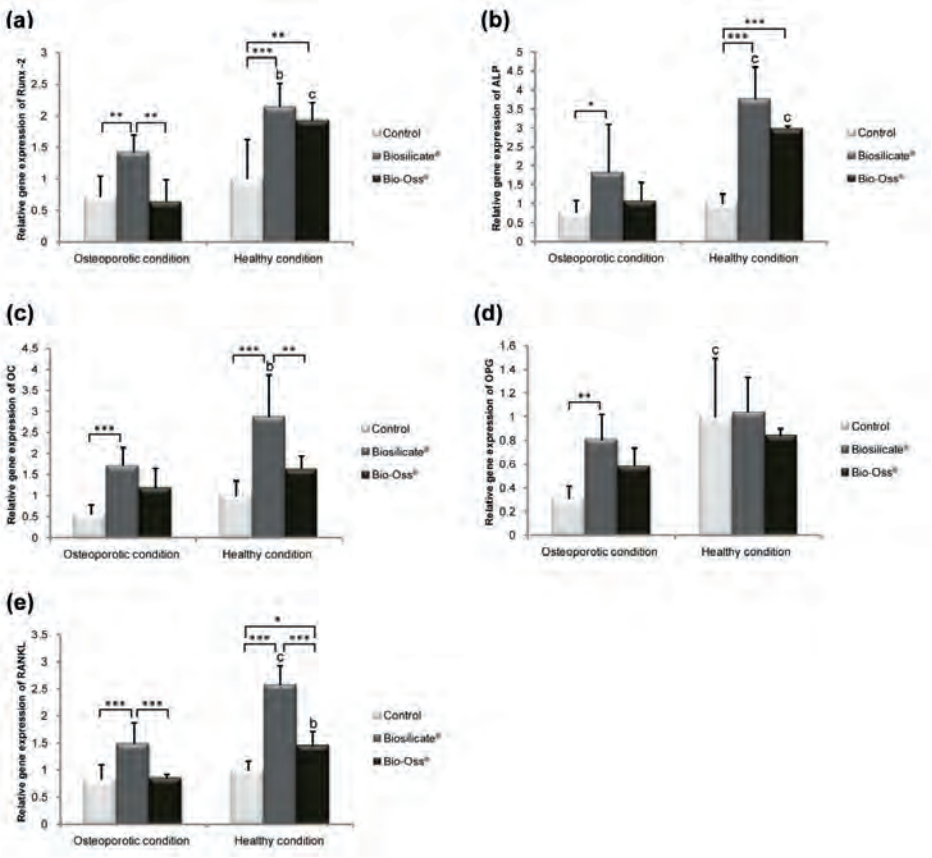

Figure 7 (a-e): In vivo results (mean ±SD) of the relative quantification of gene expression in osteoporotic (n≥6) and healthy conditions (n≥5); **(a)** Runx-2 gene-expression. **(b)** ALP gene-expression **(c)** OC gene-expression (d) OPG gene-expression (e) RANKL gene-expression; * p<0.05, ** p<0.01 and *** p<0.001, b) p<0.01 and c) p<0.001 compared to osteoporotic condition of same material

Discussion

The biological performance as well as the effects on in vivo gene expression of Biosilicate® and Bio-Oss® were comparatively examined using a rat femoral condyle bone defect model for rats that had either or not undergone ovariectomy to induce an osteoporotic bone condition [34]. Additionally, we evaluated the in vitro cellular response to these bone substitute materials.

Our in vitro experiments showed BMSCs can proliferate on tissue culture plastic. More importantly however, the addition of Biosilicate® and Bio-Oss® stimulated osteogenic differentiation compared to controls. These data corroborates the results of Ozawa et al. [37] showing stimulated osteogenic differentiation of rat BMSCs upon culturing rat bone marrow cells on hydroxyapatite (HA). When cultured on Biosilicate®, there was significantly more mineralization compared to Bio-Oss®, suggesting Biosilicate® to have more osteogenic potential in vitro. These findings are supported by the study by Renno et al. [38], who using in vitro experiments observed that osteogenic cells were successfully grown on Biosilicate® scaffolds. Moreover, the study by Herten et al. [39] showed, when seeding cells on Bio-Oss® granules, a smaller number of viable osteoblasts were detectable on the granules compared to other bone graft substitutes.

A significant up-regulation of Runx-2 was induced in vitro by Biosilicate® after 14 days. Although in our study Bio-Oss® did not induce an up-regulation of Runx-2, Sollazzo et al. [40] showed that cells cultured on Bio-Oss® for 7 days increase the osteoblast transcriptional factor Runx-2 together with other bone-related genes, i.e. SPP1 and FOSL1. Both Biosilicate® and Bio-Oss® increased the expression of OC, which corroborates with our biochemical results showing an increased mineralization compared to controls.

For evaluation of the effect of osteoporosis on bone healing in animal studies, several animal models have been utilized [41,42]. The ovariectomised rat model is a well-established small animal model for local osteoporosis [41-44]. Ovariectomy leads to estrogen deficiency and hence mimics post-menopausal osteoporosis. Since dietary factors play an important role in the multi-factorial nature of bone loss, an additional low calcium diet can further establish the osteoporotic effect [34,45]. Previous studies based on in vivo micro-CT analysis demonstrated significant effects on bone density and morphological characteristics within the femoral condyles of rats at six weeks after ovariectomy and a low calcium diet [34].

Our serum analysis results for TRAP enzyme activity are in agreement with the study of Rissannen et al. [46], who also showed significantly lower serum TRAP-activity in the OVX operated rats. Serum TRAP is a marker for the bone homeostasis, providing information about bone resorption, as the TRAP enzyme activity is derived exclusively from osteoclasts [46]. The amount of active osteoclasts on a systemic level is indicated by serum TRAP-activity. Initially, serum TRAP-activity is expected to rise after OVX surgery, because bone resorption is

increased. However, due to the resorption the absolute number of osteoclasts is significantly decreased, consequently lowering TRAP-activity in serum [46]. The additional value of serum TRAP analysis has over in vivo micro-CT, is to confirm that the osteoporotic condition is still effective locally at defect site (created 6 weeks post-ovariectomy) and even systemically after an additional implantation period of 4 weeks.

Images from ex vivo micro-CT 3D reconstructions provide information on the amount and space between trabecular bone as well as the distribution of and space between the particles. An osteoporotic condition had apparently less trabecular bone compared to healthy condition and the trabecular spacing appeared larger. Filling of the defects with Biosilicate® and Bio-Oss® showed different packing, with a loose filling for Biosilicate® and more compact filling for Bio-Oss®. Despite similar granule sizes and amounts, granule size distribution differences, apparently led to packing differences in the defects [47]. Also surface area can vary due to these granule size distribution differences. Both materials were used in the form available for clinical application for translational power.

The histological images clearly showed a gel-like layer on the Biosilicate® particles implanted in both conditions. It is well known that bioactive glasses (BG) undergo a series of reactions following implantation [47]. Release of ions (Si, Na, Ca and P) occurs immediately upon contact of BG with fluids, resulting in an increased pH [23,47,48]. Dissolution and repolymerisation of silica occur to form a silica gel on the surface. Amorphous calcium phosphate nucleates and grows onto and into the SiO_2-rich layer. With time, the CaO-P_2O_5 mineral incorporates carbonate and hydroxyl species from the ambient fluid, and hydroxycarbonate apatite (HCA) crystallizes. This layer is a necessary requirement for bone bonding to occur [17].

In the osteoporotic conditions, Bio-Oss® significantly improved bone formation. Several studies on Bio-Oss® already described the excellent in vivo performance of this bone graft material [49,50]. The in vivo results of this study demonstrate that local osteogenic effects are significantly induced by Bio-Oss® compared to empty defects. The surfaces of the Bio-Oss® granules provide a source of calcium ions, possibly facilitating bone formation around the granules [51].

For the healthy condition, both Biosilicate® and Bio-Oss® did not improve bone formation, showing the limits of using bone substitute materials in non-critical sized defect in healthy conditions. Because trabecular bone is spaced, to calculate the maximal amount of bone normally present in that area of the femur, a reference measurement could be taken from undamaged bone. This was performed earlier in the study of van de Watering et al. [52], where a femoral condyle defect was used filled with injectable calcium phosphate cement. Bone formation was calculated and comparatively evaluated to the contra lateral undamaged bone. These bone volumes were 43 ±3% and 32 ±2% at 4 weeks after ovariectomy respectively for healthy and osteoporotic bone conditions (unpublished data by van de Watering et al. 2013), using a similar strain of rats and dietary protocol as in our study. Our results show

that bone formation has not reached the optimal amount after 4 weeks, because even for the empty bone defects a lower amount of bone area was detected. To understand more about the long term results, a second and later time point is needed.

Bioactive glasses and glass-ceramics, including Biosilicate®, belong to the third generation of biomaterials that are able to stimulate bone regeneration by cell response at a molecular level [29,33,47]. Our study confirms the positive effect of Biosilicate® at a molecular level by an increased relative expression of Runx-2, ALP, OPG, OC and RANKL. However, by histomorphometry bone formation was not increased significantly compared to Bio-Oss®. These results are in line with the study of Välimäki et al. [48], who found that bioactive glass-ceramics not only promote osteoblastic functions, but also osteoclastic bone resorption and thereby enhancing bone turnover. Our study showed a significant up-regulation of osteoclastic RANKL expression by Biosilicate®, leading to a stimulation of osteoblasts enhancing bone turnover. The exact underlying mechanism of this effect remains unclear, but an enhanced bone turnover could explain why up-regulated osteogenic gene-expression does not lead to more bone formation. An additional explanation for the discrepancy between gene-expression and histomorphometric quantification is related to the osteoconductive capacity of both Biosilicate® and Bio-Oss®. The bone formation toward the centre of the defect is guided over the surface of the particulate materials, which likely masks the osteopromotive effects of Biosilicate®.

Conclusions

The present study comparatively evaluated the performance of two commercially available bone substitutes, Biosilicate® and Bio-Oss®, by measuring in vitro biological responses and in vivo experiments with rats in osteoporotic and healthy bone conditions. The main in vitro findings showed that Biosilicate® had a favourable osteopromotive effect on rat bone marrow-derived mesenchymal stem cells compared to Bio-Oss®.

While for the healthy condition, both Biosilicate® and Bio-Oss® did not improve bone formation, the in vivo performance of both materials showed improved bone regeneration in osteoporotic bone condition, particularly for Bio-Oss®. Gene-expression analysis in vivo showed that Biosilicate® increases the expression for both osteoblast and osteoclast regulating genes, while Bio-Oss® only increases expression of genes for osteoblast differentiation. Since both materials improved bone regeneration in osteoporotic conditions, these data suggest that bone defects in osteoporotic conditions can be efficiently treated with synthetic bone substitutes.

Acknowledgements

The authors thank CAPES (Coordenação de Aperfeiçoamento de Pessoal de Nível Superior) for financial support. Author 1 and Author 2 contributed equally to this work. E.D. Zanotto, O. Peitl and M.C. Crovacce are thankful to CNPq and the São Paulo funding agency Fapesp - grant# 2013/07793-6.

References

1 Urist MR, Mazet R, Jr., McLean FC. The pathogenesis and treatment of delayed union and non-union; a survey of eighty-five ununited fractures of the shaft of the tibia and one hundred control cases with similar injuries. J Bone Joint Surg Am 1954;36-A(5):931-80; passim.

2 Giannoudis PV, Einhorn TA, Marsh D. Fracture healing: the diamond concept. Injury 2007;38 Suppl 4:S3-6.

3 Van der Stok J, Van Lieshout EM, El-Massoudi Y, Van Kralingen GH, Patka P. Bone substitutes in the Netherlands - a systematic literature review. Acta Biomater 2011;7(2):739-50.

4 Dimitriou R, Mataliotakis GI, Angoules AG, Kanakaris NK, Giannoudis PV. Complications following autologous bone graft harvesting from the iliac crest and using the RIA: a systematic review. Injury 2011;42 Suppl 2:S3-15.

5 Goulet JA, Senunas LE, DeSilva GL, Greenfield ML. Autogenous iliac crest bone graft. Complications and functional assessment. Clin Orthop Relat Res 1997(339):76-81.

6 Bongio M, van den Beucken JJJP, Leeuwenburgh SCG, Jansen JA. Development of bone substitute materials: from 'biocompatible' to 'instructive'. J Mater Chem 2010;20(40):8747-59.

7 Kurien T, Pearson RG, Scammell BE. Bone graft substitutes currently available in orthopaedic practice: the evidence for their use. Bone Joint J 2013;95-B(5):583-97.

8 Carmona RH, Beato C, Lawrence A, Moritsugu K, Noonan AS, Katz SI. Bone Health and Osteoporosis: A Report of the Surgeon General. In: McGowan JA, Raisz LG, Noonan AS, Elderkin AL, editors. Bone Health and Osteoporosis: A Report of the Surgeon General. Rockville (MD): Office of the Surgeon General (US) 2004.

9 Johnell O, Kanis JA. An estimate of the worldwide prevalence and disability associated with osteoporotic fractures. Osteoporos Int 2006;17(12):1726-33.

10 Burge R, Dawson-Hughes B, Solomon DH, Wong JB, King A, Tosteson A. Incidence and economic burden of osteoporosis-related fractures in the United States, 2005-2025. J Bone Miner Res 2007;22(3):465-75.

11 Baran DT. Osteoporosis: which current treatments reduce fracture risk? Cleve Clin J Med 2000;67(10):701-3.

12 Meyer D, Stavropolous S, Diamond B, Shane E, Green PH. Osteoporosis in a north american adult population with celiac disease. Am J Gastroenterol 2001;96(1):112-9.

13 Xiao Y, Fu H, Prasadam I, Yang YC, Hollinger JO. Gene expression profiling of bone marrow stromal cells from juvenile, adult, aged and osteoporotic rats: with an emphasis on osteoporosis. Bone 2007;40(3):700-15.

14 Kubo T, Shiga T, Hashimoto J, Yoshioka M, Honjo H, Urabe M, Kitajima I, Semba I, Hirasawa Y. Osteoporosis influences the late period of fracture healing in a rat model prepared by ovariectomy and low calcium diet. J Steroid Biochem 1999;68(5-6):197-202.

15 Hollinger JO, Onikepe AO, MacKrell J, Einhorn T, Bradica G, Lynch S, Hart CE. Accelerated fracture healing in the geriatric, osteoporotic rat with recombinant human platelet-derived growth factor-BB and an injectable beta-tricalcium phosphate/collagen matrix. J Orthop Res 2008;26(1):83-90.

16 Clupper DC, Gough JE, Hall MM, Clare AG, LaCourse WC, Hench LL. In vitro bioactivity of S520 glass fibers and initial assessment of osteoblast attachment. J Biomed Mater Res A 2003;67(1):285-94.

17 Thomas MV, Puleo DA, Al-Sabbagh M. Bioactive glass three decades on. J Long Term Eff Med Implants 2005;15(6):585-97. Epub 2006/01/06.

18 Greenwald AS, Boden SD, Goldberg VM, Khan Y, Laurencin CT, Rosier RN, Implants American Academy of Orthopaedic Surgeons. The Committee on Biological. Bone-graft substitutes: facts, fictions, and applications. J Bone Joint Surg Am 2001;83-A Suppl 2 Pt 2:98-103.

19 Tapety FI, Amizuka N, Uoshima K, Nomura S, Maeda T. A histological evaluation of the involvement of Bio-Oss in osteoblastic differentiation and matrix synthesis. Clin Oral Implants Res 2004;15(3):315-24.

20 Orsini G, Scarano A, Degidi M, Caputi S, Iezzi G, Piattelli A. Histological and ultrastructural evaluation of bone around Bio-Oss particles in sinus augmentation. Oral Dis 2007;13(6):586-93.

21 Abushahba F, Renvert S, Polyzois I, Claffey N. Effect of grafting materials on osseointegration of dental implants surrounded by circumferential bone defects. An experimental study in the dog. Clin Oral Implants Res 2008;19(4):329-34.

22 Orsini G, Traini T, Scarano A, Degidi M, Perrotti V, Piccirilli M, Piattelli A. Maxillary sinus augmentation with Bio-Oss particles: a light, scanning, and transmission electron microscopy study in man. J Biomed Mater Res B Appl Biomater 2005;74(1):448-57.

23 Lu HH, Tang A, Oh SC, Spalazzi JP, Dionisio K. Compositional effects on the formation of a calcium phosphate layer and the response of osteoblast-like cells on polymer-bioactive glass composites. Biomaterials 2005;26(32):6323-34.

24 Maquet V, Boccaccini AR, Pravata L, Notingher I, Jerome R. Preparation, characterization, and in vitro degradation of bioresorbable and bioactive composites based on Bioglass-filled polylactide foams. J Biomed Mater Res A 2003;66(2):335-46.

25 Freeman CO, Brook IM, Johnson A, Hatton PV, Hill RG, Stanton KT. Crystallization modifies osteoconductivity in an apatite-mullite glass-ceramic. J Mater Sci Mater Med 2003;14(11):985-990.

26 Peitl O, Zanotto ED, Serbena FC, Hench LL. Compositional and microstructural design of highly bioactive P2O5-Na2O-CaO-SiO2 glass-ceramics. Acta Biomater 2012;8(1):321-32.

27 Vogel M, Voigt C, Knabe C, Radlanski RJ, Gross UM, Muller-Mai CM. Development of multinuclear giant cells during the degradation of Bioglass particles in rabbits. J Biomed Mater Res A 2004;70(3):370-9.

28 Hench LL. The story of Bioglass. J Mater Sci Mater Med. 2006;17(11):967-78.

29 Hench LL, Polak JM. Third-generation biomedical materials. Science 2002;295(5557):1014-7.

30 Granito RN, et al. In vivo biological performance of a novel highly bioactive glass-ceramic (Biosilicate(R)): A biomechanical and histomorphometric study in rat tibial defects. J Biomed Mater Res B Appl Biomater 2011;97(1):139-47.

31 Granito RN, Ribeiro DA, Renno AC, Ravagnani C, Bossini PS, Peitl-Filho O, Zanotto ED, Parizotto NA, Oishi J. Effects of biosilicate and bioglass 45S5 on tibial bone consolidation on rats: a biomechanical and a histological study. J Mater Sci Mater Med 2009;20(12):2521-6.

32 Bossini PS, Renno AC, Ribeiro DA, Fangel R, Peitl O, Zanotto ED, Parizotto NA. Biosilicate(R) and low-level laser therapy improve bone repair in osteoporotic rats. J Tissue Eng Regen Med 2011;5(3):229-37.

33 Xynos ID, Edgar AJ, Buttery LD, Hench LL, Polak JM. Gene-expression profiling of human osteoblasts following treatment with the ionic products of Bioglass 45S5 dissolution. J Biomed Mater Res 2001;55(2):151-7.

34 Alghamdi HS, van den Beucken JJ, Jansen JA. Osteoporotic rat models for evaluation of osseointegration of bone implants. Tissue Eng Part C Methods 2014;20(6):493-505.

35 Zanotto ED, Ravagnani C, Peitl O, Panzeri H, Lara EHG. Process and compositions for preparing particulate, bioactive or resorbable biosilicates for use in the treatment of oral ailments. Universidade Federal de São Carlos, Universidade de São Paulo. Patent Application No. Int. C. C03C10/00, WO 2004/074199, 2004

36 Wallace KE, Hill RG, Pembroke JT, Brown CJ, Hatton PV. Influence of sodium oxide content on bioactive glass properties. J Mater Sci Mater Med 1999;10(12):697-701.

37 Ozawa S, Kasugai S. Evaluation of implant materials (hydroxyapatite, glass-ceramics, titanium) in rat bone marrow stromal cell culture. Biomaterials 1996;17(1):23-9.

38 Renno AC, McDonnell PA, Crovace MC, Zanotto ED, Laakso L. Effect of 830 nm laser phototherapy on osteoblasts grown in vitro on Biosilicate scaffolds. Photomed Laser Surg 2010;28(1):131-3.

39 Herten M, Rothamel D, Schwarz F, Friesen K, Koegler G, Becker J. Surface- and nonsurface-dependent in vitro effects of bone substitutes on cell viability. Clin Oral Investig 2009;13(2):149-55.

40 Sollazzo V, Palmieri A, Scapoli L, Martinelli M, Girardi A, Alviano F, Pellati A, Perrotti V, Carinci F. Bio-Oss(R) acts on Stem cells derived from Peripheral Blood. Oman Med J 2010;25(1):26-31.

41 Jee WS, Yao W. Overview: animal models of osteopenia and osteoporosis. J Musculoskelet Neuronal Interact 2001;1(3):193-207.

42 Turner RT, Maran A, Lotinun S, Hefferan T, Evans GL, Zhang M, Sibonga JD. Animal models for osteoporosis. Rev Endocr Metab Disord 2001;2(1):117-27.

43 Thompson DD, Simmons HA, Pirie CM, Ke HZ. FDA Guidelines and animal models for osteoporosis. Bone 1995;17(4 Suppl):125S-33S.

44 Francisco JI, Yu Y, Oliver RA, Walsh WR. Relationship between age, skeletal site, and time post-ovariectomy on bone mineral and trabecular microarchitecture in rats. J Orthop Res 2011;29(2):189-96.

45 El Khassawna T, et al. Effects of multi-deficiencies-diet on bone parameters of peripheral bone in ovariectomized mature rat. PloS One 2013;8(8):e71665.

46 Rissanen JP, Suominen MI, Peng Z, Halleen JM. Secreted tartrate-resistant acid phosphatase 5b is a Marker of osteoclast number in human osteoclast cultures and the rat ovariectomy model. Calcif Tissue Int 2008;82(2):108-15.

47 Jones JR. Review of bioactive glass: from Hench to hybrids. Acta Biomater 2013;9(1):4457-86.

48 Valimaki VV, Yrjans JJ, Vuorio EI, Aro HT. Molecular biological evaluation of bioactive glass microspheres and adjunct bone morphogenetic protein 2 gene transfer in the enhancement of new bone formation. Tissue Eng 2005;11(3-4):387-94.

49 Chaves MD, de Souza Nunes LS, de Oliveira RV, Holgado LA, Filho HN, Matsumoto MA, Ribeiro DA. Bovine hydroxyapatite (Bio-Oss((R))) induces osteocalcin, RANK-L and osteoprotegerin expression in sinus lift of rabbits. J Craniomaxillofac Surg 2012;40(8):e315-20.

50 Wong RW, Rabie AB. Effect of bio-oss collagen and collagen matrix on bone formation. Open Biomed Eng J 2010;4:71-6.

51 Desterro Fde P, Sader MS, Soares GD, Vidigal GM, Jr. Can inorganic bovine bone grafts present distinct properties? Braz Dent J 2014;25(4):282-8.

52 van de Watering FC, Laverman P, Cuijpers VM, Gotthardt M, Bronkhorst EM, Boerman OC, Jansen JA, van den Beucken JJJP. The biological performance of injectable calcium phosphate/PLGA cement in osteoporotic rats. Biomed Mat 2013;8(3):035012.

3

CHAPTER 3

The performance of CPC/ PLGA and Bio-Oss® for bone regeneration in healthy and osteoporotic rats

van Houdt CIA, Ulrich DJO, Jansen JA, van den Beucken JJJP.

J Biomed Mater Res B Appl Biomater. 2018 Jan;106(1):131-142.

Introduction

An estimated number of >500,000 bone grafting procedures are performed annually in the United States and this number easily doubles on a global basis [1]. Autologous bone grafting still is the gold standard despite of the disadvantages, such as shortage in the availability of donor tissue, donor site morbidity, and increased surgery and recovery time. Allografts and xenografts can be used as a substitute for autologous grafts, but have the disadvantage of immunological issues and an increased risk of cross-species transmission of viral contaminants [1]. Alternatively, synthetic bone grafts have an increasing interest to overcome these disadvantages and worldwide endeavors are made to develop safe and reliable synthetic bone grafts [2, 3].

In view of the increasing number of osteoporotic patients encountered in the clinics [4] and the limitations in quantity and quality of autologous bone transplants in these patients [4], the question to what extent an osteoporotic bone condition affects the biological performance of bone grafts is important from a clinical perspective. It has already been reported that patients with osteoporosis present an impaired healing process of the bone wound [5]. Osteoporosis is characterized by reduced bone mineral density causing lower bone mass and deterioration of bone tissue micro-architecture. This results from an imbalance in the continuous bone remodeling process, involving bone formation and resorption, and an altered variety of proteins in the bone [4]. Osteoporosis is primarily observed after menopause in women, or by age in both women and men (ratio of 2:1), or secondarily by chronic predisposing medical problems. The number of elderly people is expected to significantly increase over the next 50 years as will the sex ratio of the older population, increasing the number of elderly women. As osteoporosis is related to age and is more prominent in women, this will result in bone grafting in osteoporotic patients being an even greater challenge in the future, which hence causes a major challenge for healthcare professionals.

In view of the aforementioned, patients with bone defects suffering from osteoporosis could greatly benefit from synthetic bone grafts. Several 'off-the-shelf' synthetic bone substitutes are available for clinical bone regenerative treatments nowadays and worldwide research is done to enhance the properties of synthetic bone substitutes. For dental applications, Bio-Oss® [6-9] is the mostly used commercially available bone substitute, consisting of devitalized bovine bone [8]. Alternatively, calcium phosphate (CaP) based materials are synthetic inorganic biomaterials that show high similarity to bone tissue by resembling the mineral phase of bone and are already popular implant materials in several fields of surgery [10-17]. Among the CaPs, CaP cement (CPC) is injectable and hence can be molded to perfectly fit within any irregularly-shaped bone defect [18]. The main disadvantage of CPC is its low degradation rate mainly due to the inadequate intrinsic porosity of the material. By adding poly(lactic-co-glycolic acid) (PLGA) particles to CPC, a composite system (CPC/PLGA) has been obtained that allows for controlled CPC degradation [19] as well as the possibility of controlled release of bioactive agents, e.g. osteoinductive growth factors [19].

For the evaluation of the performance of bone substitute materials in osteoporotic conditions, several pre-clinical animal models are available [20-22]. Osteoporotic conditions can be induced by either a chemical stimulation, for example by the administration of prednisolone [23] or via ovariectomy or orchidectomy in respectively female and male animals [20, 21]. The removal of the ovaries or testis induces a decline in estrogen or androgen levels, respectively, which leads to a rapid loss of cancellous bone mass and strength [20, 21]. The most conventional osteoporotic animal model is the ovariectomized (OVX) rat, which mimics the bone changes in humans following menopause or oöphorectomy [20, 21, 24]. Bone loss occurs first in trabecular bone, after which cortical bone is affected [20, 21, 24]. Furthermore, the degree of bone loss at various trabecular bone sites occurs in different time lapses after OVX surgery [20, 21, 24]. Consequently, studying the performance of bone substitute materials in OVX rats requires adequate selection of timing and location.

The present study comparatively evaluated the biological performance of CPC/PLGA and the dental predicate device Bio-Oss® in ovariectomized and healthy rats. We hypothesized that osteoporotic conditions would affect the biological performance of both bone substitute materials. Additionally, we hypothesized that the differences in degradation rate between CPC/PLGA and Bio-Oss® would lead to different bone forming capacity. The assessments were performed by histology, histomorphometry and micro-CT after implantation periods of 4 and 12 weeks in rat femoral condyle bone defects.

Materials and Methods

Materials

The chemical composition of CPC/PLGA consisted of 70 wt% milled, pure alpha tri-calcium phosphate (α-TCP) powder with a mean particle size of ~4.0 µm (CAM Bioceramics BV, Leiden, The Netherlands) and 30 wt% PLGA powder with a mean particle size of ~60 µm, containing both a lactic and glycolic weight percentage of 50% (manufactured at Corbion Purac®, Amsterdam, The Netherlands, and provided at the given particle size by CAM Bioceramics BV) and 0,5% carboxymethylcellulose (CMC) with a mean particle size ~106 µm (CAM Bioceramics BV). An aqueous solution of 4 wt% sodium dihydrogen phosphate dihydrate ($NaH_2PO_4 \cdot 2H_2O$) was used as liquid component to create the cement paste and was made by dissolving 4.0 g of $NaH_2PO_4 \cdot 2H_2O$ in 100 ml Milli-Q water. Bio-Oss® (Geistlich Pharma AG, Wolhusen, Switzerland) in the form of small granules of 0.25-1 mm was used as a dental predicate device after consultation of the Food and Drug Administration (FDA).

Preparation of CPC/PLGA scaffolds

To the CPC/PLGA powder fraction, a liquid solution was applied of $NaH_2PO_4 \cdot 2H_2O$ dissolved in sterile distilled water, with a ratio of 750 µl solution per 1.5 g powder. Then, CPC/PLGA was manually mixed with a spatula and applied into a Teflon mold containing cylindrical holes (2.5 mm in diameter and 5 mm in height). After setting for 24 h at room temperature, CPC/PLGA scaffolds were removed from the mold and sterilized by gamma radiation at a maximum of 50 kGy (SynergyHealth Ede B.V., Ede, Netherlands).

Animals

For this experiment, thirty-two healthy mature female Wistar rats were used at 3 months of age with an average weight of ~200 g. Animals were allowed to acclimatize for 7 days and housing was provided per pair in a standard macrolon type 3 cage, with sawdust as bedding material. In order to induce an osteoporotic condition, the rats were subjected to bilateral ovariectomy (OVX) or sham operation (SHAM). All rats received two surgical procedures during the course of the experiment, i.e. either OVX or SHAM surgery and bone defect surgery. Standard rodent chow and bottled tap water was provided ad libitum, except for the OVX group, which received a low calcium diet with pellets containing 0.01% calcium and 0.77% phosphorous (Ssniff Spezialdiäten GmbH, Soest, Germany). The housing room was maintained under standard laboratory conditions (light-dark cycle: 12:12h, temperature: 20-22°C, relative humidity: 45-55%). All experiments were conducted in accordance with institutional, national and international guidelines for animal care and the Dutch law concerning animal welfare. The studies were reviewed and approved by the Experimental Animal Committee of the Radboud University (RUDEC 2013-047).

Methods

Surgical procedure to induce osteoporotic conditions

Sixteen randomly assigned animals received OVX surgery through two separate incisions in the lateral abdominal wall. The remaining sixteen rats received a SHAM surgery. The surgical approach was the same as for the OVX animals, exposing both ovaries but these were not removed.

Anesthesia was induced and maintained by Isoflurane inhalation (Rhodia Organique Fine Limited) combined with oxygen delivered by mask. Pre-operatively pain medication was provided by an injection of Carprofen (Rimadyl®, Pfizer Animal Health, New York, USA) in dosage of 5 mg/kg, given 15min before surgery.

After confirmation of effective anesthesia, the animal was placed on an electric heating blanket in prone position exposing the dorsal part of the lumbar region. The area was shaved with electric clippers and disinfection was performed by application of a povidone iodine solution. To enter the abdominal cavity a dorsal midline incision was created caudal to the posterior border of the ribs. The incision was approximately 2 cm in length at the midpoint between the costal inferior border and the iliac crest, and a few millimeters lateral to the lateral margin of the lumbar muscle. Using blunt dissection, the muscles of the posterior abdominal wall were separated. The ovary was located in a fat pad just beneath the muscles and exteriorized by gentle retraction using forceps. Then using a mosquito forceps, the fallopian tube was clamped and a single ligature was performed using a surgical polyester suture (Terylene® 2.0 undyed, Serag-Wiessner GmbH & Co, Naila, Germany). The ovary was disconnected by cutting above the clamped area and the tuba including surrounding fat was returned into the abdomen. After checking for hemostasis, the abdominal wall (peritoneum and muscle layers) was closed with continuous absorbable sutures (Vicryl® 3.0, Ethicon, Amersfoort, The Netherlands) after which the skin was stapled by metal wound clips (Agraven®, InstruVet Bv, Cuijk, The Netherlands). The procedure was repeated for the opposite ovary using the same incision design. The SHAM group received the same surgical procedure except for the clamping and removal of the ovaries. For a minimum duration of 2 days postoperatively, Carprofen was given every 24h. Additionally, to diminish postoperative pain, Buprenorfine (Temgesic®, Reckitt Benckiser Health Care Limited, Schering-Plough, UK) was given every 12h in a dosage of 0.02 mg/kg.

Validation of osteoporotic bone condition

Of six animals (3 OVX and 3 SHAM), in vivo CT images of both femoral condyles were acquired 6 weeks after the first surgery, using an animal micro-CT scanner (Inveon, Siemens Preclinical Solutions, Knoxville, TN, USA). To acquire CT images, anesthesia was induced and maintained by isoflurane inhalation (Rhodia Organique Fine Limited, Avonmouth, Bristol, UK). The animals were placed in supine position in the scanner with the legs fixed with tape in order for optimal acquirement of the micro-CT images (spatial resolution 30 µm,

80 kV, 500 µA, exposure time 1000 ms). Projected files were then reconstructed using a cone beam algorithm. The bone architecture was analyzed using image analysis software (Inveon Research Workplace 2.0, Siemens Medical Solutions USA Inc., Knoxville, USA). From reconstructed CT scans, 3D models were built for visualization and morphometric analysis. For the morphometric analysis, a region of the femoral condyle was selected, which included the metaphysal bone of the femoral condyle head starting at the growth plate (without cortical bone layer) until 300 micro-tomographic slices more proximal. By auto-interpolation of the layers, a volume of interest (VOI) was obtained. Within this VOI, the amount of trabecular bone and bone marrow were determined on basis of the density in Houndsfield units. Thereafter, bone morphometric parameters (bone volume, trabecular spacing, and trabecular thickness) were calculated using the Inveon Research Workplace Bone Morphometry tool (Siemens Medical Solutions USA Inc.).

Surgical procedure to create and fill femoral bone defects

Six weeks after OVX or SHAM surgery, and after confirmation of significantly altered bone morphometric parameters (via *in vivo* CT; see previous section "Validation of osteoporotic bone condition"), a defect was created in both femoral condyles of each animal. Alternating the left and right femur, the materials CPC/PLGA and Bio-Oss® were used to fill the defects. Anesthesia and pain medication were administered similarly as described for the first surgical procedure (see section "Surgical procedure leading to osteoporotic conditions").

Before starting the operation of creating the femoral defect, both hind limbs of the rats were shaved and disinfected with povidone iodine. The rats were immobilized in supine position and with the knee maximally flexed a longitudinal incision through skin and muscle was made on the medial surface. After exposure of the medial side of the distal femoral condyle the knee capsule was incised. Then, the knee was extended to luxate the patella laterally. When a clear view of the knee joint was established, a bone defect (Ø 2.5 mm, depth 5 mm) was created longitudinal to the axis of the femur, using a dental drill (Elcomed 9927 SPS; W&H Dentalwerk Burmoos GmbH, Burmoos, Austria). A series of increasing bur diameters (1.5–2.0–2.3–2.5 mm) were used at a speed of maximum 5000 rpm and a constant cooling by dripping saline. The drilled cavity was then washed with saline and dried using sterile gauze.

Subsequently, the materials were alternatingly placed into the defect. Firstly, the small Bio-Oss® granules (0.25 - 1mm in diameter) were manually mixed with a drop of saline using a spatula and inserted. For the CPC/PLGA, preset cylinders were used (see section "Preparation of CPC/PLGA cylinders"). After introducing the materials into the defects, the muscular tissue layer was closed with absorbable sutures (Vicryl® 4.0, Ethicon, Amersfoort, The Netherlands) after which the skin was closed by small staples (Agraven®; InstruVet BV, Cuijk, The Netherlands).

After implant surgery, both experimental groups (OVX and SHAM) had free access to normal pellet food and water. In the initial postoperative period, the intake of water and food was

monitored as well as the weight of the animals. In addition, the animals were observed for signs of pain, infection and proper activity and weighed again postoperatively once a week to identify significant weight loss (>20%) compared to preoperative body weight of each rat.

Fluorochrome labeling for bone dynamics

The rats in the 12 week groups received a series of four fluorochromes by subcutaneous injection, with a 2-week interval, starting two weeks after implantation surgery. Calcein blue (product no. M1255, dose 30mg/kg; week 2), calcein green (C0875, 10mg/kg; week 4), alizarine complexone (A3882, 25mg/kg; week 6) and rolitetracycline (R2253, 25mg/kg; week 8) were consecutively used. All fluorochromes were obtained from SigmaAldrich (Munich, Germany). Before injection, the solutions were set to a pH between 7.2-7.4, then filtered through a 0.22 sterile millipore filter, and finally checked for fluorescence.

Specimen retrieval

After both implantation periods of 4 and 12 weeks, the animals were euthanized by suffocation with CO_2. The femurs including the implanted materials were harvested, stripped from soft tissues and immediately fixed in 10% formalin solution. Using a diamond saw, the specimens were cut smaller to become suitable for ex vivo micro-CT scanning and histological processing. After fixation, specimens were stored in 70% ethanol.

Micro-CT

A desktop X-ray micro-CT system was used (Skyscan-1072, TomoNT version 3N.5, Skyscan®, Kontich, Belgium) for 3D imaging. The specimens were placed onto the sample holder with the long axis of the femur perpendicular to the scanning beam. 3D reconstruction and imaging processing was performed using NRecon V1.4 and CTvox v2.7 (Skyscan®, Kontich, Belgium), respectively.

Histological processing

After performing micro-CT scanning, the specimens were dehydrated in a graded series of ethanol (70% - 100%), after which they were embedded in polymethylmethacrylate (pMMA). After polymerization, thin sections of 10µm were prepared in a cross-sectional direction perpendicular on the longitudinal direction of the defect using a diamond blade microtome (Leica Microsystems SP 1600, Nussloch, Germany). The first section of each specimen was aimed at the center of the defect or slightly more proximal on the femur and continued distally. Then, three sections of each specimen were stained with methylene blue and basic fuchsine. For the 12-week group, first 3 sections were made and left unstained for fluorescence analysis and immediately stored in the dark.

One specimen of each experimental group was decalcified in ethylenedinitrilotetraacetic acid (EDTA; Merck KGaA, Darmstadt, Germany), dehydrated through a series of graded ethanol and embedded in paraffin. Using a microtome (Leica RM 2165, Leica Microsystems, Nussloch, Germany) 6µm thick sections were prepared. The sections were stained with hematoxylin-

eosin (HE) to verify bone tissue within the defect area. In addition, tartrate-resistant acid phosphatase (TRAP) staining was applied to determine osteoclastic activity.

Descriptive histology and histomorphometrical analysis

At both implantation periods of 4 and 12 weeks, the pMMA and paraffin histological sections (3 sections per specimen) were examined by light microscopy (Leica Microsystems AG, Wetzlar, Germany). Using different filters on the light microscope, pictures could be made of the fluorescent labels at the four different time points. Quantitative assessment of the pMMA specimens was performed using ImageJ computer-based image analysis software (Java® ImageJ 1.47, Image processing and analysis in Java) [25]. From digitalized images of the sections (magnification: 5x), a circular region of interest (ROI) with a diameter equal to the created defects was positioned. Within this ROI, the amount of newly formed bone and material remnants were measured using color discrimination and morphology for verification. The baseline values (zero time point) for material area within this ROI were determined as described previously[26] or theoretically set at 100% (CPC/PLGA).

Statistical analysis

Data are presented as mean with SD. Statistical analysis of quantitative data was performed using one-way analysis of variance (ANOVA) with a Tukey post-hoc test for comparison between the three different time points. GraphPad Software (PRISM; La Jolla CA, USA) was used to carry out the statistical analysis. For a comparison between both conditions at selected time points and for the analysis of the ***in vivo*** micro CT analysis, Student's t-tests were used. Values of $p<0.05$ were considered statistically significant.

Results

Animals

Of the thirty-two animals, two animals were excluded from the experiment. One animal (assigned to OVX 4 weeks) died due to a respiratory depression near the end of the bone defect surgery. A second animal had an opened wound on the left leg two days after implantation surgery, for which antibiotics and further pain medication was provided. Initially, this rat seemed to recover well, but on the fourth postoperative day, the animal was limping. At this point, it was decided that the animal (assigned to SHAM 12 weeks) had reached the humane endpoint and was euthanized. After examining the leg post-mortem, no signs of infection or active bleeding were observed but the femur shaft was fractured (data not shown).

The thirty remaining animals remained in good health during the entire experimental period. One week after subcutaneous injection of the fourth fluorochrome (Rolitetracycline), nine animals showed a skin reaction by hair loss and crust formation. This did not seem to hinder the animals and the skin healed for all animals within two weeks. At sacrifice, no signs of inflammation or adverse tissue reaction were seen in the wound areas.

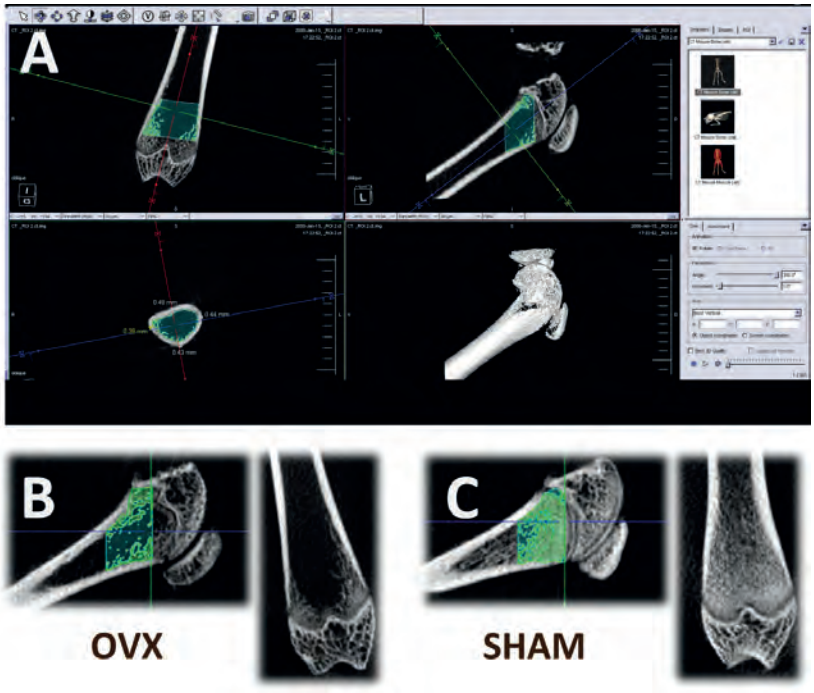

Figure 1 A-C: [A] Screenshot of in vivo micro CT analysis program of trabecular bone in osteoporotic and healthy animals. Representative in vivo CT image of **[B]** osteoporotic and **[C]** healthy rat femur.

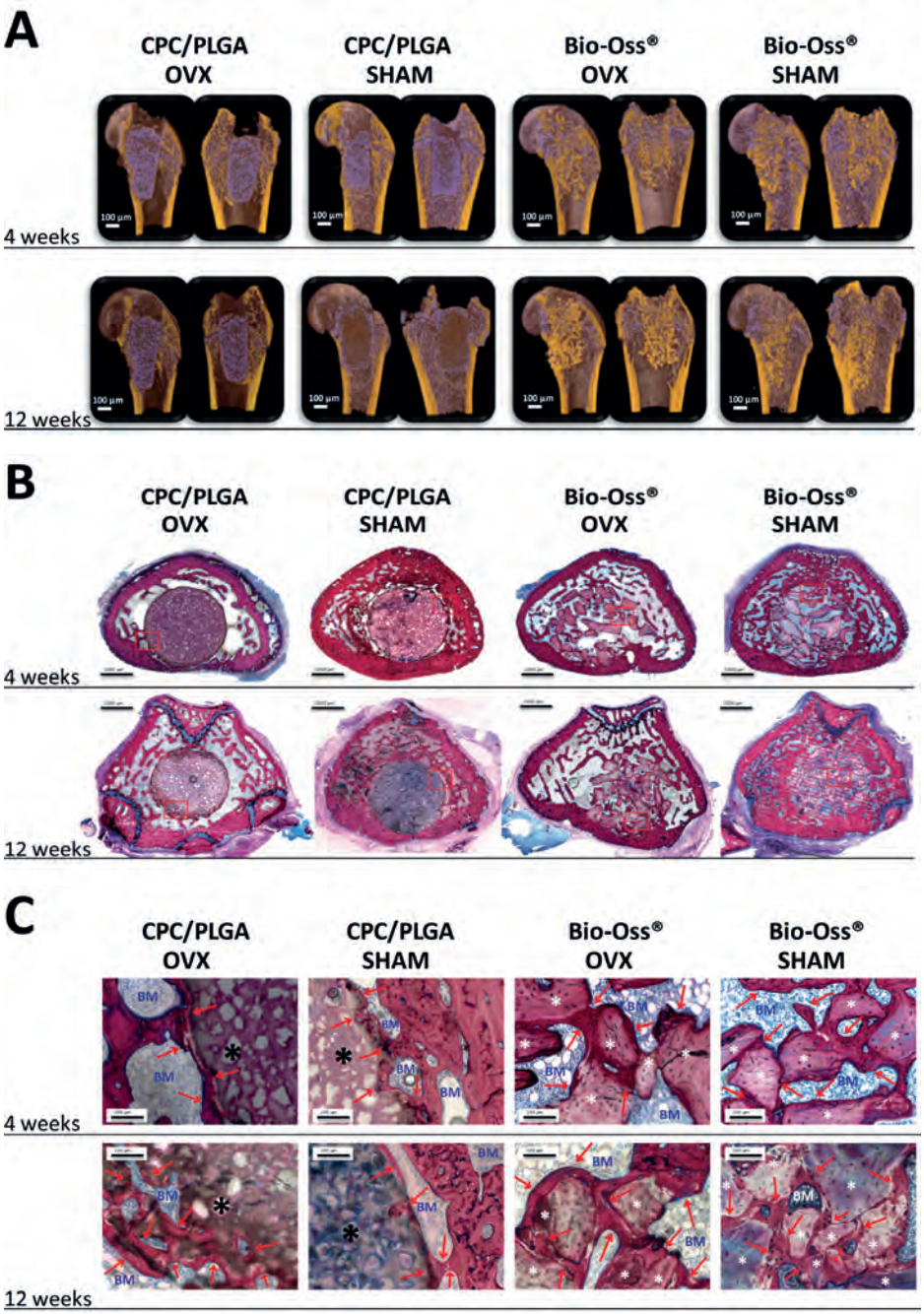

Figure 2A-C: [A] Representative micro CT images of each experimental group. Representative histological images of pMMA sections for each experimental group with images at **[B]** 4 weeks and 12 weeks and **[C]** corresponding images at 20x magnification; methylene blue and basic fuchsine staining; red arrows] new bone (pink color); *] CPC/PLGA (black*) or Bio-Oss® (white*); BM] bone marrow (blue color).

Confirmation of the osteoporotic bone condition by in vivo micro-CT

Six weeks after OVX or SHAM surgery, three of the OVX rats and three of the SHAM rats underwent *in vivo* micro-CT (**Figure 1A-C**). The bone morphometric data deduced from CT images are shown in **Table 1**, which revealed that OVX surgery significantly reduced trabecular bone volume and disorganized trabecular architecture in the femoral condyle compared to SHAM surgery. These alterations in bone morphology were further confirmed by significant effects on quantitative parameters ($p<0.01$), shown by lower trabecular bone volume, trabecular thickness and number, and higher trabecular separation for OVX compared to SHAM.

Micro-CT analysis

Reconstructed 3D micro-CT images were sliced to obtain an internal view of the bone defects. An overview with sagittal, frontal and transversal slices through the defect region for each experimental group is presented in **Figure 2A**. Color settings were adjusted to distinguish between different densities of bone and material, coloring bone yellow. The slices showed lower amounts of trabecular bone for osteoporotic rats with apparently larger spacing between the trabeculae compared to healthy rats. Further, the bone substitute materials showed clear differences in appearance, with CPC/PLGA present as a mass within the created femoral condyle bone defect and Bio-Oss® as dispersed particulate material. Color differences between both bone substitute materials showed higher radio density for Bio-Oss® particles (yellow color) compared to CPC/PLGA (purple color).

Descriptive histological evaluation of pMMA and paraffin sections

Representative images of the histological sections of specimens embedded in pMMA are depicted in **Figure 2B**. In general, histology of the pMMA-sections showed higher trabecular number and denser spacing for SHAM compared to OVX bone condition. Descriptive histology confirmed that Bio-Oss® granules presented as a more dispersed material, allowing more space within the defect area, compared to the more dense filled defects by CPC/PLGA, at both 4 and 12 weeks. New bone formation was observed at both 4 and 12 weeks for Bio-Oss®, and at 12 weeks for CPC/PLGA in both OVX and SHAM rats.

Table 1: Quantitative bone morphometric data using in vivo micro-CT (mean ±SD) for trabecular bone in distal femurs of rats 6 weeks following OVX and SHAM operations, **] Student's t-test showed significant difference between columns ($p<0.01$).

	OVX		SHAM	
Bone volume fraction %	28.2	*± 4.2*	71.8	*± 2.5***
Trabecular thickness (Tb.Th) µm	0.1	*± 0.01*	0.2	*± 0.01***
Trabecular number (Tb.N) mm^{-1}	3.1	*± 0.4*	4.2	*± 0.2***
Trabecular separation (Tb.Sp) µm	0.2	*± 0.01*	0.1	*± 0.01***

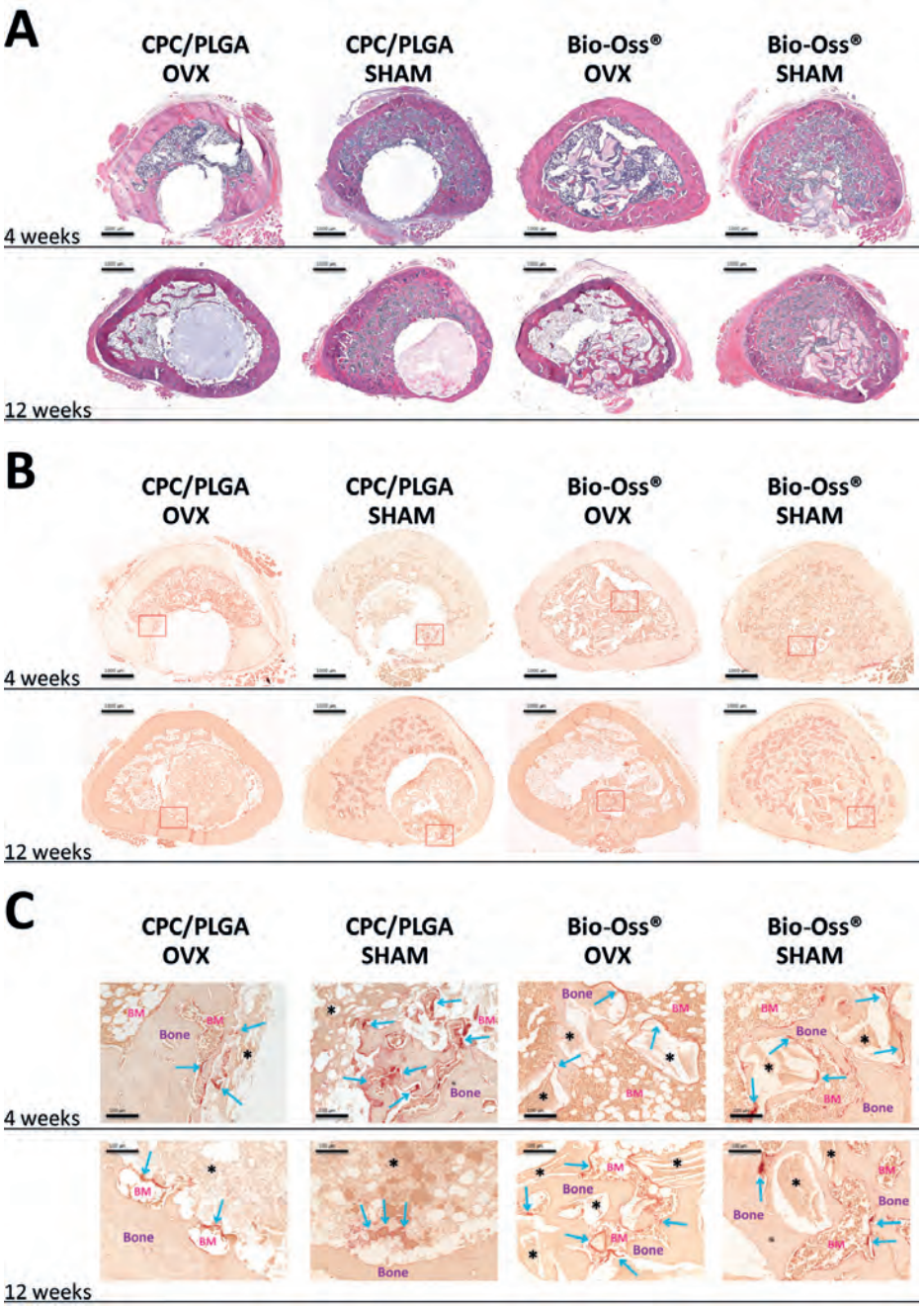

Figure 3A-C: Representative images of **[A]** HE stained paraffin section images of each experimental group, **[B]** TRAP stained paraffin sections with **[C]** detailed images at 20x magnification for each corresponding experimental group; Bone] bone; BM] bone marrow; *] materials CPC/PLGA or Bio-Oss®; blue arrows] TRAP staining red colored.

Images at 20x magnification (**Figure 2C**) showed new bone formation that was in direct contact with the implanted material, i.e. CPC/PLGA or Bio-Oss®. For CPC/PLGA, newly formed bone was mainly formed at the peripheral edge of the material and where degradation had occurred. Almost no bone formation was seen in the center of the material, except for one OVX specimen after 4 weeks and three specimens after 12 weeks. For Bio-Oss®, the granules were surrounded by newly formed bone and bridging was observed by newly formed bone between Bio-Oss® granules. At 12 weeks, the Bio-Oss® granules seemed to be completely covered by newly formed bone. Areas within the ROI where neither bone nor material was present, were filled with bone marrow. Material degradation became apparent at 12 weeks for CPC/PLGA, showing marginal degradation predominantly on the peripheral edge of the material. At 4 weeks CPC/PLGA did not show clear degradation and PLGA seemed still

present within most pores. After 12 weeks, PLGA was dissolved and bone marrow was able to penetrate the cement and fill the pores, including the center. Still, only few specimens (all OVX) contained slides showing gross degradation of CPC/PLGA that could reach to the center of the defect (data not shown).

HE-stained paraffin sections (**Figure 3A**) showed in general similar observations as described for pMMA sections. The sections showed an increased bone formation into the defect for SHAM animals compared to OVX when using Bio-Oss® at both time points. For the defects filled with CPC/PLGA, bone formation was seen mainly at the edges of the original defect.

Paraffin sections stained with TRAP (**Figure B-C**) showed low osteoclastic activity for OVX, irrespective of bone substitute material used. For SHAM, more activity was observed mostly where bone made contact with the surface of the bone substitute materials.

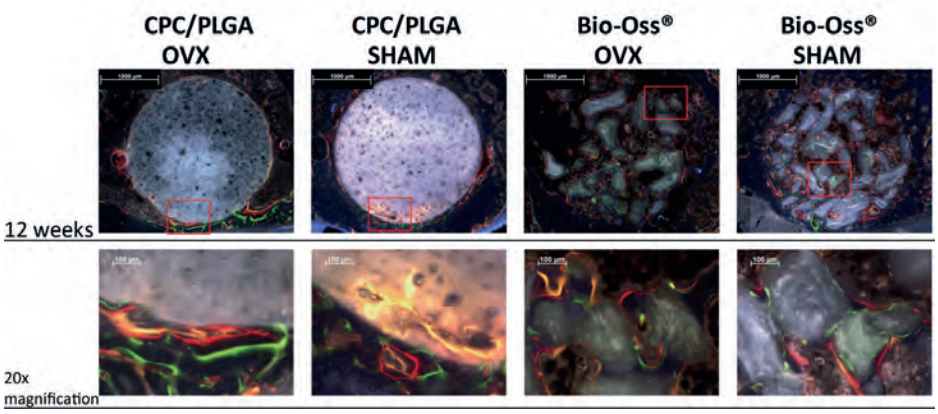

Figure 4: Representative fluorochrome microscopy images at 12 weeks for both OVX and SHAM using both CPC/PLGA and Bio-Oss® with 20x magnification images; red box] area of 20x magnification; green color] calcein green (week 4); red color] alizarine complexone (week 6); yellow color] rolitetracycline (week 8).

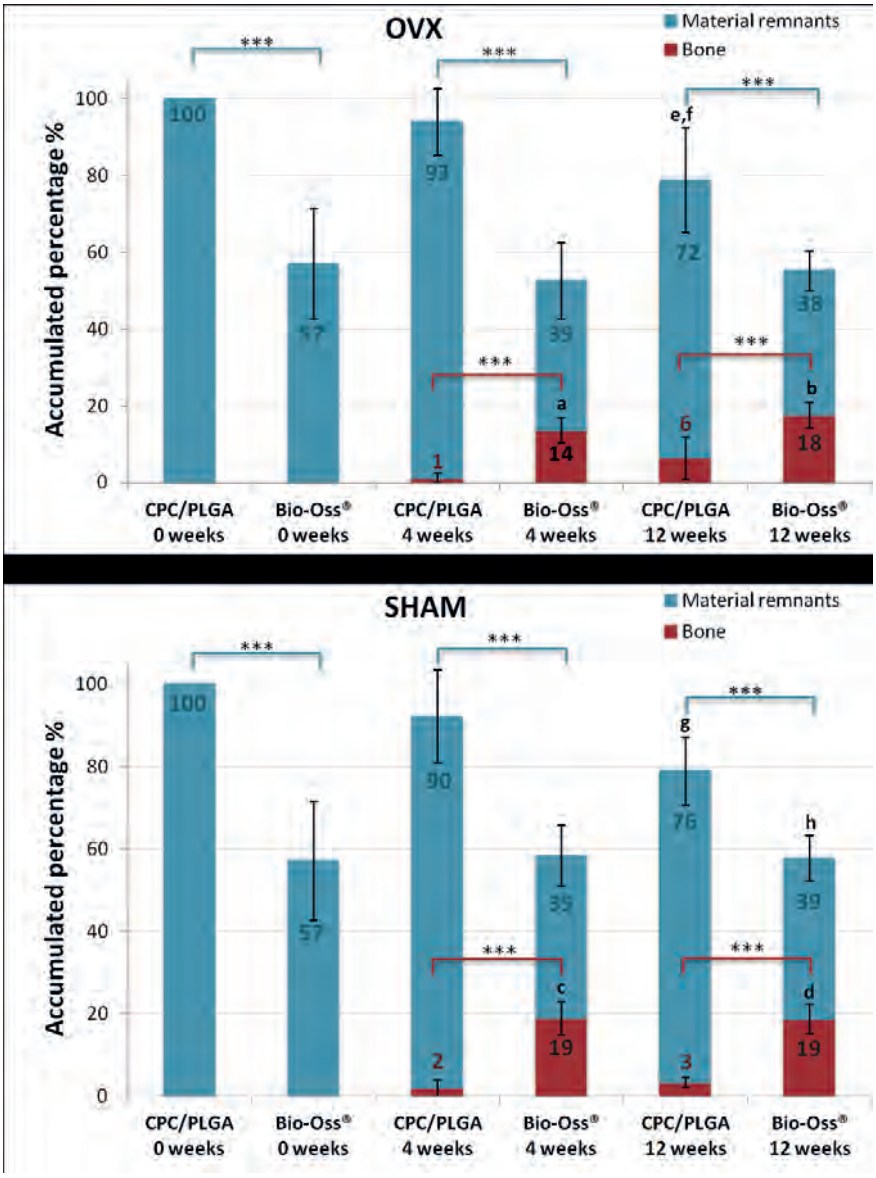

Figure 5: Accumulated area percentages (mean ±SD) of new bone formation (red bars) and material remnants (blue bars) within ROI at 0, 4 and 12 weeks after implantation (numbers in bars indicate percentages, blue for material, red for bone); ANOVA showed significant difference for both bone formation and material remnants between CPC/PLGA and Bio-Oss® of similar time point and condition, *] p<0.05, ***] p<0.001; [a]] significant increase (ANOVA, p<0.001) in bone volume compared to 0 time point for Bio-Oss® in OVX after 4 weeks and [b]] 12 weeks and [c]] in SHAM after 4 weeks and [d]] 12 weeks; significant decrease in material remnants for CPC/PLGA in [e]] OVX between 0 and 12 weeks (ANOVA, p<0.005), [f]] between 4 and 12 weeks (ANOVA, p<0.05) and [g]] in SHAM between 0 and 12 weeks (ANOVA, p<0.05) and for Bio-Oss® only in [h]] OVX between 0 to 12 weeks (ANOVA, p<0.05).

Bone dynamics by fluorochrome labeling

Incorporation of fluorochrome labels into newly formed bone (**Figure 4**) was observed for calcein green (green; week 4), alizarine complexone (red; week 6) and rolitetracycline (yellow; week 8). However, none of the sections showed calcein blue (blue; week 2).

Bone dynamics by fluorescent microscopy showed that bone was formed in the center of the defect for defects filled with Bio-Oss®, for both osteoporotic and healthy conditions, at 4, 6 and 8 weeks. For CPC/PLGA, these fluorochrome labels were observed at the defect edge (i.e. interface between bone and bone substitute material). For the CPC/PLGA three sections in OVX group the center of the defect was reached by all three colors and in one section of the SHAM group.

For OVX incorporation of all three colors was homogeneous containing Bio-Oss®, whereas CPC/PLGA showed more yellow incorporation, followed by red and then green. For the SHAM animals the incorporation of fluorochrome calcein green was the most abundant in both Bio-Oss® and CPC/PLGA, followed by yellow and then red for Bio-Oss® and followed by yellow and red equally in CPC/PLGA.

Histomorphometrical analysis

For histomorphometrical analysis, the baseline material area within the region of interest (zero-time point) was (theoretically) set at 100% for CPC/PLGA and (experimentally) determined to be 57.0 ± ***14.3***% for Bio-Oss®. Histomorphometry in OVX rats after 4 weeks showed material areas within the ROI of 92.7 ± ***8.6***% for CPC/PLGA and 38.9 ± ***10.0***% for Bio-Oss®. After 12 weeks, materials areas within the ROI were 72.4 ± ***13.6***% for CPC/PLGA and 37.7 ± ***5.2***% for Bio-Oss®. In SHAM rats, material areas within the ROI after 4 weeks were 90.3 ± ***11.2***% for CPC/PLGA and 39.5 ± ***7.4***% Bio-Oss® and after 12 weeks 75.6± ***8.2***% and 39.1 ± 5.5%, respectively. Statistical analysis showed material remnants were significantly lower for Bio-Oss® compared to CPC/PLGA at all time points and in both conditions (ANOVA, all $p<0.001$; **Figure 5**). There were no significant differences between both conditions at each time point for each material (Students t-test, $p>0.05$).

Temporal material degradation has been depicted separately in a graph for both CPC/PLGA and Bio-Oss® (**Figure 6**). In order to better illustrate the differences between the materials, data for Bio-Oss® was to set to 100% and therefore Figure 6 is showing relative percentages. Material remnants decreased significantly over a time period from 0 to 12 weeks for CPC/PLGA in both conditions (ANOVA, $p<0.01$ in OVX and $p<0.05$ in SHAM; Figure 5 & 6) and only in OVX for Bio-Oss® (ANOVA, $p<0.05$). Only CPC/PLGA in OVX showed a significant temporal decrease of materials remnants from 4 to 12 weeks (ANOVA, $p<0.05$). None of the other groups showed significant temporal decrease of material.

New bone formation within the ROI after 4 weeks in OVX rats was 1.2 ± ***1.2***% for CPC/PLGA and 13.7 ± ***3.3***% for Bio-Oss®. After 12 weeks, bone formation in OVX rats was 6.5 ± ***5.5***% for

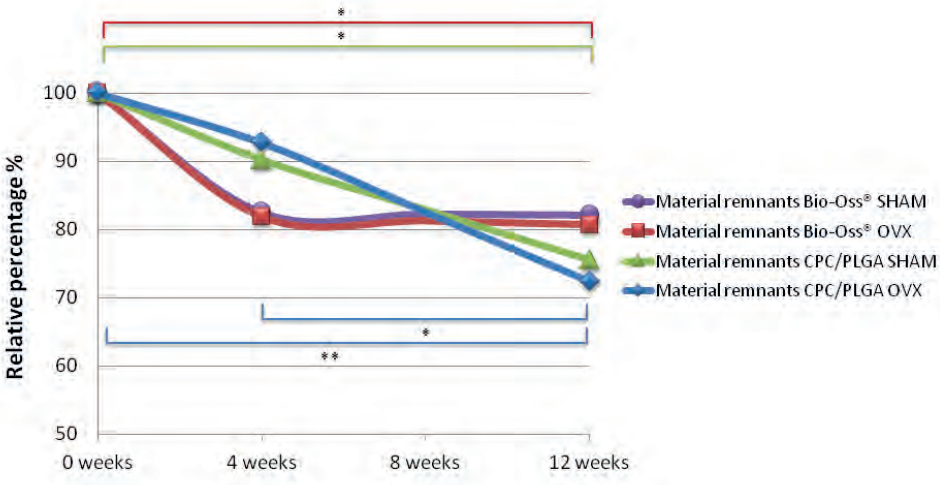

Figure 6: Temporal graph showing relative percentage and decrease of material remnants [all lines are to guide the eye]; ANOVA showed a significant temporal decrease of material remnants indicated by colored bars; red bar] Bio-Oss® OVX from 0 to 12 week; green bar] CPC/PLGA SHAM from 0 to 12 weeks; blue bars] for CPC/PLGA OVX from 0 to 12 and 4 to 12 weeks; *] $p<0.05$ and **] $p<0.01$.

CPC/PLGA and 17.5 ± *3.4*% for Bio-Oss®. For SHAM rats at 4 weeks this was 1.9 ± *2.0*% and 18.8 ± *4.1*%, respectively and at 12 weeks 3.3 ± *1.2*% and 18.6 ± *3.6*%, respectively. Bone formation was significantly increased for Bio-Oss® compared to CPC/PLGA at 4 and 12 weeks in both OVX and SHAM animals (ANOVA, all $p<0.001$; Figure 5). There was a significant temporal increase in bone formation using Bio-Oss® after both 4 and 12 weeks compared to the 0 week time point in both OVX and SHAM (ANOVA, all $p<0.001$). After 12 weeks, bone formation was twice as high in OVX as for SHAM for CPC/PLGA, however, this difference did not prove to be significant. No significant differences were observed between both conditions at each time point for each material (Students t-test, $p>0.05$).

Discussion

The aim of this study was to comparatively evaluate the performance of CPC/PLGA and Bio-Oss® in ovariectomized and healthy rats. We hypothesized that osteoporotic conditions would affect the performance of bone substitute materials. Additionally, we hypothesized that the differences in degradation rate between CPC/PLGA and Bio-Oss® would lead to different bone forming capacity. The main findings by histomorphometry showed significant degradation, especially in the period from 4 till 12 weeks, for CPC/PLGA over implantation time in both healthy and osteoporotic conditions, whereas Bio-Oss® degraded slightly within the first 4 weeks and showed no further degradation till 12 weeks. Bone formation was similar in healthy and osteoporotic conditions, with a rapid increase from 0-4 weeks for BioOss® and no further increase till week 12, whereas CPC/PLGA showed marginal bone formation over the course of 12 weeks.

Despite the overall higher degradation rate for CPC/PLGA compare to Bio-Oss®, we found relatively high amounts (>72%) of CPC/PLGA after 12 weeks, when compared to previous studies [19, 27]. An explanation for the relatively high amounts of CPC/PLGA material remnants could be the use of CMC in this study. To promote cohesion and improve injectability as well as washing resistance, previous studies have shown that addition of cellulose-based lubricants can be used [28-30]. Recent work by An et al., who also used CMC to enhance injectability of CPC and filled defects created in rabbit femoral condyles [31], showed corroborating degradation data. In their work, the CPC with CMC was compared to a composite of CPC with CMC and PLGA particles (60/40 wt% CPC/PLGA), as well as the commercially available apatite-forming cement, HydroSet™. After an implantation period of 26 weeks, they showed material remnants of 87 ± 8% for CPC/CMC and 59 ± 6% for CPC/CMC/PLGA, and also speculated that the limited degradation was caused by the use of CMC. Histologically, they noticed the presence of an acellular layer formed around the CPC, which they interpreted as a CMC-rich capsule formed after swelling of CMC. Although we did not observe this capsule, CMC likely compromises the accessibility of the intrinsic porosity within the CPC matrix, and hence prevents perfusion and cellular infiltration, reducing degradation rate. Future studies should be performed to examine the effect of CMC addition on CPC degradation.

For this study, preset cylinders of CPC/PLGA were used to exactly fit into the created defect. This allowed for shorter surgery time and more consistent and complete filling of the defects. Theoretically, this could have influenced CPC/PLGA performance, when compared to injecting directly into the defect. It could be hypothesized, when CPC/PLGA is injected directly into the bone defect, that mixing of bodily fluids (i.e. blood) could influence CPC hardening and comprise stability of the cement. Future studies should be performed to evaluate the effect of hardening of cement ***in vivo*** compared to the use of preset samples.

Irrespective of bone condition, our histomorphometrical data showed a temporal increase in bone to a maximum of 6.5% for CPC/PLGA and 18.8% for Bio-Oss®, which was significantly

higher for Bio-Oss®. Since Bio-Oss® already initially had space between the granules, bone formation could occur relatively early in comparison to the initially dense CPC/PLGA. Previous studies have shown that CPC/PLGA completely degrades over time, being replaced by new bone formation [19, 27, 32-35]. Bio-Oss®, on the other hand, is known to degrade slowly and remains present till years after implantation [36, 37], hampering more bone formation and full regeneration in those areas.

An osteoporotic bone condition significantly accelerated material degradation compared to a healthy condition, as observed for CPC/PLGA from 4 to 12 weeks and for Bio-Oss® from 0 to 12 weeks. TRAP staining showed no apparent increased intensity for osteoporotic bone versus healthy bone. This observation corroborates earlier studies [27, 38], and indicates that osteoclastic activity is not solely responsible for enhanced degradation in osteoporotic conditions [4]. On the other hand, degradation of especially CPC/PLGA can be both active (i.e. based on osteoclastic activity) and passive (i.e. based on dissolution) [39-41]. Because TRAP staining did not show increased osteoclastic activity, the increased surface area of CPC/PLGA after PLGA porogen degradation likely enhanced the passive dissolution of the CPC matrix in the period from 4-12 weeks.

In osteoporotic bone, CPC/PLGA showed a 5.4-fold increase in bone from 4 to 12 weeks, whereas in healthy bone only a 1.7-fold increase was observed. Similarly, Bio-Oss® showed a 1.3-fold increase in bone in osteoporotic bone and no increase in healthy bone. Furthermore, analyses of bone dynamics using fluorochromes for CPC/PLGA showed an apparent higher bone formation in the late period of implantation for osteoporotic versus healthy bone conditions, based on more incorporation of fluorochromes administered in this period. The earlier mentioned faster degradation rate of CPC/PLGA in osteoporotic conditions could explain the increased bone growth after 4 weeks, as bone formation can only occur after sufficient material degradation. In view of this, the use of a relatively porous and fast degrading material seems recommendable for treating bone defects in osteoporotic conditions. Additionally, it needs to be emphasized that osteoporotic patients often receive systemic medical treatments (i.e. bisphosphonates), possibly influencing material degradation and new bone formation. Consequently, further research is necessary, comparing treated to untreated osteoporotic conditions, to examine the effect on the biological performance of bone substitute materials.

Conclusion

This study showed CPC/PLGA degraded relatively faster and more steadily compared to Bio-Oss®. However, in absolute values, Bio-Oss® showed significantly less material remnant and more bone growth compared to CPC/PLGA. Our data confirmed our hypothesis that osteoporotic conditions affect degradation of CPC/PLGA, which is of vital information for its future use in osteoporotic patients. Alternatively, no effects of an osteoporotic condition on bone formation were observed. Consequently, different bone conditions require the selection of a bone graft material with suitable degradation characteristics.

Acknowledgements

The authors would like to acknowledge ms. N. van Dijk for her assistance with the histological sectioning and fluorochrome labeling and dr. V. Cuijpers for his assistance on the ***ex vivo*** micro-CT and histological imaging.

References

1 Greenwald AS, Boden SD, Goldberg VM, Khan Y, Laurencin CT, Rosier RN (2001) Bone-Graft Substitutes: Facts, Fictions, and Applications. J Bone Joint Surg Am 83-A:98-103

2 Van der Stok J, Van Lieshout EM, El-Massoudi Y, Van Kralingen GH, Patka P (2011) Bone substitutes in the Netherlands - a systematic literature review. Acta biomaterialia 7:739-750

3 Bongio M, van den Beucken JJJP, Leeuwenburgh SCG, Jansen JA (2010) Development of bone substitute materials: from 'biocompatible' to 'instructive'. J Mater Chem 20:8747-8759

4 Fini M, Giavaresi G, Torricelli P, Borsari V, Giardino R, Nicolini A, Carpi A (2004) Osteoporosis and biomaterial osteointegration. Biomedicine & pharmacotherapy = Biomedecine & pharmacotherapie 58:487-493

5 Sanfilippo F, Bianchi AE (2003) Osteoporosis: the effect on maxillary bone resorption and therapeutic possibilities by means of implant prostheses -a literature review and clinical considerations. Int J Periodontics Resorative Dent 23:447-457

6 Abushahba F, Renvert S, Polyzois I, Claffey N (2008) Effect of grafting materials on osseointegration of dental implants surrounded by circumferential bone defects. An experimental study in the dog. Clinical oral implants research 19:329-334

7 Orsini G, Scarano A, Degidi M, Caputi S, Iezzi G, Piattelli A (2007) Histological and ultrastructural evaluation of bone around Bio-Oss particles in sinus augmentation. Oral diseases 13:586-593

8 Orsini G, Traini T, Scarano A, Degidi M, Perrotti V, Piccirilli M, Piattelli A (2005) Maxillary sinus augmentation with Bio-Oss particles: a light, scanning, and transmission electron microscopy study in man. Journal of biomedical materials research Part B, Applied biomaterials 74:448-457

9 Tapety FI, Amizuka N, Uoshima K, Nomura S, Maeda T (2004) A histological evaluation of the involvement of Bio-Oss in osteoblastic differentiation and matrix synthesis. Clinical oral implants research 15:315-324

10 Bohner M (2010) Design of ceramic-based cements and putties for bone graft substitution. European cells & materials 20:1-12

11 Bohner M, Gbureck U, Barralet JE (2005) Technological issues for the development of more efficient calcium phosphate bone cements: a critical assessment. Biomaterials 26:6423-6429

12 Kolk A, Handschel J, Drescher W, Rothamel D, Kloss F, Blessmann M, Heiland M, Wolff KD, Smeets R (2012) Current trends and future perspectives of bone substitute materials - from space holders to innovative biomaterials. Journal of cranio-maxillo-facial surgery : official publication of the European Association for Cranio-Maxillo-Facial Surgery 40:706-718

13 LeGeros RZ (2002) Properties of osteoconductive biomaterials: calcium phosphates. Clinical orthopaedics and related research 81-98

14 Low KL, Tan SH, Zein SH, Roether JA, Mourino V, Boccaccini AR (2010) Calcium phosphate-based composites as injectable bone substitute materials. Journal of biomedical materials research Part B, Applied biomaterials 94:273-286

15 Verron E, Bouler JM, Guicheux J (2012) Controlling the biological function of calcium phosphate bone substitutes with drugs. Acta biomaterialia 8:3541-3551

16 Zhang J, Liu W, Schnitzler V, Tancret F, Bouler JM (2014) Calcium phosphate cements for bone substitution: chemistry, handling and mechanical properties. Acta biomaterialia 10:1035-1049

17 Brown WE, Chow LC (1983) A New Calcium-Phosphate Setting Cement. J Dent Res 62:672-672

18 Habraken WJEM, Wolke JG, Mikos AG, Jansen JA (2008) PLGA microsphere/calcium phosphate cement composites for tissue engineering: in vitro release and degradation characteristics. J Biomater Sci Polym Ed 19:1171-1188

19 Felix Lanao RP, Leeuwenburgh SC, Wolke JG, Jansen JA (2011) Bone response to fast-degrading, injectable calcium phosphate cements containing PLGA microparticles. Biomaterials 32:8839-8847

20 Jee WSS, Yao W (2001) Overview: animal models of osteopenia and osteoporosis. J Musculoskelet Neuronal Interact 1:193-207

21 Turner A (2001) Animal models of osteoporosis-necessity and limitations. Eur Cells Mater 1:66-81

22 Bongio M, van den Beucken JJ, Leeuwenburgh SC, Jansen JA (2015) Preclinical evaluation of injectable bone substitute materials. Journal of tissue engineering and regenerative medicine 9:191-209

23 Grardel B, Sutter B, Flautre B, Viguier E, Lavaste F, Hardouin P (1994) Effects of glucocorticoids on skeletal growth in rabbits evaluated by dual-photon absorptionmetry, microscopic connectivity and vertebral compressive strenght. Osteoporos Int 4:204-210

24 Alghamdi HS, van den Beucken JJ, Jansen JA (2014) Osteoporotic rat models for evaluation of osseointegration of bone implants. Tissue engineering Part C, Methods 20:493-505

25 Lopez-Heredia MA, Bongio M, Cuijpers VM, van Dijk NW, van den Beucken JJ, Wolke JG, Jansen JA (2012) Bone formation analysis: effect of quantification procedures on the study outcome. Tissue engineering Part C, Methods 18:369-373

26 Grosfeld EC, Hoekstra JW, Herber R-P, Ulrich DJO, Jansen JA, van den Beucken JJJP (2017) Long-term biological performance of injectable and degradable calcium phosphate cement. Biomedical Materials 12:015009

27 van de Watering FC, Laverman P, Cuijpers VM, Gotthardt M, Bronkhorst EM, Boerman OC, Jansen JA, van den Beucken JJ (2013) The biological performance of injectable calcium phosphate/PLGA cement in osteoporotic rats. Biomedical materials 8:035012

28 Ginebra MP, Espanol M, Montufar EB, Perez RA, Mestres G (2010) New processing approaches in calcium phosphate cements and their applications in regenerative medicine. Acta biomaterialia 6:2863-2873

29 Liu W, Zhang J, Weiss P, Tancret F, Bouler JM (2013) The influence of different cellulose ethers on both the handling and mechanical properties of calcium phosphate cements for bone substitution. Acta biomaterialia 9:5740-5750

30 An J, Wolke JG, Jansen JA, Leeuwenburgh SC (2016) Influence of polymeric additives on the cohesion and mechanical properties of calcium phosphate cements. Journal of materials science Materials in medicine 27:58

31 An J, Liao H, Kucko NW, Herber RP, Wolke JG, van den Beucken JJ, Jansen JA, Leeuwenburgh SC (2016) Long-term evaluation of the degradation behavior of three apatite-forming calcium phosphate cements. Journal of biomedical materials research Part A 104:1072-1081

32 van Houdt CI, Preethanath RS, van Oirschot BA, Zwarts PH, Ulrich DJ, Anil S, Jansen JA, van den Beucken JJ (2015) Toward accelerated bone regeneration by altering poly(d,l-lactic-co-glycolic) acid porogen content in calcium phosphate cement. Journal of biomedical materials research Part A

33 Ruhe PQ, Hedberg EL, Padron NT, Spauwen PH, Jansen JA, Mikos AG (2005) Biocompatibility and degradation of poly(DL-lactic-co-glycolic acid)/calcium phosphate cement composites. Journal of biomedical materials research Part A 74:533-544

34 del Real RP, Ooms E, Wolke JG, Vallet-Regi M, Jansen JA (2003) In vivo bone response to porous calcium phosphate cement. Journal of biomedical materials research Part A 65:30-36

35 de Falco R, Scarano E, Di Celmo D, Grasso U, Guarnieri L (2005) Balloon kyphoplasty in traumatic fractures of the thoracolumbar junction. Preliminary experience in 12 cases. Journal of neurosurgical sciences 49:147-153

36 Artzi Z, Weinreb M, Givol N, Rohrer MD, Nemcovsky CE, Prasad HS, Tal H (2004) Biomaterial resorption rate and healing site morphology of inorganic bovine bone and beta-tricalcium phosphate in the canine: a 24-month longitudinal histologic study and morphometric analysis. The International journal of oral & maxillofacial implants 19:357-368

37 Piattelli M, Favero GA, Scarano A, Orsini G, Piattelli A (1999) Bone reactions to anorganic bovine bone (Bio-Oss) used in sinus augmentation procedures: a histologic long-term report of 20 cases in humans. The International journal of oral & maxillofacial implants 14:835-840

38 Alghamdi HS, Cuijpers VM, Wolke JG, van den Beucken JJ, Jansen JA (2013) Calcium-phosphate-coated oral implants promote osseointegration in osteoporosis. J Dent Res 92:982-988

39 Grossardt C, Ewald A, Grover LM, Barralet JE, Gbureck U (2010) Passive and active in vitro resorption of calcium and magnesium phosphate cements by osteoclastic cells. Tissue engineering Part A 16:3687-3695

40 LeGeros RZ (1993) Biodegradation and bioresorption of calcium phosphate ceramics. Clinical materials 14:65-88

41 Koerten HK, van der Meulen J (1999) Degradation of calcium phosphate ceramics. Journal of biomedical materials research 44:78-86

4

CHAPTER 4

Towards accelerated bone regeneration by altering PLGA porogen content in calcium phosphate cement

van Houdt CIA, Preethanath RS, van Oirschot BAJA, Zwarts PH, Ulrich DJO, Anil S, Jansen JA, van den Beucken JJJP

J Biomed Mater Res A. 2016 Feb;104(2):483-92

Introduction

Synthetic bone substitutes are widely accepted materials in the field of bone reconstruction to promote bone regeneration and replace autologous bone grafting. Commercially available synthetic bone substitutes are available in various forms and shapes, adapted to the specific needs of different bone defects [1,2]. Synthetic bone substitutes can be subdivided into three material classes, i.e. polymers, ceramics and composites [1]. Ceramics, especially those based on calcium phosphates (CaPs), are favorable materials due to their biocompatible, bioactive and osteoconductive properties resulting from a chemical composition that is similar to the mineral phase of bone [4-8]. In view of optimized handling properties, CaP ceramics have become available in the form of injectable CaP cement (CPC) [3]. First proposed in the early 80s, CPCs were designed to overcome the handling difficulties of the traditional ceramic blocks and granules [9,10].

Depending on the end-product after setting, CPCs can be classified into two main groups, i.e. brushite and apatitic CPCs. Brushite CPCs have the ability to be resorbed under physiological conditions, whereas apatitic cements degrade relatively poorly, limiting new bone formation [11]. Resorption of CPC occurs either via active resorption (a cell-mediated process of osteoclasts and macrophages) or via passive resorption (based on the cement solubility) [12-15]. Passive resorption is mainly influenced by porosity and cement composition, i.e. apatite being less soluble than brushite. Brushite CPCs, however, have low mechanical properties and handling can be difficult due to a fast setting time (~30 s) [11]. The favorable mechanical and handling properties of apatitic cements lead research to focus on improving their degradation properties.

Ideally, the rate of material degradation is equal to the rate of bone formation gradually providing room for bone to grow [16]. Balancing degradation rate to new bone formation rate is an important material property to control. Accelerated degradation of CPC has been achieved via addition of porogens [17,18]. Generally, macropores (pores>100µm) are used to increase the surface of the CPC leading to a faster degradation. The term “macropores” is used to distinguish between the pores from the scaffold’s own micro- or nanoporosity [18]. Macropores are mainly created by leaching or degradation of incorporated particles, gas foaming, and droplet emulsion. [10,17,19-24].

Poly(D,L-lactic-co-glycolic) acid (PLGA) is a rapidly degradable synthetic polymer and hence interesting to use as porogen in CPC. PLGA has a long clinical history and already several PLGA incorporated medical devices have been approved by the FDA for clinical use [25]. In vivo degradation of PLGA occurs via hydrolysis and is a relatively fast process. During degradation, lactic acid and glycolic acid monomers are released, which are metabolized into carbon dioxide and water and excreted by the body [25]. Parameters influencing the degradation of PLGA are molecular weight, end-group functionalization (acid terminated or end capped) and ratio of lactic and glycolic acids [8,26-31]. Previously, it was shown that PLGA microspheres

enhance the degradation of apatitic CPC and improve bone regeneration [26,27,32,33]. When incorporated into CPC, the degradation is influenced by the particle size, morphology (hollow or dense spheres), and relative amount of PLGA [8,26-31].

PLGA porogens can be fabricated following several methods, such as water-in-oil-in-water emulsion or oil-in-water emulsion [25]. These chemical processes are associated with an acceptable yield (i.e. 60-80%), but such loss of product during synthesis and the time consuming nature are impeding large-scale utilization. Alternatively, PLGA milling can be applied to generate PLGA porogens [32,33]. In this way, irregularly-shaped PLGA particles are obtained relatively fast and in a cost-effective manner.

The aim of this study was to comparatively evaluate the in vitro degradation effects of dense PLGA microspheres with milled PLGA particles as porogens in apatitic CPC. We hypothesized that milled PLGA particles would degrade CPC/PLGA similarly when compared to dense PLGA microspheres. Additionally, we aimed to examine the effect of PLGA porogen amount in CPC/PLGA via an in vivo rat femoral bone defect model to determine degradation and bone formation. For this, we hypothesized that a higher PLGA porogen amount would increase the porosity, leading to faster degradation and consequently more bone formation in vivo.

Materials & methods

Materials

The CPC used for both in vitro and in vivo experiments consisted of 100% α-TCP (kindly provided by CAM Bioceramics B.V., Leiden, the Netherlands) sieved at <150 µm. Carboxymethyl cellulose (CMC; 0.75 wt%) was added to the CPC to improve injectabilty. PLGA (Purasorb®, PDLG 5002A, Mw=17kDa, acid-terminated) was obtained from Corbion B.V. (Gorinchem, the Netherlands). Milled PLGA (PDLG 5002A, acid-terminated) was kindly provided by CAM Bioceramics B.V. Custom-made cylindrical thumbtack-shaped titanium implants (grade 2) were obtained from Machinefabriek G. Jansen B.V. (Valkenswaard, the Netherlands).

Preparation of dense PLGA microspheres

Dense PLGA microspheres, used for in vitro analysis, were fabricated by an emulsion technique as described previously [30]. Briefly, PLGA was dissolved in 12 ml of dichloromethane (DCM, Merck, Germany). The solution was decanted over three beakers containing 150 ml of 0.3% polyvinyl alcohol (PVA, Acros Organics, the Netherlands). This second emulsion was stirred (800 rpm) for 5 minutes and then 200 ml of 2% isopropanol (Labscan Ltd., the Netherlands) was added. The suspension was stirred for 1 hour, after which the PLGA microspheres were allowed to precipitate. Thereafter, the supernatant was decanted and the sediment was washed twice with ultrapure water. The microspheres were lyophilized and stored at -20°C.

Preparation of CPC/PLGA scaffolds (for in vitro analysis)

The α-TCP, CMC, and PLGA porogen were combined to obtain formulations with either 30 or 50 wt% PLGA (**Table 1**). Per 1 gram of powder, a solution of 500 µl 4% NaH2PO4 was added. For the preparation of the scaffolds, a Teflon® mold was used with holes of 4.5 mm in diameter

Table 1: Overview of CPC/PLGA formulations

In vitro	CPC/PLGA	PLGA
70/30-MS	70/30 wt%	microspheres
50/50-MS	50/50 wt%	microspheres
70/30-MP	70/30 wt%	milled particles
50/50-MP	50/50 wt%	milled particles
In vivo	**CPC/PLGA**	**PLGA**
Ti-70/30-MP	70/30 wt%	milled particles
Ti-50/50-MP	50/50 wt%	milled particles

CPC, calcium phosphate cement; PLGA, poly(lactic-co-glycolic acid); MS, microspheres; MP milled particles

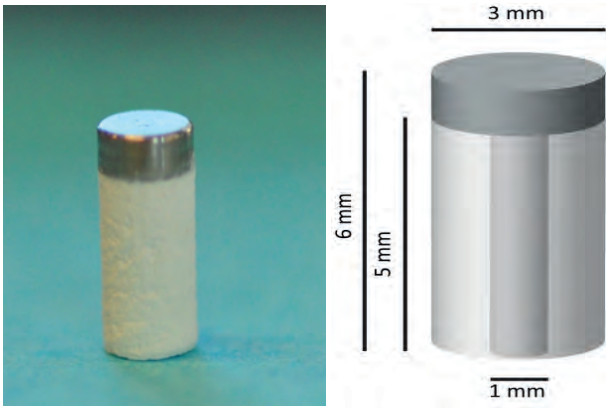

Figure 1: Schematic representation of titanium landmarks with CPC/PLGA (left) with dimensions of a diameter of maximum 3mm and minimum 1mm, length maximum 6mm; Photograph of titanium landmarks with CPC/PLGA (right); CPC, calcium phosphate cement; PLGA, poly(D,L-lactic-co-glycolic) acid

and 9.2 mm in depth. During injection into the Teflon® mold, attention was paid to completely fill the space and any air being trapped under the cement was removed. The cement was left to air dry at room temperature for a minimum of 24 hours.

Preparation of titanium-CPC/PLGA scaffolds (for in vivo analysis)

Titanium implants (thumbtack-shape; length 6 mm, base diameter 3 mm, core diameter 1 mm), were cleaned using a tabletop ultrasonic cleaner via consecutive rinsing with acetone and alcohol, and then air dried. Then, the titanium implants were placed into a Teflon® mold, with holes of 3 mm in diameter and 6 mm in length.

CPC/PLGA was mixed with 500 µl of 4% NaH_2PO_4 solution per 1 gram powder and injected with an 18G needle into the space around the titanium implants. During injection, attention was paid to completely fill the space and any air being trapped under the cement was removed. Then, the cement was left to air dry at room temperature for a minimum of 24 hours, after which the implants were gently removed from the mold. Dimensions of the Ti-CPC/PLGA implants are depicted in **Figure 1**. Finally, sterilization was performed by gamma irradiation (25-50 kGy; SynergyHealth Ede B.V., Ede, the Netherlands).

In vitro material characterization

PLGA porogens

The size of the PLGA microspheres was measured by optical microscopy (DM RBE Leica, Germany) with image analysis software (Qwin Leica, Germany).

CPC/PLGA scaffolds

After removal from the mold, scaffolds were each placed in 1.5 ml of phosphate buffered saline (PBS) and left on a shaking apparatus at 37°C.

Scaffold morphology

A scanning electron microscope (SEM; JEOL JSM 6340, 10 kV) was used for morphological analysis. For each material group, samples were scanned after 4 weeks and 8 weeks of incubation.

Porosity calculations and measurements

The macroporosity of the different CPC/PLGA experimental formulas (n=3) was determined as previously described by Habraken et al. [34]. The equations used to calculate the total porosity and macroporosity are as shown in **Figure 2**.

Degradation and pH changes

Degradation of the scaffolds was determined by analyzing Ca^{2+} release into the PBS,

$$\varepsilon_{tot} = \left(1 - \frac{m\ burnt}{V * \rho\ \mathrm{HAP}}\right) * 100\% \quad \text{Equation 1}$$

$$\varepsilon_{macro} = \left(1 - \frac{m\ burnt}{m\ microporous}\right) * 100\% \quad \text{Equation 2}$$

Legend

ε tot	=	total porosity (%)
ε macro	=	macroporosity (%)
m burnt	=	average mass sample (after burning out polymer) (g. n=3)
m microporous	=	average mass microporous sample (g. n=3)
V	=	volume sample (cm3)
ρ HAP	=	density hydroxyapatite (g/cm3)

Figure 2: Equations 1 and 2 used to calculate macro- and microporosity (%) of the scaffolds

measured at the end of each week, for 8 consecutive weeks. The absolute amounts of $Ca2^{+}$-ions in the PBS media were analyzed by the orthocresolphtalein complexone (OCPC) method (Sigma-Aldrich Chemie B.V., Zwijndrecht, the Netherlands) as described previously [30]. Additionally, the pH of the PBS media was monitored, using pH-indicator strips, at the same weekly time points.

In vivo analysis

Animals

Twenty healthy mature male Wistar rats were used for this experiment at 3 months of age with an average weight of 250 grams at the start of the experiment. An acclimatization period of 7 days was used and housing was provided per pair in a standard macrolon type 3 cage with sawdust as bedding material. Standard rodent chow and bottled tap water was provided ad libitum. The housing room was maintained under standard laboratory conditions (light-dark cycle: 12:12 hours, temperature: 20-22°C, relative humidity: 45-55%). All experiments were conducted in accordance with institutional, national and international guidelines for animal care and the Dutch law concerning animal welfare. The studies were reviewed and approved by the Experimental Animal Committee of the Radboud University (RUDEC 2012-243).

Surgical procedure

A rat femoral bone defect model was used, as described previously [35]. Pre-operatively, pain medication was provided by an injection of Carprofen (5 mg/kg; Rimadyl®, Pfizer Animal Health, New York, USA) given 15 minutes before surgery. Anesthesia was induced and maintained by Isoflurane inhalation (Rhodia Organique Fine Ltd., Avonmouth, Bristol, UK) combined with oxygen. After confirmation of effective anesthesia, the surgical area was shaved and disinfection was performed by application of a povidone iodine solution. The rats were placed on a heating mat to prevent hypothermia and immobilized in supine position. With the knee maximally flexed, a longitudinal incision through skin and muscle was made on the medial surface. After exposure of the medial side of the distal femoral condyle, the knee capsule was incised. Then, the knee was extended to luxate the patella laterally. When a clear view of the knee joint was established, a femoral bone defect (diameter 3 mm, depth 6 mm) was created in the same direction as the axis of the femur, using a dental drill (Elcomed 9927 SPS; W&H Dentalwerk Burmoos GmbH, Burmoos, Austria). A series of increasing bur diameters were used with the final drill of 3 mm in diameter, at a speed of maximum 5000 rpm and constant cooling by dripping saline. The drilled cavity was then washed with a spray of saline and dried using sterile gauze, after which the pre-set titanium-CPC/PLGA scaffolds were placed into the defects. Each rat received both implants (Ti-50/50-MP and Ti-70/30-MP), alternating between each rat the two weight percentages for the left and right knee. After introducing the implants into the defects, the muscular tissue layer was closed with resorbable sutures (Vicryl® 4.0) after which the skin was closed with small staples (Agraven®; InstruVet B.V., Cuijk, the Netherlands). To diminish postoperative discomfort, Buprenorfine (0.02 mg/kg; Temgesic® Reckitt Benckiser Pharmacueticals Ltd., Slough, UK)

was given every 12 hours till 2 days after surgery. All animals had free access to pellet food and water. In the initial postoperative period, the intake of water and food was monitored daily as well as the weight of the animals. In addition, the animals were observed for signs of pain, infection and proper activity. Weekly weighing of each animal was continued until the end of the experiment.

Implant retrieval

After implantation periods of 4 and 8 weeks, the animals were euthanized by CO2-suffocation. The retrieved specimens were harvested and fixed in 10% neutral buffered formalin solution for 24 hours, after which the specimens were dehydrated in a graded series of ethanol.

Histological processing

All specimens were embedded in poly(methylmethacrylate) (pMMA). After polymerization, three sections per specimen of ~10 µm were prepared perpendicular to the axis of the femur using a diamond blade saw (Leica Microsystems SP 1600, Nussloch, Germany). Methylene blue and basic fuchsine staining was performed for each section.

Descriptive histology and histomorphometry

Descriptive histology was performed by light microscopy examination (Leica Microsystems AG, Wetzlar, Germany) comparing all histological sections. Staining allowed for discrimination between soft tissue, bone tissue and CPC. Attention was paid to bone and CPC morphology, and amounts of bone and CPC.

Histomorphometry for both implantation periods of 4 and 8 weeks, pMMA histological sections (n=3 per femoral bone defect) were assessed quantitatively using computer-based image analysis techniques (Leica® Qwin Pro-image analysis system, Wetzlar, Germany). From the digitalized images of the sections at a 5x magnification, a circular region of interest (ROI) of 3mm in diameter was selected to assign the defect area with the titanium pin as the center. Quantitative measurements within this ROI for area of newly formed bone and area of CPC material, were performed using the Leica® Qwin computer-based image analysis techniques. Vital bone could be distinguished by the pink colour and distinctive cell morphology including a nucleus, allowing to be easily discerned from other tissues as well as from CPC. The maturity of bone was differentiated by morphology, as mature trabecular bone is formed in lamellae, whereas newly formed bone has a more woven structure. Relative bone forming capacity is defined as relative increment in bone area per relative decline in CPC area. Bone-to-implant contact (BIC) area was defined as the length around the circumference of the titanium pin that is in contact with bone. The standardized diameter of the defect and titanium pin allowed to calculate areas of bone, CPC and BIC into percentages.

Statistical analysis

Data for new bone formation and CPC remnants were presented as means with standard deviations (SD). The mean area percentages were statistically compared between the groups

using one-way ANOVA (GraphPad, Prism 5, GraphPad Software Inc., La Jolla, California USA) with a post-hoc Tukey-Kramer Multiple Comparisons test. Differences were considered significant at $p<0.05$.

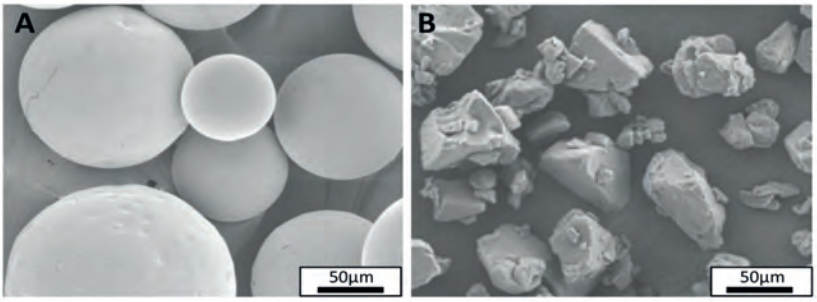

Figure 3 A-B: Representative SEM images of PLGA; A) microspheres and B) milled particles; SEM, scanning electron microscope; PLGA, poly(D,L-lactic-co-glycolic) acid

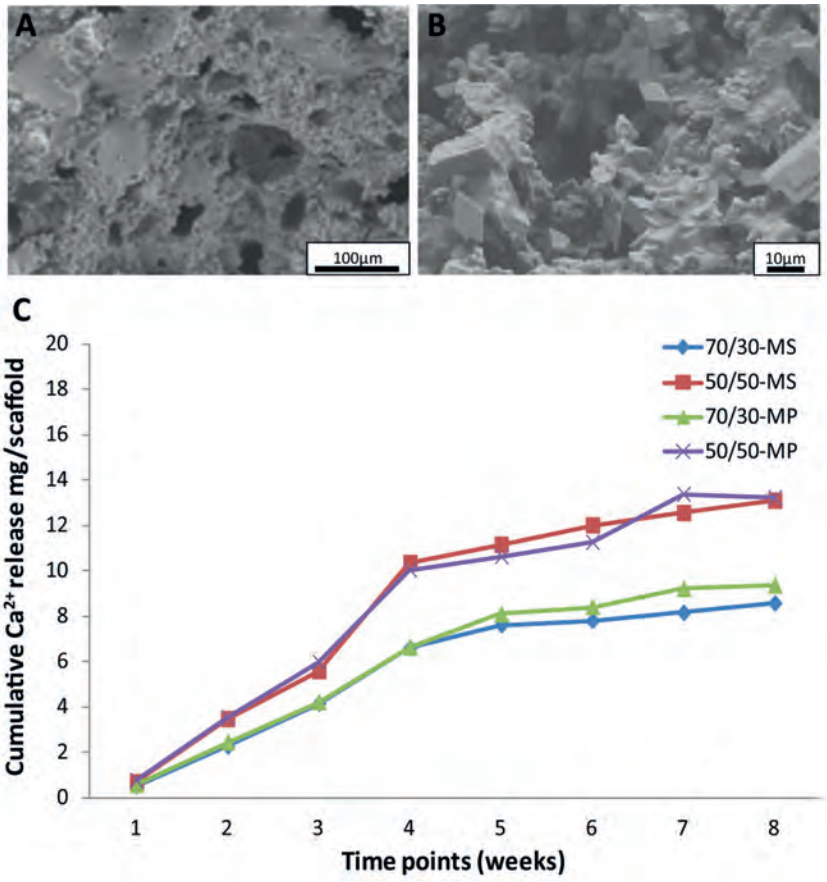

Figure 4 A-B: **A)** SEM images of CPC/PLGA with pore formation by degraded PLGA; **B)** higher magnification showing detail of brushite crystal formation; C) In vitro cumulative $Ca2^{+}$ release in mg/scaffold for each CPC/PGLA formulation, differences between 70/30-MS and 70/30-MP formulations were significantly different at all time points compared to 50/50-MS and 50/50-MP; CPC, calcium phosphate cement; PLGA, poly(D,L-lactic-co-glycolic) acid; MS, microspheres; MP, milled particles

Results

Material characterization

PLGA porogen

Representative images of both PLGA porogens are depicted in **Figure 3A-B**, showing spherically-shaped PLGA microspheres and irregularly-shaped milled particles. The mean particle size was 39.95 ± 9.21 µm for the microspheres and 48.65 ± 22.07 µm for the milled particles.

CPC/PLGA scaffolds

Scaffold morphology

SEM images revealed that at the start of the in vivo experiment, the PLGA microspheres and milled PLGA particles were embedded within the CPC. Already after 4 weeks of incubation in PBS, the PLGA porogens in all four groups were degraded and the CPC showed signs of degradation (**Figure 4A**). At higher magnifications, precipitate formation in the form of brushite crystals was detected (**Figure 4B**).

Porosity calculations

Porosity calculations showed that differences in porogen amount led to significant differences in porosity, comparing 70/30-MS to 50/50-MS and 70/30-MP to 50/50-MP (both $p<0.001$; **Table 2**). Comparing the two types of porogens at the same wt% (i.e. 70/30-MS to 70/30-MP and 50/50-MS to 50/50-MP) the differences were not significant ($p>0.05$; **Table 2**).

Degradation and pH changes

At all time points, the cumulative $Ca2^{+}$ amount was significantly higher for the 70/30 CPC/

Table 2: Porosity calculations of the scaffolds*

	Mean mass (g)	Density (g/cm3)	Total porosity (%)	Macroporosity (%)	Microporosity (%)
CPC only	0.213 ± 0.003	0.0305 ± 0.0004	52.9 ± 0.7	n.a.	52.9 ± 0.7
70/30-MS	0.095 ± 0.004	0.0136 ± 0.0005	78.9 ± 0.8	55.3 ± 1.8	23.7 ± 0.9
50/50-MS	0.068 ± 0.005	0.0097 ± 0.0007	85.0 ± 1.1	68.1 ± 2.3	16.9 ± 1.2
70/30-MP	0.099 ± 0.003	0.0141 ± 0.0005	78.2 ± 0.7	53.7 ± 1.6	24.5 ± 0.8
50/50-MP	0.068 ± 0.006	0.0097 ± 0.0008	85.0 ± 1.2	68.1 ± 2.6	16.8 ± 1.4

**Porosity calculations were performed based on CPC with burned out PLGA; The differences were significant ($p<0.001$) comparing both 70/30-MS and 70/30-MP to 50/50-MS and 50/50-MP; CPC, calcium phosphate cement; MS, microspheres; MP milled particles*

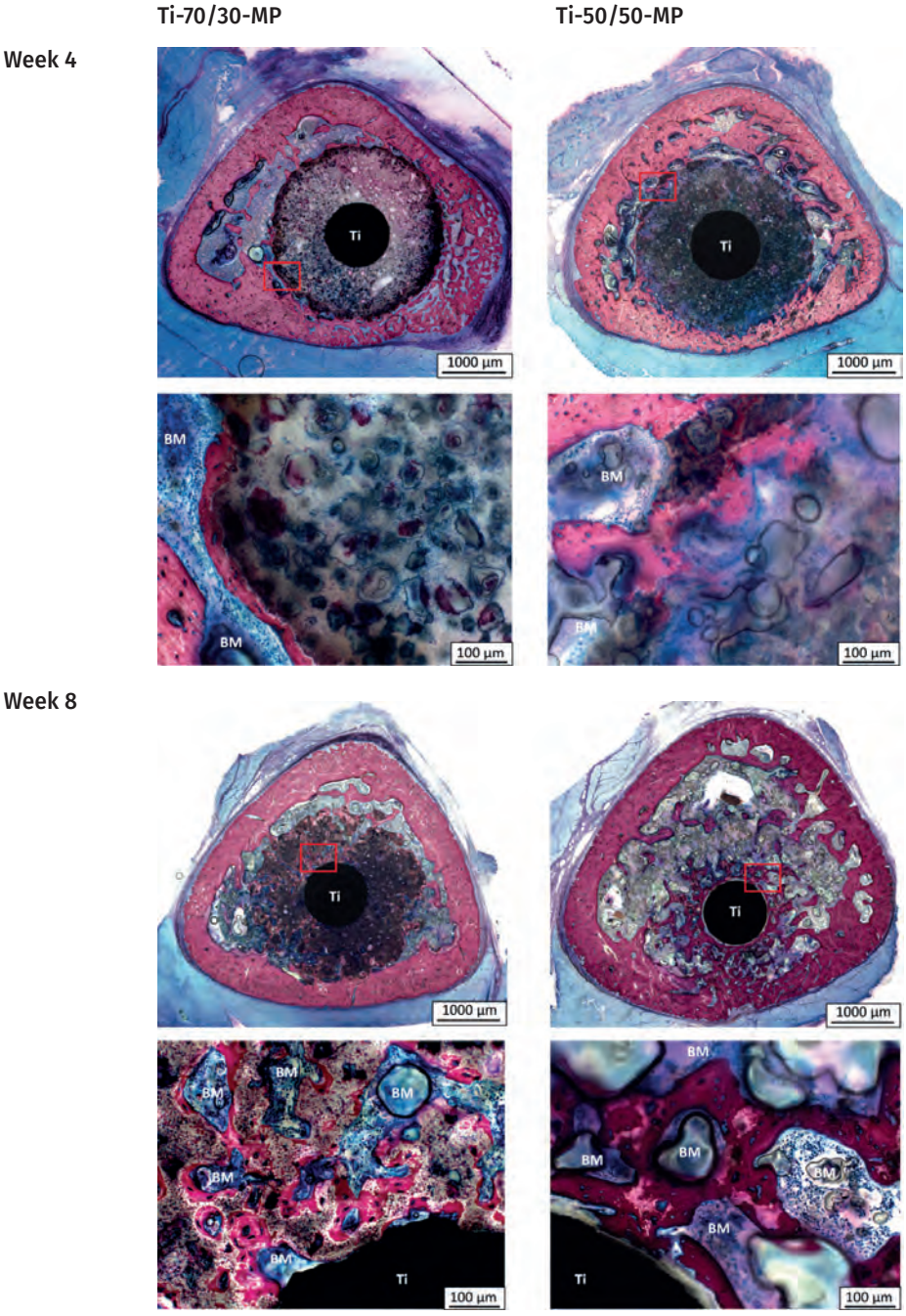

Figure 5: Representative histological images (5x magnification) of both materials at time points of 4 and 8 weeks with detailed images (20x magnification); Ti, titanium landmarks; BM, bone marrow

PLGA formula compared to the 50/50 CPC/PLGA (**Figure 4C**). CPC/PLGA formulations with the same amount of PLGA (microspheres or milled particles) showed similar $Ca2^+$ release profiles ($p>0.05$) with an accelerated release from 3 to 4 weeks. In contrast, significantly higher ($p<0.05$) $Ca2^+$ release profiles were observed for both 50/50-MS and 50/50-MP compared to both 70/30-MS and 70/30-MP, at all time points.

For the pH-values of the incubation media (data not shown), the initial pH-value of 7.4 dropped to ~4 within the first week for all CPC/PLGA formulas. Subsequently, a further gradual decrease of the pH was observed to ~3.3 after 8 weeks of incubation.

In vivo analysis

Clinical evaluation following surgery

All twenty rats recovered well from surgery and remained in good health during the course of the experiment. None of the animals showed signs of illness or compromised wound healing. Examination of the wound and implantation areas after euthanasia at either 4 or 8 weeks showed no inflammatory or other adverse tissue reaction. All installed implants were retrieved and used for further analysis.

Descriptive histology

Representative histological overview images are provided in **Figure 5**, with additional detailed images at 20x magnification. Newly formed bone could be macroscopically detected at the periphery of the CPC after both 4 and 8 weeks of implantation for both Ti-70/30-MP and Ti-50/50-MP. In all groups, this bone was in direct contact with the CPC, without intervening soft tissue layers. Additionally, no signs of inflammatory responses were observed for any of the groups. In several cases of each group, cracks were observed within the CPC with bone tissue growing into these cracks.

At 4 weeks, no apparent differences in CPC degradation were observed between Ti-70/30-MP and Ti-50/50-MP. At 8 weeks, however, a clear difference was observed, with Ti-50/50-MP showing faster CPC degradation than Ti-70/30-MP. Within the newly formed bone, some remnant CPC was detectable at a higher magnification for both Ti-70/30-MP and Ti-50/50-MP. For specimens showing almost fully degraded CPC, the new bone present within the defect area was trabecular-shaped with bone marrow between bone trabeculae.

Histomorphometry

CPC area (%)

The CPC area within the ROI showed a temporal decrease for both Ti-50/50-MP and Ti-70/30-MP (**Table 3** & **Figure 6A**). The area of CPC measured at 0 weeks were 81.0 ± 0.6% for Ti-70/30-MP and 74.8 ± 0.7% for Ti-50/50-MP ($p<0.001$). After 4 weeks of implantation, the CPC area was 60.9 ± 13.5% for Ti-70/30-MP and 53.5 ± 17.3% for Ti-50/50-MP ($p>0.05$). After 8 weeks of implantation were 35.2 ± 21.2% for Ti-70/30-MP and 9.1 ± 9.7% for Ti-50/50-MP ($p<0.001$).

Comparing the different time points revealed a significant temporal decrease after the first 4 weeks in CPC area for Ti-50/50-MP ($p<0.05$). After 8 weeks the CPC area was decreased further, significantly for both Ti-70/30-MP ($p<0.01$) and Ti-50/50-MP ($p<0.001$). The decrease was also significant from 4 to 8 weeks for both Ti-70/30-MP ($p<0.01$) and Ti-50/50-MP ($p<0.001$).

Bone area (%)

Newly formed bone within the ROI increased over time for both Ti-70/30-MP and Ti-50/50-MP (**Table 3** & **Figure 6B**). After 4 weeks, the bone area within the ROI was 5.8 ± 5.0% for Ti-70/30-MP and 8.3 ± 2.8% for Ti-50/50-MP ($p>0.05$). After 8 weeks, the bone area revealed a significant temporal increase ($p<0.001$) for both experimental groups and a significant inter-group difference ($p<0.05$) with values of 22.9 ± 5.2% and 35.0 ± 15.0% for Ti-70/30-MP and Ti-50/50-MP, respectively.

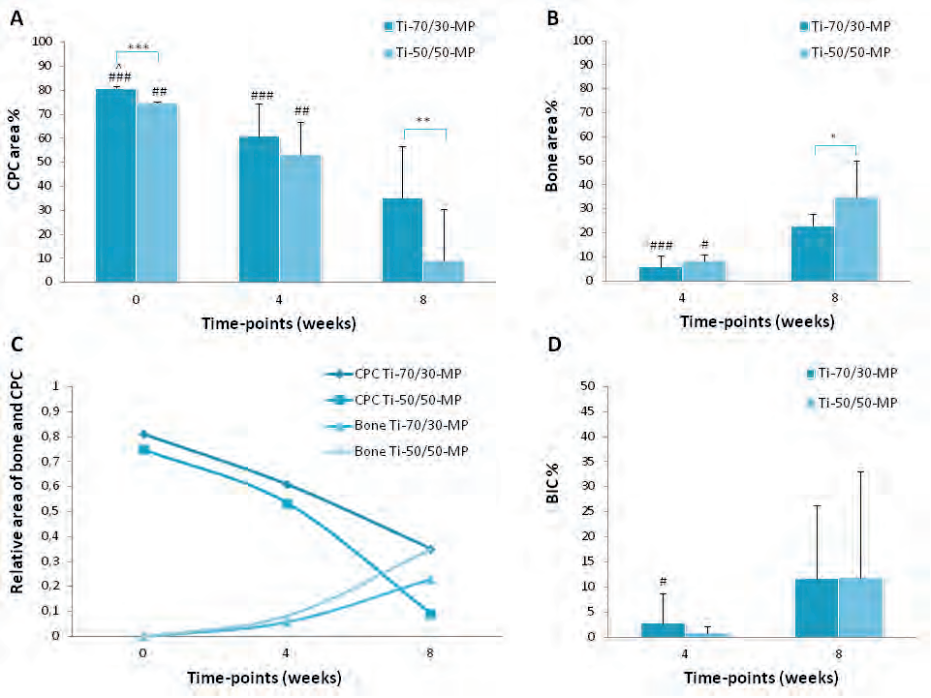

Figure 6 A-D: A) CPC area in the ROI (mean +SD); B) Bone area in the ROI (mean ±SD); C) Graph of CPC degradation rate versus bone formation rate; D) Bone to implant contact (BIC) (mean ±SD); Intergroup differences *) $p<0.05$, **) $p<0.01$, ***) $p<0.001$; Temporal differences $^{\wedge}$) $p<0.05$ compared to 4 week equivalent, $^{\#}$) $p<0.05$ compared to 8-week equivalent; $^{\#\#}$) $p<0.01$ compared to 8-week equivalent, $^{\#\#\#}$) $p<0.001$ compared to 8-week equivalent

Bone forming capacity

For extended visualization of temporal decreases of CPC area and increases in bone area (**Figure 6C**), calculations were made on the relative bone forming capacity (**Table 4**).

In the first 4 weeks, 1% CPC degradation resulted in 0.29% new bone for the Ti-70/30-MP compared to 0.39% for the Ti-50/50-MP. From week 4 to 8, 1% CPC degradation allowed for 0.67% new bone for Ti-70/30-MP compared to 0.60% for Ti-50/50-MP. Overall, more bone was formed within the ROI of Ti-50/50-MP over the time period of 0 to 8 weeks with a total of 0.53% new bone per 1% CPC degradation for Ti-50/50-MP, compared to 0.50% for Ti-70/30-MP.

Bone-to-implant contact (BIC%)

Bone-to-implant contact was calculated for both time periods for each experimental group (**Table 3** & **Figure 6D**). At 4 weeks, similar marginal BIC values ($p>0.05$) of 2.4 ± 4.7% and 0.5 ± 0.7% were found for Ti-70/30-MP and Ti-50/50-MP, respectively. At 8 weeks, BIC values for

Table 3: Data (means +SD) for bone area, CPC area and BIC percentages at all time points

	Ti-70/30-MP		Ti-50/50-MP	
CPC area	**Mean(%) ± SD**	**n**	**Mean(%) ± SD**	**n**
week 0	81.0 ± 0.6	3	74.8 ± 0.7	3
week 4	60.9 ± 13.5	10	53.4 ± 17.3	10
week 8	35.2 ± 21.6	10	9.1 ± 9.7	10
Bone area	**Mean(%) ± SD**	**n**	**Mean(%) ± SD**	**n**
week 0	0.0 ± 0.0	0	0.0 ± 0.0	0
week 4	5.8 ± 4.9	10	8.3 ± 2.8	10
week 8	22.9 ± 5.2	10	35.0 ± 15.0	10
BIC	**Mean(%) ± SD**	**n**	**Mean(%) ± SD**	**n**
week 0	0.0 ± 0.0	0	0.0 ± 0.0	0
week 4	2.4 ± 4.7	10	0.5 ± 0.7	10
week 8	11.7 ± 14.6	10	11.9 ± 21.2	10

BIC, bone-to-implant contact; Ti, titanium MP, milled particles; SD, standard deviation

both experimental groups showed a temporal increase of 11.7 ±14.7% for Ti-70/30-MP and 11.9 ±21.2% for Ti-50/50-MP. Between the groups the difference at both time points was not significant. The increase of BIC% between 4 and 8 weeks was significant for Ti-70/30-MP (p=0.0371), but not for Ti-50/50-MP (p=0.0536).

Table 4: Relative bone formation per 1% degraded material

	Ti-70/30-MP	Ti-50/50-MP
0-4 weeks	0.29 %	0.39 %
4-8 weeks	0.67 %	0.60 %
0-8 weeks	0.50 %	0.53 %

Discussion

The aim of this study was to comparatively evaluate the in vitro degradation effects of dense PLGA microspheres and milled PLGA particles as porogens within CPC. We hypothesized that milled PLGA particles would evoke similar CPC/PLGA degradation compared to dense PLGA microspheres. Additionally, we aimed to examine the effect of PLGA porogen amount in CPC/PLGA via an in vivo rat femoral bone defect model to determine CPC degradation and bone formation. We hypothesized that a higher PLGA porogen amount would increase the porosity leading to faster degradation and consequently more bone formation in vivo. The main finding of the in vitro study was that equal amounts of either PLGA microspheres or milled PLGA particles resulted in similar CPC/PLGA degradation characteristics, while increased amount of PLGA porogens within CPC accelerated CPC/PLGA degradation. In vivo results further showed that CPC/PLGA with milled PLGA particles showed favorable bone responses without adverse events, for which a higher amount of milled PLGA particles (i.e. 50 versus 30 wt%) incorporated within the CPC accelerated both CPC degradation and new bone formation within the defect area.

Previous studies have shown that properties of PLGA porogens are critical for the characteristics of CPC/PLGA degradation [26,27,31]. For example, dense PLGA microspheres accelerate CPC degradation compared to hollow PLGA microspheres, with inferior additional effects related to PLGA molecular weight and chemical end-group modification [26,27]. In view of future clinical application of injectable CPC/PLGA for bone regenerative purposes and the cost-effectiveness thereof, our in vitro study proved similar efficacy, in terms of porosity and degradation, in both percentages for PLGA porogens generated in the form of microspheres and milled particles.

Our in vivo results of CPC/PGLA milled particles, in two weight percentages (wt%), showed a correlation between the degradation rate and new bone formation. Increasing the degradation rate of CPC with milled PLGA particles resulted in enhanced bone formation in a non load-bearing site in rats. The correlation between degradation and new bone formation was also found in the study of Felix Lanao et al. [26]. Using a distal femoral condyle model in, they examined the influence of varying the end-group functionalization (acid terminated versus end capped) as well as morphology (hollow versus dense) of PLGA microspheres. The rate of new bone formation after 12 weeks ranged from 5 to 55% and the increase in the amount of bone within the defect area could be related to a faster dissolution rate of the CPC. The cement area was significantly reduced for the CPC containing dense microspheres, which resulted in more bone formation compared to CPC with hollow microspheres.

Ruhé et al. [31] compared different wt% of CPC/PLGA in a non-critical sized calvarial rat model using PLGA microspheres. In contrast to our results, Ruhé et al. concluded that the 70/30 wt% shows the most favorable biological response, whereas the 50/50 wt% of CPC/PLGA had less osteogenic performance compared to lower levels of PLGA. The different defect site can

explain the discrepancy compared to our results, as the calvarial bone is different in terms of vascularization and fluid exchange compared to the femoral bone.

For osteoconductive materials, the ideal rate of degradation is balanced with the rate of new bone formation [16,36]. By performing calculations of the amount of cement being replaced by bone phase over time, we proved this balance to be tunable. Although faster degradation leads to more bone formation this was not consistent over time, as seen in the period of 4 to 8 weeks where the cement of Ti-50/50-MP degraded faster than bone could regenerate, indicating the difficulty of creating a degradable material with the optimal degradation rate at different time points.

For future clinical application PLGA milled particles appear to be promising as CPC porogen, as the manufacturing yield is much higher resulting in a more cost-effective process compared to PLGA microspheres. Furthermore, the different morphology and wider range of particle size with similar mean size do not significantly influence the outcome of CPC degradation and bone formation. Moreover, by varying the PLGA porogen wt% degradation rate of CPC can be tuned to desired demands such as for different defect sites and patient conditions.

Conclusion

The results of our in vitro study of equal amounts of either PLGA microspheres or milled particles showed similar scaffold morphology, CPC porosity and degradation. By increasing the amount of PLGA porogens within CPC accelerated CPC/PLGA degradation in vitro. The in vivo results of CPC/PLGA with milled PLGA showed favorable bone responses. Furthermore, a higher amount of milled PLGA particles (i.e. 50 versus 30 wt%) accelerated both CPC degradation and new bone formation. For future clinical application, milled PLGA particles appear to be promising as CPC porogen, since the manufacturing is more cost-effective while maintaining a favorable bone response. Moreover, by varying the PLGA porogen wt%, the degradation rate of CPC is tunable to meet desired demands of different defect sites and patient conditions.

Acknowledgements

The authors would like to acknowledge ms. Natasja van Dijk for her assistance with histological sectioning and dr. Ralf-Peter Herber and mr. Wilfred Versteeg (both from CAM Bioceramics B.V.) for kindly providing the α-TCP, milled PLGA and assistance with the fabrication of the CPC/PLGA and Ti-CPC/PLGA scaffolds.

References

1. Bongio M, van den Beucken JJJP, Leeuwenburgh SCG, Jansen JA. Development of bone substitute materials: from 'biocompatible' to 'instructive'. J Mater Chem 2010;20:8747-59.

2. Van der Stok J, Van Lieshout EM, El-Massoudi Y, Van Kralingen GH, Patka P. Bone substitutes in the Netherlands - a systematic literature review. Acta Biomater 2011;7:739-50.

3. Bohner M.Design of ceramic-based cements and putties for bone graft substitution. Eur Cell Mater. 2010;20:1-12.

4. Kolk A, Handschel J, Drescher W, Rothamel D, Kloss F, Blessmann M, et al. Current trends and future perspectives of bone substitute materials - from space holders to innovative biomaterials. J Maxillofac Surg 2012;40:706-18.

5. Low KL, Tan SH, Zein SH, Roether JA, Mourino V, Boccaccini AR. Calcium phosphate-based composites as injectable bone substitute materials. J Biomed Mater Res B Appl Biomater 2010;94:273-86.

6. Verron E, Bouler JM, Guicheux J. Controlling the biological function of calcium phosphate bone substitutes with drugs. Acta Biomater 2012;8:3541-51.

7. Zhang J, Liu W, Schnitzler V, Tancret F, Bouler JM. Calcium phosphate cements for bone substitution: chemistry, handling and mechanical properties. Acta Biomater 2014;10:1035-49.

8. LeGeros RZ. Properties of osteoconductive biomaterials: calcium phosphates. Clin Orthop Relat Res 2002:81-98.

9. Brown WE, Chow LC. A New Calcium-Phosphate Setting Cement. J Dent Res 1983;62:672.

10. Bohner M, Gbureck U, Barralet JE. Technological issues for the development of more efficient calcium phosphate bone cements: a critical assessment. Biomaterials 2005;26:6423-9.

11. Tamimi F, Sheikh Z, Barralet J. Dicalcium phosphate cements: brushite and monetite. Acta biomaterialia 2012;8:474-87.

12. Grossardt C, Ewald A, Grover LM, Barralet JE, Gbureck U. Passive and active in vitro resorption of calcium and magnesium phosphate cements by osteoclastic cells. Tissue Eng Part A 2010;16:3687-95.

13. Bohner M, Galea L, Doebelin N. Calcium phosphate bone graft substitutes: Failures and hopes. J Eur Ceram Soc 2012;32:2663-71.

14. LeGeros RZ. Biodegradation and bioresorption of calcium phosphate ceramics. Clin Mater 1993;14:65-88.

15. Koerten HK, van der Meulen J. Degradation of calcium phosphate ceramics. J Biomed Mater Res 1999;44:78-86.

16. Hannink G, Arts JJ. Bioresorbability, porosity and mechanical strength of bone substitutes: what is optimal for bone regeneration? Injury 2011;42 Suppl 2:S22-5.

17. Habraken WJ, Wolke JG, Jansen JA. Ceramic composites as matrices and scaffolds for drug delivery in tissue engineering. Adv Drug Deliv Rev 2007;59:234-48.

18. Karageorgiou V, Kaplan D. Porosity of 3D biomaterial scaffolds and osteogenesis. Biomaterials 2005;26:5474-91.

19. del Real RP, Ooms E, Wolke JG, Vallet-Regi M, Jansen JA. In vivo bone response to porous calcium phosphate cement. J Biomed Mat Res A 2003;65:30-6.

20. Ginebra MP, Espanol M, Montufar EB, Perez RA, Mestres G. New processing approaches in calcium phosphate cements and their applications in regenerative medicine. Acta Biomater 2010;6:2863-73.

21. del Real RP, Wolke JG, Vallet-Regi M, Jansen JA. A new method to produce macropores in calcium phosphate cements. Biomaterials 2002;23:3673-80.

22. Panzavolta S, Fini M, Nicoletti A, Bracci B, Rubini K, Giardino R, et al. Porous composite scaffolds based on gelatin and partially hydrolyzed alpha-tricalcium phosphate. Acta Biomater 2009;5:636-43.

23. Perez RA, Del Valle S, Altankov G, Ginebra MP. Porous hydroxyapatite and gelatin/hydroxyapatite microspheres obtained by calcium phosphate cement emulsion. J Biomed Mater Res B Appl Biomater 2011;97:156-66.

24. Qi X, Ye J, Wang Y. Alginate/poly (lactic-co-glycolic acid)/calcium phosphate cement scaffold with oriented pore structure for bone tissue engineering. J Biomed Mat Res A 2009;89:980-7.

25. Felix Lanao RP, Jonker AM, Wolke JG, Jansen JA, van Hest JC, Leeuwenburgh SC. Physicochemical properties and applications of poly(lactic-co-glycolic acid) for use in bone regeneration. Tissue Eng Part B Rev 2013;19:380-90.

26. Felix Lanao RP, Leeuwenburgh SC, Wolke JG, Jansen JA. Bone response to fast-degrading, injectable calcium phosphate cements containing PLGA microparticles. Biomaterials 2011;32:8839-47.

27. Felix Lanao RP, Leeuwenburgh SC, Wolke JG, Jansen JA. In vitro degradation rate of apatitic calcium phosphate cement with incorporated PLGA microspheres. Acta Biomater 2011;7:3459-68.

28. Klijn RJ, van den Beucken JJ, Felix Lanao RP, Veldhuis G, Leeuwenburgh SC, Wolke JG, et al. Three different strategies to obtain porous calcium phosphate cements: comparison of performance in a rat skull bone augmentation model. Tissue Eng Part A 2012;18:1171-82.

29. Link DP, van den Dolder J, Jurgens WJ, Wolke JG, Jansen JA. Mechanical evaluation of implanted calcium phosphate cement incorporated with PLGA microparticles. Biomaterials 2006;27:4941-7.

30. Lopez-Heredia MA, Sariibrahimoglu K, Yang W, Bohner M, Yamashita D, Kunstar A, et al. Influence of the pore generator on the evolution of the mechanical properties and the porosity and interconnectivity of a calcium phosphate cement. Acta Biomater 2012;8:404-14.

31. Ruhe PQ, Hedberg EL, Padron NT, Spauwen PH, Jansen JA, Mikos AG. Biocompatibility and degradation of poly(DL-lactic-co-glycolic acid)/calcium phosphate cement composites. J Biomed Mater Res A 2005;74:533-44.

32. Shabir A, Alhusban F, Perrie Y, Mohammed AR. Effects of ball-milling on PLGA polymer and its implication on lansoprazole-loaded nanoparticles. J Basic Clin Pharm 2011;2:71-82.

33. Sawkins MJ, Brown BN, BonassarLJ, Rose FRAJ, Shakesheff KM. Bioplotting of novel scaffold materials and complex constructs for osteochondral tissue engeneering. Eur Cell Mater 20012;24(4):36

34. Habraken WJ, Wolke JG, Mikos AG, Jansen JA. Injectable PLGA microsphere/calcium phosphate cements: physical properties and degradation characteristics. J Biomater Sci Polym Ed 2006;17:1057-74.

35. Bongio M, van den Beucken JJ, Leeuwenburgh SC, Jansen JA. Preclinical evaluation of injectable bone substitute materials. J Tissue Eng Reg Med 2012; Doi: 10.1002/term.1637 Epub ahead of print.

36. Chow LC. Next generation calcium phosphate-based biomaterials. Dent Mater J 2009;28:1-10.

37. Babis GC, Soucacos PN. Bone scaffolds: the role of mechanical stability and instrumentation. Injury 2005;36 Suppl 4:S38-44.

38. Gisep A, Wieling R, Bohner M, Matter S, Schneider E, Rahn B. Resorption patterns of calcium-phosphate cements in bone. J Biomed Mater Res A 2003;66(3):532-40.

39. Mantripragada VP, Lecka-Czernik B, Ebraheim NA, Jayasuriya AC. An overview of recent advances in designing orthopedic and craniofacial implants. J Biomed Mater Res A 2013;101:3349-64.

40. Albrekston T, Branemark PI, Hansson HA, Lindstrom J. OSSEOINTEGRATED TITANIUM IMPLANTS Requirements for Ensuring a Long-Lasting, Direct Bone-to-Implant Anchorage in Man. Acta Orthop Scand 1981;52:155-70.

41. De Kam DC, Busch VJ, Veth RP, Schreurs BW. Total hip arthroplasties in young patients under 50 years: limited evidence for current trends. A descriptive literature review. Hip Int 2011;21:518-25.

42. Morshed S, Bozic KJ, Ries MD, Malchau H, Colford JM, Jr. Comparison of cemented and uncemented fixation in total hip replacement: a meta-analysis. Acta Orthop 2007;78:315-26.

43. Gandhi R, Tsvetkov D, Davey JR, Mahomed NN. Survival and clinical function of cemented and uncemented prostheses in total knee replacement A META-ANALYSIS. J Bone Joint Surg Br 2009;91:889-95.

44. Brown TE, Harper BL, Bjorgul K. Comparison of cemented and uncemented fixation in total knee arthroplasty. Orthopedics 2013;36:380-7.

5

CHAPTER 5

Porous titanium scaffolds with injectable hyaluronic acid-DBM gel for bone substitution in a rat critical-sized calvarial defect model

van Houdt CIA, Cardoso DA, van Oirschot BAJA, Ulrich DJO, Jansen JA, Leeuwenburgh SCG, van den Beucken JJJP.

J Tissue Eng Regen Med. 2017 Sep;11(9):2537-2548.

Introduction

Bone grafting is a well-described surgical technique in trauma and reconstructive surgery to repair and augment (damaged or diseased) bone. The 'golden standard' in bone grafting still is transplantation of autologous bone, which possesses osteogenic (by osteogenic cells), osteoconductive (guiding bone growth), and osteoinductive properties (by growth factors and/or cells) (Dimitriou et al. 2011). Despite these desirable properties, several downsides accompany the use of autologous bone, including limited availability, increased donor site morbidity, and additional surgical efforts (Dimitriou et al. 2011, Finkemeier 2002). In view of these disadvantages, multiple biological and synthetic bone substitutes have been explored over the last few decades.

In addition to the desired biological properties related to bioactivity, osteoconductivity, and osteoinductivity (Bongio et al. 2010), a stable environment is mandatory to achieve uneventful bone healing (Calori et al. 2011, Giannoudis et al. 2007, Van der Stok et al. 2013). Bone grafts alone do not possess the mechanical properties to secure a stable environment under load-bearing conditions or at vital locations. Therefore, bone grafts are often combined with a stabilization method such as pins, screws, plates, and intramedullary nails, often made out of stainless steel or alloys of cobalt, titanium or tantalum (Mantripragada et al. 2013). Titanium is a metallic material that is successfully used for a wide variety of medical applications due to its strength, low density and resistance to corrosion (Mantripragada et al. 2013, Matassi et al. 2013). With the use of selective laser sintering (SLS), tailor-made titanium implants can be generated in the form of porous scaffolds, which can provide stability and are osteoconductive (Van der Stok et al 2013, Mantripragada et al. 2013).

Allograft is an alternative for autologous bone, although immunological issues need to be considered regarding safe use. Allografts have a long track of clinical use and already several approved products are commercially available, i.e. Bio-Oss® by Geistlich (devitalised bovine bone) or DBX™ by DePuy Synthes (demineralised human bone) (Gruskin et al. 2012, Kurien et al. 2013, Urist 1965). In view of demineralized bone matrix (DBM), demineralization can be achieved by treatment with either an acidic solution (e.g. hydrochloric acid, HCl), or a chelating agent (e.g. ethylene-diamine-tetra-acetic acid, EDTA) (Bowman 1996, Catanese III et al. 1999, Urist 1965, Urist et al. 1967).

To improve the handling properties of DBM during surgery, efforts have focused on combinations with other materials (Schwartz et al. 2007, Moore et al. 2011). Carriers, such as glycerol, poloxamer, gelatine, calcium sulphate, lecithin, and hyaluronic acid have been used to obtain DBM in different forms, such as pastes, putties and gels (Drosos et al. 2007). These carriers can help to improve moldability, which is especially of interest for minimally invasive surgical procedures. The composite material must maintain graft containment during wound irrigation and graft localization until stabilization by new bone formation. Hyaluronic acid (HA) is an interesting material for bone regeneration, as it is a natural derivative found

in the extracellular matrix of many tissues in the body. Interestingly, several studies already demonstrated that HA accelerates bone formation by stimulating mesenchymal stem cell differentiation (Aslan et al. 2006, Kim et al. 2007, Patterson et al. 2010, Sasaki et al. 1995). These favourable biological properties together with its ability to be used as a cohesive material render HA an interesting material to combine with other bone substitute materials.

The aim of this study was to evaluate the bone-forming capacity and biological performance of porous titanium scaffolds filled with novel injectable HA+DBM formulations in a critical-sized calvarial defect model in rats. A comparison was made for DBM obtained via treatment with either HCl or EDTA. Our hypothesis was that DBM demineralised by HCl would result better outcomes in terms of osteoinductivity and biodegradability compared to DBM demineralised by EDTA. Secondly, we hypothesized that implantation of these constructs in a critical-sized calvarial defect would enhance bone regeneration compared to empty scaffolds, with DBM demineralised by HCl performing better compared to DBM demineralised by EDTA.

Materials and Methods

Materials

DBM (EMCM B.V., Nijmegen, the Netherlands) used in this experiment was prepared using either HCl or EDTA as the demineralization agent (**Table 1**). After obtaining DBM granules from a tissue bank, these were sieved in order to obtain particles with size between 250 µm and 500 µm. The sieved DBM particles were tested for calcium content with the objective of obtaining a calcium concentration between 4% and 8%. The HA gel (pre-cross linked; HyalTech Ltd., Livingstone, UK) was used as received.

The preparation of the composite formulations was performed by mixing each component using a luer-lock syringe. The DBM particles (10, 20 or 30 wt%) were put in one of the syringes and the HA gel in the other syringe. After connecting the two syringes with a luer-lock adapter, the two different components were mixed for 20 cycles.

Swelling ratio

For evaluation of fold swelling ratios, pre-set HA+DBM_{HCl} and HA+DBM_{EDTA} formulations were prepared by injection of the formulation into Teflon® moulds (Ø 10 mm, height 5 mm) and leaving them to cure at room temperature for 4 hours. The formulations (n=3) were placed in 5 ml of conventional simulated body fluid (SBF; ionic concentrations: 142.0 mm Na^+, 5.0 mm K^+, 1.5 mm Mg^{2+}, 2.5 mm Ca^{2+}, 103,0 mm Cl^-, 4.2 mm HCO_3^{2-}, 1.0 mm HPO_4^{2-} and 0.5 mm SO_4^{2-}) according to the protocol from Kokubo (Kokubo et al. 1990). The mass of the formulations was measured before immersion, 4 hours after and 24 hours after immersion. The formulations were removed from the solution and the liquid removed with filtration paper. The calculated swelling ratio (SR) was obtained using the following formula:

SR % = ((Wt - W0)/W0) x 100%

where Wt is weight of the formulation after a respective immersion time (t) in SBF and W0 is the weight of the formulation before immersion.

Table 1: Material composition used for ***in vitro*** analysis

DBM Demineralization process	wt%	Name
HCl	10	HA+10%DBM_{HCl}
	20	HA+20%DBM_{HCl}
	30	HA+30%DBM_{HCl}
EDTA	10	HA+10%DBM_{EDTA}
	20	HA+20%DBM_{EDTA}
	30	HA+30%DBM_{EDTA}

Rheology

Immediately after curing and after 7 days immersion in SBF, the storage modulus G' and damping coefficient tan delta of the HA+DBM formulations (n=3) were tested using oscillatory rheometry (geometry diameter 8 mm, normal force < 0.03 N, constant stress of 0.05 Pa).

Preparation of constructs for critical-sized calvarial defect surgery

A porous titanium scaffold (Ø 8mm, height 2 mm; Future Innovations B.V., Boxmeer, the Netherlands) was used to contain the composite HA+DBM formulations within the calvarial defects and provide load-bearing strength. Preparation of the constructs was carried out in sterile conditions, using HA and DBM sterilized by gamma irradiation (>20 kGy; SynergyHealth B.V., Ede, the Netherlands). The composite formulations with 30% DBM were obtained as described above and the porous titanium scaffolds were loaded with the HA+DBM formulations using a sealed chamber using luer-lock. For in vivo implantation, the experimental groups Ti-HA+DBM_{HCl} and Ti-HA+DBM_{EDTA} were included.

Animals

Thirty-six healthy mature male Wistar rats (weight: ~250g) were used for this experiment for the calvarial defects, five of which were additionally used for subcutaneous implantation of DBM (Charles River Laboratories Nederland B.V., Leiden, the Netherlands). Housing was provided per pair in a standard macrolon type 3 cage with sawdust as bedding material. Standard rodent chow and bottled tap water was provided ***ad libitum***. The housing room was maintained under standard laboratory conditions (light-dark cycle: 12:12h, temperature: 20-22°C, relative humidity: 45-55%). All experiments were performed according to institutional, national and international guidelines for animal care and the Dutch law concerning animal welfare. The studies were reviewed and approved in advance by the Experimental Animal Committee of the Radboud University (RUDEC 2011-299 and RUDEC 2013-206).

Surgical procedures

Subcutaneous implantation

Preoperative pain medication was provided by an injection of Carprofen (5 mg/kg; Rimadyl®, Pfizer Animal Health, New York, USA) given at a minimum of 15 minutes before surgery. Anaesthesia was induced and maintained by isoflurane inhalation (Rhodia Organique Fine Ltd., Avonmouth, Bristol, UK) combined with oxygen. The surgical area was shaved with electric clippers and disinfection was performed using a povidone iodine solution. The rats were placed in ventral position on a heating mat. Small incisions of 1 cm were made on the back of the rats on each side parallel to the spine, after which subcutaneous pockets were created using blunt dissection with scissors. Before placing ~0.1 gram of DBM_{HCl} or DBM_{EDTA} in the subcutaneous pocket, several drops of 0.9% NaCl were added to the material to improve handling properties. For three animals, DBM_{HCl} (n=3) was placed on the right side and the DBM_{EDTA} (n=3) on the left side. For two animals, also 5 µg of BMP-2 (InductOs™, Medtronic BioPharma B.V., Heerlen, the Netherlands) was added to the 0.9% NaCl solution, for positive

control purposes, again placing DBM_{HCl} right (n=2) and DBM_{EDTA} left (n=2). The skin was closed with a resorbable suture (Vicryl® 4.0, Johnson & Johnson, St-Stevens-Woluwe, Belgium). Carprofen was given every 24 hours for a minimum of 2 days postoperatively.

Critical-sized calvarial defect

For the preparation of critical-sized calvarial defects, the same pre-operative pain

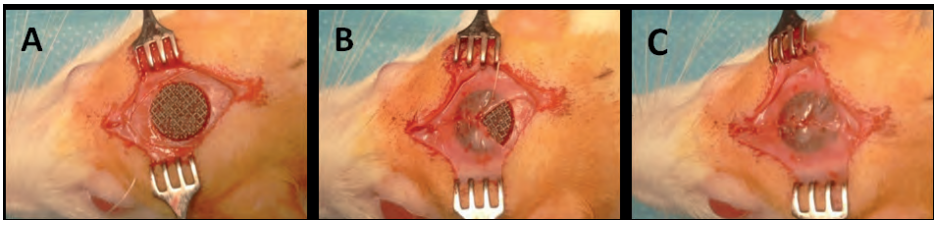

Figure 1: Representative intra-operative images of **A)** the construct placed inside the calvarial bone defect, **B)** halfway closure of the periosteum over the construct and **C)** full closure of the periosteum over the construct.

medication, anaesthesia and animal preparations were used as described for the subcutaneous implantation surgery. After confirmation of effective anaesthesia, the rats were intubated in order to maintain an open airway and secured anaesthesia during surgery and a pulse-oximeter was placed to monitor the capillary blood oxygen level during surgery. The calvarium was exposed using a longitudinal incision through the skin, starting just caudal from between the eyes to ventral between the ears. After retracting the skin sideways, the periosteum was incised from nasal bone to just caudal of the midsagittal crest. With an elevator, the periosteum was pushed laterally to fully expose the bone. To further ensure pain management and reduce blood loss, a solution of Xylocaine® 1% with epinephrine 1:100.000 (AstraZeneca B.V., Zoetermeer, the Netherlands) was used. After waiting for the solution to have effect, the bone was drilled with a dental trephine drill (8.4 mm inner and 8.5 mm outer diameter) at a maximum speed of 1500 rpm with constant cooling by saline dripping. By tilting the drill laterally left and right toward the more sloped sides, an all around even depth into the calvarial bone was ensured. To prevent damage of the underlying soft tissues, such as the sagittal blood vessels and dura, the depth of the drill was frequently checked during surgery by slight pressure on the edges of the defect. When the correct depth was reached all around the defect, the bone within the defect was carefully lifted, first from the lateral side to release the dura and blood vessels still (partially) attached. After blunt dissection with a gauze sideways, the bone was freed and removed from the defect. The defect area was then washed with saline and checked for haemostasis before a construct was placed into the defect (n=6 for each group).

After introducing a construct into a calvarial defect and ensuring correct positioning, first

the periosteum layer was closed (**Figure 1 A-C**), using a single continuous resorbable suture (Monocryl® 4.0, Johnson & Johnson, St-Stevens-Woluwe, Belgium). Then, the skin was closed with multiple single sutures of Monocryl (Johnson & Johnson). To diminish postoperative discomfort, for a minimum duration of 2 days postoperatively Buprenorfine (0.02 mg/kg; Temgesic®, Reckitt Benckiser Pharmaceuticals Ltd., Slough, UK) was given every 12 hours. Additionally, Carprofen (5 mg/kg; Rimadyl®, Pfizer Animal Health, New York, USA) was given every 24 hours for a minimum of 2 days postoperatively.

All animals were housed as described above and had free access to pellet food and water. In the initial postoperative period, the intake of water and food was monitored as well as the weight of the animals. In addition, the animals were observed for signs of pain, infection and proper activity and weighed again postoperatively once a week to identify significant weight loss (>20%) compared to preoperative body weight of each rat.

Explantation and histological processing

The animals were euthanized by CO_2 suffocation after implantation periods of 12 weeks for the animals that received subcutaneous implants and after implantation periods of 2 and 8 weeks for animals with calvarial defects. After the animals were euthanized, the subcutaneous implants and calvarial bones including the implanted materials were harvested and immediately fixed in 10% neutral buffered formalin solution. After 24 hours of fixation, the specimens were dehydrated in a graded series of ethanol.

Encapsulated materials from the subcutaneous pocket were processed for paraffin embedding. Using a microtome (Leica® RM 2165, Leica Microsystems, Nussloch Germany), thin sections (6 µm) were made and stained with haematoxylin-eosin (HE) or Elastic-Van Gieson (EVG).

All calvarial bone specimens were embedded in poly(methylmethacrylate) (pMMA). Sections were prepared in the coronal plane of ~10 µm using an inner circular diamond saw and constant cooling (Leica® Microsystems SP 1600, Nussloch, Germany). Staining was performed for each section with methylene blue and basic fuchsine.

Descriptive histology and histomorphometry

Histological slides, either from paraffin or pMMA sections, were examined by light microscopy (Zeiss® Imager Z1 Microscope, Carl Zeiss Microimaging GmbH, Göttingen, Germany). Descriptive histology and histomorphometry were performed based on colour discrimination and morphological aspect.

For the paraffin sections, HE and EVG staining allowed to distinguish soft tissue from bone or DBM. Descriptive analysis was performed on all sections to detect whether bone formation had occurred and if DBM remnants were present.

For sections of calvarial defects, the amount of bone formation and DBM remnants were quantitatively assessed using computer-based image analysis techniques (Leica® Qwin Microsystems Imaging Solutions Ltd., Cambridge, UK). Within the digitalized images of the sections, a rectangular region of interest (ROI) was set around the porous titanium constructs. The area percentage of newly formed bone and DBM remnants within this ROI was quantitatively measured for each section separately.

Statistical analysis

Data were presented as means with standard deviations (SD). The *in vitro* data and mean area percentages of new bone formation and DBM remnants were statistically analysed using GraphPad Prism 5 (GraphPad Software Inc., La Jolla, California USA). The statistical comparisons between experimental groups were analyzed with one-way analysis of variances (ANOVA) combined with a Tukey Multi Comparisons post-hoc test. All intra-group temporal analyses, *in vitro* and *in vivo,* and *in vivo* inter-group analyses on DBM-remnants were performed using unpaired ***t***-tests. Differences were considered significant at a p-value < 0.05.

Results

Materials

Swelling ratio

Figure 2 shows the effect of SBF immersion on the mass of HA+DBM formulations. All formulations displayed a mass increase after 4 hours, which continued after leaving the formulations for up to 24 hours in solution. The initial mass increased significantly between 4 and 24 hours for all formulations (HA+10%DBM_{HCl} p=0.0006, HA+20%DBM_{HCl} p=0.0119, HA+30%DBM_{HCl} p=0.0138, HA+10%DBM_{EDTA} p=0.0004, HA+20%DBM_{EDTA} p=0.0034 and HA+30%DBM_{EDTA} p=0.0056). Formulations with relatively less DBM displayed significantly more swelling. These differences were increased after 24 hours of immersion, when the formulations with 10% and 20% DBM_{HCl} or DBM_{EDTA} swelled significantly more than those with 30% DBM_{HCl} or DBM_{EDTA} ($p<0.001$ and $p<0.01$ respectively). The difference between 10% and 20% DBM_{HCl} was also significant after 24 hours ($p<0.05$).

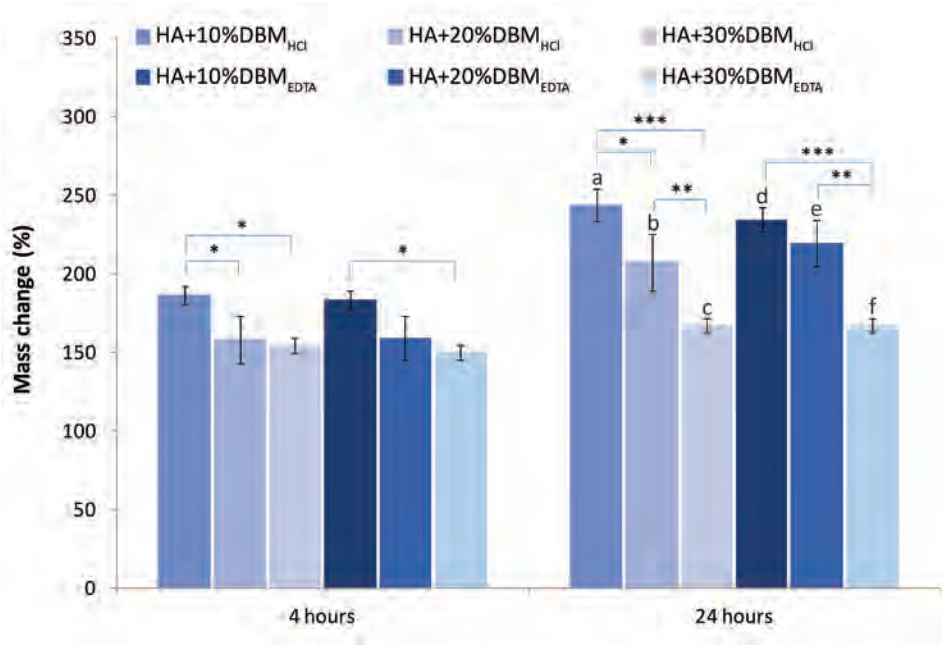

Figure 2: Percentage mass change, samples measured after 4 and 24 hours of immersion, compared to the mass measured before immersion (n=3); between the different formulas there is more mass change with a lower amount of DBM: *) p<0.05, **) p<0.01 and ***) p<0.001; between 4 and 24 hours the mass significantly increased for all formulations: a) p=0.0006, b) p=0.0119, c) p= 0.0138, d) p= 0.0004, e) p=0.0034 and f) p=0.0056.

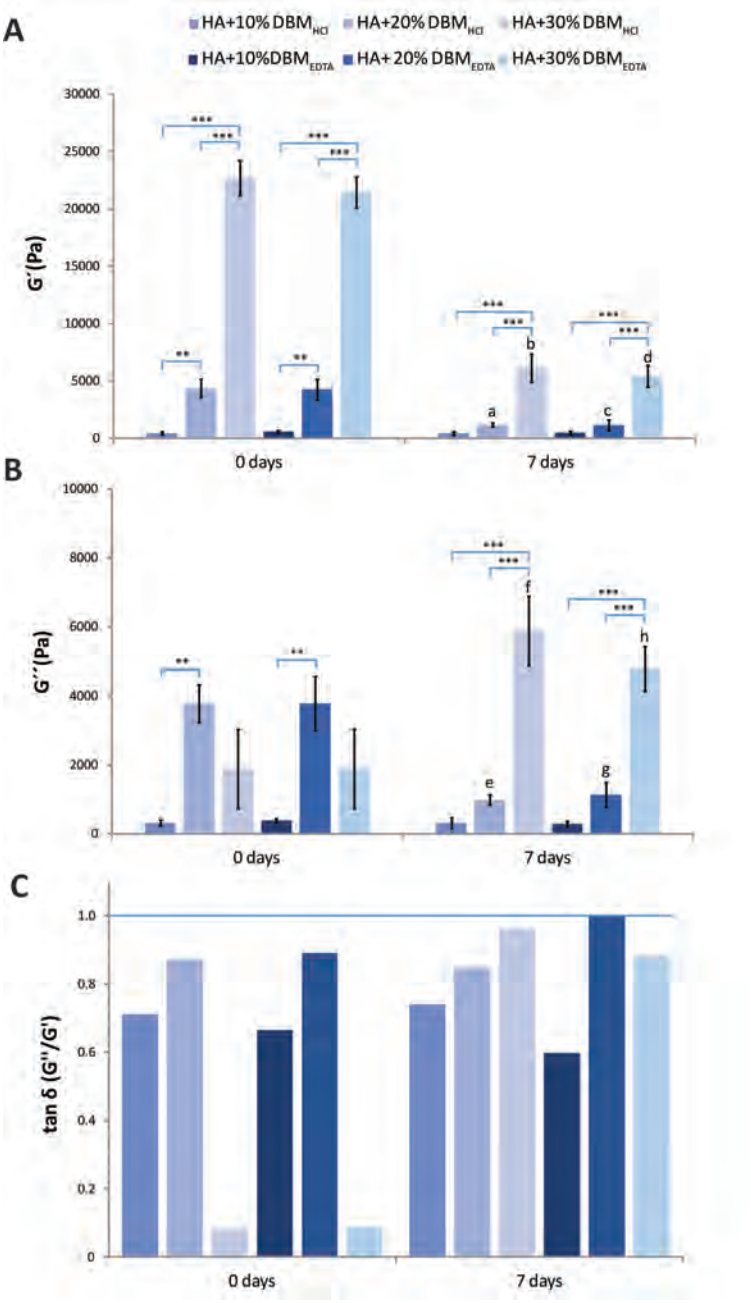

Figure 3: A) Storage moduli of experimental HA+DBM composites (G', n=3) (**p<0.01 and ***p<0.001; a, HA+20%DBM$_{HCl}$ p=0.0013, b, HA+30%DBM$_{HCl}$ p<0.0001, c, HA+20%DBM$_{EDTA}$ p= 0.0029, and d, HA+30%DBM$_{EDTA}$ p<0.0001). B) Loss moduli of experimental HA+DBM composites (G'', n=3) (**p<0.01, ***p<0.001; e p=0.0005, f, p=0.0052, g, p= 0.0030, and h, p=0.0098. C) Tan δ values (=G''/G') of experimental HA+DBM composites showing values below 1 for all composites.

Rheology

The storage modulus (G´) of each formulation strongly increased with increasing DBM content. All formulations had a tan delta value below 1, which reflects that solid-like behaviour dominated viscous behaviour for all formulations. After leaving each formulation for seven days in contact with SBF, a decrease in the storage modulus was observed for all formulations. The highest difference was observed for the formulations containing 30% of DBM, followed by the formulations containing 20% and 10%. No difference in viscoelastic parameters were observed related to the preparation method of the DBM particles.

Clinical observations of the experimental animals

In three of the total thirty-six animals receiving critical-sized calvarial defects, extensive haemorrhaging from the sagittal sinus occurred during surgery and the animals were euthanized whilst still under anaesthesia. All other animals recovered well from surgery and remained in good health during the entire experimental period without any signs of illness or postoperative wound healing complications. At sacrifice for all implantation periods, the wound areas showed no signs of inflammation or adverse tissue reaction and all porous titanium constructs were in correct position. All remaining constructs were retrieved and used for further analysis.

Descriptive histological evaluation

Subcutaneous implants

Light microscopy of the encapsulated materials from the subcutaneous pockets revealed that the positive controls of DBM_{HCl} and DBM_{EDTA} with BMP-2 showed newly formed bone (**Table 2**). None of the DBM specimens without BMP-2 (i.e. neither DBM_{HCl} nor DBM_{EDTA}) showed bone formation. Remnants of DBM were observed for all specimens containing DBM_{EDTA} (with or without BMP-2). In contrast, DBM_{HCl} remnants were observed for only 1 specimen in combination with BMP-2.

Critical-sized calvarial defects

Representative histological images for each experimental group are presented in **Figure 4**. Examination by light microscopy revealed periosteal swelling at 2 weeks, but this effect seemed to be fully recovered at 8 weeks for all implanted constructs. Further visual examination revealed no signs of severe inflammation or other adverse tissue reaction. New bone growing into the porous titanium construct could easily be distinguished by colour discrimination following the applied staining techniques. Since staining of DBM particles can appear similar to that of vital bone, attention was paid to cell morphology and presence of nuclei to distinguish between newly formed bone and DBM.

At 2 weeks, the defects with Ti-Empty constructs showed apparent bone formation in all sections, whereas Ti-HA+DBM_{HCl} and Ti-HA+DBM_{EDTA} only occasionally showed bone formation. For each experimental group, evidently more bone ingrowth and new bone formation was

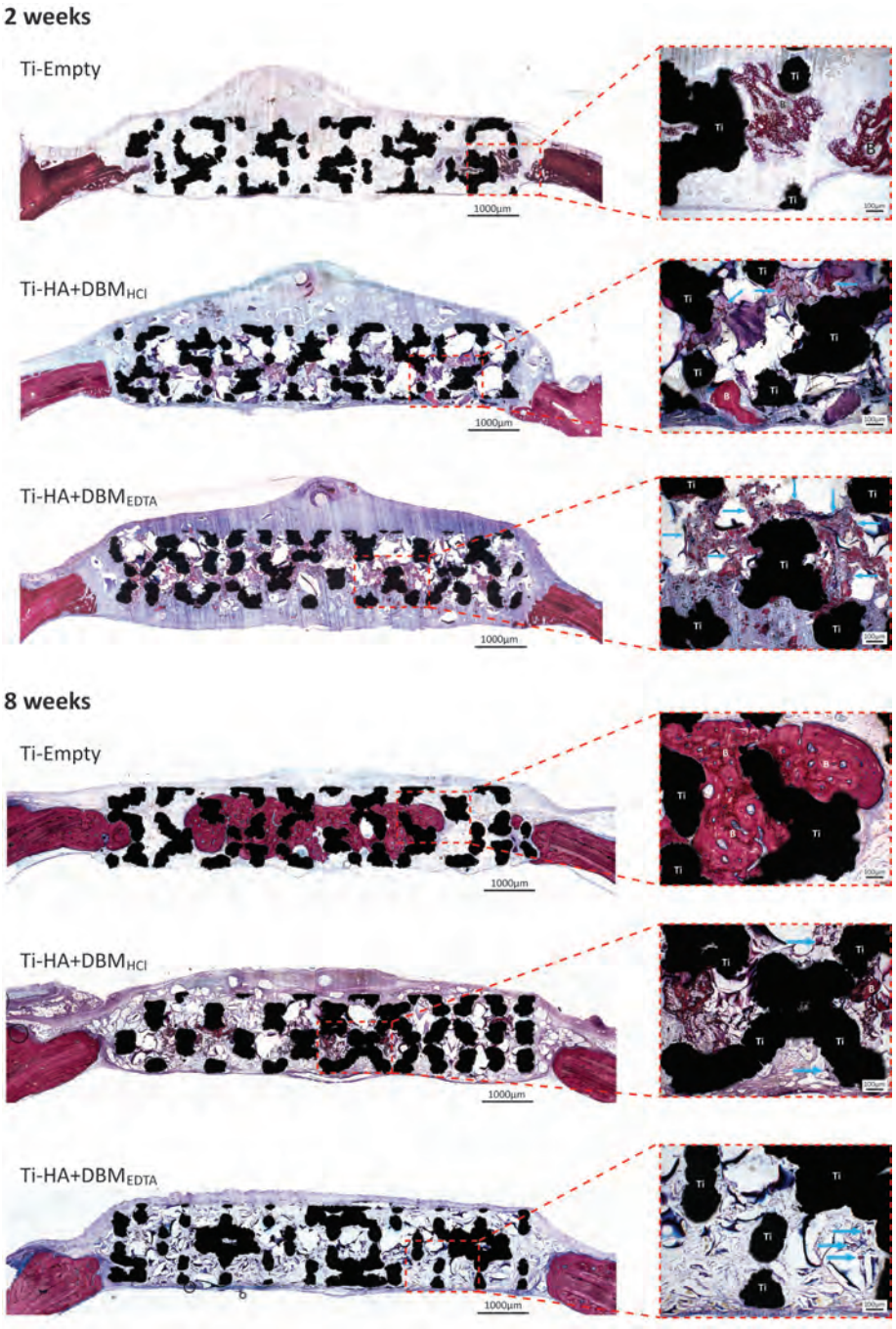

Figure 4: Representative histology for all experimental groups obtained by light microscopy, showing an overview (left panel) and detail (right panel) after 2 and 8 weeks of implantation; Ti= titanium, B= bone, blue arrows indicate DBM remnants.

observed after 8 weeks compared to 2 weeks implantation. For 8 week implantation, the most obvious bone ingrowth and formation was observed for Ti-Empty constructs. Bone ingrowth reached to the centre in several sections of Ti-Empty constructs, while remaining rather peripheral for both Ti-HA+DBM$_{HCl}$ and Ti-HA+DBM$_{EDTA}$ constructs.

Bone formation beneath the porous titanium construct was observed for four defects, all of which received Ti-HA+DBM$_{HCl}$ constructs. For these constructs, relatively limited bone formation was observed for two defects at 2 weeks and more prominent bone formation was seen in two cases at 8 weeks (**Figure 5**).

Histomorphometrical analysis

Newly formed bone (%) in critical-sized calvarial defects

Mean percentages of newly formed bone within the calvarial defects are shown in Figure 6. At 2 weeks, significantly more bone was present for Ti-Empty (3.8 ± 2.2%) compared to Ti-HA+DBM$_{HCl}$ (0.8 ±0.6%; p=0.022), but not to Ti-HA+DBM$_{EDTA}$ (1.5 ±1.3%; p>0.05). At 8 weeks, newly formed bone values were similar among the experimental groups (p>0.05), with values of 12.6 ± 13.0%, 3.7 ± 2.8%, and 1.5 ± 1.0% for Ti-Empty, Ti-HA+DBM$_{HCl}$, and Ti-HA+DBM$_{EDTA}$, respectively. The amount of bone formation improved significantly for both Ti-Empty and Ti-HA+DBM$_{HCl}$ from 2 to 8 weeks (p=0.0155 and p=0.134 respectively), while Ti-HA+DBM$_{EDTA}$ showed similar values for both implantation periods (p>0.05).

DBM remnants (%) in critical-sized calvarial defects

At 2 weeks, the percentage of DBM inside Ti-HA+DBM$_{HCl}$ and Ti-HA+DBM$_{EDTA}$ constructs showed significantly different values of 4.3 ± 2.0% and 7.2 ± 1.0%, respectively (p=0.0087; Figure 6). At 8 weeks, DBM remnants for Ti-HA+DBM$_{HCl}$ showed a similar value of 3.2 ± 1.5% (p>0.05), while Ti-HA+DBM$_{EDTA}$ showed a temporally reduced value for DBM remnants of 3.0 ± 1.8% (p<0.0003).

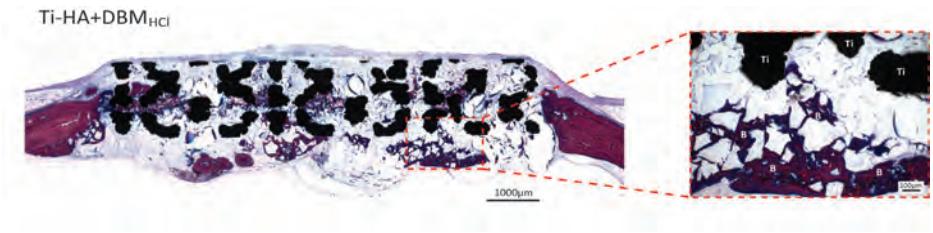

Figure 5: Representative histological image (light microscopy) of a Ti-HA+DBM$_{HCl}$ construct placed in a rat calvarial defect after 8 weeks of implantation. The panel on the right shows a magnification of bone formation below the construct. (Ti= titanium, B= bone).

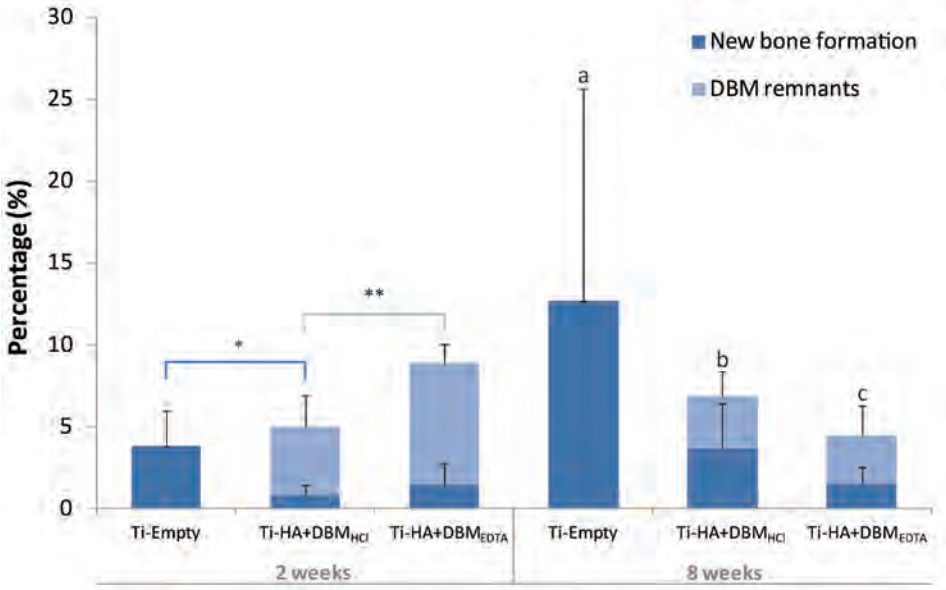

Figure 6: Histomorphometrical data on new bone formation (dark blue) and DBM remnants (light blue; in area percentage ± SD). *p=0.022 for new bone formation, **p= 0.01 for DBM remnants. Temporal differences on new bone formation: a, p=0.00155, b, p=0.0134; temporal difference on DBM remnants: c, p=0.003.

Discussion

The aim of this study was to evaluate the bone-forming capacity and biological performance of porous titanium scaffolds filled with novel injectable HA+DBM formulations in a critical-sized calvarial defect model in rats. A comparison was made for DBM obtained via a demineralization treatment with either HCl or EDTA. Our hypothesis was that DBM demineralised by HCl would result better outcomes in terms of osteoinductivity and biodegradability compared to DBM demineralised by EDTA. Secondly, we hypothesized that implantation of these constructs in a critical-sized calvarial defect would enhance bone regeneration compared to empty scaffolds, with EDTA demineralised by HCl performing better compared to DBM demineralised by EDTA. Our observations did not reveal any osteoinductive properties of DBM upon ectopic implantation. Bone forming capacity of the HA gel containing DBM was not enhanced compared to the osteoconductive properties of an empty porous titanium scaffold in a critical-sized calvarial defect in rats. Although the empty porous titanium scaffolds demonstrated an accelerated bone formation, similar amounts of newly formed bone were found after 8 weeks.

Using DBM in dry form can become cumbersome regarding its delivery to and containment at the surgical site (Moore et al. 2011, Schwartz et al. 2007). To overcome these handling difficulties, multiple types of carriers are available to improve applicability of DBM, such as pastes, putties and gels (Drosos et al. 2007). Several studies have shown that HA can improve bone formation and serve as a suitable carrier, i.e. for cells, growth factors or drugs (Aslan et al. 2006, Kim et al. 2007, Martinez-Sanz et al. 2011, Patterson et al. 2010). HA is one of the major components of the extracellular matrix found in the human body. Although predominantly present in soft tissues, it has been reported that HA is capable of accelerating new bone formation ***in vivo*** by stimulating the differentiation of mesenchymal stem cells (Aslan et al. 2006, Kim et al. 2007, Patterson et al. 2010, Sasaki et al. 1995). We examined different formulations of HA and DBM with 10, 20 or 30 wt% DBM that was demineralised using either treatment HCl or EDTA. Formulations with relatively more DBM displayed significantly less swelling. Moreover, the storage modulus (G´) of each formulation increased with increasing DBM content, thereby confirming that the DBM particles stiffened the formulations. The 30 wt% DBM prepared via treatment with either HCl or EDTA in HA-gel had the highest storage modulus and hence was chosen as composite formulation for the ***in vivo*** study. In view of loading and retention issues within the porous titanium scaffold used for the in vivo model, only experimental groups combining HA and DBM within the porous titanium scaffold were used.

DBM has the advantage of excellent biocompatibility and the demineralization process has been suggested to expose growth factors such as BMPs rendering DBM osteoinductive (Calori et al. 2011, Wildeman et al. 2007, Dinopoulos et al. 2006). The osteoinductive properties, however, can vary depending on the donor but also on DBM processing technique (Drosos et al. 2007, Li et al. 2000, Pietrzak et al. 2006, Schwartz et al. 2007, Takikawa et al. 2003). We

aimed to detect differences in degradation and osteoinductive capacity between DBM that was demineralised by treatment with either HCl or EDTA. Already in 1965, Urist examined bone allograft demineralised by HCl and EDTA and stated that it is an excellent substitute for a bone graft (Urist 1965). He noticed that bone demineralised by HCl showed a slightly more positive result of bone formation, measured by histological and radiographic assessment, compared to EDTA. Our subcutaneously implanted DBM_{HCl} and DBM_{EDTA} showed no bone formation. On the other hand, positive controls consisting of either type of DBM with the osteoinductive agent BMP-2 showed extensive bone formation. Regarding degradation of DBM at this ectopic site, less remnants of DBM_{HCl} remained after 8 weeks compared to DBM_{EDTA}. The concentration of osteoinductive agents in bone matrix can greatly vary per donor (Takikawa et al. 2003, Pietrzak et al. 2006). To eliminate this variable and better compare the two preparation methods within our study, only one DBM donor was used. Current donor selection for bone banking is mainly based on transmittable diseases and not on osteoinductive properties (Schwartz et al. 1998, Abbas et al. 2007). A correlation between increased age and low BMP amounts has been suggested (Lohmann et al. 2001, Schwartz et al. 1998, Traianedes et al. 2004, Zhang et al. 1997). However, there are controversial results and the exact underlying mechanism remains unknown (Pietrzak et al. 2006). To improve donor selection more research is needed to better predict osteoinductive properties of allografts. Although our DBM did not present osteoinductive properties, the reported favourable biocompatibility (Moore et al. 2011, Schwartz et al. 2007) and long clinical history of DBM as a bone substitute made us hypothesize that these types of DBM might still have a positive effect on bone formation orthotopically, when incorporated into the HA gel.

The critical-sized calvarial defect in rats is a reproducible and versatile model to observe bone forming capacity of bone substitute material. The model is convenient due to its easy accessibility and allows for evaluation of biomaterials for bone tissue engineering approaches within an orthotopic site (Mendes Brazão et al. 2010, Spicer et al. 2012). Several previous studies have shown bone growth within the defect already after 2 weeks after implantation (Jansen et al. 2005, MacIsaac et al. 2013). Depending of the different clinical relevance, animal models are chosen and should represent the complex environment in which clinical bone regeneration procedures are performed. The calvarial defect model can represent several cranial reconstructions in the clinic, representing a non-load bearing site. The calvarium is easily accessible, however, when creating a critical-sized bone defect, there is a risk of damaging the dura or sagital sinus. Generally, calvarial defects of 8 mm are considered as critically-sized (for extended evaluation periods; i.e. >6 weeks). Although 5 mm defects have been suggested, this only seems to be critical for shorter time periods up to 2 weeks (Porto et al. 2012, Spicer et al. 2012). In the past, ultrasonic devices have been used, only cutting hard tissue without damaging soft tissues due to the ultrasonic frequency. However, in the study of Bodde et al. it was found that calvarial defects created with an ultrasonic device had less optimal bone/implant contact compared with the trephine bur method at 4 weeks of implantation (Bodde et al. 2008). Therefore, for this study we chose to create an 8 mm defect using a trephine drill to test the optimal bone regenerative properties.

Histomorphometry was used in this study to perform bone volume analysis. There is an ongoing development based on analyses of bone mineral content by micro CT (Sehmisch et al. 2008, Umoh et al. 2009). This technique provides several advantages, such as comparison per subject over time (i.e. in vivo micro CT) and 3D reconstruction with quantitative measurements. Despite improvements in spatial resolution of micro CT images, the combination of histology and histomorphometry still provides the highest resolution. For future research, however, micro CT images can be considered simultaneously to compare and further improve understanding of both techniques.

In this study, we combined an injectable HA and DBM gel with a porous titanium scaffold. These scaffolds not only provided structural support, but additionally demonstrated osteoconductive capacity, as previously demonstrated by Van der Stok et al. (Van der Stok et al. 2013). In more detail, the osteoconductive properties of the porous titanium scaffold proved beneficial in a critical-sized segmental femoral defect in rats. Our result confirmed the osteoconductive properties of the titanium constructs, as bone reached the centre of the empty scaffolds after 8 weeks. Overall, our results showed bone formation into the scaffolds in all groups, but surprisingly both our composite constructs showed less bone formation compared to the empty scaffolds. Hypothetically, the lack of pores in the HA gel at time of implantation prevents osteogenic cells to reach the inner part of the material. The study of Klijn et al. showed the importance of instantaneously versus delayed porosity examined in a rat skull augmentation model. Instantaneous pores in calcium phosphate cement showed an increased amount of bone formation and also bone reached further into the scaffold (Klijn et al. 2010). The advantage of instantaneous porosity was hypothesized to allow direct influx of body fluid, proteins and cells. It was shown by Ruhé et al. using fluorochrome labelling that bone formation can already proceed into the macropores within one week after implantation (Ruhé et al. 2004). Our histological images showed that the titanium scaffolds with HA gel had little bone ingrowth and still contained HA gel after 8 weeks. Most likely the HA gel with DMB inside the scaffold hampered tissue ingrowth and hence was limiting the osteoconductive properties of the titanium and DBM within the constructs.

The limited infiltration of cells into the gel was also observed by others (Bongio et al. 2013, Nejadnik et al. 2014). In the study by Nedjadnik et al., covalently cross-linked HA gel with and without bisphosphonate (BP) or calcium phosphate (CaP), respectively denoted as HA, HA_{BP} and HA+CaP, were compared to non-covalent cross-linked HA gel with BP and CaP (HA_{BP}·CaP) in rats subcutaneously and in a femoral bone defect model. Bone formation was detected for all gels only at the bone-material interface after 1 week. However, after 4 weeks the HA_{BP}·CaP showed newly-formed trabecular-like bone homogeneously interspersed throughout the material. It was suggested that the more homogeneous nanostructure contributed to a more stable environment for attachment of osteoprogenitor cells resulting in a more homogeneous degradation.

Beside the possible lack of pores and inhomogeneous degradation, other issues need to

be considered when working with HA as a carrier. Previous studies have proven that HA gel alone is not a suitable bone substitute material and several explanations are given (Aslan et al. 2006, de Brito Bezerra et al. 2012, Maus et al. 2008, Mendes Brazão et al. 2010). De Brito Bezerra et al. examined a HA gel and collagen sponge in a critical-sized calvarial defect and also found no additional effect of the HA gel (de Brito Bezerra et al. 2012). In their reflection, this issue was related to HA being available in different molecular weights and this having an effect on the osteogenesis. In the study of Maus et al., a HA gel with or without BMP-2 was used in a femoral defect in sheep (Maus et al. 2008). Less bone formation was found compared to autologous graft and even slightly less to an empty defect. It was argued that the effect of HA is transmitted by different receptors and that HA stimulates the expression of RANKL as proven by Cao et al. (Cao et al. 2005). This could explain the negative effect of the HA gel, as RANKL is associated with osteoclast differentiation and activation and thus indicates the need for an osteoinductive addition to the gel. Maus et al. postulated that possibly the BMP-2 group did not contain BMP-2 due to washing of the material intra-operatively and therefore there was a lack of bone growth.

Our data showed no significant difference in amount of bone formation between the two preparation methods of DBM when placed in a critical-sized calvarial defect. However, there was a significant temporal increase in bone growth for Ti-HA+DBM_{HCl} constructs from 2 to 8 weeks of implantation. Moreover, only in Ti-HA+DBM_{HCl} constructs bone was formed outside the scaffold. These data corroborate the first results of Urist (Urist 1965) and it could indicate that DBM_{HCl} degrades faster and is slightly more osteopromotive compared to DBM_{EDTA}. The amount of DBM_{EDTA} remnants at 2 weeks was significantly lower in comparison to DBM preparation with HCl, however, after 8 weeks both DBM amounts were reduced to similar levels. This indicates that within the first two weeks after implantation, DBM_{HCl} degrades faster compared to DBM_{EDTA}. Also ectopically the results showed DBM_{HCl} to have a faster degradation rate than DBM_{EDTA}. The exact underlying mechanism of this effect remains unclear, however, this could possibly explain the significant temporal increase of bone formation when using DBM_{HCl}.

Conclusion

Our results showed under the current experimental conditions no osteoinductive capacity of ectopically placed DBM. Hyaluronic gel composite with DBM in titanium constructs was generally well tolerated in the rat calvarial defects. Bone forming capacity of the gel containing DBM was not enhanced compared to the osteoconductive properties of an empty porous titanium scaffold.

Acknowledgements

The authors thank the funding of this research by the European Community's Seventh Framework Programme (MultiTERM, grant agreement No. 238551) and BONE-IP research program of the BioMedical Materials institute, co-funded by the Dutch Ministry of Economic Affairs, Agriculture and Innovation (BONE-IP project P2.04).

References

1. Abbas G, Bali SL, Abbas N, Dalton DJ. 2007, Demand and supply of bone allograft and the role of the orthopaedic surgeons, ***Acta Orthop Belg***, 73: 507-11

2. Aslan M, Simsek G, and Dayi E. 2006, The effect of hyaluronic acid-supplemented bone graft in bone healing: experimental study in rabbits, ***J Biomater Appl***, 20: 209-20

3. Bodde EW, Boerman OC, Russel FG, Mikos AG, Spauwen PH, Jansen JA. 2008, The kinetic and biological activity of different loaded rhBMP-2 calcium phosphate cement implants in rats. ***J Biomed Mater Res A***, 87: 780-91

4. Bowman SM, Zeind J, Gibson LJ, Hayes WC, McMahon TA. 1996, The tensile behavior of demineralized bovine cortical bone, ***J Biomech***, 29: 1497-501

5. Bongio M, van den Beucken JJJP, Leeuwenburgh SCG, Jansen JA. 2010, Development of bone substitute materials: from 'biocompatible' to 'instructive', ***J Mater Chem***, 20: 8747-59

6. Bongio M, Nejadnik MR, Birgani ZT, Habibovic P, Kinard LA, Kasper FK, Mikos AG, Jansen JA, Leeuwenburgh SCG, van den Beucken JJJP. 2013, In Vitro and In Vivo Enzyme-Mediated Biomeineralization of Oligo(poly(ethylene glycol) Fumarate Hydrogels, ***Macromol Biosci***, 13: 777-88

7. Calori GM, Mazza E, Colombo M, Ripamonti C. 2011, The use of bone-graft substitutes in large bone defects: any specific needs?, ***Injury***, 42 Suppl 2: S56-63

8. Cao J J, Singleton PA, Majumdar S, Boudignon B, Burghardt A, Kurimoto P, Wronski PJ, Bourguignon LY, Halloran BP. 2005, Hyaluronan increases RANKL expression in bone marrow stromal cells through CD44, ***J Bone Miner Res***, 20: 30-40

9. Catanese III J, Iverson EP, Ng RK, Keaveny TM. 1999, Heterogeneity of the mechanical properties of demineralized bone, ***J Biomech***, 32: 1365-9

10. de Brito Bezerra B, Mendes Brazao MA, de Campos ML, Casati MZ, Sallum EA, Sallum AW. 2012, Association of hyaluronic acid with a collagen scaffold may improve bone healing in critical-size bone defects, ***Clin Oral Implants Res***, 23: 938-42

11. Dimitriou R, Mataliotakis GI, Angoules AG, Kanakaris NK, Giannoudis PV. 2011, Complications following autologous bone graft harvesting from the iliac crest and using the RIA: a systematic review, ***Injury***, 42 Suppl 2: S3-15

12. Dinopoulos HTH, Giannoudis PV. 2006, Safety and efficacy of use of deminieralised bone matrix in orthopaedic and trauma surgery, ***Expert Opin Drug Saf,*** 5: 847-66

13. Drosos GI, Kazakos KI, Kouzoumpasis P, Verettas D-A. 2007, Safety and efficacy of commercially available demineralised bone matrix preparations: A critical review of clinical studies, ***Injury***, 38 Suppl 4: S13-S21

14. Finkemeier CG. 2002, Bone-grafting and bone-graft substitutes, ***J Bone Joint Surg Am***, 84-A: 454-64

15. Giannoudis PV, Einhorn TA, Marsh D. 2007, Fracture healing: the diamond concept, ***Injury***, 38: S3-6

16. Gruskin E, Doll BA, Futrell FW, Schmitz JP, Hollinger JO. 2012, Demineralized bone matrix in bone repair: history and use, ***Adv Drug Deliv Rev***, 64: 1063-77

17. Jansen JA, Vehof JW, Ruhé PQ, Kroeze-Deutman H, Kuboki Y, Takita H, Hedberg EL, Mikos AG. 2005, Growth factor-loaded scaffolds for bone engineering. ***J Control Release***, 101: 127-36

18. Kim J, Kim IS, Cho TH, Lee KB, Hwang SJ, Tae G, Noh I, Lee SH, Park Y, Sun K. 2007, Bone regeneration using hyaluronic acid-based hydrogel with bone morphogenic protein-2 and human mesenchymal stem cells, ***Biomaterials***, 28: 1830-7

19. Klijn RJ, van den Beucken JJJP, Félix Lanao RP, Leeuwenburgh SCG, Wolke JGC, Meijer GJ, Jansen JA. 2012, Three different strategies to obtain porous calcium phosphate cements: Comparison of performance in a rat skull bone augmentation model, ***Tissue Eng Part A***, 18: 1171-82

20. KokuboT, Kushitani H, Sakka S, Kitsugi T, Yamamuro T. 1990, Solutions able to reproduce in vivo surface-structure changes in bioactive glass-ceramic A-W3, ***J Biomed Mater Res***, 24: 721-34

21. Kurien T, Pearson RG, Scammell BE. 2013, Bone graft substitutes currently available in orthopaedic practice. THE EVIDENCE FOR THEIR USE, ***Bone Joint J***, 95-B: 583-97

22. Li H, Pujic Z, Xiao Y, Bartold PM. 2000, Identification of bone morphogenetic proteins 2 and 4 in commercial demineralized freeze-dried bone allograft preparations: pilot study, ***Clin Implant Dent Relat Res***, 2: 110-7

23. Lohmann CH, Andreacchio D, Koster G, Carnes DL Jr, Cochran DL, Dean DD, Boyan BD, Schwartz Z. 2001, Tissue response and osteoinduction of human bone grafts in vivo, ***Arch Orthop Trauma Surg***, 121: 583-90

24. Mantripragada VP, Lecka-Czernik B, Ebraheim NA, Jayasuriya AC. 2013, An overview of recent advances in designing orthopedic and craniofacial implants, ***J Biomed Mater Res A***, 101: 3349-64

25. Martinez-Sanz E, Ossipov DA, Hilborn J, Larsson S, Jonsson KB, Varghese OP. 2011, Bone reservoir: Injectable hyaluronic acid hydrogel for minimal invasive bone augmentation, ***J Control Release***, 152: 232-40

26. Matassi F, Botti A, Sirleo L, Carulli C, Innocenti M. 2013, Porous metal for orthopedic implants, ***Clin Cases Miner Bone Metab***, 10: 111-5

27. Maus U, Andereya S, Gravius S, Siebert CH, Ohnsorge JA, Niedhart C. 2008, Lack of effect on bone healing of injectable BMP-2 augmented hyaluronic acid, ***Arch Orthop Trauma Surg***, 128: 1461-6

28. MacIsaac ZM, Levine BA, Smith DM, Cray JJ, Shaw M, Naran S, Kinsella C, Mooney MP, Cooper GM, Losee JE. 2013, Novel animal model of calvarial defect: part IV. Reconstruction of a calvarial wound complicated by durectomy, ***Plast Reconstr Surg,*** 131: 512-9

29. Mendes Brazão MA, de Brito Bezerra B, Casati MZ, Sallum EA, Sallum AW. 2010, Hyaluronan does not improve bone healing in critical size calvarial defects in rats - a radiographic evaluation, ***Braz J Oral Sci***, 9: 124-7

30. Moore ST, Katz JM, Zhukauskas RM, Hernandez RM, Lewis CS, Supronowicz PR, Gill E, Grover SM, Long NS, Cobb RR. 2011, Osteoconductivity and osteoinductivity of Puros(R) DBM putty, ***J Biomater Appl***, 26: 151-71

31. Nejadnik MR, Yang X, Bongio M, Alghamdi HS, van den Beucken JJJP, Huysmans MC, Jansen JA, Hilborn J, Ossipov D, Leeuwenburgh SCG. 2014, Self-healing hybrid nanocomposites consisting of bishposphonated hyaluronan and calcium phosphate nanoparticles, ***Biomaterials***, 35: 6918-29

32. Patterson J, Siew R, Herring SW, Lin AS, Guldberg R, Stayton PS. 2010, Hyaluronic acid hydrogels with controlled degradation properties for oriented bone regeneration, ***Biomaterials***, 31: 6772-81

33. Pietrzak WS, Woodell-May J, McDonald N. 2006, Assay of Bone Morphogenetic Protein-2, -4, and -7 in Human Demineralized Bone Matrix, ***J Craniofac Surg***, 17: 84-90

34. Porto GG, Vasconcelos BCdE, Andrade ESdS, Carneiro SCdAS, Frota MSM. 2012, Is a 5 mm rat calvarium defect really critical?, ***Acta Cir Bras***, 27: 757-60

35. Ruhé PQ, Kroese-Deutman HC, Wolke JG, Spauwen PH, Jansen JA. 2004, Bone inductive properties of rhBMP-2 loaded porous calcium phosphate cement implants in cranial defects in rabbits, ***Biomaterials***, 25: 2123-32

36. Sasaki T, Watanabe C. 1995, Stimulation of osteoinduction in bone wound healing by high-molecular hyaluronic acid, ***Bone***, 16: 9-15

37. Schwartz Z, Goldstein M, Raviv E, Hirsch A, Ranly DM, Boyan BD. 2007, Clinical evaluation of demineralized bone allograft in a hyaluronic acid carrier for sinus lift augmentation in humans: a computed tomography and histomorphometric study, ***Clin Oral Implants Res***, 18: 204-11

38. Schwartz Z, Somers A, Mellonig JT, Carnes DL Jr, Dean DD, Cochran DL, Boyan BD. 1998, Ability of Commercial Demineralized Freeze-Dried Bone Allograft to Induce New Bone Formation Is Dependent on Donor Age But Not Gender, ***J Periodontol***, 69: 470-8

39. Sehmisch S, Dullin C, Zaroban A, Tezval M, Rack T, Scmelz U, Seidlova-Wuttke D, Dunkelberg H, Wuttke W, Marten K, Stuermer K-M, Stuermer EK. 2008, The Use of Flat Panel Volumetric Computed Tomography (fpVCT) in Osteoporosis Research, ***Acad Radiol***, 16: 394-400

40. Spicer PP, Kretlow JD, Young S, Jansen JA, Kasper FK, Mikos AG. 2012, Evaluation of bone regeneration using the rat critical size calvarial defect, ***Nat Protoc***, 7: 1918-29

41. Takikawa S, Bauer TW, Kambic H, Togawa D. 2003, Comparative evaluation of the osteoinductivity of two formulations of human demineralized bone matrix, ***J Biomed Mater Res A***, 65A: 37-42

42. Traianedes K, Russell JL, Edwards JT, Stubbs HA, Shanahan IR, Knaack D. 2004, Donor age and gender effects on osteoinductivity of demineralized bone matrix, ***J Biomed Mater Res***, 70B: 21-9

43. Umoh JU, Sampaio AV, Welch I, Pitelka V, Goldber HA, Underhill TM, Holdsworth DW. 2009, In vivo micro-CT analysis of bone remodeling in a rat calvarial defect model, ***Phys Med Biol,*** 54: 2147-61

44. Urist MR. 1965, Bone: formation by autoinduction, ***Science***, 150: 893-9

45. Van der Stok J, Van der Jagt OP, Amin Yavari S, De Haas MF, Waarsing JH, Jahr H, Van Lieshout EM, Patka P, Verhaar JA, Zadpoor AA, Weinans H. 2013, Selective laser melting-produced porous titanium scaffolds regenerate bone in critical size cortical bone defects, ***J Orthop Res***, 31: 792-9

46. Wildemann B, Kadow-Romacker A, Haas NP, Schmidmaier G. 2007, Quantification of various growth factors in different demineralized bone matrix preparations, ***J Biomed Mater Res A***, 81: 437-42

47. Zhang M, Powers RM Jr, Wolfinbarger L Jr. 1997, Effect(s) of the demineralization process on the osteoinductivity of demineralized bone matrix, ***J Periodontol,*** 68: 1085-92

6

CHAPTER 6

Alendronate release from calcium phosphate cement for bone regeneration in osteoporotic conditions

van Houdt CIA, Cardoso DA, van Oirschot BAJA, Ulrich DJO, Jansen JA, Leeuwenburgh SCG, van den Beucken JJJP.

J Tissue Eng Regen Med. 2017 Sep;11(9):2537-2548

Introduction

Osteoporosis is the most frequent human metabolic bone disorder affecting over 75 million people in Europe, Japan and the USA [1]. As such, osteoporosis represents a major health problem in terms of compromising bone strength and increasing the risk of bone fractures [2]. In patients suffering from osteoporosis, the bone healing process is negatively influenced [3], which challenges the treatment of bone defects or bone fractures. Bone grafting is a widely-used therapy to reconstruct bone defects, although it remains a challenging problem particularly for compromised conditions such as osteoporosis. Autologous bone transplantation can be employed to regenerate bone defects, but its use is hampered by the need for additional surgical procedures and potential limitations in bone quality and quantity. Alternatively, the use of allografts and xenografts is related to immunological issues and an increased risk of cross-species disease transmission [4,5]. In contrast, the use of synthetic biomaterials as a bone substitute has many advantages, including off-the-shelf availability in various shapes and sizes. Still, the biological performance of synthetic bone substitutes is inferior to autologous bone [6]. Consequently, optimization of the biological performance of synthetic bone substitutes via e.g. the release of biologically active factors is a highly explored field within bone biomaterials research [7].

Osteoporosis is characterized by reduced bone mineral density causing lower bone mass and deterioration of bone tissue micro-architecture. This results from an imbalance between the continuous bone formation and resorption during bone remodeling and an altered variety of proteins in the extracellular matrix of the bone [8,9]. Osteoporosis is primarily observed after menopause in women, with increasing age in both women and men (ratio of 2:1), or secondary by chronic predisposing medical problems [10]. World-wide life expectancy has increased over the last couple of decades for both men and women, resulting in an aging population [1,2,11,12]. This increase in elderly people is expected to continue, ultimately resulting in a further increased need of reliable bone grafting materials for elderly, osteoporotic patients.

The mostly prescribed medication for osteoporosis are bisphosphonates [13]. The regular route of administration is oral, for which it has been observed that 24h excretion levels by the renal system reach percentages of 38% to 73% [14]. The major disadvantage of oral administration of bisphosphonates is their poor absorption from the gastro-intestinal tract, generally less than 1% [15]. This is further negatively influenced when the stomach contains food or has the presence of calcium [15]. The bisphosphonate fraction remaining in the body predominantly localizes to areas with high bone turnover by exploiting its affinity to mineral within the bone extracellular matrix. After localizing to these areas, bisphosphonates can remain within the bone for many years. Among the different types of bisphosphonates, ALN and risedronate are frequently chosen because these both increase bone mineral density, reduce the risk of fracture, and are well tolerated [16].

In view of the aforementioned, optimization of synthetic bone substitutes with bisphosphonates to locally adjust the imbalance in bone remodeling seems a straightforward approach to aid bone regeneration in osteoporotic conditions. Among the currently available synthetic bone substitutes, calcium phosphate (CaP) based materials are inorganic biomaterials that show high similarity to bone tissue by resembling the mineral phase of bone and are already popular implant materials in several fields of surgery [17]. Calcium phosphate cement (CPC) represents a suitable scaffold material for bone regenerative treatment [18,19]. CPC has the advantage of being injectable and moldable, for which it allows perfect filling directly into a bone defect or by pre-setting it in a specifically designed mold fitted to the defect requirements. When adding porogens, (e.g. poly(lactic-co-glycolic acid) (PLGA) microspheres) to CPC, controlled degradation of the material can be obtained as well as the possibility to release bioactive agents, e.g. osteoinductive growth factors or therapeutic drugs [18,20]. Previous ***in vitro*** studies proved a successful incorporation of bisphosphonates into ceramic bone substitutes [21-33]. Generally, these studies showed altered but still acceptable material properties, steady release of the bisphosphonate with inhibition of osteoclasts and stimulation of osteoblast. Only a few reported on ceramic implants used ***in vivo*** [34-37]. These all showed positive results of the material on bone formation.

Here, we used the anti-osteoporotic drug ALN to functionalize CPC/PLGA. We characterized the material morphologically and crystallographically, analyzed setting time and mechanical properties, and determined ALN release kinetics. In addition, we used a femoral condyle bone defect model in osteoporotic rats to comparatively evaluate the biological performance of ALN-loaded CPC/PLGA. We hypothesized that loading CPC/PLGA composites with ALN would (i) not critically affect material morphology and crystallography, (ii) promote controlled ALN release, and hence (iii) enhance the biological performance of CPC/PLGA in osteoporotic conditions by increasing bone formation rate and volumes.

Materials and Methods

Materials

Alpha tri-calcium phosphate (α-TCP) was provided by Cam Bioceramics B.V. (mean particle ~4.0 µm; Leiden, The Netherlands). Poly(DL-lactic-co-glycolic acid) PLGA particles (containing both a lactic and glycolic weight percentage of 50%; particle size ~60 µm) was obtained from Corbion (PLGA, Purasorb®, Gorinchem, The Netherlands). Carboxymethylcellulose (CMC) was purchased from Kelco (Georgia, USA) and Alendronate (ALN) was purchased from AK Scientific (Union City, California, USA).

Preparation of CPC/PLGA and CPC/PLGA-ALN composites

CPC/PLGA composites were prepared by weighing 0.597 g of α-TCP, 0.398 g of PLGA and 0.005 g of CMC in a beaker. Subsequently, the liquid component (4% NaH_2PO_4 solution) was added in a liquid/power ratio of 0.50 and the composition was mixed with a spatula. Afterwards, the composite was injected, using a 2 ml syringe (BD Plastipakt, Becton Dickinson S.A., Madrid, Spain), into teflon molds to obtain cylinders of 5 mm x 3 mm (diameter and height) for ***in vitro*** analysis. For mechanical tests, cylinders of 6 mm x 12 mm (diameter and height) were prepared utilizing different molds.

ALN was introduced into CPC/PLGA scaffolds via the liquid CPC component. Briefly, ALN was dissolved in 4% NaH_2PO_4 at different concentrations (range: 0-6 wt% for setting time investigations) and the pH was adjusted to ~7.4. The selected experimental groups are presented in Table 1.

For ***in vivo*** experiments, pre-set cylindrical CPC/PLGA composites (2.5 mm in diameter and 5 mm in height) were prepared, either or not containing ALN (2 µg/ml for the CPC/PLGA-lowALN) within the liquid component. This concentration corresponds to 0.5 wt.% ALN. After setting for 24h at room temperature, composites were removed from the mold and sterilized using ethylene oxide (Synergy Health, Venlo, The Netherlands).

Material characterization

Setting time

The setting time of CPC-formulations was determined using the Gillmore needle method at 37°C, as described previously (ASTM C266, 1999) [67]. For this purpose, a bronze block containing six holes was used as a mold (6 mm in diameter, 12 mm in height). The different formulations (n=3) were inserted into the mold in order to assess the initial and final setting.

Morphology

Immediately after setting, the samples were mounted on stubs with carbon tape and sputter coated with gold. SEM (SEM, JEOL 6310) was performed to examine the structural morphology of the composites.

Physico-chemical analysis

Immediately after preparation and setting, the samples were pulverized and submitted to Fourier transform infrared spectroscopy (FTIR; Perkin-Elmer 1700, UK). FTIR was performed to characterize the chemical bonds present in the samples. Analyses were done using pulverized samples in the range of 520-4000 cm^{-1} with a resolution of 2 cm^{-1}. The samples were scanned 100 times for each FTIR measurement and the spectrum acquired was the average of all these scans.

X-ray diffraction (XRD, Cu-Ka, 45 kV, 30 mA, Philips BV, the Netherlands) patterns of pulverized samples were collected (2θ range: 20-40°) to crystallographically characterize the phases. XRD evaluation was done at days 0, 3, 7 and 148 after incubation in 1.0 ml of phosphate buffered saline solution (PBS; pH 7.4).

Mechanical testing

After setting, the compressive strength (CS) of the CPC cylinders was measured, in the longitudinal direction of the specimens, at a loading rate of 1 mm/min using a testing bench machine (Model 858, Mini-Bionix II, MTS Systems Corp., Eden Prairie, MN, USA) using three cylinders per experimental group (n=3).

ALN release from CPC/PLGA-ALN composites

In vitro release tests were performed by soaking one sample cylinder of each CPC formulation in 1.0 ml of PBS and incubating the samples (n=3) under agitating conditions at 37°C. ALN release was determined using a ninhydrin assay on releasates collected after selected time periods (range: 1-148 days) [68]. Briefly, 100 µL of releasate (complete removal of 1 ml and addition of 1 ml of fresh PBS) or standard (serial dilutions of ALN; range: 0-200 µM) was pipetted in a 96-well plate, after which 75 µL of ninhydrin color reagent (Sigma-Aldrich, St. Louis, USA) was added for incubation at 80°C for 30 min. Subsequently, the well plate was cooled and 100 µL of stabilizing solvent (50% ethanol) was added into each well. The absorbance of each well was measured on a microplate spectrophotometer at 570 nm (Bio-Tech Instruments, Winooski, VT, USA).

Biological performance

Animals

For this experiment, twelve healthy mature female Wistar rats were used at 3 months of age with an average weight of ~200 g. Animals were allowed to acclimatize for 7 days and housing was provided per pair in a standard macrolon type 3 cage. To induce an osteoporotic condition, rats were subjected to bilateral ovariectomy (OVX). All rats received two surgical procedures during the course of the experiment: OVX surgery and 6 weeks later bone defect surgery. After OVX surgery, a low calcium diet was provided during six weeks with pellets containing 0.01% calcium and 0.77% phosphorous (Ssniff Spezialdiäten GmbH, Soest, Germany). After the bone defect surgery, a standard rodent chow was provided ad libitum.

The housing room was maintained under standard laboratory conditions (light-dark cycle: 12:12h, temperature: 20-22°C, relative humidity: 45-55%). All experiments were conducted in accordance with institutional, national and international guidelines for animal care and the Dutch law concerning animal welfare. The studies were reviewed and approved by the Experimental Animal Committee of the Radboud University (RUDEC 2013-080).

Surgical procedure to induce osteoporotic conditions

All animals received OVX surgery through two separate incisions in the lateral abdominal wall. The same procedure was followed as previously described by Alghamdi et al [69].

Surgical procedure to create and fill femoral bone defects

Six weeks after OVX surgery, a bone defect was created in both femoral condyles of each animal. Alternating the left and right femur, CPC/PLGA-blank and CPC/PLGA-lowALN, pre-set composites were used to fill the defects. Anesthesia was induced and maintained by Isoflurane inhalation (Rhodia Organique Fine Limited) combined with oxygen delivered by mask. Pre-operatively pain medication was provided by an injection of Carprofen (Rimadyl®, Pfizer Animal Health, New York, USA) in dosage of 5 mg/kg, given 15 min before surgery. For a minimum duration of 2 days postoperatively, Carprofen was given every 24h. Additionally, to diminish postoperative pain, Buprenorfine (Temgesic®, Reckitt Benckiser Health Care Limited, Schering-Plough, UK) was given every 12h in a dosage of 0.01 mg/kg. Additionally, to ensure adequate postoperative analgesia, before closing the wound local drop anaesthesia was provided by Lidocaïne (10 mg/ml Lidocaïne FNA, Centrafarm B.V., Etten-Leur, the Netherlands) and Bupivacaïne (5 mg/ml Bupivacaïne Actavis, Actavis B.V., Baarn, the Netherlands) diluted with NaCl using ~1 ml per rat containing 1 mg of Lidocaïne and 0.25 mg of Bupivacaïne.

Before creating femoral defects, both hind limbs of the rats were shaved and disinfected with povidone iodine. The rats were immobilized in supine position and with the knee maximally flexed a longitudinal incision through skin and muscle was made on the medial surface. After exposure of the medial side of the distal femoral condyle, the knee capsule was incised. Then, the knee was extended to luxate the patella laterally. When a clear view of the knee joint was established, a bone defect (Ø 2.5 mm, depth 5 mm) was created longitudinal to the axis of the femur, using a dental drill (Elcomed 9927 SPS; W&H Dentalwerk Burmoos GmbH, Burmoos, Austria). A series of increasing bur diameters (1.5–2.0–2.3–2.5 mm) were used at a speed of maximum 5000 rpm and a constant cooling by dripping saline. The drilled cavity was then washed with saline and dried using sterile gauze.

Subsequently, the CPC/PLGA composites were alternatingly placed into the defect. A total of 24 implants were used, resulting in n=6 per group. To increase statistical power paired analysis was made possible by combining CPC/PLGA-blank with CPC/PLGA-lowALN in each rat. After local drop anesthesia, the muscular tissue layer was closed with absorbable sutures (Vicryl® 4.0, Ethicon, Amersfoort, The Netherlands) after which the skin was closed by small staples (Agraven®; InstruVet BV, Cuijk, The Netherlands). In the initial postoperative period,

the intake of water and food was monitored as well as the weight of the animals. In addition, the animals were observed for signs of pain, infection and proper activity and weighed again postoperatively once a week to identify significant weight loss (>20%) compared to preoperative body weight of each rat.

Fluorochrome labeling for bone dynamics analysis

Animals assigned to a 12-week implantation period received a series of four fluorochromes (SigmaAldrich; Munich, Germany) by subcutaneous injection with a 2-week interval, starting two weeks after implantation surgery: Calcein blue (product no. M1255, dose 30 mg/kg; week 2), calcein green (C0875, 10 mg/kg; week 4), alizarine complexone red (A3882, 25 mg/kg; week 6) and rolitetracycline yellow (R2253, 25 mg/kg; week 8). Before injection, the solutions were set to neutral pH (7.2-7.4), then filtered through a 0.22 sterile millipore filter, and finally checked for fluorescence.

Specimen retrieval

After implantation periods of 4 and 12 weeks, the animals were euthanized by suffocation with CO_2. The femurs including the implanted materials were harvested, stripped from soft tissues and immediately fixed in 10% formalin solution. Using a diamond saw, the specimens were cut to become suitable for ex vivo micro-CT scanning and histological processing. After fixation, specimens were stored in 70% ethanol.

Micro-CT

A desktop X-ray micro-CT system was used (Skyscan-1072, TomoNT version 3N.5, Skyscan®, Kontich, Belgium) for 3D imaging. The specimens were placed onto the sample holder with the long axis of the femur perpendicular to the scanning beam. 3D reconstruction and imaging processing was performed using NRecon V1.4 and CTvox v2.7 (Skyscan®, Kontich, Belgium), respectively.

Histological processing

After performing micro-CT scanning, the specimens were dehydrated in a graded series of ethanol (70%-100%), after which they were embedded in polymethylmethacrylate (pMMA). After polymerization, thin sections of 10 µm were prepared in a cross-sectional direction perpendicular on the longitudinal direction of the defect using a diamond blade microtome (Leica Microsystems SP 1600, Nussloch, Germany) using a sawing technique as previously described [69,70]. Using this microtome sawing technique, at least three sections of ~10 µm thick per specimen are cut with intermediate loss of ~300 µm (thickness of sawing blade). With this loss the sections are therefore 300 µm separated from each other. The first section of each specimen was aimed at the center of bone defect or slightly proximally and then continued distally on the femur. The bone defect was created at distal end of the femur with a diameter of 2.5 mm and depth of 5 mm (for further information also see section "***Surgical procedure to create and fill femoral bone defects")***. Three sections of each specimen were stained with methylene blue and basic fuchsine. For the 12-week group, 3 additional sections were

made and left unstained for fluorescence analysis and immediately stored in the dark. All sectioning and histological processing was performed at the Radboudumc, department of Biomaterials (Nijmegen, the Netherlands).

Descriptive histology and histomorphometrical analysis

At both implantation periods of 4 and 12 weeks, the pMMA histological sections (3 sections per specimen) were examined by light microscopy (Leica Microsystems AG, Wetzlar, Germany); non-stained images were used for fluorescence microscopy. Digital images of the sections were assessed histologically and quantitative histomorphometry was performed using ImageJ computer-based image analysis software (Java® ImageJ 1.47, Image processing and analysis in Java) [71]. For quantitative analysis, a circular region of interest (ROI) with a diameter equal to the created defects (i.e. 2.5 mm) or an enlarged ROI (eROI; 3 mm) were superimposed on the defect area. Within the ROI and eROI, the amounts of newly formed bone and material remnants were measured using a combination of color discrimination (staining) and morphological appearance (for verification).

Statistical analysis

Data are presented as mean with SD for characterization, bone dynamics by fluorochorme labeling and histomorphometrical data. Statistical analyses were performed using STATISTICA 7.0 (StatSoft, Tulsa, Oklahoma, USA) or GraphPad Software (PRISM; La Jolla CA, USA). Shapiro-Wilk normality test was used to check distribution. A Kruskal-Wallis test and Dunn post hoc were used for nonparametric data. One-way analysis of variance (ANOVA) and Tukey multiple comparisons post-tests were used for parametric data. Student's t-tests were used for comparison of histomorphometrical data between time points for selected materials and paired t-tests were used for comparison between the two composites. Values of $p<0.05$ were considered statistically significant.

Results

Material characterization

After mixing both CPC and CPC/PLGA materials with ALN, all formulations remained injectable using standard syringes. Setting times (**Figure 1A**) of CPC and CPC/PLGA formulations showed to range from 4 to 28 min for initial and from 8 to 58 min for final setting. ALN loading via the liquid phase significantly increased setting times of both CPC and CPC/PLGA formulations. For subsequent ***in vitro*** experiments, we chose ALN doses of 0.5 wt% (low dose) and 5.0 wt% (high dose), which respectively presented initial setting times of ~10-12 min and ~20-22 min for both CPC formulations.

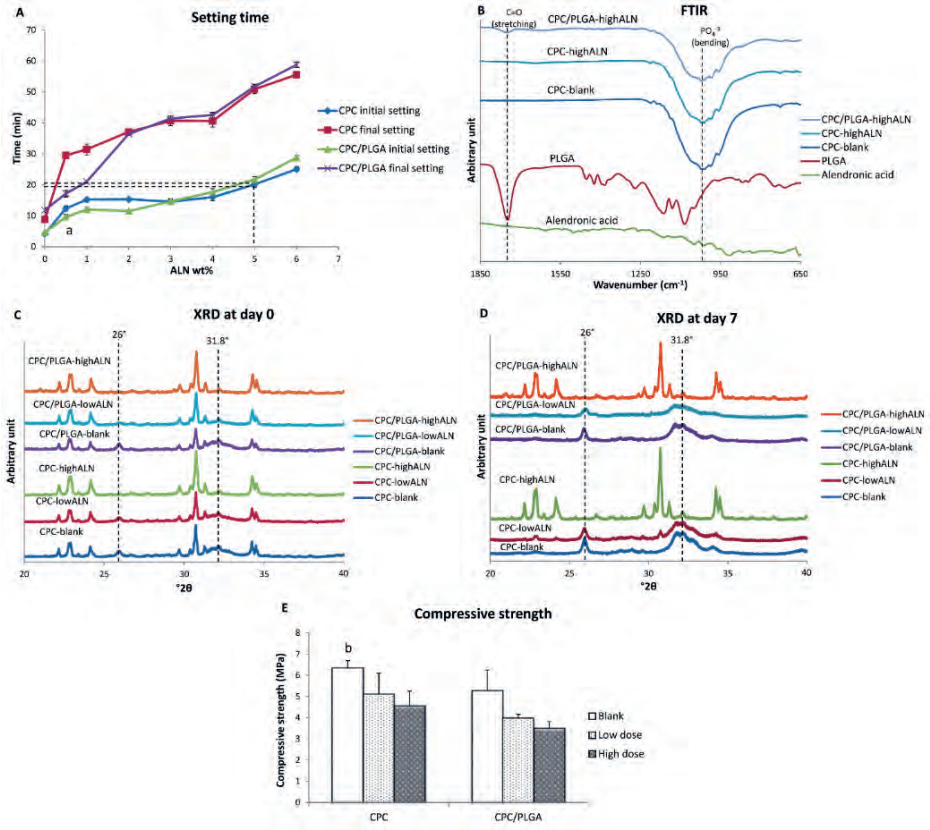

Figure 1A-E. Characterization analysis for CPC/PLGA-ALN composites. **[A]** initial and final setting time at different ALN wt%, dashed lines indicate the initial setting time at 5wt% ALN for CPC and CPC/PLGA, [a]] $p<0.05$ for CPC initial compared to CPC/PLGA initial setting; **[B]** FTIR of Alendronic acid, PLGA, CPC, CPC-highALN and CPC/PLGA-highALN. Dashed lines indicate peaks associated to PLGA (C=O stretching) and CPC (PO_4^{-3} bending) in the materials; **[C]** and **[D]** XRD at days 0 and 7 for the materials, dashed lines indicate HA peaks (26 and 31.8 °2θ); **[E]** compressive strength, [b]] $p<0.05$ for CPC-blank compared to CPC/PLGA-highALN. Error bars represent the SD.

Figure 2 shows SEM micrographs for all CPC formulations. PLGA could be discriminated due to morphological and size differences compared to the CPC matrix. The composites presented a homogenous aspect with PLGA particles dispersed throughout the CPC matrix (**Figures 2B, 2D & 2F**).

FTIR analysis (**Figure 1B**) showed absorption peaks representative for α-TCP and PLGA. A strong peak of carbonyl at ~1750 cm^{-1} was detected in PLGA containing samples, while representative peaks for PO_4^{-3} at the range of 900 to 1100 cm^{-1} were observed for all formulations. Due to low crystallinity of ALN, no characteristic peaks were observed for this component.

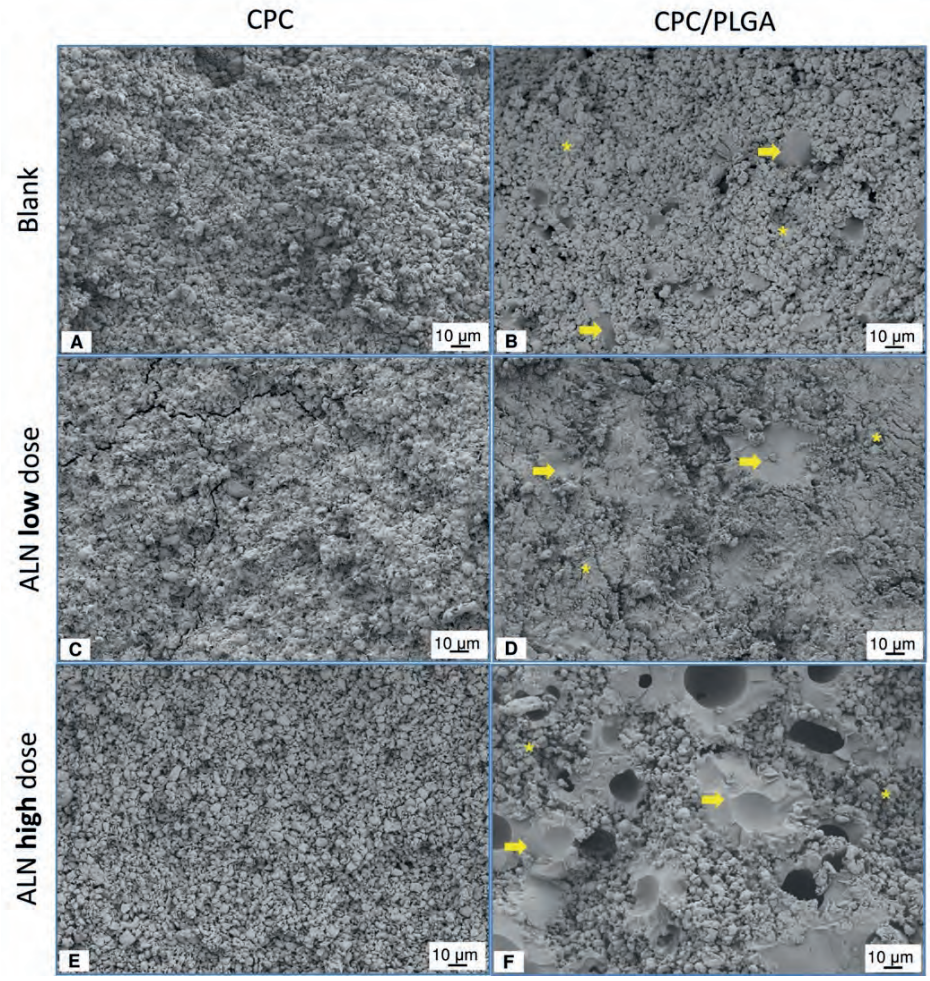

Figure 2A-F. Micrographs obtained by SEM. **[A]** CPC-blank; **[B]** CPC/PLGA-blank; **[C]** CPC-lowALN; **[D]** CPC/PLGA-lowALN; **[E]** CPC-highALN and **[F]** CPC/PLGA-highALN. Asterisks and arrows indicate CPC and PLGA particles respectively. Magnification of 500x.

XRD patterns of the composites at day 0 (after setting) showed an initial phase transition from α-TCP to hydroxyapatite (HA; **Figure 1C**; dashed lines) for CPC-blank, CPC-lowALN, CPC/PLGA-blank and α-CPC/PLGA-lowALN. After 3 and 7 days of incubation, peaks for HA formation were observed (at ~26 and 31.8 2°θ; **Figure 1D**), but no HA peaks were observed for CPC-highALN and CPC/PLGA-highALN, indicating that phase transformation was not taking place for high ALN formulations. This pattern was also observed after 148 days (data not shown).

The compressive strength for CPC and CPC/PLGA formulations assessed by mechanical test ranged from ~4 to 6 MPa (**Figure 1E**). The addition of ALN to CPC or CPC/PLGA tended to decrease the compressive strength for CPC and CPC/PLGA formulations. Statistical differences were found for CPC-blank compared to CPC/PLGA-highALN (p=0.0115).

ALN release kinetics

The ALN release data assessed via ninhydrin assay showed negligible ALN release for CPC-formulations (**Figure 3**). In contrast, the CPC/PLGA formulations showed a 2-week lag phase with negligible release followed by a biphasic ALN release with 2 distinct sustained release phases. A first fast and sustained ALN release from day 15 to 42 (~0.02 and ~0.20 mg ALN/day for low and highALN, respectively) reached ~15 % (~0.7 mg) and 20 % (~10 mg) of the initially loaded ALN amount for CPC/PLGA-lowALN and CPC/PLGA-highALN, respectively. Thereafter, a second sustained release phase with lower ALN release was observed (~9.40 x 10^{-4} and ~0.02 mg ALN/day for low and highALN, respectively), which after 148 days cumulatively reached ~16 % (~0.8 mg) and 25 % (~12.0 mg) of the initially loaded ALN amount for CPC/PLGA low and high dosages, respectively.

Based on the ***in vitro*** data of ALN incorporation into CPC and CPC/PLGA, we proceeded with ***in vivo*** analysis using only degradable CPC/PLGA, since no ALN release was detected from CPC. Additionally, CPC/PLGA-highALN was excluded for ***in vivo*** studies, as it showed incomplete phase transformation (based on setting time and physicochemical analysis).

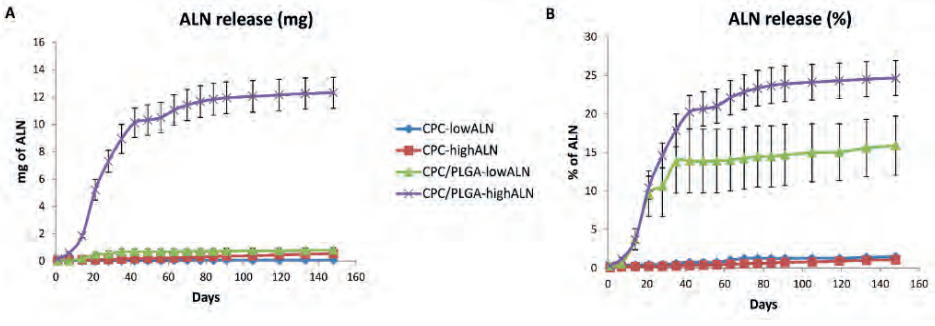

Figure 3. Cumulative Alendronate release from CPC and CPC/PLGA cylinders loaded with the bisphosphonate for up to 148 days. **[A]** Absolute ALN release (mg) **[B]** Relative ALN release (% of loaded dose). Error bars represent the SD.

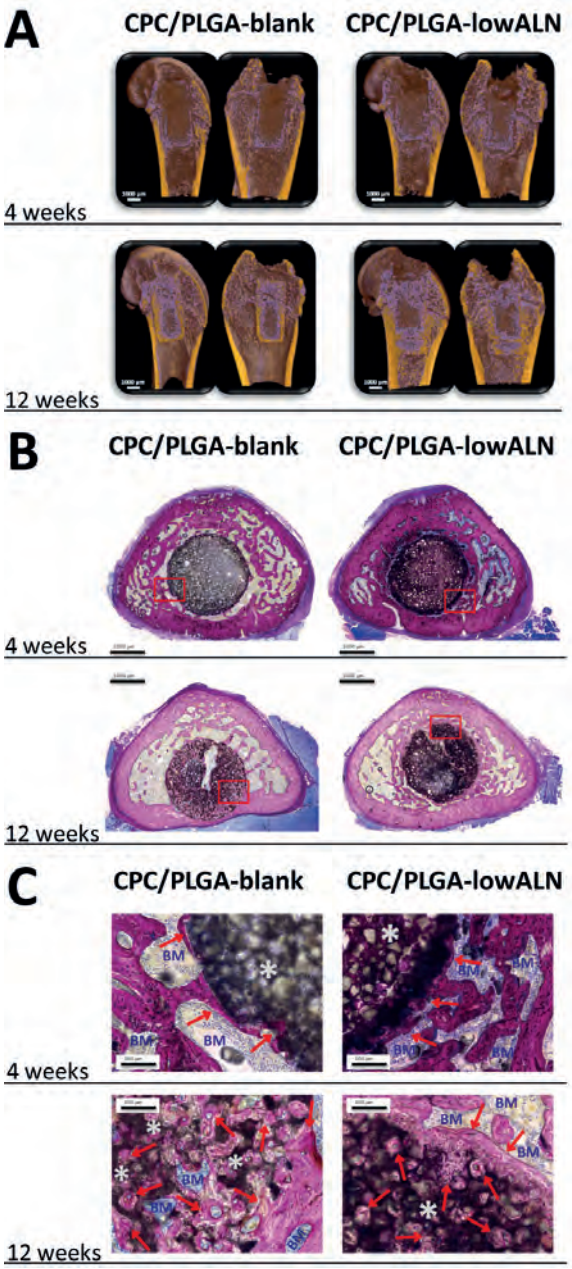

Figure 4A-C: [A] Representative micro-CT images of each experimental group. Color settings were adjusted to distinguish between different densities of bone and material, coloring bone yellow and CPC/PLGA purple. Representative histological images of pMMA sections for each experimental group with images at **[B]** 4 weeks and 12 weeks and **[C]** corresponding images at high magnification; methylene blue and basic fuchsine staining; red arrows] new bone (pink color); *] CPC/PLGA; BM] bone marrow (blue color).

Biological performance

Micro-CT analysis

The micro-CT data were reconstructed to 3D representations and then sliced to obtain an internal view of the bone defects. A representative overview with sagittal, frontal and transversal slices through the defect region for each experimental group is presented in **Figure 4A**. Color settings were adjusted to distinguish between different densities of bone and material. After 4 and 12 weeks, both CPC/PLGA-blank and CPC/PLGA-lowALN showed presence of CPC in contact with surrounding bone tissue. With implantation time, both CPC/PLGA-blank and CPC/PLGA-lowALN showed more bone formation around the composites.

Descriptive histology

Representative images of the histological sections of specimens embedded in pMMA are depicted in **Figure 4B**. In general, histological analysis showed differential material degradation and bone formation depending on the composition of the implant. For CPC/PLGA-blank and CPC/PLGA-lowALN, no apparent degradation was visible at 4 weeks, and peripheral degradation was observed after 12 weeks. There was an increased amount of bone formation, macroscopically, around the composites for CPC/PLGA-lowALN compared to CPC/PLGA-blank. Similar as with the micro-CT images, this difference was more apparent after 12 weeks. The histological slides of CPC/PLGA-lowALN further showed an apparently higher bone density outside the ROI. At higher magnification (**Figure 4C**), newly formed bone in direct contact with CPC/PLGA-blank and CPC/PLGA-lowALN was observed. Within the ROI, both CPC/PLGA-blank and CPC/PLGA-low ALN showed that bone had reached the center of the ROI.

Bone dynamics by fluorochrome labeling

Incorporation of fluorochrome labels into newly formed bone (**Figure 5A**) was observed for calcein green (green; week 4), alizarine complexone (red; week 6) and rolitetracycline (yellow; week 8). However, none of the sections showed incorporation of calcein blue (blue; week 2). For both CPC/PLGA-blank and CPC/PLGA-lowALN, calcein green was mostly present

Table 1: Labels and descriptions of the experimental groups

Labels	Descriptions
CPC-blank	Only α-TCP
CPC-lowALN	α-TCP + 0.5 wt % ALN
CPC-highALN	α-TCP + 5.0 wt % ALN
CPC/PLGA-blank	60 % α-TCP / 40 % PLGA
CPC/PLGA-lowALN	60 % α-TCP/40 % PLGA + 0.5 wt % ALN
CPC/PLGA-highALN	60 % α-TCP/40 % PLGA 5.0 wt % ALN

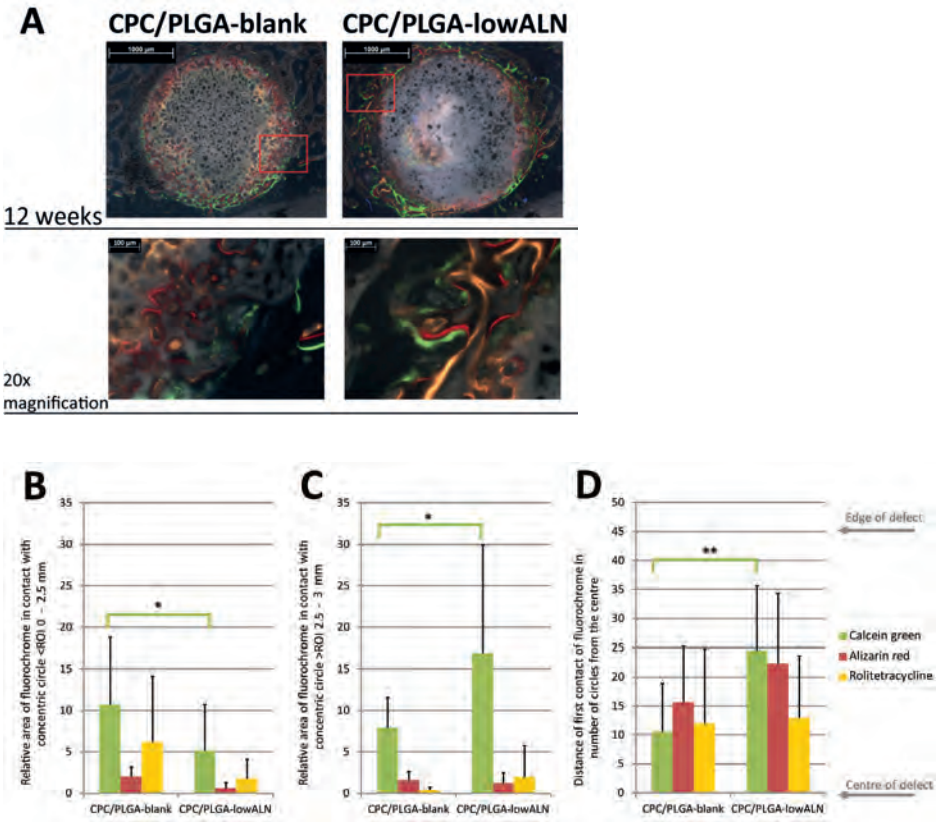

Figure 5A-D: [A] Representative fluorochrome microscopy images at 12 weeks, with high magnification images; red box] area of high magnification; green color] calcein green (week 4); red color] alizarine complexone (week 6); yellow color] rolitetracycline (week 8). **B-D:** Relative volume areas (mean *+SD*) of fluorochrome labels in contact with concentric circles for calcein green (week 4), alizarine complexone (week 6) and rolitetracycline (week 8) for both CPC/PLGA-blank and CPC/PLGA-lowALN **[B]** within ROI (0-2.5 mm) and **[C]** extended ROI (eROI, 2.5-3 mm); statistical analysis showed significantly more calcein green within ROI for CPC/PLGA-blank compared to CPC/PLGA-lowALN (Student's t-test, $p<0.05$); analysis showed significantly more calcein green in the eROI for CPC/PLGA-lowALN compared to CPC/PLGA-blank (Student's t-test, $p<0.05$); **[D]** Distance of the first ring that is in contact with a fluorochrome (mean *+SD*) for both CPC/PLGA-blank and CPC/PLGA-lowALN; statistical analysis showed significantly closer contact with calcein green for CPC/PLGA-blank compared to CPC/PLGA-lowALN (Student's t-test, $p<0.01$); Range] 0 to 55 rings, edge of defect] ring 45 (2.5 mm from centre).

within the ROI (**Figure 5B**). This was significantly more for CPC/PLGA-blank compared to CPC/PLGA-lowALN ($p<0.05$). However, in the peripheral area of 2.5 to 3 mm from the center of the ROI (**Figure 5C**), CPC/PLGA-lowALN showed significantly higher presence of calcein green compared to CPC/PLGA-blank ($p<0.05$). Bone formation dynamics by fluorescent microscopy showed that significantly more bone was formed near the center of the defect at 12 weeks for CPC/PLGA-lowALN compared to CPC/PLGA-blank ($p<0.01$; **Figure 5D**).

Histomorphometrical analysis

Histomorphometry data (**Table 1** & **Figure 6**) showed CPC remnants within the ROI after 4 weeks of 74.2 ± ***5.7***% for CPC/PLGA-blank and 71.7 ± ***5.4***% for CPC/PLGA-lowALN. After 12 weeks, CPC remnants within the ROI were 60.7 ± ***8.9***% for CPC/PLGA-blank and 66.5 ± ***7.1***% for CPC/PLGA-lowALN. Statistical analysis showed significant temporal decrease from 4 to 12 weeks of material remnants was seen for CPC/PLGA-blank ($p<0.05$), but not for CPC/PLGA-lowALN ($p>0.05$).

Bone areas within the ROI after 4 weeks were 4.1 ± ***1.4***% for CPC/PLGA-blank and 5.5 ± ***1.4***% for CPC/PLGA-lowALN. After 12 weeks, bone areas within the ROI were 22.8 ± ***8.0***% for CPC/PLGA-blank and 16.4 ± ***4.1***% for CPC/PLGA-lowALN. Statistical analysis for bone area within ROI showed no significant difference between CPC/PLGA-blank and CPC/PLGA-lowALN for both time points ($p>0.05$). Data showed significant temporal increase from 4 to 12 weeks of bone for CPC/PLGA-blank and CPC/PLGA-lowALN (Student's t-test, both $p<0.001$).

Descriptive histology suggested increased bone formation outside the ROI, therefore, bone areas were also measured in an extended ROI (eROI, from 2.5 to 3 mm). After 4 weeks bone area outside the ROI were 17.3 ± ***2.0***% for CPC/PLGA-blank and 15.5 ± ***3.7***% for CPC/PLGA-lowALN. Bone area for the eROI after 12 weeks, were 10.9 ± ***1.8***% for CPC/PLGA-blank and 18.1 ± ***2.1***% for CPC/PLGA-lowALN. Statistical analysis for bone area for the eROI showed significantly more bone at 12 weeks there was significantly more bone for CPC/PLGA-lowALN compared to CPC/PLGA-blank (Student's t-test, $p<0.05$). Data showed significant temporal increase from 4 to 12 weeks of bone only for CPC/PLGA-lowALN (Student's t-test, $p<0.01$). There was significantly less bone formation outside the ROI for CPC/PLGA-blank at 12 weeks compared to at 4 weeks ($p<0.001$).

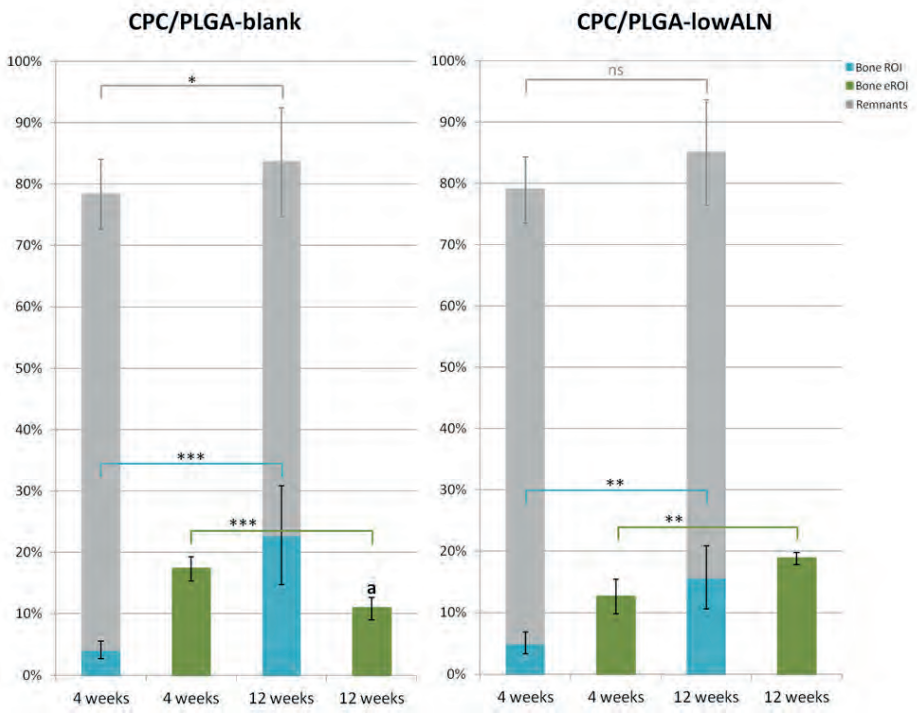

Figure 6: Accumulated volume percentages (mean ±*SD*) of new bone formation (green bars for eROI and blue bars within ROI) and material remnants (grey bars) at 4 and 12 weeks after implantation for CPC/PLGA-blank and CPC/PLGA-lowALN; statistical analysis showed significant increase of bone formation within ROI from 4 to 12 weeks for both CPC/PLGA-blank and CPC/PLGA-lowALN (***=$p<0.001$, **=$p<0.01$); bone formation over time in the eROI significantly decreased for CPC/PLGA-blank ($p<0.001$), but significantly increased for CPC/PLGA-lowALN ($p<0.001$); material remnants significantly decreased for CPC/PLGA-blank (*=$p<0.05$) but not significantly for CPC/PLGA-lowALN (ns=$p>0.05$); [a] At 12 weeks there was a significant higher amount of bone in the eROI for CPC/PLGA-lowALN compared to CPC/PLGA-blank ($p<0.05$).

Discussion

The aim of this study was to develop CPC/PLGA composites loaded with ALN and investigate the morphological features, physicochemical properties and ALN release kinetics. Furthermore, we evaluated the efficacy of CPC and CPC/PLGA as a local ALN release system in a rat femoral condyle bone defect in osteoporotic rats. We hypothesized that addition of ALN would (i) not critically affect material physicochemical properties, (ii) promote controlled ALN release, and (iii) enhance the biological performance of the CPC for bone regeneration in osteoporotic rats. We showed that ALN loading increased CPC and CPC/PLGA setting times and marginally affected compressive strength. Loading ALN at a dose of 5 wt% impeded with the conversion of the alpha-TCP base powder to HA within 3 days of incubation in PBS, while a dose of 0.5 wt% did not. ALN release kinetics showed hardly any release from CPC, whereas CPC/PLGA showed a controlled release of ALN up to 148 days with 2 consecutive sustained release phases following a 2-week lag phase. The main ***in vivo*** findings by micro-CT imaging, descriptive histology and quantitative histomorphometry showed that loading of ALN within CPC/PLGA did not increase bone formation within the defect region, but enhanced bone formation within the peri-defect region compared to control CPC/PLGA.

Previous ***in vitro*** studies proved a successful incorporation of bisphosphonates into ceramic bone substitutes [21-32]. These studies showed decrease of the mechanical properties and increases the setting time of the ceramic, however the range was still within acceptable limits [21,26,31,32]. This is consistent with our study and dependent of dose of the bisphosphonate added. By ***in vitro*** analysis the previous studies showed the release of the drug to be generally steady and not cytotoxic [21,22,27-29,31,32]. Moreover, there was a inhibition of osteoclasts and stimulation of osteoblasts [22-27,29,30]. Most of these studies also used ALN, however there were different ways of incorporation the drug into the cement. Most of the studies used the technique of loading the drug onto the surface of an inorganic implant by soaking the implant in a solution containing the drug [21-25,28-32]. However, this technique has the disadvantage of limited drug loading content and results in a uncontrolled burst release on administration [38]. The study by Panzavolta et al. incorporated the drug (both ALN and pamidronate) into the liquid phase, they do not report on the release properties [26]. In the study by Shi et al. the ALN was incorporated into the liquid phase of PLGA which was then incorporated as a porogen into the cement [27]. Their results showed a controlled release which is in concurrence with our study. There are previous ***in vivo*** studies using a cement enhanced with bisphophonate, showing positive results on bone formation [34-37]. However, a fair comparison between these four studies is compromised, due to use of all different cements in combination with other bisphosphonates and also the animal models were different.

For clinical application, handling properties of injectable bone substitutes that harden in situ are of utmost importance. Alterations in the composition of CPC or CPC/PLGA have shown to affect important handling properties, including injectability [39] and setting time [40,41]. Here, addition of ALN into the liquid phase of the cement formulation make it possible to obtain

injectable materials that were extruded by standard syringes [42], which corroborates previous work [43]. For setting time evaluation, we used systematic increases of ALN loading (0.5-6 wt%) and observed clinically acceptable initial setting times (i.e. <20 min) [19] for ALN amounts up to 5 wt%. ALN act on the CPC hydration process which is a reaction of dissolution-precipitation of CPC particles and Ca^{2+}/PO_4^{-3} ions respectively, affecting the curing of CPC [43]. In view of eventual clinical application, CPC/PLGA composites with low (0.5 wt%) and high (5.0 wt%) doses of ALN were subsequently used for further experimental in vitro work. As a less important characteristic for injectable bone substitutes meant for application under minimal loading, ALN loading showed marginal lowering effects on compressive strength. Panzavolta et al. [44] and Li et al. [45] also demonstrated a lowering effect of ALN on the CPC compressive strength, but with values of ~5.0 MPa these remain close to those of human cancellous bone [45].

From a material perspective, FTIR analysis and XRD confirmed the conversion of the alpha-TCP base powder to HA formed through hydration (HA, JCPDS 01-074-0566) [46] within 3 days of incubation in PBS for CPC and CPC/PLGA formulations without or low ALN loading. In contrast, high ALN loading inhibited this conversion. It is well-known that α-TCP hydrolyses to hydroxyapatite through dissolution and successive precipitation of the more stable phase, and the high affinity of ALN for calcium ions retards this process [43].

ALN release kinetics showed negligible release from CPC, whereas CPC/PLGA showed a controlled release of ALN with 2 distinct consecutive sustained release phases after a 2-week lag phase. Apparently, the dense configuration of the CPC and related lack of degradation is responsible for the observed negligible ALN release. Similarly, the relatively dense CPC/PLGA composite configuration upon setting limits ALN release during a 2-week lag phase. Subsequently, sustained ALN release coincides with the generation of a porous network within the ceramic matrix due to PLGA degradation. The second sustained ALN release phase takes place after PLGA degradation from ~day 40 onwards, when liquid can penetrate the ceramic matrix via an interconnective porosity system [47]. The difference in average daily ALN relative release (~20 and ~10 times greater in the 1st compared to 2nd phase for CPC-lowALN and CPC-highALN, respectively) is likely due to the additional acidifying effect of PLGA degradation products in the 1st phase, while a sole dissolution-controlled release process from a porous ceramic matrix remains thereafter [48,49]. Our observations are in accordance with those of Panyam and coworkers [50], who studied the use of PLGA micro- and nanoparticles for drug-delivery, and previous work from our group using CPC/PLGA as a drug-delivery vehicle [51,52].

Over the last decade, several studies examined the effect of bisphosphonates on peri-implant bone response using metallic bone implants [53-66] and showed enhanced bone formation (using mainly ALN and Zolendronate) compared to controls without bisphosphonate, with evaluation periods up to one year [59]. This is in accordance with our results, which showed enhanced peri-defect bone formation in response to locally released ALN from CPC/PLGA

composites. However, these studies differ in the use of non-degradable metallic implants versus degradable CPC/PLGA in our study. Remarkably, we did not observe any influence of ALN loading on bone formation within the defect region, for which the reason remains unclear.

CPC has the advantage as a bone substitute material of being injectable and moldable, allowing to directly adapt or being pre-set to the shape of a bone defect [18,19]. For this study we used pre-set composite of CPC/PLGA with and without ALN, specifically shaped to the measurements of our defect. With these pre-set CPC/PLGA composites we aimed to ensure the implants contained consistent amounts of cement and alendronate for both our ***in vitro*** and ***in vivo*** studies, as well as reduce operative time.

Conclusion

This study showed by *in vitro* analysis that ALN-loaded CPC/PLGA presents clinically acceptable handling, suitable compressive strength, and a controlled ALN release. The *in vivo* bone defect model showed that a relative low dose of ALN (0.5 wt%) significantly increases bone formation in the peri-defect region in osteoporotic conditions, without effects on CPC/PLGA degradation. The data suggest that future clinical application of ALN-loaded CPC/PLGA could be benificial for bone healing in compromised conditions.

Author Contribution statement

Authors Claire IA van Houdt and Paulo R Gabbai-Armelin equally contributed in writing of the main manuscript text. Paula M Lopez-Perez aided in the in vitro part of this study. Ana Claudia M Renno and Jeroen JJP van den Beucken supervised both the experimental analysis and the writing of the manuscript. All authors reviewed the manuscript. All the listed authors have agreed to all of the contents.

Acknowledgements

The authors would like to acknowledge ms. N. van Dijk for her assistance with the histological sectioning and fluorochrome labeling, dr. V. Cuijpers for his assistance on the ***ex vivo*** micro-CT and histological imaging and dr. ing. Bronkhorst for his with statistical and methodological guidance. The author P. R. Gabbai-Armelin would like to acknowledge the Conselho Nacional de Desenvolvimento Científico e Tecnológico (CNPq) and Fundação de Amparo à Pesquisa do Estado de São Paulo (FAPESP) for the scholarships (grants no. 209507/2013-6 and 2015/20704-8 respectively).

Additional Information

We have no conflicts of interest to disclose. We confirm that all experiments were performed in accordance with relevant guidelines and regulations.

References

1 Prevention and management of osteoporosis. ***World Health Organization technical report series*** 921, 1-164, back cover (2003).

2 Riggs, B. L. & Melton, L. J., 3rd. The worldwide problem of osteoporosis: insights afforded by epidemiology. ***Bone*** 17, 505S-511S (1995).

3 Kubo, T. ***et al.*** Osteoporosis influences the late period of fracture healing in a rat model prepared by ovariectomy and low calcium diet. ***The Journal of steroid biochemistry and molecular biology*** 68, 197-202 (1999).

4 Greenwald, M. A., Kuehnert, M. J. & Fishman, J. A. Infectious disease transmission during organ and tissue transplantation. ***Emerging infectious diseases*** 18, e1, doi:10.3201/eid1808.120277 (2012).

5 Greenwald, A. S. ***et al.*** Bone-graft substitutes: facts, fictions, and applications. ***The Journal of bone and joint surgery. American volume*** 83-A Suppl 2 Pt 2, 98-103 (2001).

6 Klijn, R. J., Meijer, G. J., Bronkhorst, E. M. & Jansen, J. A. A meta-analysis of histomorphometric results and graft healing time of various biomaterials compared to autologous bone used as sinus floor augmentation material in humans. ***Tissue Eng Part B Rev*** 16, 493-507, doi:10.1089/ten.TEB.2010.0035 (2010).

7 Agarwal, R. & Garcia, A. J. Biomaterial strategies for engineering implants for enhanced osseointegration and bone repair. ***Adv Drug Deliv Rev*** 94, 53-62, doi:10.1016/j.addr.2015.03.013 (2015).

8 Fini, M. ***et al.*** A new austenitic stainless steel with a negligible amount of nickel: an in vitro study in view of its clinical application in osteoporotic bone. ***Journal of biomedical materials research. Part B, Applied biomaterials*** 71, 30-37, doi:10.1002/jbm.b.30068 (2004).

9 Finigan, J. Bone up on osteoporosis. ***Nursing standard*** 17, 104, doi:10.7748/ns2003.09.17.51.104.c3449 (2003).

10 Fitzpatrick, L. A. Secondary causes of osteoporosis. ***Mayo Clin Proc*** 77, 453-468, doi:10.4065/77.5.453 (2002).

11 Anderson, G. F. & Hussey, P. S. Population aging: a comparison among industrialized countries. ***Health affairs*** 19, 191-203 (2000).

12 Blume, S. W. & Curtis, J. R. Medical costs of osteoporosis in the elderly Medicare population. ***Osteoporosis international : a journal established as result of cooperation between the European Foundation for Osteoporosis and the National Osteoporosis Foundation of the USA*** 22, 1835-1844, doi:10.1007/s00198-010-1419-7 (2011).

13 Duque, G. Osteoporosis in older persons: current pharmacotherapy and future directions. ***Expert Opin Pharmacother*** 14, 1949-1958, doi:10.1517/14656566.2013.822861 (2013).

14 Russell, R. G., Watts, N. B., Ebetino, F. H. & Rogers, M. J. Mechanisms of action of bisphosphonates: similarities and differences and their potential influence on clinical efficacy. ***Osteoporosis international : a journal established as result of cooperation between the European Foundation for Osteoporosis and the National Osteoporosis Foundation of the USA*** 19, 733-759, doi:10.1007/s00198-007-0540-8 (2008).

15 Ezra, A. & Golomb, G. Administration routes and delivery systems of bisphosphonates for the treatment of bone resorption. ***Adv Drug Deliv Rev*** 42, 175-195 (2000).

16 G, D. in ***Expert Opin Pharmacother*** Vol. 14 1949-1958 (2013).

17 Dorozhkin, S. V. Calcium orthophosphates: occurrence, properties, biomineralization, pathological calcification and biomimetic applications. ***Biomatter*** 1, 121-164, doi:10.4161/biom.18790 (2011).

18 Habraken, W. J., Wolke, J. G., Mikos, A. G. & Jansen, J. A. PLGA microsphere/calcium phosphate cement composites for tissue engineering: in vitro release and degradation characteristics. ***Journal of biomaterials science. Polymer edition*** 19, 1171-1188, doi:10.1163/156856208785540136 (2008).

19 Komath, M. & Varma, H. K. Development of a fully injectable calcium phosphate cement for orthopedic and dental applications. ***Bulletin of Materials Science*** 26, 415-422, doi:Doi 10.1007/Bf02711186 (2003).

20 Felix Lanao, R. P., Leeuwenburgh, S. C., Wolke, J. G. & Jansen, J. A. Bone response to fast-degrading, injectable calcium phosphate cements containing PLGA microparticles. ***Biomaterials*** 32, 8839-8847, doi:10.1016/j.biomaterials.2011.08.005 (2011).

21 Denissen, H., van Beek, E., Lowik, C., Papapoulos, S. & van den Hooff, A. Ceramic hydroxyapatite implants for the release of bisphosphonate. ***Bone Miner*** 25, 123-134 (1994).

22 Josse, S. ***et al.*** Novel biomaterials for bisphosphonate delivery. ***Biomaterials*** 26, 2073-2080, doi:10.1016/j.biomaterials.2004.05.019 (2005).

23 Seshima, H. ***et al.*** Control of bisphosphonate release using hydroxyapatite granules. ***Journal of biomedical materials research. Part B, Applied biomaterials*** 78, 215-221, doi:10.1002/jbm.b.30446 (2006).

24 Boanini, E., Torricelli, P., Gazzano, M., Giardino, R. & Bigi, A. Alendronate-hydroxyapatite nanocomposites and their interaction with osteoclasts and osteoblast-like cells. ***Biomaterials*** 29, 790-796, doi:10.1016/j.biomaterials.2007.10.040 (2008).

25 Boanini, E., Torricelli, P., Gazzano, M., Fini, M. & Bigi, A. The effect of alendronate doped calcium phosphates on bone cells activity. ***Bone*** 51, 944-952, doi:10.1016/j.bone.2012.07.020 (2012).

26 Panzavolta, S., Torricelli, P., Bracci, B., Fini, M. & Bigi, A. Alendronate and Pamidronate calcium phosphate bone cements: setting properties and in vitro response of osteoblast and osteoclast cells. ***J Inorg Biochem*** 103, 101-106, doi:10.1016/j.jinorgbio.2008.09.012 (2009).

27 Shi, X., Wang, Y., Ren, L., Gong, Y. & Wang, D. A. Enhancing alendronate release from a novel PLGA/hydroxyapatite microspheric system for bone repairing applications. ***Pharm Res*** 26, 422-430, doi:10.1007/s11095-008-9759-0 (2009).

28 Capra, P. ***et al.*** A preliminary study on the morphological and release properties of hydroxyapatite-alendronate composite materials. ***J Microencapsul*** 28, 395-405, doi:10.3109/02652048.2011.576783 (2011).

29 Schnitzler, V. ***et al.*** Investigation of alendronate-doped apatitic cements as a potential technology for the prevention of osteoporotic hip fractures: critical influence of the drug introduction mode on the in vitro cement properties. ***Acta Biomater*** 7, 759-770, doi:10.1016/j.actbio.2010.09.017 (2011).

30 Zhang, X., Hu, J., Li, Y., Yin, G. & Luo, E. Effects of ibandronate-hydroxyapatite on resorptive activity of osteoclasts. ***Arch Med Sci*** 7, 53-60, doi:10.5114/aoms.2011.20604 (2011).

31 Gong, T. ***et al.*** Preparation, characterization, release kinetics, and in vitro cytotoxicity of calcium silicate cement as a risedronate delivery system. ***Journal of biomedical materials research. Part A*** 102, 2295-2304, doi:10.1002/jbm.a.34908 (2014).

32 Pascaud, P. ***et al.*** Adsorption on apatitic calcium phosphates for drug delivery: interaction with bisphosphonate molecules. ***J Mater Sci Mater Med*** 25, 2373-2381, doi:10.1007/s10856-014-5218-0 (2014).

33 Faucheux, C. ***et al.*** Controlled release of bisphosphonate from a calcium phosphate biomaterial inhibits osteoclastic resorption in vitro. ***Journal of biomedical materials research. Part A*** 89, 46-56, doi:10.1002/jbm.a.31989 (2009).

34 Matuszewski, L. ***et al.*** Effect of implanted bisphosphonate-enriched cement on the trabecular microarchitecture of bone in a rat model using micro-computed tomography. ***Int Orthop*** 37, 1187-1193, doi:10.1007/s00264-013-1855-z (2013).

35 Verron, E. ***et al.*** Vertebroplasty using bisphosphonate-loaded calcium phosphate cement in a standardized vertebral body bone defect in an osteoporotic sheep model. ***Acta Biomater*** 10, 4887-4895, doi:10.1016/j.actbio.2014.07.012 (2014).

36 Gong, T. ***et al.*** Osteogenic and anti-osteoporotic effects of risedronate-added calcium phosphate silicate cement. ***Biomed Mater*** 11, 045002, doi:10.1088/1748-6041/11/4/045002 (2016).

37 Ma, J. H., Guo, W. S., Li, Z. R. & Wang, B. L. Local Administration of Bisphosphonate-soaked Hydroxyapatite for the Treatment of Osteonecrosis of the Femoral Head in Rabbit. ***Chin Med J (Engl)*** 129, 2559-2566, doi:10.4103/0366-6999.192768 (2016).

38 Cattalini, J. P., Boccaccini, A. R., Lucangioli, S. & Mourino, V. Bisphosphonate-based strategies for bone tissue engineering and orthopedic implants. ***Tissue Eng Part B Rev*** 18, 323-340, doi:10.1089/ten.TEB.2011.0737 (2012).

39 Habraken, W. J., Wolke, J. G., Mikos, A. G. & Jansen, J. A. Injectable PLGA microsphere/calcium phosphate cements: physical properties and degradation characteristics. ***Journal of biomaterials science. Polymer edition*** 17, 1057-1074 (2006).

40 Renno, A. C. ***et al.*** Incorporation of bioactive glass in calcium phosphate cement: material characterization and in vitro degradation. ***Journal of biomedical materials research. Part A*** 101, 2365-2373, doi:10.1002/jbm.a.34531 (2013).

41 Klijn, R. J. ***et al.*** Three different strategies to obtain porous calcium phosphate cements: comparison of performance in a rat skull bone augmentation model. ***Tissue engineering. Part A*** 18, 1171-1182, doi:10.1089/ten.TEA.2011.0444 (2012).

42 Bohner, M. & Baroud, G. Injectability of calcium phosphate pastes. ***Biomaterials*** 26, 1553-1563, doi:10.1016/j.biomaterials.2004.05.010 (2005).

43 Shen, Z., Yu, T. & Ye, J. Microstructure and properties of alendronate-loaded calcium phosphate cement. ***Mater Sci Eng C Mater Biol Appl*** 42, 303-311, doi:10.1016/j.msec.2014.05.043 (2014).

44 Panzavolta, S., Torricelli, P., Bracci, B., Fini, M. & Bigi, A. Functionalization of biomimetic calcium phosphate bone cements with alendronate. ***J Inorg Biochem*** 104, 1099-1106, doi:10.1016/j.jinorgbio.2010.06.008 (2010).

45 Li, Y. H. ***et al.*** The biocompatibility of calcium phosphate cements containing alendronate-loaded PLGA microparticles in vitro. ***Experimental biology and medicine*** 240, 1465-1471, doi:10.1177/1535370215579142 (2015).

46 Kumar, S. A. ***Eco-Friendly Nano-Hybrid Materials for Advanced Engineering Applications***. (Apple Academic Press, 2016).

47 Lodoso-Torrecilla, I. ***et al.*** Multimodal pore formation in calcium phosphate cements. ***Journal of biomedical materials research. Part A*** 106, 500-509, doi:10.1002/jbm.a.36245 (2018).

48 Tung, I. C. In vitro drug release of antibiotic-loaded porous hydroxyapatite cement. ***Artif Cells Blood Substit Immobil Biotechnol*** 23, 81-88, doi:10.3109/10731199509117669 (1995).

49 Mitra, A. K., Mitra, C. C. P. P. S. U. M. K. C. M. A. K., Kwatra, D. & Vadlapudi, A. D. ***Drug Delivery***. (Jones & Bartlett Learning, LLC, 2014).

50 Panyam, J. ***et al.*** Polymer degradation and in vitro release of a model protein from poly(D,L-lactide-co-glycolide) nano- and microparticles. ***J Control Release*** 92, 173-187, doi:https://doi.org/10.1016/S0168-3659(03)00328-6 (2003).

51 Felix Lanao, R. P. ***et al.*** RANKL delivery from calcium phosphate containing PLGA microspheres. ***Journal of biomedical materials research. Part A*** 101, 3123-3130, doi:10.1002/jbm.a.34623 (2013).

52 Felix Lanao, R. P. ***et al.*** Porous calcium phosphate cement for alveolar bone regeneration. ***Journal of tissue engineering and regenerative medicine*** 8, 473-482, doi:10.1002/term.1546 (2014).

53 Kurth, A. H. ***et al.*** The bisphosphonate ibandronate improves implant integration in osteopenic ovariectomized rats. ***Bone*** 37, 204-210, doi:10.1016/j.bone.2004.12.017 (2005).

54 McKenzie, K., Dennis Bobyn, J., Roberts, J., Karabasz, D. & Tanzer, M. Bisphosphonate remains highly localized after elution from porous implants. ***Clinical orthopaedics and related research*** 469, 514-522, doi:10.1007/s11999-010-1527-x (2011).

55 Tanzer, M., Karabasz, D., Krygier, J. J., Cohen, R. & Bobyn, J. D. The Otto Aufranc Award: bone augmentation around and within porous implants by local bisphosphonate elution. ***Clinical orthopaedics and related research*** 441, 30-39 (2005).

56 Peter, B. ***et al.*** Local delivery of bisphosphonate from coated orthopedic implants increases implants mechanical stability in osteoporotic rats. ***Journal of biomedical materials research. Part A*** 76, 133-143, doi:10.1002/jbm.a.30456 (2006).

57 McLeod, K. ***et al.*** Adsorption of bisphosphonate onto hydroxyapatite using a novel co-precipitation technique for bone growth enhancement. ***Journal of biomedical materials research. Part A*** 79, 271-281, doi:10.1002/jbm.a.30792 (2006).

58 Jakobsen, T. ***et al.*** Local bisphosphonate treatment increases fixation of hydroxyapatite-coated implants inserted with bone compaction. ***J Orthop Res*** 27, 189-194, doi:10.1002/jor.20745 (2009).

59 Bobyn, J. D., McKenzie, K., Karabasz, D., Krygier, J. J. & Tanzer, M. Locally delivered bisphosphonate for enhancement of bone formation and implant fixation. ***The Journal of bone and joint surgery. American volume*** 91 Suppl 6, 23-31, doi:10.2106/JBJS.I.00518 (2009).

60 Jakobsen, T., Baas, J., Bechtold, J. E., Elmengaard, B. & Soballe, K. The effect on implant fixation of soaking tricalcium phosphate granules in bisphosphonate. ***The open orthopaedics journal*** 6, 371-375, doi:10.2174/1874325001206010371 (2012).

61 Bobyn, J. D. ***et al.*** Local alendronic acid elution increases net periimplant bone formation: a micro-CT analysis. ***Clinical orthopaedics and related research*** 472, 687-694, doi:10.1007/s11999-013-3120-6 (2014).

62 Meraw, S. J., Reeve, C. M. & Wollan, P. C. Use of alendronate in peri-implant defect regeneration. ***Journal of periodontology*** 70, 151-158, doi:10.1902/jop.1999.70.2.151 (1999).

63 Niu, S. ***et al.*** Peri-implant and systemic effects of high-/low-affinity bisphosphonate-hydroxyapatite composite coatings in a rabbit model with peri-implant high bone turnover. ***BMC musculoskeletal disorders*** 13, 97, doi:10.1186/1471-2474-13-97 (2012).

64 Linderback, P., Areva, S., Aspenberg, P. & Tengvall, P. Sol-gel derived titania coating with immobilized bisphosphonate enhances screw fixation in rat tibia. ***Journal of biomedical materials research. Part A*** 94, 389-395, doi:10.1002/jbm.a.32708 (2010).

65 Peter, B. ***et al.*** Calcium phosphate drug delivery system: influence of local zoledronate release on bone implant osteointegration. ***Bone*** 36, 52-60, doi:10.1016/j.bone.2004.10.004 (2005).

66 Alghamdi, H. S. ***et al.*** Synergistic effects of bisphosphonate and calcium phosphate nanoparticles on peri-implant bone responses in osteoporotic rats. ***Biomaterials*** 35, 5482-5490, doi:10.1016/j.biomaterials.2014.03.069 (2014).

67 ASTM. Standard Test Method for Time of Setting of Hydraulic-Cement Paste by Gillmore Needles, Document Number: ASTM C266-99, ASTM International. (1999).

68 Taha, E. A. & Youssef, N. F. Spectrophotometric determination of some drugs for osteoporosis. ***Chemical & Pharmaceutical Bulletin*** 51, 1444-1447, doi:DOI 10.1248/cpb.51.1444 (2003).

69 Alghamdi, H. S., van den Beucken, J. J. & Jansen, J. A. Osteoporotic rat models for evaluation of osseointegration of bone implants. ***Tissue engineering. Part C, Methods*** 20, 493-505, doi:10.1089/ten.TEC.2013.0327 (2014).

70 van der Lubbe, H. B., Klein, C. P. & de Groot, K. A simple method for preparing thin (10 microM) histological sections of undecalcified plastic embedded bone with implants. ***Stain Technol*** 63, 171-176 (1988).

71 Lopez-Heredia, M. A. ***et al.*** Bone formation analysis: effect of quantification procedures on the study outcome. ***Tissue engineering. Part C, Methods*** 18, 369-373, doi:10.1089/ten.TEC.2011.0353 (2012).

7

CHAPTER 7

Regenerating critical size rat segmental bone defects with a self-healing hybrid nano-composite hydrogel: effect of bone condition and BMP-2 incorporation

van Houdt CIA, Koolen MKE, Lopez-Perez PM, Ulrich DJO, Jansen JA, Leeuwenburgh SCG, Weinans HH, van den Beucken JJJP.

Introduction

Severe trauma, bone tumors, congenital malformation or extensive infection of bone tissue can be the cause of critical size bone defect. The term critical size bone defect is defined as an orthotopic intraosseous wound that does not spontaneously heal without surgical intervention [1]. Urist concluded in 1954 that there is no limited amount of time after which a pseudarthrosis cannot unite anymore by prolonged immobilization [2]. Urist further concluded that a new proliferative process begins after any surgical intervention and after the implantation of any type of bone graft [2]. In case of a critical size defect, bone grafting surgery is generally performed to obtain bone healing and reduce recovery time. An estimated 500,000 bone grafting procedures are performed annually in the United States and this number easily doubles on a global basis [3].

Autologous bone grafting is the golden standard for treating bone defects [4-7]. Drawbacks of autologous bone grafting are need for two surgical sites, donor site morbidity, increased surgery and recovery time, and shortage in the availability of donor tissue [8]. Over the next 50 years, the number of elderly patients with the need for bone grafting is expected to increase, including their comorbidities. Especially the increase in osteoporotic patients represents a major challenge for medical care [9]. Osteoporosis compromises bone strength (both trabecular and cortical), hence increases fracture risks, and further negatively influences the bone healing process [10-13].

Over the past decades, different types of synthetic bone graft have emerged, of which particularly calcium phosphate (CaP) based ceramics have shown large potential [14,15]. In view of increased demands for synthetic bone grafts with advantageous properties, we previously designed an injectable, self-healing hydrogel consisting of bisphosphonated (BP) hyaluronan (HA) and CaP nanoparticles [16]. The major biological advantage of this material was the observed ingrowth of newly-formed trabecular-like bone interspersed throughout the material after 4 weeks in a femoral condyle defect in rats [16].

In view of the BP-moiety in the material and the used of BPs as a drug in the treatment of osteoporosis, in the current study bone regeneration was challenged using a rat critical size segmental defect model, in which the effect of bone condition (healthy versus osteoporotic bone) on bone defect healing using HA_{BP}-CaP gel was comparatively evaluated. Additionally, the effect of enriching this HA_{BP}-CaP gel with BMP-2 was explored. We hypothesized that (i) an osteoporotic condition would negatively affect defect healing, and (ii) that enrichment of the HA_{BP}-CaP gel with BMP-2 would improve defect healing in both healthy and osteoporotic conditions.

Materials and Methods

Materials

The hyaluronan with bisphosphonate and calcium phosphate hydrogel (HA_{BP}-CaP) was prepared as previously described [16], mixing equal volumes of hyaluronan-bisphosphonate with a CaP suspension in connected syringe. This resulted in a non-covalently cross-linked HA_{BP}-CaP hybrid nanocomposite gel.

To further enhance bone healing, BMP-2 (InductOs™, Medtronic BioPharma B.V., Heerlen, The Netherlands) was added to the liquid component of the gel in 3 µg (HA_{BP}-CaP-lowBMP2) and 30 µg (HA_{BP}-CaP-highBMP2) per implant from a 1.5 mg/ml solution.

In order to maintain the gel inside the defect, we used polytetrafluorethylene (PTFE) tubing of ±7 mm in length, 4.2 mm in diameter of 0.25 mm ± 0.07 mm (Polyfluor Plastics BV, Breda, the Netherlands), as is used in e.g. vascular surgery. To allow for fluid exchange, the tubing was perforated using a 1 mm biopsy punch (Kai Europe GmbH, Solingen, Germany) creating 4 holes in a row in 4 directions resulting in 16 holes per tube.

Animals

For this experiment, 56 healthy mature male Wistar rats (age: 3 months; weight: ± 250 g) were used. All animals received either orchidectomy to induce an osteoporotic bone condition or sham surgery, as described previously [17]. Six weeks after, all animals received 1 unilateral segmental defect in the right femur, which was treated with HA_{BP}-CaP (8 healthy and 8 osteoporotic animals), HA_{BP}-CaP-lowBMP2 (8 healthy and 8 osteoporotic animals), HA_{BP}-CaP-highBMP2 (8 healthy and 8 osteoporotic animals), empty PTFE tubing (4 healthy animals), or left empty (4 healthy animals).

All experiments were conducted in accordance with institutional, national and international guidelines for animal care and the Dutch law concerning animal welfare. The studies were reviewed and approved by the Experimental Animal Committee of the Radboud University (RUDEC 2013-206).

Surgical procedure to induce osteoporotic condition

Anaesthesia was induced and maintained by Isoflurane inhalation (Rhodia Organique Fine Limited) combined with oxygen delivered by mask. Pre-operative pain medication was provided by an injection of Carprofen (5 mg/kg; Rimadyl®, Pfizer Animal Health, New York, USA), given 15 min before surgery. After confirmation of effective anaesthesia, the animal was placed on an electric heating blanket in supine position. The area disinfection was performed by application of a povidone iodine solution. A skin incision was made over the scrotum, followed by blunt dissection of subcutaneous connective tissue and creating a 5 mm opening in the tip of the scrotal sac. The gonadal tissue was pulled through, including the caudal epididymis, caput epididymis, vas deferens, and spermatic blood vessels. A single

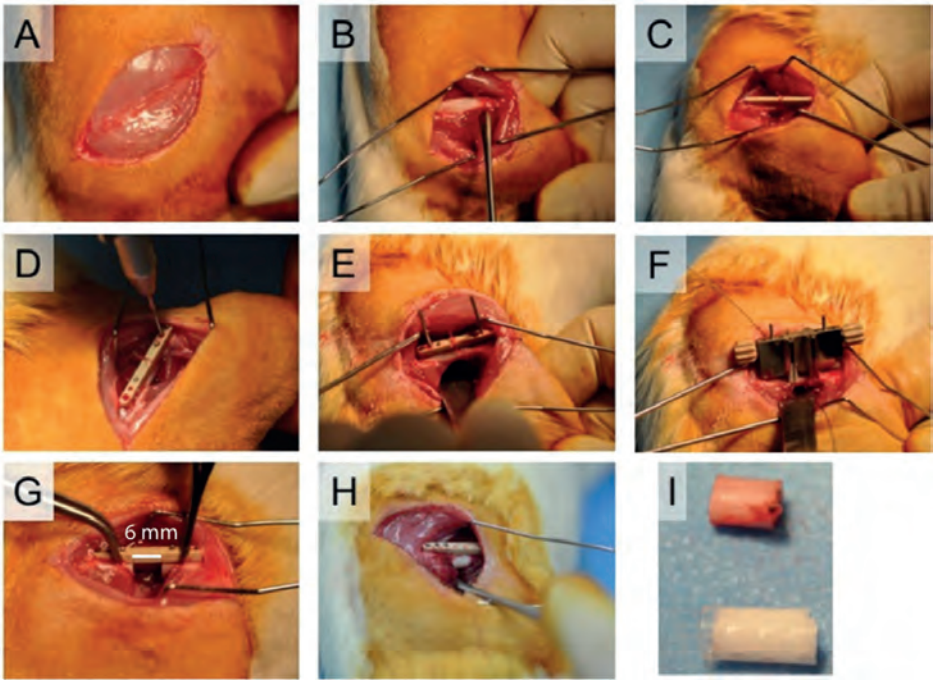

Figure 1 A-I: A-H] Photographs during surgery of creating the critical-sized segmental defect in male rats and implantation of the material (in chronological order from left to right and top to bottom). **I]** A removed bone segment of 6 mm next to a polyurethane tube containing experimental HABP-CaP gel.

ligature was performed around the blood vessels and the vas deferens using a surgical polyester suture (Terylene® 2.0 undyed, Serag-Wiessner GmbH & Co, Naila, Germany) after testis and epididymis were removed. Remaining vas deferens and fat was replaced in the sac. After haemostasis, the skin was closed with subcutaneous absorbable sutures (Vicryl® 3.0, Ethicon, Amersfoort, The Netherlands). Finally, the animals were covered with paper or cloth in order to avoid hypothermia. The ORX animals received a low calcium diet for six weeks. The sham operated animals underwent the same surgical procedure except for the actual removal of the gonads and normal food pellets were provided. For a minimum duration of 2 days postoperatively, Carprofen was given every 24 h. Additionally, to diminish postoperative pain, Buprenorfine (Temgesic®, Reckitt Benckiser Health Care Limited, Schering-Plough, UK; 0.02 mg/kg) was given every 12 h.

Surgical procedure to create critical size segmental femur defect and placement of bone substitute material

A critical size segmental defect was created unilaterally in the femur of the rats. A single dose of antibiotics (Enrofloxacin, 5 mg/kg body weight) was administered 1 h before surgery. To reduce intra-operative and post-operative pain, Temgesic® (0.02 mg/kg) was administered

subcutaneously pre-operatively. All surgeries were performed under general inhalation anaesthesia with pre-operative pain medication and sterile conditions as mentioned above (see Surgical procedure to induce osteoporotic conditions). The right leg was shaved, and the rat was placed in a left lateral position on heating mat. The surgical area was disinfected with povidone iodine. Through an anterolateral approach, the vastus lateralis and biceps femoris were separated and elevated while cautioning to keep the periosteum intact along the surface of the bone (**Figure 1A-B**). Firstly, a PEEK plate was inserted and fixed in the anterolateral plane (RatFix, RISystem AG, AOFoundation, Davos, Switzerland; **Figure 1C-E**). Then, a segmental defect was created with the use of a Gigli saw with saw guide to ensure the 6 mm length of the femoral segment (both saw and guide were purchased from RISystem) under constant cooling with saline (**Figure 1F-G**). After removing the segment, we left the defect empty or placed a tube of polytetrafluorethylene in the defect, filled with our experimental material (HA_{BP}-CaP, HA_{BP}-CaP-lowBMP2 or HA_{BP}-CaP-highBMP2) or with an empty tube (**Figure 1H-I**). Subsequently, the muscles and fascia were closed with absorbable sutures (Vicryl® 4.0, Ethicon Products, Amersfoort, the Netherlands) and the skin with both absorbable suture and agraves (Vicryl® 4.0 and agraves, Ethicon Products, Amersfoort, the Netherlands). Postoperatively, Temgesic® (0.02 mg/kg) and Carprofen® (5.0 mg/kg) were administered for 2 days post-operatively every 12 h.

Animal euthanasia and specimen retrieval

Twelve weeks post-operatively, specimens were retrieved for ex vivo X-ray imaging and micro-CT scanning, as well as histological assessment. All rats were euthanized by CO^2-suffocation in accordance with ISO standards and protocols of the Radboud University Nijmegen Medical Center, The Netherlands. The femurs including the implanted materials were harvested, stripped from soft tissues and immediately fixed in 10% formalin solution. After fixation, specimens were stored in 70% ethanol.

Validation of osteoporotic condition by ELISA for serum TRAP analysis

During specimen retrieval, blood was taken from several rats of both SHAM and ORX (8 and 10 rats respectively) to validate osteoporotic condition. This was evaluated by a serum analysis for TRAP enzyme activity performed with the RatTRAP™ Assay kit (Immunodiagnostic Systems GmbH, Frankfurt am Main).

X-ray imaging

After specimen retrieval and formalin fixation, X-ray images were made of the femora using dental X-ray equipment and imaging plate (Planmeca ProX™ 2016 & Soredex™ DIGORA™ Optime 2015; Dental Union Plandent, Nieuwegein, the Netherlands).

Micro-CT scanning

Micro-computed tomography (micro-CT) scanning of the femora were performed to assess bone formation at the end point of 12 weeks with a micro-CT imaging system (Quantum FX; PerkinElmer, Waltham, MA, USA). Three minutes of scan time was required per bone for an

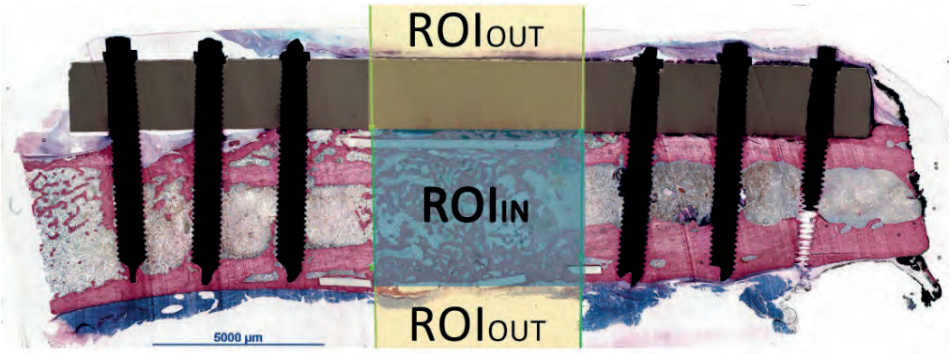

Figure 2: Example of a histological image with all three analyzed regions (colors and lettering are only drawn to indicate the areas in this image). ROIIN] Region of Interest within defect area; ROIOUT] Region of interest outside the defect area.

isotropic voxel size of 42 µm (voltage 90 kV, current 180 mA, field of view = 21 mm). To analyze the results, all datasets were aligned. A region of interest (ROI) of 4.6 x 5 x 6 mm (bone volume inside the defect; BVi) and of 6 x 8.4 x 8.4 mm (total bone volume; TBV) was selected. The ROI was segmented with a global threshold. Bone volume was measured in mm3 using image processing software (Image-J; Java, Redwood Shores, CA, USA).

For 3D imaging, one sample of each group was selected and scanned with a desktop X-ray micro-CT system (Skyscan-1072, TomoNT version 3N.5, SkyscanVR, Kontich, Belgium). The specimens were placed onto the sample holder with the long axis of the femur perpendicular to the scanning beam. The 3D reconstruction and imaging processing was performed using NRecon V1.4 and Dataviewer V1.4.3.0 (SkyscanVR, Kontich, Belgium), respectively.

Histological processing

After performing the X-ray imaging and micro-CT scanning, the obtained specimens were dehydrated in a graded series of ethanol (70-100%), and embedded in polymethylmethacrylate (PMMA). After polymerization, thin sections of the defect of ~10 µm were prepared in a plane parallel to the axis of the femur using a diamond blade microtome (Leica Microsystems SP 1600, Nussloch, Germany) as previously described [17,18]. At least three sections of each specimen were made and stained with methylene blue and basic fuchsine.

Descriptive histology and histomorphometrical analysis

After an implantation period of 12 weeks, PMMA histological sections (3 sections per specimen) were examined by light microscopy (Leica Microsystems AG, Wetzlar, Germany) and digitalized with an automatic scanning microscope (Panoramic250, 3DHISTECH Ltd.,

Budapest, Hungary). Quantitative assessment of the PMMA sections was performed using ImageJ computer-based image analysis software (Java® ImageJ 1.47, Image processing and analysis in Java) 19. From digitalized images of the sections (magnification: 5x), a rectangular region of interest (ROI) was created with dimensions equal to the created defects (ROIIN). Secondly, a rectangular ROI above and below the implant was positioned as ROIOUT (**Figure 2**). Within all ROIs, the amount of newly formed bone and material remnants were measured using colour discrimination and morphology for verification. Evaluation of the gel capacity to overcome the critical size defect included whether or not the defect was bridged. This was defined by bone formation from both ends of the defect that is connected in the middle, with visible cortical bone connection or by relatively thick trabecular-like bone dispersed throughout the whole defect.

Statistical analysis

Data are presented as mean with SD for histomorphometric data and CT-scan analysis. Statistical analysis of quantitative data was performed using one-way analysis of variance (ANOVA) with a Tukey post-hoc test for comparison between the three different groups. Student's t-tests were used for comparison between both conditions for selected materials. GraphPad Software (PRISM, La Jolla CA, USA) was used to carry out the statistical analysis. Values of $p<0.05$ were considered statistically significant.

Results

Animals

All of the 56 animals recovered well after orchidectomy or sham surgery. There were no wound problems and all but one animal remained in good condition. Two days after surgical segmental defect creation, one animal was found dead (sham-operated, HABP-CaP); obduction did not reveal issues in the operated leg, however, ascitis and pleural effusion were observed. All 55 remaining animals were healthy and recovered well, presenting normal activity without signs of infection or other wound healing problems.

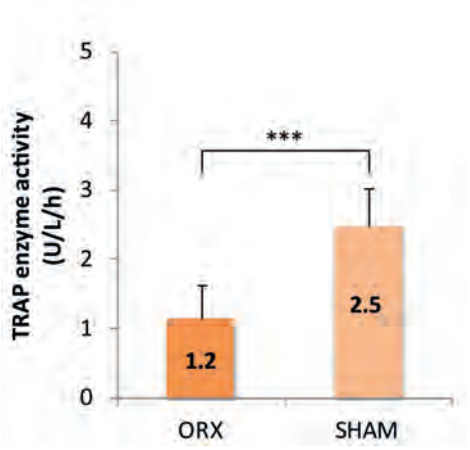

Figure 3: Serum TRAP enzyme activity (mean ±SD) comparing ORX and SHAM operated animals, ***] significant difference between ORX and SHAM ($p<0.001$)

Validation of osteoporotic condition by serum TRAP analysis

The induced osteoporotic bone condition after orchidectomy resulted in significantly decreased serum TRAP enzyme activity ($p<0.001$) compared to healthy animals (**Figure 3**), with activity values of 1.2 ±0.5 and 2.5 ±0.6 U/L/h, respectively.

X-ray imaging

Representative X-ray images are depicted in **Figure 4**. These images showed substantial healing for HA_{BP}-CaP-lowBMP2 and HA_{BP}-CaP-highBMP2, but low radiopacity in the defect region for HA_{BP}-CaP and empty tube controls. In one of the four femurs with no tube the screws were broken and in a second animal of this group the screws were loosened resulting in a 45° angle of the distal femur.

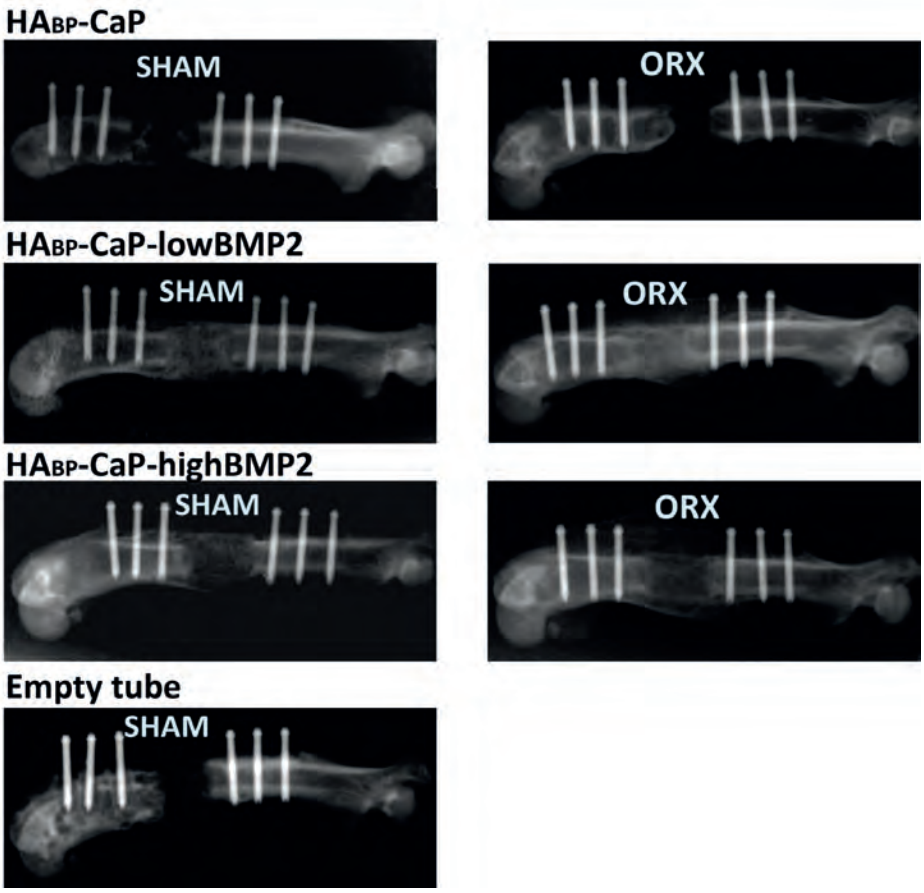

Figure 4: Representative X-ray images of all material groups in SHAM and ORX animals, and of the SHAM animals with an empty tube control

Micro-CT analysis

Representative micro-CT images of the segmental defects are depicted in **Figure 5A**. Data of the micro-CT analysis are shown in **Table 1A** and **Figure 5B**. Overall bone formation in ROIIN demonstrated that defects could not be bridged by the gel alone. Only two out of eight defects in the ORX animals showed bridging. For SHAM animals this material had the least amount of bone formation compared to other materials and none bridged the defect.

Further specification within the different experimental groups showed bone formation to be highest for HA_{BP}-CaP-lowBMP2 in both SHAM and ORX animals (38.5% and 37.0% respectively). Bone formation was significantly highest for HA_{BP}-CaP-lowBMP2 compared to all other groups for both conditions ($p<0.001$, $p<0.001$ and $p<0.01$ compared to, respectively, control group, HA_{BP}-CaP and HA_{BP}-CaP-highBMP2). Bone formation was not only seen within the original

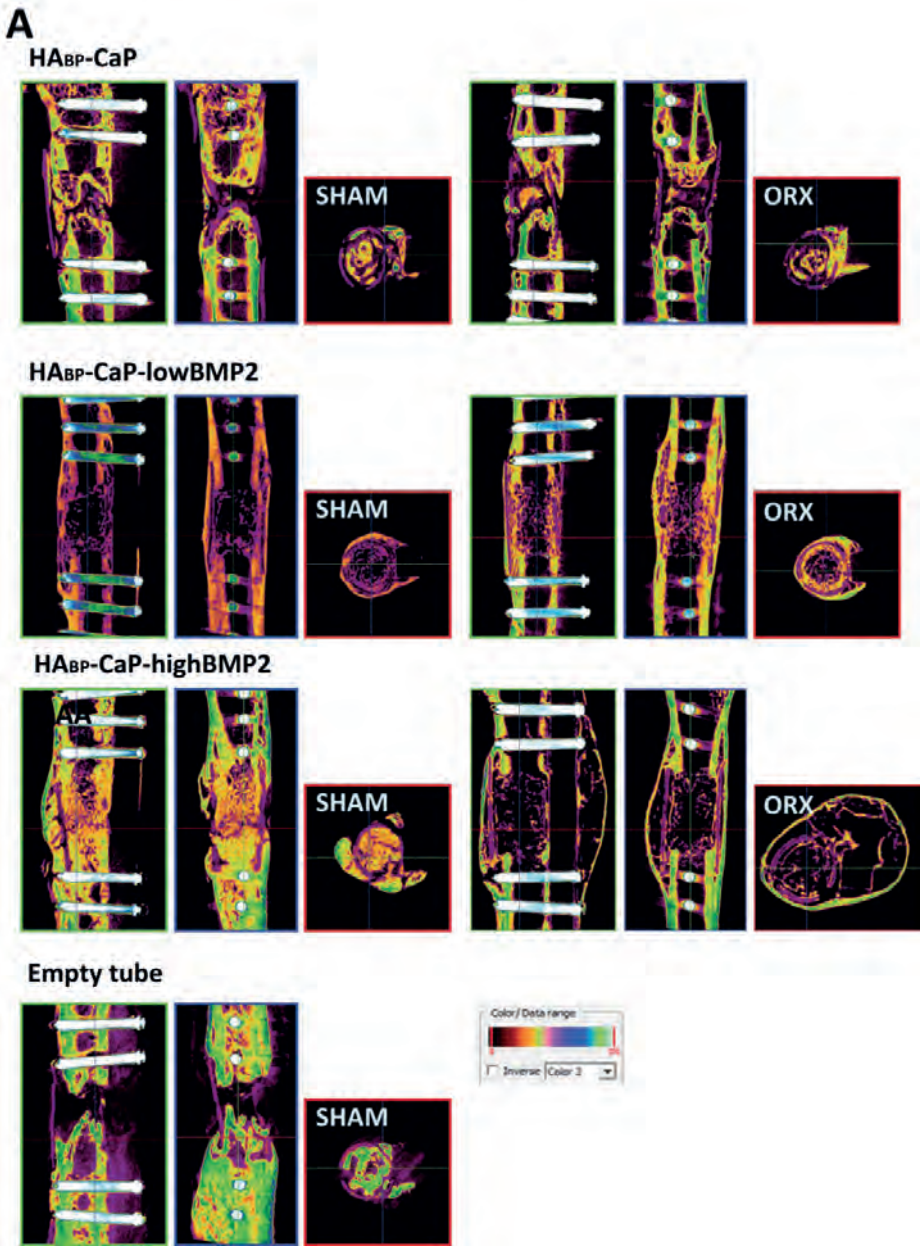
A
HABP-CaP
SHAM
ORX
HABP-CaP-lowBMP2
SHAM
ORX
HABP-CaP-highBMP2
AA
SHAM
ORX
Empty tube
SHAM
Color / Data range
Inverse
Color 3

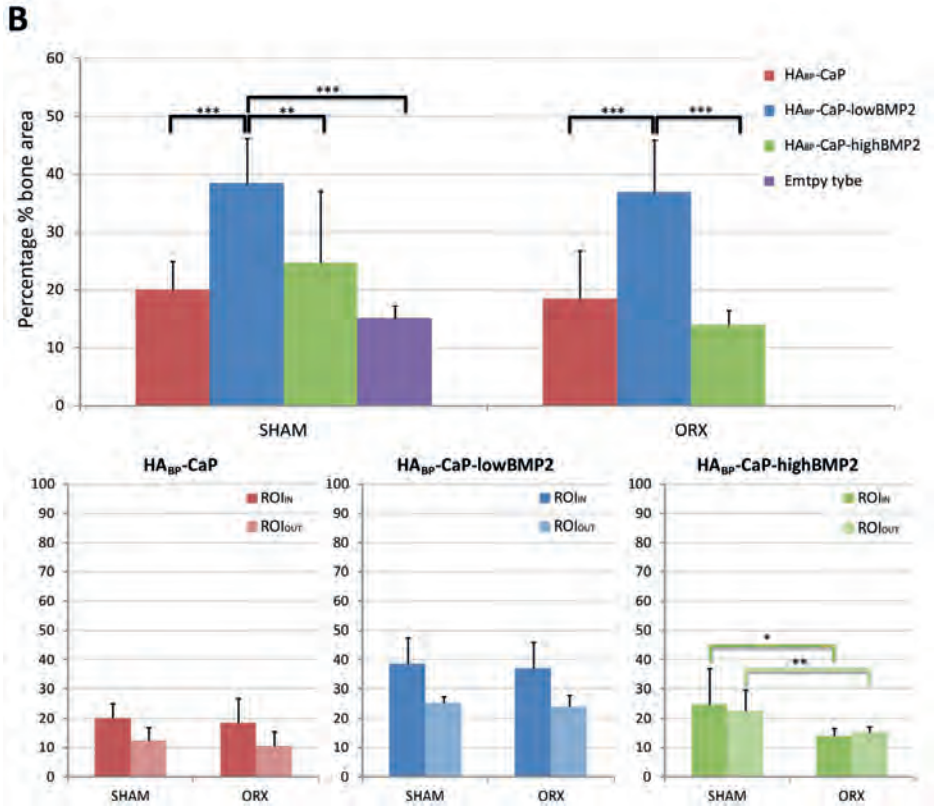

Figure 5 A-B: A] Representative micro-CT images (reproduced with DataViewer) of all 3 experimental groups of SHAM and ORX animals and of the SHAM animals with an empty tube control. Green boxed images are coronal cross-sections with the plate to the right side of the image, being the anterolateral side of the femur. The blue boxed (middle) images are of sagittal planes through the femur. The red boxes are transverse planes with the plate to the right side of the image. The colors are a pre-selected setting in DataViewer (Color 2), which represents density **B]** Quantitative analysis based on micro-CT images of bone formation (percentage % bone area in mean data ±SD) within and outside the ROI. With the larger graph comparing between groups and the smaller between ROIIN and ROIOUT and per material group; showing significant differences of *] p<0.05, **] p<0.01 and ***] p<0.001.

Table 1 A-B; Mean data ±SD of bone formation percentage (%) by A] micro-CT analysis and B] histomorphometry.

	SHAM				ORX			
	ROI_{IN}		ROI_{OUT}		ROI_{IN}		ROI_{OUT}	
Table A								
HA_{BP}-CaP	20.0	± 4.9	12.4	± 4.4	18.5	± 8.3	10.6	± 4.8
HA_{BP}-CaP-lowBMP2	38.5	± 7.7	25.2	± 2.3	37.0	± 9.0	24.0	± 4.0
HA_{BP}-CaP-highBMP2	24.8	± 12.3	22.4	± 7.1	14.0	± 2.5	15.3	± 1.8
Empty tube	15.2	± 2.1	8.5	± 1.0	NA		NA	
Table B								
HA_{BP}-CaP	24.9	± 6.1	4.9	± 3.2	28.3	± 7.8	4.8	± 4.6
HA_{BP}-CaP-lowBMP2	34.2	± 5.5	23.5	± 3.8	38.5	±11.4	22.6	± 5.1
HA_{BP}-CaP-highBMP2	26.4	± 7.4	24.6	± 6.6	15.2	± 3.8	21.8	± 3.0
Empty tube	26.2	± 3.6	6.2	± 3.0	NA		NA	

Table 2; Segmental defect bridging*.

	SHAM		ORX	
	ROI_{IN}	ROI_{OUT}	ROI_{IN}	ROI_{OUT}
HA_{BP}-CaP	1/7	0/7	2/8	0/8
HA_{BP}-CaP-lowBMP2	8/8	8/8	8/8	8/8
HA_{BP}-CaP-highBMP2	4/8	8/8	3/8	8/8
Empty tube	0/4	0/4	NA	NA

** Bridging was assessed histologically; numbers indicate number of defects showing complete segmental defect bridging out of total number of defects per experimental group.*

defect area, but also outside of this area. Particularly for those groups with added BMP-2, substantial bone tissue was formed outside the original defect area. Outside the ROI there was significantly less bone in SHAM animals for HA_{BP}-CaP compared to HA_{BP}-CaP-lowBMP2 and HA_{BP}-CaP-highBMP2 (both $p<0.001$). In ORX animals the bone in ROIOUT was significantly higher for HA_{BP}-CaP-lowBMP2 compared to HA_{BP}-CaP and HA_{BP}-CaP-highBMP2 (both $p<0.001$). Between conditions there was a significant difference in the favor of SHAM for HA_{BP}-CaP-highBMP2 both inside and outside the ROI (ROIIN $p<0.05$ and ROIOUT $p<0.01$).

Descriptive histology

Representative histology images of the segmental defects are depicted in **Figure 6A**. Histological images of both control groups (with no tube or empty tube) confirmed that the used segmental defect can be classified as critical size defect.

In all three of the experimental groups (HA_{BP}-CaP, HA_{BP}-CaP-lowBMP2, HA_{BP}-CaP-highBMP2) there was apparent bone formation. There was a difference between bone formed with or without BMP-2. When using the gel only (HA_{BP}-CaP) bone regeneration was seen at both ends of the defect as a cortical edge growing towards the center. However, none of the samples with HA_{BP}-CaP had fully bridged bone defects (**Table 2**). For the HA_{BP}-CaP-lowBMP2 samples all had complete filling of bone within the defect areas for both ORX and SHAM. The newly formed bone in these samples was spongeous-like and dispersed throughout the ROIIN. In the HA_{BP}-CaP-highBMP2 samples bone defects were filled with bone but the bone formation was cyst-like with a very thin shell. Also, around the tube and both side of the fixation plate an even thinner layer of bone was formed.

Magnifications of the samples showed almost all material has degraded. Only in a few samples material remnants were detected, as small uncouloured particles with irregular shaped edges, entrapped within the newly formed bone (**Figure 6A**, black arrows indicate material remnants). Higher magnification showed the cysts formed with high dosage of BMP-2 were filled with adipose cells (**Figure 6A**). Defects bridged by bone with low dose of BMP-2 also contained more adipose cells within the defect area compared to the defects without BMP-2.

Histomorphometry analysis

Histomorphometrical data are depicted in **Figure 6B**. For SHAM animals this material had the least amount of bone formation compared to other materials and none bridged the defect. Histomorphometry analysis between the different experimental groups bone formation showed to be highest for HA_{BP}-CaP-lowBMP2 in both SHAM and ORX animals (34.2% and 38.5% respectively). As already mentioned bone formation was not only seen within the original defect area, but also outside of this area. Particularly for those groups with added BMP-2, substantial bone tissue was formed outside the original defect area.

Statistical analysis for histomorphometric bone formation was significantly higher for HA_{BP}-CaP-lowBMP2 compared other material groups ($p<0.05$ compared to HA_{BP}-CaP in both conditions and $p<0.01$ compared to HA_{BP}-CaP-highBMP2 for SHAM animals). In ORX, HA_{BP}-CaP-highBMP2 showed significantly less bone compared to HA_{BP}-CaP ($p<0.01$). Bone formation outside the ROI was significantly lower for HA_{BP}-CaP compared to HA_{BP}-CaP-lowBMP2 and HA_{BP}-CaP-highBMP2 in both SHAM and ORX animals (all $p<0.001$).

Between the two bone conditions, there was more bone in favour of SHAM for HA_{BP}-CaP-highBMP2 within the defect area compared to osteoporotic bone conditions ($p<0.05$).

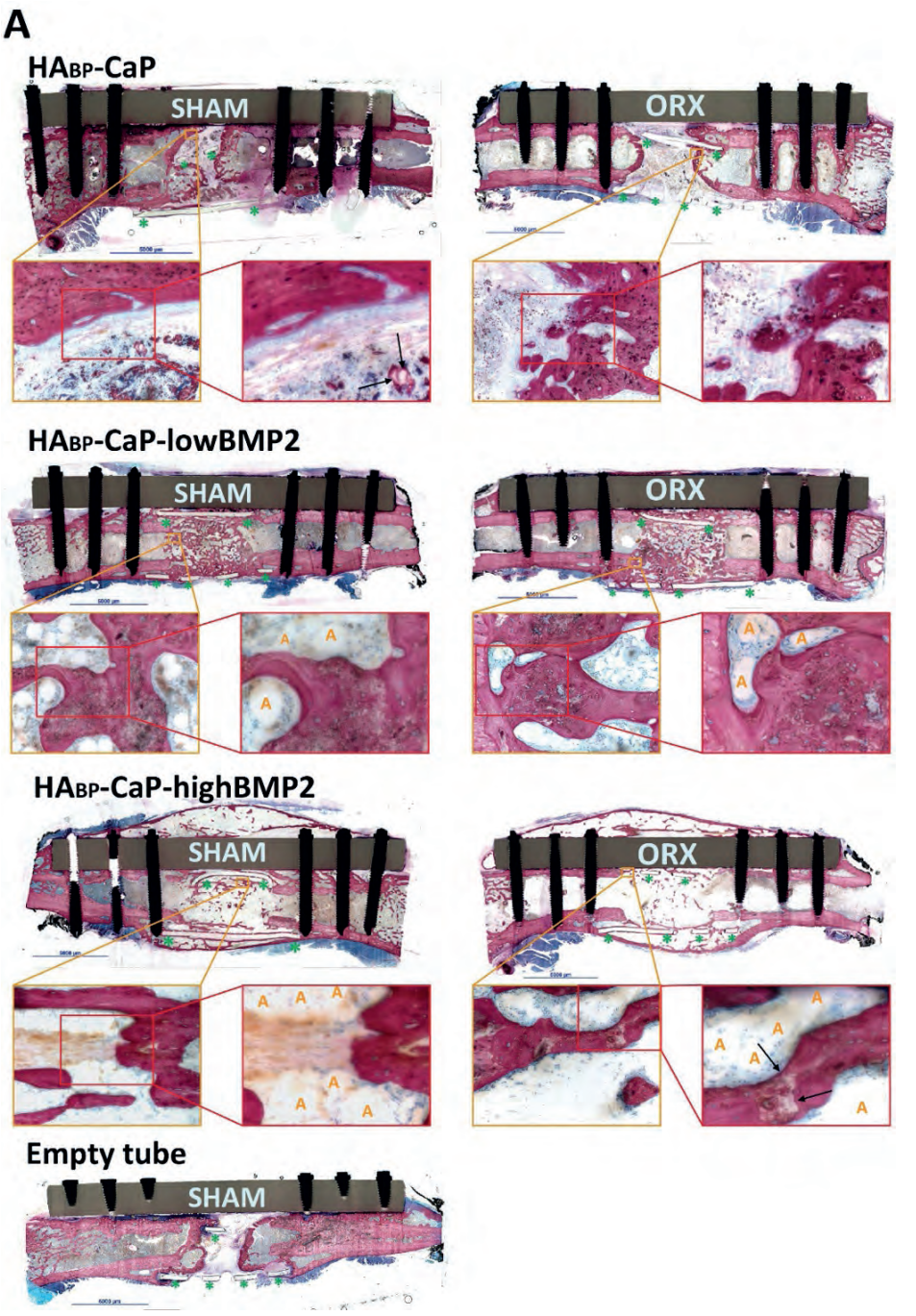
A
HABP-CaP
SHAM
ORX
HABP-CaP-lowBMP2
SHAM
ORX
HABP-CaP-highBMP2
SHAM
ORX
Empty tube
SHAM

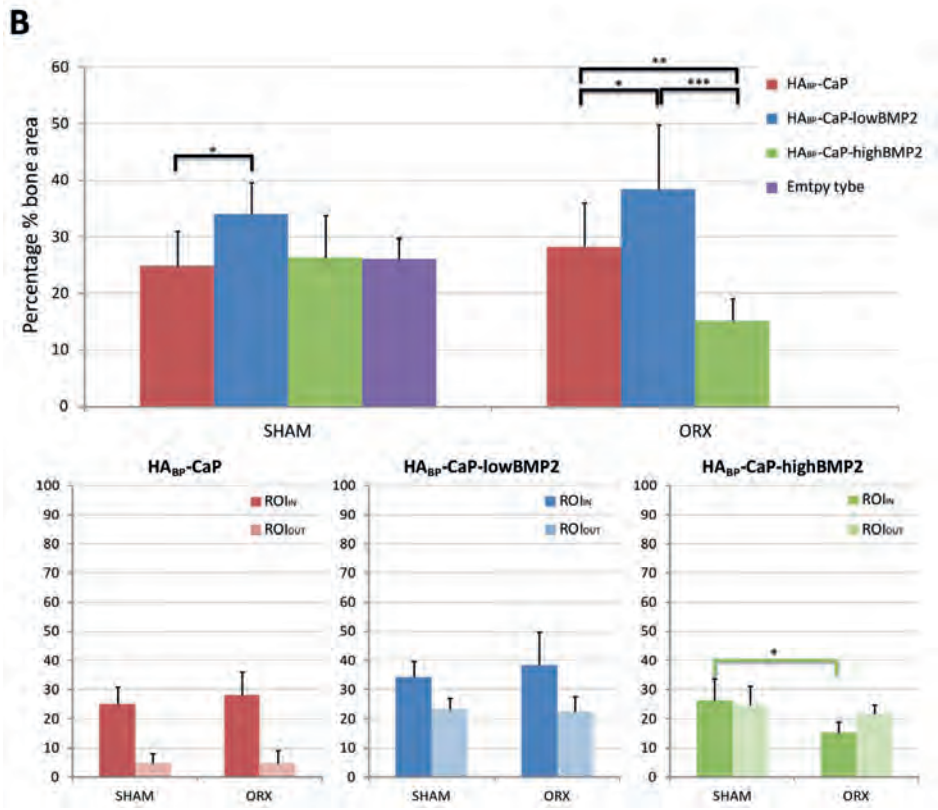

Figure 6 A-B: **A]** Representative histological images and magnifications (orange =20x and red 40x) of all 3 material groups of SHAM and ORX animals and of the SHAM animals with an empty tube. Green asterisks are placed below pieces of the tube. Black arrows indicate material remnants. Orange A's are placed in adipose tissue. **B]** Quantitative analysis based on histomorphometry of bone formation (percentage % bone area in mean data ±SD) within and outside the ROI. With the larger graph comparing between groups and the smaller between ROIIN and ROIOUT and per material group; analysis showing significant differences of *] p<0.05, **] p<0.01 and ***] p<0.001.

Discussion

In the current study, bone regeneration was examined using a rat critical sized femoral defect model, in which the effects of bone condition (healthy versus osteoporotic bone) and BMP-2 incorporation into the HA_{BP}-CaP hydrogel were comparitively evaluated. We hypothesized that (i) an osteoporotic condition would negatively affect defect healing, and (ii) that enrichment of the HA_{BP}-CaP gel with BMP-2 would improve defect healing in both healthy and osteoporotic conditions.

The osteoporotic model was validated by serum TRAP analysis. In a previous study, we used in vivo micro-CT to analyze trabecular bone morphometry after orchidectomy and found less trabecular bone compared to healthy rats [17]. Also, the segmental femoral bone defect model of 6 mm proved to be of critical size as none of the control groups showed bridging. This corroborates with other studies using the RatFix system [20-24].

For this study, the hydrogel was applied in a PTFE tube to contain it within the defect area. The strong bond of the cabon-fluorine gives PTFE the durable properties, inertness and resistance to chemical, biological and physical degradation [25]. PTFE as biomaterial has been widely used in clinics for several years [26-35], and is generally considered to be a well-tolerated material and useful when autologous tissue is not available. One major drawback is the risk of infection. In our study, no infection was observed in any of the animals. To study the effect of the tube on the bone formation two control groups were included, one with and one without the tube. The distal femur of two out of four defects without tube were found to be loosened. The other two femurs had intact plate and screws and showed some bone formation on the plate side of the defect. The four femurs with an empty tube showed more equally distributed bone formation starting from each side of the defect, suggesting a scaffolding effect of the tube. However, none of the control group, with or without tube, showed complete bridging of the defect.

In view of increased demands for synthetic bone grafts with advantageous properties, we previously designed an injectable, hydrogel consisting of bisphosphonated hyaluronan and CaP nanoparticles 16. The major biological advantage of this material at the time was ingrowth of newly-formed trabecular-like bone interspersed throughout the material after 4 weeks in a femoral condyle defect in rats 16. Our results show that the hydrogel was almost all resorbed by 12 weeks and did allow for bone ingrowth. However, the results of this study demonstrate that this material alone is insufficient to regenerate 6 mm rat critical size segmental bone defects.

Additionally, the efficacy of BMP-2 loading in the hydrogel was examined in this study and found to be effective and dose-dependent. Qualitative and quantitative analysis for bone formation by radiography, micro-CT and histomorphometry showed optimal healing for HA_{BP}-CaP-lowBMP2 in both healthy and osteoporotic bone conditions. Qualitative data showed

the type of bone formation was different depending on the material used. When the tube was empty or filled with gel only more cortical bone was formed from the edges of the bone inwards. Whereas when BMP-2 was used bone formation was more spongeous-like, especially for low dose BMP-2. A more cyst-like formation was seen when high dosage of BMP-2 was used. The quantitative data showed the most bone volume for the hydrogel with low dosage of BMP-2. However, the spongious-like bone was not tested for strength and more research should be performed to further inform on the quality of the two different bone formations with or without BMP-2.

Since the discovery of BMP-2 by Urist in 1965, many studies show similar promising effect of BMP-2. In 2007 it was first approved by the FDA (Food and Drug Administration) for clinical purpose reporting "near perfect" safety [36]. In the recent years, however, several (pre-)clinical studies with the use of BMP-2 for bone regeneration do show several adverse effects [36,37]. These include in general inflammatory and wound complications, ectopic bone, osteoclast activation, osteolysis and graft subsidence 36. More specifically for spinal fusion, complications can be radiculopathy, urogenital events (retrograde ejaculation and bladder retention) and most concerning cervical spine swelling to the extent of being potentially life-threatening [36,37]. Remarkably, we observed significantly less bone and lower quality of formed bone for HA_{BP}-CaP-highBMP2 compared to HA_{BP}-CaP-lowBMP2. Studies analyzing the signaling of BMP-2 have found that BMP-2 induces expression of numerous inflammatory cytokines and chemokines, including TNF-α and interleukins [38-40]. Yamazaki et al. found that TNF-α represses BMP-2, which is increased by the use of BMP-2, therefore not only resulting in inflammation but also in inhibition of osteoblastgenesis [41]. Liao et al. found that BMP-2 not only affects MSCs by inducing both osteogenic and chondrogenic differentiation through RUNX2 pathway, but also can promote adipogenic differentiation [36,42]. The latter could be related to bone cyst formation with decreased overall bone quality [36]. This was also seen in the study by Zara et al., who used the same segmental defect as was used in this study, filled with collagen sponges infused with several dosages of BMP-2 [43]. Their study showed that high dosages of BMP-2 induce inflammation resulting in structurally abnormal bone in vivo, with the formation of cyst-like bony shells filled with adipose tissue [43]. This corroborates with our results of high BMP-2 dosage showing bone formation outside the defect in a similar matter. Also, the increased number of adipose cells within the defect area for both high and low dose BMP-2 corresponds with these studies [36,42,43]. Zara et al. postulated that high dosage of BMP-2 disregulates Wnt signaling and activate PPARγ leading to abnormal structure decreasing bone quality and probably influencing the mechanical properties.

As osteoporosis is increasingly becoming a major health problem, we aimed to examine bone regenerating capacity of a bone substitute material in both healthy and osteoporotic conditions. However, very few differences were observed between the healthy and osteoporotic conditions. Only for the HA_{BP}-CaP-highBMP2, superior regeneration in healthy conditions was found. This observation corroborates with one of our other studies, in which CPC/PLGA and Bio-Oss® were compared in healthy and osteoporotic conditions in a rat

femoral bone defect model and also no significant differences between the two conditions in terms of bone regeneration were found [44]. As already mentioned, a high dosage BMP-2 can have adverse effects, such as general inflammatory and wound complications, ectopic bone, osteoclast activation, osteolysis and graft subsidence. In this study these adverse effects of a high dosage of BMP-2 on bone regeneration seems less pronounced in osteoporotic conditions. An explanation for this could be found in the serum TRAP analysis. Our results show significantly lower amounts of serum TRAP in osteoporotic conditions, which is in concurrence with a previous studies [45,46]. We concluded that the lower amount of TRAP indicates a decreased absolute number of active osteoclast due to a decreased amount of bone [45,46]. This absolute decreased amount of active osteoclasts combined with less bone volume can explain why BMP-2 has less effect in osteoporotic conditions. Furthermore, the high dosage of BMP-2 could result in more bone resorption by further increasing the number of active osteoclast [36,43]. To confirm this hypothesis more research with gene expression analysis in osteoporotic conditions should be performed.

Conclusion

The current study shows that critical size, segmental femoral bone defects cannot be healed with HA_{BP}-CaP gel alone. Loading of the HA_{BP}-CaP gel with low dose BMP-2 significantly improved bone formation and resulted in defect bridging in 100% of the defects. Alternatively, high dose BMP-2 loading of the HA_{BP}-CaP gel did not improve bone formation within the defect area, but led to excessive bone outside the defect area by cyst-like formation. Surprisingly, bone defect healing was not negatively affected by osteoporotic bone conditions, except when using high dose BMP-2.

Acknowledgements

The authors would like to acknowledge ms. N. van Dijk for her assistance with the histological sectioning and dr. V. Cuijpers for his assistance on the histological imaging and histomorphometrical analysis. We further acknowledge the department of pathology, especially ms. M. Hermsen, for assistance with automated scanning of histological sections.

References

1. Spicer PP, Kretlow JD, Young S, Jansen JA, Kasper FK, Mikos AG. Evaluation of bone regeneration using the rat critical size calvarial defect. *Nat Protoc* 2012; **7**(10): 1918-29.

2. Urist MR, Mazet R, Jr., Mc LF. The pathogenesis and treatment of delayed union and non-union; a survey of eighty-five ununited fractures of the shaft of the tibia and one hundred control cases with similar injuries. *J Bone Joint Surg Am* 1954; **36-A**(5): 931-80; passim.

3. Greenwald AS, Boden SD, Goldberg VM, et al. Bone-graft substitutes: facts, fictions, and applications. *J Bone Joint Surg Am* 2001; **83-A Suppl 2 Pt 2**: 98-103.

4. Berggren A, Weiland AJ, Dorfman H. Free vascularized bone grafts: factors affecting their survival and ability to heal to recipient bone defects. *Plast Reconstr Surg* 1982; **69**(1): 19-29.

5. Weiland AJ, Phillips TW, Randolph MA. Bone grafts: a radiologic, histologic, and biomechanical model comparing autografts, allografts, and free vascularized bone grafts. *Plast Reconstr Surg* 1984; **74**(3): 368-79.

6. Muramatsu K, Bishop AT. Cell repopulation in vascularized bone grafts. *J Orthopaed Res* 2002; **20**(4): 772-8.

7. Arata MA, Wood MB, Cooney WP, 3rd. Revascularized segmental diaphyseal bone transfers in the canine. An analysis of viability. *J Reconstr Microsurg* 1984; **1**(1): 11-9.

8. Dimitriou R, Mataliotakis GI, Angoules AG, Kanakaris NK, Giannoudis PV. Complications following autologous bone graft harvesting from the iliac crest and using the RIA: a systematic review. *Injury* 2011; **42 Suppl 2**: S3-15.

9. Prevention and management of osteoporosis. *World Health Organ Tech Rep Ser* 2003; **921**: 1-164, back cover.

10. Sanfilippo F, Bianchi AE. Osteoporosis: the effect on maxillary bone resorption and therapeutic possibilities by means of implant prostheses--a literature review and clinical considerations. *Int J Periodontics Restorative Dent* 2003; **23**(5): 447-57.

11. Fini M, Giavaresi G, Torricelli P, et al. Osteoporosis and biomaterial osteointegration. *Biomed Pharmacother* 2004; **58**(9): 487-93.

12. Finigan J. Bone up on osteoporosis. *Nurs Stand* 2003; **17**(51): 104.

13. Ott SM. Cortical or Trabecular Bone: What's the Difference? *Am J Nephrol* 2018; **47**(6): 373-5.

14. Bongio M, van den Beucken JJJP, Leeuwenburgh SCG, Jansen JA. Development of bone substitute materials: from 'biocompatible' to 'instructive'. *J Mater Chem* 2010; **20**(40): 8747-59.

15. Hench LL. The story of Bioglass. *J Mater Sci Mater Med* 2006; **17**(11): 967-78.

16. Nejadnik MR, Yang X, Bongio M, et al. Self-healing hybrid nanocomposites consisting of bisphosphonated hyaluronan and calcium phosphate nanoparticles. *Biomaterials* 2014; **35**(25): 6918-29.

17. Alghamdi HS, van den Beucken JJ, Jansen JA. Osteoporotic rat models for evaluation of osseointegration of bone implants. ***Tissue Eng Part C Methods*** 2014; **20**(6): 493-505.

18. van der Lubbe HB, Klein CP, de Groot K. A simple method for preparing thin (10 microM) histological sections of undecalcified plastic embedded bone with implants. ***Stain Technol*** 1988; **63**(3): 171-6.

19. Lopez-Heredia MA, Bongio M, Cuijpers VM, et al. Bone formation analysis: effect of quantification procedures on the study outcome. ***Tissue Eng Part C Methods*** 2012; **18**(5): 369-73.

20. Poser L, Matthys R, Schawalder P, Pearce S, Alini M, Zeiter S. A standardized critical size defect model in normal and osteoporotic rats to evaluate bone tissue engineered constructs. ***Biomed Res Int*** 2014; **2014**: 348635.

21. Chatterjea A, van der Stok J, Danoux CB, et al. Inflammatory response and bone healing capacity of two porous calcium phosphate ceramics in critical size cortical bone defects. ***J Biomed Mater Res A*** 2014; **102**(5): 1399-407.

22. van der Stok J, Koolen MK, Jahr H, et al. Chondrogenically differentiated mesenchymal stromal cell pellets stimulate endochondral bone regeneration in critical-sized bone defects. ***Eur Cell Mater*** 2014; **27**: 137-48; discussion 48.

23. Van der Stok J, Van der Jagt OP, Amin Yavari S, et al. Selective laser melting-produced porous titanium scaffolds regenerate bone in critical size cortical bone defects. ***J Orthop Res*** 2013; **31**(5): 792-9.

24. Sato K, Watanabe Y, Harada N, et al. Establishment of reproducible, critical-sized, femoral segmental bone defects in rats. ***Tissue Eng Part C Methods*** 2014; **20**(12): 1037-41.

25. Henry BJ, Carlin JP, Hammerschmidt JA, et al. A critical review of the application of polymer of low concern and regulatory criteria to fluoropolymers. ***Integr Environ Assess Manag*** 2018; **14**(3): 316-34.

26. Bellon JM, Bujan J, Contreras LA, Hernando A, Jurado F. Similarity in behavior of polytetrafluoroethylene (ePTFE) prostheses implanted into different interfaces. ***J Biomed Mater Res*** 1996; **31**(1): 1-9.

27. Grimme FA, Reijnen MM, Pfister K, Martens JM, Kasprzak P. Polytetrafluoroethylene covered stent placement for focal occlusive disease of the infrarenal aorta. ***Eur J Vasc Endovasc Surg*** 2014; **48**(5): 545-50.

28. Baker LD, Jr., Johnson JM, Goldfarb D. Expanded polytetrafluoroethylene (PTFE) subcutaneous arteriovenous conduit: an improved vascular access for chronic hemodialysis. ***Trans Am Soc Artif Intern Organs*** 1976; **22**: 382-7.

29. Feliciano DV, Mattox KL, Graham JM, Bitondo CG. Five-year experience with PTFE grafts in vascular wounds. ***J Trauma*** 1985; **25**(1): 71-82.

30. Bellon JM, Contreras LA, Bujan J, Carrera-San Martin A. The use of biomaterials in the repair of abdominal wall defects: a comparative study between polypropylene meshes (Marlex) and a new polytetrafluoroethylene prosthesis (Dual Mesh). ***J Biomater Appl*** 1997; **12**(2): 121-35.

31. Gillion JF, Begin GF, Marecos C, Fourtanier G. Expanded polytetrafluoroethylene patches used in the intraperitoneal or extraperitoneal position for repair of incisional hernias of the anterolateral abdominal wall. *Am J Surg* 1997; **174**(1): 16-9.

32. Lukasiewicz A, Drewa T. Synthetic implants in hernia surgery. *Adv Clin Exp Med* 2014; **23**(1): 135-42.

33. Fotek PD, Neiva RF, Wang HL. Comparison of dermal matrix and polytetrafluoroethylene membrane for socket bone augmentation: a clinical and histologic study. *J Periodontol* 2009; **80**(5): 776-85.

34. Jacob T, LaCour OJ, Burgoyne CF, LaFleur PK, Duzman E. Expanded polytetrafluoroethylene reinforcement material in glaucoma drain surgery. *J Glaucoma* 2001; **10**(2): 115-20.

35. Sevy A, Arriaga M. The Stapes Prosthesis: Past, Present, and Future. *Otolaryngol Clin North Am* 2018; **51**(2): 393-404.

36. James AW, LaChaud G, Shen J, et al. A Review of the Clinical Side Effects of Bone Morphogenetic Protein-2. *Tissue Eng Part B Rev* 2016; **22**(4): 284-97.

37. Epstein NE. Complications due to the use of BMP/INFUSE in spine surgery: The evidence continues to mount. *Surg Neurol Int* 2013; **4**(Suppl 5): S343-52.

38. Liu J, Chen L, zhou Y, Liu X, Tang K. Insulin-like growth factor-1 and bone morphogenetic protein-2 jointly mediate prostaglandin E2-induced adipogenic differentiation of rat tendon stem cells. *PLoS One* 2014; **9**(1): e85469.

39. Jeon MJ, Kim JA, Kwon SH, et al. Activation of peroxisome proliferator-activated receptor-gamma inhibits the Runx2-mediated transcription of osteocalcin in osteoblasts. *J Biol Chem* 2003; **278**(26): 23270-7.

40. Suda T, Takahashi N, Udagawa N, Jimi E, Gillespie MT, Martin TJ. Modulation of osteoclast differentiation and function by the new members of the tumor necrosis factor receptor and ligand families. *Endocr Rev* 1999; **20**(3): 345-57.

41. Yamazaki M, Fukushima H, Shin M, et al. Tumor necrosis factor alpha represses bone morphogenetic protein (BMP) signaling by interfering with the DNA binding of Smads through the activation of NF-kappaB. *J Biol Chem* 2009; **284**(51): 35987-95.

42. Liao X, Wu L, Fu M, et al. [Chondrogenic phenotype differentiation of bone marrow mesenchymal stem cells induced by bone morphogenetic protein 2 under hypoxic microenvironment in vitro]. *Zhongguo Xiu Fu Chong Jian Wai Ke Za Zhi* 2012; **26**(6): 743-8.

43. Zara JN, Siu RK, Zhang X, et al. High doses of bone morphogenetic protein 2 induce structurally abnormal bone and inflammation in vivo. *Tissue Eng Part A* 2011; **17**(9-10): 1389-99.

44. van Houdt CIA, Ulrich DJO, Jansen JA, van den Beucken J. The performance of CPC/PLGA and Bio-Oss((R)) for bone regeneration in healthy and osteoporotic rats. *J Biomed Mater Res B Appl Biomater* 2018; **106**(1): 131-42.

45. van Houdt CI, Tim CR, Crovace MC, et al. Bone regeneration and gene expression in bone defects under healthy and osteoporotic bone conditions using two commercially available bone graft substitutes. *Biomed Mater* 2015; **10**(3): 035003.

46. Rissanen JP, Suominen MI, Peng Z, Halleen JM. Secreted tartrate-resistant acid phosphatase 5b is a Marker of osteoclast number in human osteoclast cultures and the rat ovariectomy model. *Calcif Tissue Int* 2008; **82**(2): 108-15.

8

CHAPTER 8

Summary and closing remarks

Summary

Chapter 1
General introduction

Bone has the regenerative capacity to completely heal defects and fracture, and restore its properties as was before the damage (Thorne et al. 2014, Gianoudis et al. 2007). A disruption to this regenerative capacity can lead to uncomplete healing (Gianoudis et al. 2007). Surgical intervention using bone grafting is used to repair and augment damaged or diseased bone in cases that exceed the critical boundaries for spontaneous healing. The gold standard in bone regeneration is the use of autologous bone graft; however, there are several disadvantages when using autologous bone, such as an additional surgical site and patient-related compromised bone quality. Therefore, synthetic bone substitutes have been developed to overcome these drawbacks. Beside the material choice, it is also important to consider the conditions in which the bone substitutes have to perform, which may not be optimal. This thesis focuses specifically on critically sized defects and the systemically compromised bone condition osteoporosis. When using autologous bone graft to aid bone healing, osteoporosis causes added complexity because of the systemic nature of the disease (Fini et al. 2004). Because osteoporosis is an age-related disease, the challenge of bone regeneration in osteoporotic conditions is becoming more relevant with the number of elderly patients expecting to increase significantly over the next several decades (Carmona et al. 2004, Johnell et al. 2006, Burge et al. 2007).

Based on the above mentioned, the main objective of this thesis was to evaluate bone regeneration using bone graft substitutes, both commercially available and novel materials, in healthy and compromised conditions using ***in vivo*** animal models. For this, we focused on evaluation of bone regeneration in osteoporotic conditions, challenged bone regeneration using defect size, and explored novel experimental bone substitute materials with appealing properties for stimulation of bone regeneration. The following sections recapitulate the specific objectives and performed experimental work for this thesis.

Chapter 2
Evaluate the efficacy of two commercially available materials, Biosilicate® and Bio-Oss®, in healthy and osteoporotic conditions at both tissue and molecular level by gene-expression analysis.

Biosilicate® and Bio-Oss® are two commercially available bone substitutes, however, little is known regarding their efficacy in osteoporotic conditions. The purpose of this study was to evaluate the osteogenic properties of both materials, at tissue and molecular level. Thirty-six Wistar rats were submitted to ovariectomy (OVX) for inducing osteoporotic conditions and sham surgery (SHAM) as a control. Bone defects were created in both femurs, which were filled with Biosilicate® or Bio-Oss®, and empty defects were used as control. Results showed for the healthy condition both Biosilicate® and Bio-Oss® did not improve bone formation after 4 weeks. Histomorphometric evaluation of osteoporotic bone defects with

bone substitutes showed more bone formation compared to empty controls. To determine effects of the bone condition on mesenchymal stem cells (MSCs), molecular biological evaluation was performed by gene-expression analysis (Runx-2, ALP, OC, OPG, RANKL). The relative gene expression was increased with Biosilicate® for all genes in MSCs from OVX rats and for Runx-2, ALP, OC and RANKL in MSCs from SHAM rats. In contrast, with Bio-Oss®, the relative gene expression of MSCs from OVX rats was similar for all three groups. For MSCs from SHAM rats, gene expression was increased for Runx-2, ALP, OC and RANKL. Since both materials improved bone regeneration in osteoporotic conditions, our results suggest that bone defects in osteoporotic conditions can be efficiently treated with these two bone substitutes.

Chapter 3

Evaluate the efficacy of calcium phosphate cement with porogens in bone defects created in healthy and osteoporotic conditions.

Next to the two commercially available bone substitutes mentioned in the previous chapter, we aimed to analyse the efficacy of a novel biomaterial with appealing handling properties and controllable degradation. Calcium phosphate (CaP) based materials are synthetic inorganic biomaterials that show high similarity to bone tissue by resembling the mineral phase of bone and are already popular implant materials in several fields of surgery. CaP based materials are available in several forms, such as pre-set samples as well as in an injectable form. As an injectable CaP cement (CPC), the main disadvantage is its low degradation rate mainly due to the inadequate intrinsic porosity. We questioned to what extent an osteoporotic bone condition affects the biological performance of CPC, more specifically material degradation and bone regenerative capacity. To answer these questions, we aimed to comparatively evaluate the biological performance of CPC combined with polylactic-co-glycolic acid (PLGA) micro-particles and Bio-Oss® in ovariectomized and healthy rats. Thirty-two Wistar rats received alternating experimental CPC/PLGA and Bio-Oss® in femoral condyle defects in both femurs 6 weeks after ovariectomy (OVX, n=16) or sham operation (SHAM, n=16). Six weeks after OVX or SHAM surgery, bone morphology was analysed by ***in vivo*** computed tomography (CT) to confirm osteoporotic bone condition. Analysis of bone formation and material remnants at 4 and 12 weeks after material implantation was performed by micro-CT, descriptive histology, histomorphometry and bone dynamics by fluorochrome labelling. The ***in vivo*** CT scans showed effective induction of an osteoporotic bone condition by ovariectomy. Our data showed that CPC/PLGA degraded faster and more steadily in osteoporotic conditions. However, Bio-Oss® had significantly less material remnants and showed significantly more bone formation compared to CPC/PLGA. Overall, our data showed relatively high amounts of CPC/PLGA at each time point, hampering new bone formation within the defect area. Osteoporotic conditions proved to significantly affect degradation rates, but did not significantly influence bone formation. We concluded that an osteoporotic bone condition affects degradation of CPC/PLGA, which is vital information for its potential use in osteoporotic conditions.

Chapter 4

Evaluate bone regeneration and material degradation by altering the PLGA porogen content in calcium phosphate cement.

To futher analyse the degradation rate of CPC and increase bone regeneration, this chapter aimed to improve both using different porogens and ratios. We comparatively evaluated the ***in vitro*** degradation effects of dense PLGA microspheres and milled PLGA particles as porogens within CPC. We hypothesized that milled PLGA particles would evoke similar CPC/PLGA degradation compared to dense PLGA microspheres. Additionally, we aimed to examine the effect of PLGA porogen amount in CPC/PLGA via an ***in vivo*** rat femoral bone defect model to determine CPC degradation and bone formation. We hypothesized that a higher PLGA porogen amount would increase the porosity leading to faster degradation and consequently more bone formation ***in vivo***. Our in vitro results showed no differences between both forms of PLGA particles (as porogens in CPC) regarding morphology, porosity and degradation. Using milled PLGA particles as porogens within CPC/PLGA, we evaluated the effect of porogen amount on degradation and bone forming capacity in a rat femoral bone defect model. Titanium landmarks surrounded by CPC/PLGA, at a weight percentage of 50/50 and 70/30wt%, were implanted in the femurs of twenty male Wistar rats. Histomorphometric results showed a significant temporal decrease in the amount of cement for both formulas, and confirmed that 50/50wt% of CPC/PLGA degrades faster than 70/30wt% and allows for a 1.5-fold higher amount of newly formed bone tissue. Taken together, this study demonstrated that (i) PLGA porogens in the form of milled particles perform equal to dense PLGA microspheres, and (ii) tuning of the PLGA content in CPC/PLGA is a feasible approach to leverage material degradation and bone formation.

Chapter 5

Challenge bone regeneration by introducing demineralized bone matrix as bone substitute material into a critical sized calvarial bone defect.

Further challenging bone healing, we examined bone regeneration in a critical sized calvarial bone defect. For this study, we examined demineralised bone matrix (DBM), which is an allograft bone substitute used for bone repair surgery to overcome drawbacks of autologous bone grafting such as limited supply and donor-site comorbidities. In view of different demineralization treatments to obtain DBM, we examined the biological performance of two differently demineralised types of DBM (i.e. by acidic treatment using hydrochloric acid, HCl, or treatment with the chelating agent ethylenediaminetetraacetate, EDTA). Firstly, we evaluated osteoinductive properties of both DBMs by implanting the materials subcutaneously in rats. Secondly, we evaluated effects on bone formation by incorporating DBM in a hyaluronic acid (HA) gel to fill a porous titanium scaffold for use in a critical-sized calvarial defect model in 36 male Wistar rats. These porous titanium scaffolds were implanted empty or filled with HA-gel containing either DBM_{HCl} or DBM_{EDTA}. Ectopically implanted DBM_{HCl} and DBM_{EDTA} did not induce ectopic bone formation over the course of 12 weeks. For the calvarial defects, mean percentages of newly formed bone at 2 weeks were significantly higher for Ti-Empty compared to Ti-HA+DBM_{HCl}, but not compared to Ti-HA+DBM_{EDTA}. Significant

temporal bone formation was observed for Ti-Empty and Ti-HA+DBM_{HCl}, but not for Ti-HA+DBM_{EDTA}. At 8 weeks, there were no significant differences in values of bone formation between the three experimental constructs. In conclusion, these results showed that under the current experimental conditions both DBM_{HCl} and DBM_{EDTA} do not possess osteoinductive properties. Additionally, in combination with an HA-gel loaded in a porous titanium scaffold, DBM_{HCl} and DBM_{EDTA} showed similar amounts of new bone formation after 8 weeks, which were lower compared to the empty porous titanium scaffold.

Chapter 6

Evaluate bone regeneration using an "improved" novel material by adding alendronate into the CPC/PLGA and test the efficacy in osteoporotic conditions.

As mentioned before, osteoporosis represents a major health problem in terms of compromising bone strength and increasing the risk of bone fractures. It can be medically treated with bisphosphonates, which act systemically upon oral or venous administration. Further, bone regenerative treatments in osteoporotic conditions present a challenge. Here, we focused on the development of a synthetic bone substitute material with local diminishing effects on osteoporosis. Composites were created using calcium phosphate cement (CPC; 60 wt%) and polylactic-co-glycolic acid (PLGA; 40 wt%), which were loaded with alendronate (ALN). *In vitro* results showed that ALN-loaded CPC/PLGA composites presented clinically suitable properties, including setting times, appropriate compressive strength, and controlled release of ALN, the latter being dependent on composite degradation. Using a rat femoral condyle bone defect model in osteoporotic animals, ALN-loaded CPC/PLGA composites demonstrated stimulatory effects on bone formation both within and outside the defect region.

Chapter 7

Evaluate bone regeneration in a critical sized defect with osteoporotic conditions and enhance the bone substitute material (a self-healing hydrogel containing BP and calcium phosphate) with BMP-2.

Ultimately, we challenged bone regeneration by combining two compromising conditions: a critical sized defect and osteoporotic conditions. In this study, we first aimed to evaluate the biological response to experimental hydrogels with calcium phosphate (CaP) and hyaluronan (HA) with bisphosphonate (BP) physical gelation and BMP-2 in a critical-sized segmental femoral bone defect model in rats. Additionally, we aimed to evaluate the effect of the hydrogels in osteoporotic condition using the same defect model. Fifty-six Wistar rats received either a sham surgery (SHAM) or orchydectomie (ORX). After six weeks to establish osteoporotic conditions for the ORX animals, a critical-sized segmental femoral defect was created in one femur per rat. Two control groups were used: one with only a plate to fixate the defect and a second with the same plate adding an empty PTFE tube. The experimental groups consisted of the plate and tube filled with our hydrogel (HA_{BP}-CaP) and the hydrogel with BMP-2 in a low dosage (HA_{BP}-CaP-lowBMP2) or high dosage (HA_{BP}-CaP-highBMP2). Twelve weeks after the bone defect surgery, bone formation analysis was performed by

X-ray examination, micro-CT analysis, descriptive histology and histomorphometry. Our data from micro-CT analysis showed significantly more bone for HABP-CaP-lowBMP2 compared to HA_{BP}-CaP and HA_{BP}-CaP-highBMP2 in both healthy and osteoporotic bone conditions. Histomorphometry also showed significantly more bone for HA_{BP}-CaP-lowBMP2 compared to HA_{BP}-CaP and HA_{BP}-CaP-highBMP2 in both healthy and osteoporotic conditions. For defects filled with either low or high dosages of BMP-2, an increased amount of bone around the defect area was observed compared to BMP-2 free hydrogels. Only for the HA_{BP}-CaP-highBMP2, a difference between healthy and osteoporotic bone conditions was observed in favour of SHAM. We conclude that the critical-sized defects could be regenerated using our hydrogel, showing most bone formation for hydrogels with low dose BMP-2, regardless of the bone condition.

Closing remarks

Continuous progress in healthcare contributes to extended life-expectancy. With people living longer, the number of people suffering from age-related diseases also increases. Considering bone, the most common age-related disease is osteoporosis, a systemic bone condition in which the remodeling process of bone is out of balance resulting in porous and fragile bone. Patients with osteoporosis have an increased risk for bone fractures as well as impaired bone healing. An increase in the need for bone grafting surgery is expected over the coming decades. With impaired bone healing in osteoporotic patients and the drawbacks of autologous bone grafting (i.e. limited amount and quality of donor bone and extra surgical time and donor site morbidity) the possibility to replace autologous bone by bone substitutes has been explored heavily over the last century. However, the effect of osteoporosis on the performance of such bone substitutes is not clear. The overall aim of this thesis was to investigate the effect of the compromising condition osteoporosis on bone healing using bone graft substitutes. Our research showed that when using two commercially available bone graft substitutes (i.e. Bio-Oss® and Biosilicate®) both materials improve bone regeneration in osteoporotic conditions, but do not in healthy conditions (Chapter 2). These data suggest that bone defects in osteoporotic conditions can be successfully treated with synthetic bone substitutes and that bone substitutes are of additional value for bone defect treatment particularly in osteoporotic patients. When examining the effect of osteoporosis on bone substitute degradation, we found that CPC/PLGA degraded faster and more steadily compared to Bio-Oss® in osteoporotic conditions (Chapter 3). However, in absolute values, Bio-Oss® showed significantly fewer material remnants and more bone formation compared to CPC/PLGA. Our data confirmed our hypothesis that an osteoporotic condition affects degradation of CPC/PLGA, which is vital information for its future use in osteoporotic patients. Alternatively, no effects of an osteoporotic condition on bone formation were observed. Consequently, different bone conditions require the selection of a bone graft material with suitable degradation characteristics.

Continuous improvement of healthcare not only results in an increase in life-expectancy, but also comes with better survival, for example, in high energy traumas and after cancer treatment. In both cases, large bone defects can occur in a variety of forms, anatomic locations and patient ages. To overcome these critically sized defects, also here great benefit can be obtained from the use of synthetic instead of autologous bone. To provide support, such large defects often require to be combined with some form of scaffold (carrier) adapted to the bone type and anatomical location of the defect (i.e. long bone or flat, load bearing site or non-load bearing). A second aim of this thesis was to explore the possibility to overcome such large critical size defects with bone substitute materials combined with a stable supporting scaffold. Our results showed that under healthy conditions, bone forming capacity of hyaluronic gel composite with DBM in titanium constructs was not enhanced compared to the osteoconductive properties of an empty porous titanium scaffold alone (Chapter 5). In another experimental setting using segmental defects, our results showed

that a critical size segmental defect of 5mm in the rat femur can heal using a self-healing hybrid nano-composite hydrogel in both healthy and osteoporotic conditions (Chapter 7).

For almost a century, bone substitutes have been under investigation to improve surgical treatment of bone fractures and defects. Since compromising conditions more and more become an interfering factor regarding bone healing, we aimed to examine the effect of osteoporosis to better predict the outcome of bone grafting procedures. A next step is to investigate how to improve bone grafting procedures by altering properties of bone substitutes and possibly further enhance their performance by adding molecules that can elute and locally treat diseased bone. This was our third aim for this thesis. The results of our *in vitro* study with CPC containing equal amounts of either PLGA microspheres or milled particles showed similar scaffold morphology, CPC porosity and degradation (Chapter 4). By increasing the amount of PLGA porogens within CPC, we accelerated CPC/PLGA degradation *in vitro*. The *in vivo* results of CPC/PLGA with milled PLGA showed a favorable bone response. Furthermore, a higher amount of milled PLGA particles (i.e. 50 versus 30 wt%) accelerated both CPC degradation and new bone formation. For future clinical application, milled PLGA particles appear to be promising as CPC porogen. Moreover, the degradation rate of CPC is tunable to meet desired demands at different defect sites and with different patient conditions.

Addition of drugs or growth factors into the material could possibly further enhance and stimulate bone regeneration. The *in vitro* analysis in our study of alendronate (ALN; a frequently used bisphosphonate for osteoporosis) release from calcium phosphate cement for bone regeneration in osteoporotic conditions showed that ALN-loaded CPC/PLGA presents clinically acceptable handling, suitable compressive strength, and a controlled ALN release (Chapter 6). In an *in vivo* bone defect model, application of ALN-loaded CPC/PLGA showed that a relative low dose of ALN (0.5 wt%) significantly increased bone formation in the peri-defect region in osteoporotic conditions, without effect on CPC/PLGA degradation. The data suggest that future clinical application of ALN-loaded CPC/PLGA can be beneficial for the healing of bone defects in a compromised osteoporotic condition.

In another experimental set-up, our *in vivo* result showed that a critical size, segmental femoral bone defects could not be healed with HABP-CaP gel alone (Chapter 7). Loading of the HABP-CaP gel with a low dose of BMP-2 significantly improved bone formation and resulted in defect bridging in 100% of the defects. Alternatively, high dose BMP-2 loading of the HABP-CaP gel did not improve bone formation within the defect area, but led to excessive bone formation outside the defect area. Future use of BMP-2 appears to beneficial, however, the effect is highly dose dependent.

Future perspectives

The process of bone healing has been a research topic for several decades with the aim to prevent and/or treat fractures and bone defects. The multifactorial aspect of healing makes

it an interesting and complex subject for researchers worldwide. In this thesis, we aimed to examine the effect of osteoporosis as a systemic condition interfering with bone homeostasis on the performance of bone substitutes in challenging conditions to add information and hopefully provide basis for more research that can ultimately result in complete healing and/or prevention of complex fractures and bone defects in osteoporotic patients.

Development of bone substitutes with improved biological performance

Autologous bone has the advantage of having both properties of osteoconduction and osteoinduction. Therefore, autologous bone remains the gold standard in bone grafting procedures. The term osteoconduction refers to the ability of bone to grow along a surface, i.e. to conduct bone from one end of the defect to the other. In other words, bone regeneration is established by growing bone tissue that exploits the material within the defect (formed or placed) as a scaffold. Bone substitutes generally also have osteoconductive properties. This can be influenced by the number and sizes of pores within the material and also by the degradation rate. These properties can be tunable in bone substitutes, and hence can be adjusted to specific needs in different patients and/or defect properties. Since bone healing is multifactorial, tailor-made bone substitutes specifically designed to have patient-specific degradation would be desirable to optimally match physico-chemical material properties with biological conditions in a specific defect site for individual patients.

To further improve bone substitutes, more and more research is performed to engineer biomaterials that also have osteoinductive properties, in order to become capable of healing large and compromised defects. Osteoinduction involves the stimulation of osteoprogenitor cells to differentiate into osteoblasts to form new bone. Bone morphogenetic proteins (BMPs) represent a group of growth factors that are widely used to provide osteoinductive capacity. In this thesis, we found the effect of BMP-2 to be dose-dependent. Further research is needed to reveal the optimal osteoinductive material and determine the correct use of such growth factors regarding their safe loading, release, and biological activity. Also, here, more knowledge can lead to engineering bone substitutes for individual patients with specific bone defect characteristics and patient conditions.

Novel predictive & preventive medicine

As mentioned before, improving healthcare results in an increased life-expectancy and better survival. This is also true for bone trauma or bone cancer treatment, giving rise to more complex and large bone defects. In the previous paragraph, we hypothesized on how bone substitute properties can be changed to improve the biological performance of bone substitutes. To offer optimal treatment of bone defects or fractures in these complex patient conditions, however, research should also continue to focus on patient- and defect-related risk factors in order to optimize outcome. The effect of patient- and defect-related factors on bone healing is quintessential for choosing which surgical procedure and bone substitute to use in order to provide the best care for each individual patient. Nowadays, healthcare is already worldwide changing its strategy to become preventive rather than curative. For

bone fractures, this is the case especially for osteoporosis. Lifestyle changes, better diet advise, and medical treatment for the prevention of osteoporosis are already implemented in global healthcare systems to prevent osteoporotic fractures. Still, a large number of men and women, especially those above 50 years of age, will encounter the complications of this disease. Although bone substitutes cannot be used for the prevention of osteoporosis, they likely can aid in the surgical treatment of bone defects or fractures. Further, once implanted, they can provide prevention of bone fractures by locally releasing suitable anti-osteoporotic or anabolic molecules.

Predictive models for risk of non-unions have been successfully investigated (Zura et al. 2017). Still, the prevention of non-unions remains difficult and the treatment remains a challenge for surgeons and patients. In the case of non-unions, younger patients with comorbidities as smoking, alcoholism, obesity, osteo- or rheumatoid arthritis, type 2 diabetes and/or open fractures are more at risk. Using the information at hand on who will have a high risk of developing a non-union, possibly bone substitutes can be further improved in order to use as a therapeutic. Knowing which risk factor is involved in a patient with a fracture that can contribute to a non-union, adding a tailor-made bone substitute with therapeutic drugs can result in improved bone regeneration and a lower risk of non-union compared to autologous bone graft. When a fracture does not require surgery but is at risk for non-union, another bone substitute with features specifically tailored for the patient can be used. This is a time-consuming, costly and complex research strategy that, however, can help a wide variety of patients.

Local versus systemic treatment of bone conditions

To continuously improve bone substitutes, we discussed the development to upgrade bone substitutes with osteoinductive properties and exploit tunable properties specifically tailored to the need of the individual patient and defect conditions. Addition of drugs (i.e. antibiotics or anti-osteoporotic drugs) to bone substitutes is an example of such a tailor-made property. In the case of osteoporosis, bone turnover imbalance is counteracted by anti-osteoporotic drugs, such as bisphosphonates. These drugs inhibit osteoclast function, resulting in less bone resorption and reduced risk of bone fractures. There are a variety of side effects that can occur, such as stomach problems, kidney failure, osteonecrosis of the jaw, and even an increased risk of esophageal cancer (Kenal et al. 2009). When treating an osteoporotic fracture, anti-osteoporotic drugs can be added to a bone substitute to improve and speed up bone healing. An advantage of locally administered drugs is that the dosage can be reduced and therefore there is less risk of systemic side effects. Combined with preventive medicine, such as healthy nutrition and enough exercise, this can hopefully reduce the need for systemically administration.

References

1. Burge R, Dawson-Hughes B, Solomon DH, Wong JB, King A, Tosteson A. Incidence and economic burden of osteoporosis-related fractures in the United States, 2005-2025. J Bone Miner Res 2007;22(3):465-75.

2. Carmona RH, Beato C, Lawrence A, Moritsugu K, Noonan AS, Katz SI. Bone Health and Osteoporosis: A Report of the Surgeon General. In: McGowan JA, Raisz LG, Noonan AS, Elderkin AL, editors. Bone Health and Osteoporosis: A Report of the Surgeon General. Rockville (MD): Office of the Surgeon General (US) 2004.

3. Fini M, Giavaresi G, Torricelli P, Borsari V, Giardino R, Nicolini A, Carpi A () Osteoporosis and biomaterial osteointegration. Biomedicine & pharmacotherapy 2004;58:487-493.

4. Giannoudis PV, Einhorn TA, Marsh D. Fracture healing: the diamond concept. Injury 2007;38 Suppl 4:S3-6.

5. Johnell O, Kanis JA. An estimate of the worldwide prevalence and disability associated with osteoporotic fractures. Osteoporos Int 2006;17(12):1726-33.

6. Kennel KA, Drake MT. Adverse effects of bisphosphonates: implications for osteoporosis management. Mayo Clin Proc. 2009;84(7):632-638.

7. Zura R, Braid-Forbes MJ, Jeray K, Mehta S, Einhorn TA, Watson JT, Della Rocca GJ, Forbes K, Steen RG. Bone fracture nonunion rate decreases with increasing age: A prospective inception cohort stud. Bone 2017;95:26-32.

9

CHAPTER 9

Samenvatting

Samenvatting

Hoofdstuk 1
Algemene introductie

Bot heeft het regeneratieve vermogen om defecten en breuken volledig te genezen en zijn eigenschappen te herstellen zoals voordat de schade ontstond (Thorne et al. 2014, Gianoudis et al. 2007). Een verstoring van het regeneratieve vermogen van bot kan leiden tot een onvolledige genezing (Gianoudis et al. 2007). Chirurgische interventie met bottransplantatie wordt gebruikt om beschadigd of ziek bot te herstellen en bot toe te voegen in gevallen die de kritische grenzen voor spontane genezing overschrijden. De gouden standaard bij botregeneratie is het gebruik van autoloog bottransplantaat. Er zijn echter verschillende nadelen bij het gebruik van autoloog bot, zoals een extra operatie wond en patiënt gerelateerde verminderde botkwaliteit. Daarom zijn synthetische botvervangers ontwikkeld om deze nadelen te ondervangen. Naast de materiaalkeuze is het ook belangrijk om rekening te houden met de omstandigheden waarin de botvervangers moeten presteren, die wellicht niet optimaal zijn. Dit proefschrift richt zich specifiek op defecten van kritieke grootte en de systemisch botaandoening osteoporose. Bij gebruik van autoloog bottransplantaat om botgenezing te bevorderen, zorgt osteoporose voor extra complexiteit vanwege de systemische aard van de ziekte met negatieve invloed op botgenezing (Fini et al. 2004). Omdat osteoporose een leeftijdsgebonden ziekte is, wordt de uitdaging van botregeneratie bij osteoporotische aandoeningen relevanter, aangezien het aantal oudere patiënten dat verwacht aanzienlijk te stijgen in de komende decennia (Carmona et al. 2004, Johnell et al. 2006, Burge et al. 2007).

Gebaseerd op het bovenstaande, was het hoofddoel van dit proefschrift om botregeneratie te evalueren met behulp van bottransplantaatvervangers, zowel commercieel verkrijgbaar als nieuwe materialen, in gezonde en gecompromitteerde condities met behulp van in vivo diermodellen. Hiervoor hebben we ons gericht op de evaluatie van botregeneratie in osteoporotische condities, botregeneratie uitgedaagd door gebruik te maken van defectgrootte, en nieuwe experimentele botvervangende materialen onderzocht met gunstige eigenschappen voor bevorderen van botregeneratie. De volgende hoofdstukken geven een samenvatting van de specifieke doelstellingen en het de uitgevoerde experimenten die verricht zijn voor dit proefschrift.

Hoofdstuk 2
Evalueren van de werkzaamheid van twee commercieel verkrijgbare materialen, Biosilicate® en Bio-Oss®, in gezonde en osteoporotische condities op zowel weefsel- als moleculair niveau door middel van genexpressieanalyse

Biosilicate® en Bio-Oss® zijn twee in de handel te verkrijgen botvervangers, maar er is weinig bekend over hun werkzaamheid bij osteoporotische aandoeningen. Het doel van deze studie was om de osteogene eigenschappen van beide materialen te evalueren, op weefsel- en moleculair niveau. Zesendertig Wistar-ratten werden onderworpen aan een ovariëctomie (OVX) voor het induceren van osteoporotische aandoeningen en vergeleken

met gezonde (SHAM) ratten ter contole. Botdefecten werden gecreëerd in beide dijbenen, die werden gevuld met Biosilicate® of Bio-Oss®, en lege defecten werden gebruikt als controle. Resultaten toonden voor de gezonde toestand dat zowel Biosilicate® als Bio-Oss® de botvorming na 4 weken niet verbeterden. Histomorfometrische evaluatie van osteoporotische botdefecten met botvervangers liet meer botvorming zien in vergelijking met lege controles. Om de effecten van de botaandoening op mesenchymale stamcellen (MSC's) te bepalen, werd moleculair biologische evaluatie uitgevoerd door middel van genexpressie-analyse (Runx-2, ALP, OC, OPG, RANKL). De relatieve genexpressie werd verhoogd met Biosilicate® voor alle genen in MSC's van ratten met osteoporotische condities en voor Runx-2, ALP, OC en RANKL in MSC's van gezonde ratten. Bij Bio-Oss® daarentegen was de relatieve genexpressie van MSC's van ratten met osteoporotische condities vergelijkbaar voor alle drie de groepen. Voor MSC's van gezonde ratten was de genexpressie verhoogd voor Runx-2, ALP, OC en RANKL. Omdat beide materialen de botregeneratie bij osteoporotische condities verbeterden, suggereren onze resultaten dat botdefecten bij osteoporotische condities efficiënt kunnen worden behandeld met deze twee botvervangers.

Hoofdstuk 3

Evalueren van de werkzaamheid van calciumfosfaatcement met porogenen bij botdefecten die ontstaan onder gezonde en osteoporotische aandoeningen

Naast de twee commercieel verkrijgbare botvervangers die in het vorige hoofdstuk zijn genoemd, wilden we de werkzaamheid analyseren van een nieuw biomateriaal met gunstige hanteringseigenschappen en controleerbare degradatie. Materialen op basis van calciumfosfaat (CaP) zijn synthetische anorganische biomaterialen die in hoge mate gelijkenis vertonen met botweefsel doordat ze lijken op de minerale fase van bot en daardoor al populaire botvervangende materialen zijn in verschillende chirurgische vakgebieden. Op CaP gebaseerde materialen zijn verkrijgbaar in verschillende vormen, zowel in verschillende vormen en mate als ook mede in een injecteerbare vorm die zich vormt naar het defect. Als injecteerbaar CaP-cement (CPC) is het belangrijkste nadeel de lage afbraaksnelheid, voornamelijk als gevolg van de onvoldoende intrinsieke porositeit. We vroegen ons af in hoeverre osteoporotische condities de biologische prestatie van CPC in bot beïnvloedt, meer specifiek de materiaalafbraak en botregeneratieve capaciteit. Om deze vragen te beantwoorden, wilden we de biologische prestatie van CPC in combinatie met polymelk-co-glycolzuur (PLGA) microdeeltjes en Bio-Oss® in gezonde ratten die ovariëctomie hebben ondergaan, relatief evalueren. Tweeëndertig Wistar-ratten kregen 6 weken na ovariëctomie (OVX, n = 16) of schijnoperatie (SHAM, n = 16) afwisselend experimentele CPC / PLGA en Bio-Oss® in femurdefecten beiderzijds. Zes weken na OVX- of SHAM-chirurgie werd de botmorfologie geanalyseerd door in vivo computertomografie (CT) om de osteoporotische botaandoening te bevestigen. Analyse van botvorming en materiaalresten op 4 en 12 weken na implantatie van het materiaal werd uitgevoerd door micro-CT, beschrijvende histologie, histomorfometrie en botdynamica door middel van fluorochrome labeling. De in vivo CT-scans lieten een effectieve inductie zien van een osteoporotische conditie door ovariëctomie. Onze gegevens toonden aan dat CPC / PLGA sneller en gestaag degradeerde

onder osteoporotische condities. Bio-Oss® had echter significant minder materiaalresten en vertoonde significant meer botvorming in vergelijking met CPC / PLGA. Over het algemeen lieten onze gegevens op elk tijdstip relatief hoge hoeveelheden CPC / PLGA zien, waardoor de vorming van nieuw bot in het defectgebied werd belemmerd. Osteoporotische conditie bleek de afbraaksnelheid significant te beïnvloeden, maar hadden geen significante invloed op de botvorming. We concludeerden dat een osteoporotische conditie de afbraak van CPC / PLGA beïnvloedt, wat essentiële informatie is voor het mogelijke gebruik ervan bij osteoporotische aandoeningen.

Hoofdstuk 4

Evalueren van botregeneratie en materiaalafbraak door het PLGA-partikel gehalte in calciumfosfaatcement te veranderen

Om de afbraaksnelheid van CPC verder te analyseren en de botregeneratie te verhogen, had dit hoofdstuk als doel om beide te verbeteren door verschillende partikels en verhoudingen te gebruiken. We evalueerden relatief de in vitro afbraakeffecten van dichte PLGA-microsferen en gemalen PLGA-deeltjes als partikels binnen CPC. Onze hypothese was dat gemalen PLGA-deeltjes vergelijkbare CPC / PLGA-degradatie zouden oproepen in vergelijking met dichte PLGA-microsferen. Bovendien wilden we het effect van hoeveelheid PLGA partikels in CPC onderzoeken via een in vivo model van botdefecten in de femur bij ratten om CPC-afbraak en botvorming te bepalen. Onze hypothese was dat een hogere hoeveelheid PLGA partikels de porositeit zou verhogen, wat zou leiden tot snellere afbraak en bijgevolg meer botvorming in vivo. Onze in vitro resultaten toonden geen verschillen tussen beide vormen van PLGA partikels (microsferen of gemalen deeltjes) wat betreft morfologie, porositeit en degradatie. Met behulp van gemalen PLGA-deeltjes als partikels binnen CPC / PLGA, evalueerden we het effect van de hoeveelheid partikels op afbraak en botvormend vermogen in een femur botdefectmodel van de rat. Titanium oriëntatiepunten omgeven door CPC / PLGA, met een gewichtspercentage van 50/50 en 70/30 gew.%, werden geïmplanteerd in de femora van twintig mannelijke Wistar-ratten. Histomorfometrische resultaten toonden een significante geleidelijke afname van de hoeveelheid cement voor beide formules, en bevestigden dat 50/50 gew.% van CPC / PLGA sneller afbreekt dan 70/30 gew.% en 1,5 keer meer nieuw botvorming mogelijk maakt. Alles bij elkaar heeft deze studie aangetoond dat (i) PLGA partikels in de vorm van gemalen deeltjes gelijk presteren als dichte PLGA-microsferen, en (ii) afstemming van het PLGA-gehalte in CPC / PLGA is een haalbare benadering om materiaalafbraak en botvorming te benutten.

Hoofdstuk 5

Botregeneratie stimuleren door gebruik van gedemineraliseerde botmatrix als botvervangend materiaal in een schedel botdefect van kritieke grootte

Om botgenezing nog verder uit te dagen wilden we botregeneratie onderzoeken in een schedeldefectmodel van kritieke grootte. Voor deze studie hebben we gedemineraliseerde botmatrix (DBM) onderzocht, een allograft botvervanger die wordt gebruikt voor botherstelоperaties om de nadelen van autologe bottransplantatie, zoals

een beperkte voorraad en comorbiditeit op de donorplaats, te beperken. Met het oog op verschillende demineralisatiebehandelingen om DBM te verkrijgen, onderzochten we de biologische prestaties van twee verschillend gedemineraliseerde soorten DBM (d.w.z. door zure behandeling met zoutzuur, HCl of behandeling met het chelaatvormer ethyleendiaminetetraacetaat, EDTA). Ten eerste hebben we de osteo-inductieve eigenschappen van beide DBM's geëvalueerd door de materialen subcutaan in ratten te implanteren. Ten tweede hebben we effecten op botvorming geëvalueerd door DBM op te nemen in een hyaluronzuur (HA) -gel om een poreuze titanium implantaat te vullen voor gebruik in een schedeldefectmodel van kritieke grootte bij 36 mannelijke Wistar-ratten. Deze poreuze titanium implantaten werden leeg geïmplanteerd of gevuld met HA-gel die ofwel DBM-HCl of DBM-EDTA bevatte. Ectopisch geïmplanteerde DBM-HCl en DBM-EDTA veroorzaakten geen ectopische botvorming in de loop van 12 weken. Voor de schedel defecten waren de gemiddelde percentages nieuw gevormd bot na 2 weken significant hoger voor Ti-Empty vergeleken met Ti-HA + DBM-HCl, maar niet vergeleken met Ti-HA + DBM-EDTA. Significante botvorming in de tijd werd waargenomen voor Ti-Empty en Ti-HA + DBM-HCl, maar niet voor Ti-HA + DBM-EDTA. Na 8 weken waren er geen significante verschillen botvorming tussen de drie experimentele constructen. Concluderend lieten deze resultaten zien dat onder de huidige experimentele omstandigheden zowel DBM-HCl als DBM-EDTA geen osteo-inductieve eigenschappen bezitten. Bovendien vertoonden DBM-HCl en DBM-EDTA, in combinatie met een HA-gel geladen in een poreuze titanium implantaat, vergelijkbare hoeveelheden nieuwe botvorming na 8 weken, die lager waren in vergelijking met de lege poreuze titanium implantaat.

Hoofdstuk 6

Evalueren van botregeneratie met behulp van een "verbeterd" nieuw materiaal door alendronaat toe te voegen aan de CPC / PLGA en de werkzaamheid te testen bij osteoporotische condities

Zoals eerder vermeld, vormt osteoporose een groot gezondheidsprobleem in termen van verminderde botsterkte en verhoging van het risico op botbreuken. Het kan medisch worden behandeld met bisfosfonaten, die systemisch werken na orale of veneuze toediening. Bovendien vormen osteoporotische condities ook een uitdaging voor botregeneratieve behandelingen. Hier hebben we ons gericht op de ontwikkeling van een synthetisch botvervangend materiaal met lokaal afnemende effecten op osteoporose. Composieten werden gemaakt met calciumfosfaatcement (CPC; 60 gew.%) en polymelk-co-glycolzuur (PLGA; 40 gew.%), met toevoeging van alendronaat (ALN). In vitro resultaten toonden aan dat ALN-beladen CPC / PLGA-composieten klinisch geschikte eigenschappen vertoonden, waaronder tijden voor uitharding, geschikte weerstand tegen druk en gecontroleerde afgifte van ALN, waarbij de laatste afhankelijk is van de afbraak van het materiaal. Met behulp van een femoraal botdefect bij ratten met osteoporotische condities, vertoonden de CPC / PLGA-composieten met ALN toevoeging een stimulerende effect op botvorming te hebben zowel binnen als buiten het defectgebied.

Hoofdstuk 7

Evalueren van botregeneratie in een defect van kritische grootte met osteoporotische condities en verbeteren van het botvervangende materiaal (een zelfherstellende hydrogel die BP en calciumfosfaat bevat) met BMP-2.

Uiteindelijk hebben we botregeneratie nog verder willen uit dagen door twee compromitterende factoren te combineren: een defect van kritieke grootte en osteoporotische condities. In deze studie wilden we eerst de biologische respons evalueren op experimentele hydrogels met calciumfosfaat (CaP) en hyaluronan (HA) met fysische gelering van bisfosfonaat (BP) en BMP-2 in een segmentaal femoraal botdefect van kritische grootte bij ratten. Bovendien wilden we het effect van de hydrogels in osteoporotische conditie evalueren met behulp van hetzelfde defectmodel. Zesenvijftig Wistar-ratten kregen ofwel een schijnoperatie (SHAM) of orchydectomie (ORX). Na zes weken werd een segmentaal femurdefect van kritische grootte gecreëerd in één femur per rat. Er werden twee controlegroepen gebruikt: een met alleen een plaatje om het defect te fixeren en een tweede met dezelfde plaat met een lege PTFE-buis. De experimentele groepen bestonden uit de plaat en buis gevuld met onze hydrogel (HABP-CaP) en de hydrogel met BMP-2 in een lage dosering (HABP-CaP-lowBMP2) of hoge dosering (HABP-CaP-highBMP2). Twaalf weken na de botdefectoperatie werd botvormingsanalyse uitgevoerd door middel van röntgenonderzoek, micro-CT-analyse, beschrijvende histologie en histomorfometrie. Onze gegevens van micro-CT-analyse lieten significant meer bot zien voor HABP-CaP-lowBMP2 in vergelijking met HABP-CaP en HABP-CaP-highBMP2 in zowel gezonde als osteoporotische condities. Histomorfometrie toonde ook significant meer bot voor HABP-CaP-lowBMP2 in vergelijking met HABP-CaP en HABP-CaP-highBMP2 in zowel gezonde als osteoporotische condities. Voor defecten gevuld met ofwel lage of hoge doseringen BMP-2, werd een grotere hoeveelheid bot rond het defectgebied waargenomen in vergelijking met hydrogels zonder BMP-2. Alleen voor de HABP-CaP-highBMP2 werd een verschil tussen gezonde en osteoporotische botaandoeningen waargenomen in het voordeel van de gezonde conditie. We concluderen dat de defecten van kritieke grootte kunnen worden overbrugt met behulp van onze hydrogel, die de meeste botvorming vertoont voor hydrogels met een lage dosis BMP-2, ongeacht de botconditie.

Afsluitende opmerkingen

Voortdurende vooruitgang in de zorg draagt bij aan een langere levensverwachting. Doordat mensen langer leven, neemt ook het aantal mensen dat aan leeftijd gerelateerde ziekten lijdt toe. Wat bot betreft, is de meest voorkomende leeftijdsgebonden ziekte osteoporose, een systemische botaandoening waarbij het herstelling proces van bot uit balans is, wat resulteert in poreus en kwetsbaar bot. Patiënten met osteoporose hebben een verhoogd risico op botbreuken en een verminderde botgenezing. De komende decennia wordt een toename van de behoefte aan bottransplantatiechirurgie verwacht. Met verminderde botgenezing bij osteoporotische patiënten en de nadelen van autologe bottransplantatie (d.w.z. beperkte hoeveelheid en kwaliteit van donorbot en extra operatietijd en morbiditeit op de donorplaats) is de mogelijkheid om autoloog bot te vervangen door botvervangers de afgelopen eeuw intensief onderzocht. Het effect van osteoporose op de prestatie van dergelijke botvervangende materialen is echter nog niet duidelijk. Het algemene doel van dit proefschrift was om het effect van de compromitterende aandoening osteoporose op botgenezing te onderzoeken met behulp van bottransplantaatvervangers. Ons onderzoek toonde aan dat bij gebruik van twee in de handel verkrijgbare bottransplantaatvervangers (d.w.z. Bio-Oss® en Biosilicate®) beide materialen de botregeneratie verbeteren in osteoporotische condities, maar niet in gezonde omstandigheden (Hoofdstuk 2). Deze gegevens suggereren dat botdefecten bij osteoporotische condities met succes kunnen worden behandeld met synthetische botvervangers en dat botvervangers van toegevoegde waarde zijn voor de behandeling van botdefecten, met name bij osteoporotische patiënten. Bij het onderzoeken van het effect van osteoporose op de afbraak van botvervangers, ontdekten we dat CPC / PLGA sneller en gestaag degradeerde in vergelijking met Bio-Oss® in osteoporotische condities (Hoofdstuk 3). In absolute waarden vertoonde Bio-Oss® echter significant minder materiaalresten en meer botvorming in vergelijking met CPC / PLGA. Onze gegevens bevestigden onze hypothese dat een osteoporotische aandoening de afbraak van CPC / PLGA beïnvloedt, wat essentiële informatie is voor het toekomstige gebruik ervan bij osteoporotische patiënten. Als alternatief werden geen effecten van een osteoporotische aandoening op botvorming waargenomen. Daarom zijn er voor de verschillende botcondities ook een verschillende keuze van bottransplantaatmateriaal nodig met de meest geschikte degradatiekenmerken per aandoening.

Voortdurende verbetering van de zorg leidt niet alleen tot een verhoging van de levensverwachting, maar ook tot een betere overleving, bijvoorbeeld bij hoogenergetische trauma's en na een kankerbehandeling. In beide gevallen kunnen grote botdefecten optreden in verschillende vormen, anatomische locaties en leeftijd van de patiënt. Om deze defecten van kritieke grootte te overwinnen, kan ook hier een groot voordeel worden verkregen door het gebruik van synthetisch in plaats van autoloog bot. Om ondersteuning te bieden, moeten dergelijke grote defecten vaak worden gecombineerd met een of andere vorm van implantaat die is aangepast aan het bottype en de anatomische locatie van het defect (d.w.z. lang bot of plat, gewicht dragend of niet gewicht dragende locatie). Een tweede doel van dit proefschrift was om de mogelijkheid te onderzoeken om zulke grote defecten van kritische afmetingen te

overwinnen met botvervangende materialen in combinatie met een stabiele ondersteunende steiger. Onze resultaten toonden aan dat onder gezonde omstandigheden het botvormend vermogen van botvervangende gel met DBM in titaniumconstructies niet verbeterd was in vergelijking met de osteoconductieve eigenschappen van alleen een lege poreuze titanium implantaat (Hoofdstuk 5). In een andere experimentele setting waarbij gebruik werd gemaakt van segmentale defecten, toonden onze resultaten aan dat een segmentaal defect van 5 mm in het dijbeen van de rat kan genezen met behulp van een zelfherstellende hybride nano-composiet hydrogel in zowel gezonde als osteoporotische condities (Hoofdstuk 7).
Al bijna een eeuw worden botvervangers onderzocht om de chirurgische behandeling van botbreuken en defecten te verbeteren. Omdat compromitterende aandoeningen steeds meer een belemmerende factor worden bij botgenezing, wilden we het effect van osteoporose onderzoeken om de uitkomst van bottransplantatieprocedures beter te voorspellen. Een volgende stap is om te onderzoeken hoe bottransplantatieprocedures kunnen worden verbeterd door de eigenschappen van botvervangers te aanpassen en mogelijk hun prestaties verder te verbeteren door toevoeging van middelen om het aangedane bot lokaal te kunnen behandelen. Dit was ons derde doel voor dit proefschrift. De resultaten van onze in vitro studie met CPC die gelijke hoeveelheden PLGA-microbolletjes of gemalen deeltjes bevatte, lieten een vergelijkbare morfologie, CPC-porositeit en degradatie zien (Hoofdstuk 4). Door de hoeveelheid PLGA-partikels binnen CPC te verhogen, hebben we de afbraak van CPC / PLGA in vitro versneld. De in vivo resultaten van CPC / PLGA met gemalen PLGA lieten een gunstige botrespons zien. Bovendien versnelde een grotere hoeveelheid gemalen PLGA-deeltjes (d.w.z. 50 versus 30 gew.%) zowel de afbraak van CPC als de vorming van nieuw bot. Voor toekomstige klinische toepassingen lijken gemalen PLGA-deeltjes veelbelovend om de porositeit van CPC te bepalen. Bovendien is de afbraaksnelheid van CPC aan te passen om aan de gewenste eisen te voldoen op verschillende defectlocaties en met verschillende patiëntcondities.

Toevoeging van medicijnen of groeifactoren aan het materiaal zou mogelijk de botregeneratie verder kunnen versterken en stimuleren. De in vitro analyse in onze studie van de afgifte van alendronaat (ALN) uit calciumfosfaatcement voor botregeneratie bij osteoporotische aandoeningen toonde aan dat toevoeging van ALN aan CPC / PLGA een klinisch aanvaardbare behandeling is met geschikte uithardingstijden en een gecontroleerde afgifte van ALN geeft (Hoofdstuk 6). In een in vivo botdefectmodel toonde aan dat de toevoeging van een relatief lage dosis ALN (0,5 gew.%) aan CPC / PLGA de botvorming in het gebied rondom het defect bij osteoporotische condities significant verhoogde, zonder effect op CPC / PLGA-degradatie. De gegevens suggereren dat toekomstige klinische toepassing van ALN toevoeging aan CPC / PLGA gunstig kan zijn voor de genezing van botdefecten in bij patienten met een osteoporotische aandoening.
In een andere experimentele opstelling toonde ons in vivo resultaat aan dat segmentale femorale botdefecten van kritieke grootte niet konden worden genezen met alleen HABP-CaP-gel (Hoofdstuk 7). Het laden van de HABP-CaP-gel met een lage dosis BMP-2 verbeterde de botvorming significant en resulteerde in defectoverbrugging in 100% van de

defecten. Als alternatief verbeterde de hoge dosis BMP-2-belading van de HABP-CaP-gel de botvorming binnen het defectgebied niet, maar leidde tot overmatige botvorming buiten het defectgebied. Toekomstig gebruik van BMP-2 lijkt gunstig te zijn, maar het effect is sterk dosisafhankelijk.

Toekomstperspectieven

Het proces van botgenezing is al tientallen jaren een onderwerp voor onderzoek met als doel breuken en botdefecten te voorkomen en/of te behandelen. Het multifactoriële aspect van genezing maakt het een interessant en complex onderwerp voor onderzoekers over de hele wereld. In dit proefschrift wilden we het effect onderzoeken van osteoporose als een systemische aandoening die bothomeostase verstoort op de prestatie van botvervangers in uitdagende omstandigheden om informatie toe te voegen en hopelijk een basis te bieden voor meer onderzoek dat uiteindelijk kan resulteren in volledige genezing en/of preventie van complexe fracturen en botdefecten bij osteoporotische patiënten.

Ontwikkeling van botvervangers met verbeterde biologische prestaties

Autoloog bot heeft het voordeel dat het beide eigenschappen van osteoconductie en osteoinductie heeft. Daarom blijft autoloog bot de gouden standaard bij bottransplantatieprocedures. De term osteoconductie verwijst naar het vermogen van bot om langs een oppervlak te groeien, d.w.z. om bot van het ene uiteinde van het defect naar het andere te geleiden. Met andere woorden, botregeneratie wordt tot stand gebracht door botweefsel te laten groeien over het materiaal dat in het defect wordt geplaatst en als een ladder wordt gebruikt. Botvervangers hebben doorgaans ook osteoconductieve eigenschappen. Dit kan worden beïnvloed door het aantal en de grootte van de poriën in het materiaal en ook door de afbraaksnelheid. Deze eigenschappen kunnen worden afgestemd in botvervangers en kunnen daarom worden aangepast aan specifieke behoeften bij verschillende patiënten en/of defecte eigenschappen. Omdat botgenezing multifactorieel is, zouden op maat gemaakte botvervangers die specifiek zijn ontworpen om patiënt specifieke afbraak te hebben, wenselijk zijn om de fysisch-chemische materiaaleigenschappen optimaal te matchen met biologische omstandigheden op een specifieke defectlocatie voor individuele patiënten.

Om botvervangers verder te verbeteren, wordt er steeds meer onderzoek gedaan naar biomaterialen die ook osteoinductieve eigenschappen hebben, om zo grote en gecompromitteerde defecten te kunnen genezen. Osteoinductie omvat de stimulatie van osteoprogenitor cellen om zich te differentiëren tot osteoblasten om nieuw bot te vormen. Botmorfogenetische eiwitten (BMP's) vertegenwoordigen een groep groeifactoren die op grote schaal worden gebruikt om osteoinductieve capaciteit te bieden. In dit proefschrift hebben we gevonden dat het effect van BMP-2 dosisafhankelijk is. Verder onderzoek is nodig om het optimale osteoinductieve materiaal te onthullen en het juiste gebruik van dergelijke groeifactoren te bepalen met betrekking tot hun veilige lading, afgifte en biologische activiteit. Ook hier kan meer kennis leiden tot de ontwikkeling van botvervangers

voor individuele patiënten met specifieke kenmerken van botdefecten en patiëntcondities.

Nieuwe voorspellende en preventieve geneeskunde

Zoals eerder vermeld, leidt het verbeteren van de gezondheidszorg tot een hogere levensverwachting en een betere overleving. Dit geldt ook voor bottrauma of behandeling van botkanker, waardoor complexere en grotere botdefecten ontstaan. In de vorige paragraaf hebben we een hypothese opgesteld over hoe botvervangende eigenschappen kunnen worden veranderd om de biologische prestaties van botvervangers te verbeteren. Om een optimale behandeling van botdefecten of fracturen in deze complexe patiëntcondities te bieden, moet het onderzoek zich echter ook blijven richten op patiënt- en defect gerelateerde risicofactoren om de uitkomst te optimaliseren. Het effect van patiënt- en defect gerelateerde factoren op botgenezing is essentieel voor het kiezen van welke chirurgische procedure en botvervanger te gebruiken om de beste zorg voor elke individuele patiënt te bieden. Tegenwoordig verandert de gezondheidszorg al wereldwijd haar strategie om preventief in plaats van curatief te worden. Bij botbreuken is dit vooral het geval bij osteoporose. Veranderingen in levensstijl, beter voedingsadvies en medische behandeling voor de preventie van osteoporose zijn al geïmplementeerd in wereldwijde gezondheidszorgsystemen om osteoporotische fracturen te voorkomen. Toch zal een groot aantal mannen en vrouwen, vooral boven de 50 jaar, met de complicaties van deze ziekte te maken krijgen. Hoewel botvervangers niet kunnen worden gebruikt voor de preventie van osteoporose, kunnen ze waarschijnlijk helpen bij de chirurgische behandeling van botdefecten of botbreuken. Verder kunnen ze, eenmaal geïmplanteerd, botbreuken voorkomen door plaatselijk geschikte anti-osteoporotische of anabole moleculen vrij te geven.

Voorspellende modellen voor het risico van onvolledige botgenezing (non-union) zijn met succes onderzocht (Zura et al. 2017). Toch blijft het voorkomen van non-union moeilijk en blijft de behandeling een uitdaging voor chirurgen en patiënten. Bij non-union lopen jongere patiënten met comorbiditeiten zoals roken, alcoholisme, obesitas, osteo- of reumatoïde artritis, diabetes type 2 en/of open fracturen meer risico. Met behulp van de beschikbare informatie over wie een hoog risico loopt om een non-union te ontwikkelen, kunnen mogelijk botvervangers verder worden verbeterd om als een therapeutisch middel te gebruiken. Wetende welke risicofactor betrokken is bij een patiënt met een fractuur die kan bijdragen aan een non-union, kan het toevoegen van een op maat gemaakte botvervanger met therapeutische geneesmiddelen resulteren in verbeterde botregeneratie en een lager risico op niet-hechting in vergelijking met autoloog bottransplantaat. Wanneer een fractuur geen operatie vereist, maar het risico loopt om niet te genezen, kan een ander botvervangingsmiddel worden gebruikt met functies die specifiek op de patiënt zijn afgestemd. Dit is een tijdrovende, kostbare en complexe onderzoeksstrategie die echter een grote verscheidenheid aan patiënten kan helpen.

Lokale versus systemische behandeling van botaandoeningen

Om botvervangers continu te verbeteren, hebben we de ontwikkeling besproken

om botvervangers te upgraden met osteoinductieve eigenschappen en afstembare eigenschappen te benutten die specifiek zijn afgestemd op de behoefte van de individuele patiënt en defecten. Toevoeging van geneesmiddelen (d.w.z. antibiotica of anti-osteoporotische geneesmiddelen) aan botvervangers is een voorbeeld van een dergelijke op maat gemaakte eigenschap. In het geval van osteoporose wordt een onbalans in de botomzetting tegengegaan door anti-osteoporotische geneesmiddelen, zoals bisfosfonaten. Deze medicijnen remmen de osteoclastfunctie, wat resulteert in minder botresorptie en een verminderd risico op botbreuken. Er zijn verschillende bijwerkingen die kunnen optreden, zoals maagproblemen, nierfalen, osteonecrose van de kaak en zelfs een verhoogd risico op slokdarmkanker (Kenal et al. 2009). Bij de behandeling van een osteoporotische fractuur kunnen anti-osteoporotische geneesmiddelen worden toegevoegd aan een botvervanger om de botgenezing te verbeteren en te versnellen. Een voordeel van lokaal toegediende medicijnen is dat de dosering verlaagd kan worden en daardoor minder kans op systemische bijwerkingen. In combinatie met preventieve geneeskunde, zoals gezonde voeding en voldoende beweging, kan dit hopelijk de behoefte aan systemische toediening verminderen.

Referenties

1. Burge R, Dawson-Hughes B, Solomon DH, Wong JB, King A, Tosteson A. Incidence and economic burden of osteoporosis-related fractures in the United States, 2005-2025. J Bone Miner Res 2007;22(3):465-75.

2. Carmona RH, Beato C, Lawrence A, Moritsugu K, Noonan AS, Katz SI. Bone Health and Osteoporosis: A Report of the Surgeon General. In: McGowan JA, Raisz LG, Noonan AS, Elderkin AL, editors. Bone Health and Osteoporosis: A Report of the Surgeon General. Rockville (MD): Office of the Surgeon General (US) 2004.

3. Fini M, Giavaresi G, Torricelli P, Borsari V, Giardino R, Nicolini A, Carpi A () Osteoporosis and biomaterial osteointegration. Biomedicine & pharmacotherapy 2004;58:487-493.

4. Giannoudis PV, Einhorn TA, Marsh D. Fracture healing: the diamond concept. Injury 2007;38 Suppl 4:S3-6.

5. Johnell O, Kanis JA. An estimate of the worldwide prevalence and disability associated with osteoporotic fractures. Osteoporos Int 2006;17(12):1726-33.

6. Kennel KA, Drake MT. Adverse effects of bisphosphonates: implications for osteoporosis management. Mayo Clin Proc. 2009;84(7):632-638.

7. Zura R, Braid-Forbes MJ, Jeray K, Mehta S, Einhorn TA, Watson JT, Della Rocca GJ, Forbes K, Steen RG. Bone fracture nonunion rate decreases with increasing age: A prospective inception cohort stud. Bone 2017;95:26-32.

APPENDICES

Dankwoord

Curriculum Vitae

List of publications

Datamanagement plan

Dankwoord / Acknowledgements

Wetenschap heb ik altijd een belangrijk onderdeel gevonden van de opleiding tot arts. Daarom heb ik ook niet getwijfeld toen ik voor de keuze stond om te mogen solliciteren voor een promotie traject bij de afdeling Biomaterialen. Hoewel je er een voorstelling van probeert te maken, kun je nooit echt inschatten wat een impact dit heeft op jezelf en je omgeving. Zoals een van mijn stellingen luidt: “If we knew what it was we were doing, it would not be called research, would it?” (Einstein). Terugkijkend op het geheel kan ik zeggen dat ik veel heb geleerd en hoop dat dit onderzoek zal bijdragen aan de verdere ontwikkeling en verbetering van de wetenschap en de zorg.

Natuurlijk is dit allemaal niet mogelijk geweest zonder de hulp en steun van een groot aantal mensen. Een aantal wil ik in het bijzonder noemen om te bedanken.

Prof. Dr. J.A. Jansen – Beste John, bedankt voor het geloof in mij en voor de kans die ik heb gekregen. Ik kan me de dag dat ik solliciteerde nog goed herrinneren en je gaf me het vertrouwen om aan dit project te beginnen. Gedurende de jaren heb ik altijd de steun gevoeld die in het begin was gegeven. Ook bedankt voor uw geduld aangezien het toch een heel veel langer traject is geworden dan we van te voren hadden afgesproken.

Prof. Dr. D.J.O. Ulrich – Beste Dietmar, ik heb erg veel respect voor jou en ben ik blij dat je in 2011 naar de afdeling plastische chirurgie van het Radboud bent gekomen. Ik voel me ook vereerd dat ik een onderdeel heb mogen zijn van de groei die de afdeling heeft gemaakt. Ook ben ik heel blij met het vertrouwen dat je in mij hebt gehad en de kansen die ik heb gekregen door te kunnen promoveren en ook met mogelijkheid om de opleiding tot plastisch chirurg te kunnen starten. Nu er een van de twee trajecten (eindelijk) is afgerond en de tweede bijna kan ik tevreden terug kijken en zien dat ik een persoonlijke en professionele groei heb doorgemaakt, voor een groot deel door jouw hulp en steun. Dankzij onze samenwerking heb ik kunnen bijdragen aan de wetenschap en de medische zorg. Naast een harde werk ethos was er ook altijd ruimte voor gezellige momenten (bvb concerten, bbq’s en ski-uitjes) en was er ook nog ruimte voor persoonlijke steun bij wat drukkere tijden. Hoewel straks onze tijd in het kader van mijn opleiding afgerond zal zijn, hoop (en verwacht) ik dat er bij jou nooit een einde zal komen aan je inzet voor de zorg van je patienten, de steun aan je collega’s en de ambitie om de plastische chirurgie in Nijmegen, en zelfs ver daar buiten, te verbeteren.

Dr. Ing. J.J.P. van den Beucken – Beste Jeroen, ik had dit zeker nooit kunnen doen zonder jouw hulp! Door jouw wijze adviezen, heldere inzichten, aanpassingen van mijn manuscripten (en zelf mails) was dit boekje er nooit gekomen. Je directe feedback heb ik altijd erg kunnen waarderen en heeft me geholpen om snel te schakelen. Voornamelijk wil ik je bedanken voor je eeuwige beschikbaarheid, je eindeloze geduld en ook het vertrouwen dat je me hebt gegeven. We konden altijd goed kletsen over het onderzoek, maar ook heerlijk over andere levenskwesties waardoor het altijd erg gezellig was.

Paranimfen – **Kassandra van Houdt** en **Femke van de Peppel-Mauritz**, mijn lieve zus en schoonzus. Het is niet voor niets dat ik deze bijzondere vraag om mij te steunen bij mijn promoveren bij jullie leg. Jullie zijn beide zowel waardevol als familie en als vriendin! Het maakt niet uit waarover het gaat, met elke vraag kan ik bij jullie terrecht. Daarom ben ik heel blij dat jullie deze dag samen met mij willen delen.

Leden van de manuscriptcommisie; **Prof. Dr. M.J.R. Edwards**, **Dr. H.C. Kroeze-Deutman** en **Prof. Dr. P. Habibovic** – Dank voor het plaatsnemen in de commissie en het kritisch beoordelen van het proefschrift. Ook de andere leden van de promotiecommissie wil ik bedanken voor deelname in de commissie.

Collega's afdeling Biomaterialen – Hoewel alweer een hele tijd geleden ben ik natuurlijk ook zeer dankbaar voor de samenwerking met mijn mede (oud) promovendi. **Hamdan Alghamdi**, I woul like to thank you for sharing your wisdom and help me with starting this project, but also for our discussions mainly about the animal studies. **Floor van de Wateringen**, onze gesprekken aan de start van mijn promotie hebben geholpen om vooral ook de analyse met de beeldvorming een juiste richting te geven. Alle mede auteurs en specifiek **Bart van Oirschot**, **Carla Tim**, **Paulo Gabbai-Armelin**, **Paula Lopez-Perez**, **Daniel AlvesCardoso** en **Preetha Preethanath** wil ik bedanken voor een hele fijne en productieve samenwerking. Ook mijn mede promovendi **Jan-Willem Hoekstra**, **Manuela Ventura**, **Maria Cristina LoGiudice**, **Ruggero Bosco**, **Simone Mastrogiacomo, Eline-Claire Grosfeld**, **Na Yu**, **An Jie**, **Mani Diba**, **Astghik Hayarpetyan**, **Alexey Klymov**, **Xinjie Cai**, **Yue Sa**, **Kemal Sabriibrahimoglu**, **Kambiz Farbod**, **Winston Camargo**, **Matilde Bongio**, **Eva Raquel UrquíaEdreira**, **Wanxun Jang**, **Jinankan Song**, **Xiangzhen Yan**, **Rosa FelixLanao**, **Pedro DousaBabo** en iedereen die mogelijk ben vergeten over de jaren. Jullie hebben bijgedragen aan een leerzame en leuke periode van onderzoek doen bij de afdeling Biomaterialen.

Stafleden afdeling Biomaterialen – **Sander van Leeuwenburg**, **Frank Walboomers**, **Joop Wolke**, **Fang Yang**, bedankt voor jullie feedback en ondersteuning op de juiste momenten.

Collega's in het lab – Een speciale dank wil ik uitpreken naar de hulp die in het lab heb gekregen. Beste **Natasja van Dijk**, jij hebt mij gedurende mijn hele tijd bij de biomaterialen het meeste gezien en gesteund. Door jou had ik het vertrouwen om in het laboratiorium aan de slag te gaan. Voor mij een volledig nieuwe omgeving, maar door jou steun en toeverlaat was het direct een prettige werkomgeving. Naast al het eindeloze snijden en prepareren van de coupes hebben we gelukkig ook regelmatig tijdens koffie pauzes en lunch kunnen kletsen. Bedankt voor deze bijzondere tijd. Beste **Vincent Cuijpers**, ook jouw hulp is niet onopgemerkt gebleven. Jouw expertise was groots en dat bleek ook wel aangezien je ook bent gepromoveerd in 2016. Ook heb je mij geholpen met het verwerken van de data en daar ben ik je dankbaar voor. Verder kan ik natuurlijk ook **Martijn Martens**, **Monique Kersten** en **Marjon Bloemen** niet vergeten.

Dr. M. Koolen – Beste Marianne, bedankt voor de prettige samenwerking. Ik heb veel van je kunnen leren. Ons gezamenlijk project heeft voor mooie resultaten gezorgd waarvan onder andere het figuur op de voorkant van dit proefschrift. Ook dank aan **Prof. Dr. H.H. Weinans** die deze samenwerking mede mogelijk heeft gemaakt.

Collega's in het CDL – mijn onderzoek was niet mogelijk zonder de hulp en begeleiding vanuit het CDL. De biotechnichi en dierenwelzijns functionarissen hebben de dierproeven mogelijk gemaakt. Vooral wil ik mijn dank uiten naar de mensen die hier direct bij betrokken zijn geweest en altijd de wetenschap goed combineerde met de liefde en zorg voor de dieren. Dit zijn **Daphne Reijnen**, **Denise Taks**, **Linda Derks-Wagemakers**, **Bianca Lemmers-van de Weem**, **Charlene de Kluijs-Bender**, **Saskia Mulder**, **Roel Sneepers** en **Pieter Verbost**.

Afdeling Pathologie – Beste **Meyke Hermsen**, bedankt voor de mogelijkheid om onze coupes de kunnen scannen en de begeleiding hierbij.

Stafleden Plastische chirurgie – Graag bedankt ik **Till Wagner**, **Pieter Hupkens**, **Hanneke Tielemans**, **Erik Walbeehm**, nieuwe collega's **Franz Pronk**, **Tim de Jong**, **Tim Nijhuis**, **Brigitte van der Heijden** en **Marielle Vehmeijer**. Maar ook oud collega's **Dalibor Vasilic**, **Marie-Claire Schreinemachers** en **Oliver Kloeters**. In het bijzonder ook **Prof. Hovius** voor de leerzame onderwijsmomenten en **Stefan Hummelink** voor zowel de muzikale gesprekken als verzoek voor wetenschappelijke status updates.

Collega's assistenten Plastische chirurgie – **Inge Hoevenaren**, **Marijn Hameeteman** en **Marjolijn van Abeelen**, samen met jullie is het allemaal begonnen in het Radboud. Toen kwamen **Nicholas Slater**, **Vera Paulus**, **Tycho Wesselius**, **Anne-Sophie Kruit**, **Femke Mathot**, **Pepijn Sun** en later nog **Lennart Steenbeek**, **Kaj Brouwers**, **Bo Notermans**, **Laura Burlage**, **Harm Winters** en **Sakia de Roo**. Weledelgeleerde dames en heren, jullie zijn allemaal zeer lieve collega's en ook als assistentengroep is het altijd een super gezellige sfeer! Ik hoop dat waar we allemaal ook in de toekomst terrecht komen er altijd zulke lieve collega's zullen zijn. Voor jullie allemaal wens ik het allerbeste en hopelijk zien we elkaar nog regelmatig, minstens op de NVPC-dagen wanneer die weer fysiek mogen.

Personeel Plastische chirurgie – dames van de poli en het secretariaat, maar ook **Erik de Laat**, **Nienke Gort** en **Yasmille Winnen**, ook jullie steun heb ik de afgelopen jaren zeer gewaardeerd. **Stephan van Raay**, zonder jou was dit boekje zeker niet zo mooi geworden. Dank voor je hulp.

Lieve vrienden en vriendinnen

Geneeskundevriendinnen – **Barbara Muller**, **Sophie Bekman**, **Willemijn van Hoesel-van Eeten**, **Sasja LeLoup**, **Siegrid de Meer**, **Joyce Heijenman** en **Anne Schmetz**. Het was altijd fijn om werkgerelateerd te kunnen praten, grappen en reflecteren, maar ik ben vooral dankbaar voor de gezellige tijd. Ik koester jullie vriendschap.

Suzanne Oosterwijk – mijn "oudste" vriendinnetje. Met weinig woorden begrijpen wij elkaar heel goed. Momenteel ben je nog steeds ver weg op avontuur in New York, maar het maakt niet uit waar je op de wereld bent we blijven altijd vriendinnen en hoelang het ook geleden is, als we kletsen voelt het altijd als vanouds.

Vala van Beek – lieve Vala, door omstandigheden zien en spreken we elkaar minder dan ik zou willen, maar onze middelbareschool periode en de vriendschap die hieruit is ontstaan zal ik altijd koesteren.

Joyce Heijneman en **Bas de Bruin**, samen beleven wij al jaren mooie avonturen op onder andere festivals en onze weekendjes in de Ardennen. Dank jullie beide voor al deze heerlijke momenten die voor de nodige ontspanning zorgen naast al het harde werken. We hebben nog een hele bucket list te gaan en hopelijk lukt het ons om deze ervaringen allemaal samen te beleven.

Vrienden uit Wageningen – Lieve **Sander van Houwelingen**, **Maikel Boos**, **Selko Smits**, **Joost Kettmann**, **Maartje Mulders**, **Paul Eijskoot** en **Caroline van Oostveen**. Jullie hebben mijn komst naar Wageningen doen voelen als een warm bad. Alles begon in de Infinity waar we veel gezellige avonden hebben gehad. Wat fijn dat ik deze ontspannende momenten samen met jullie kan delen.

Lieve familie

Wim van Houdt en **Jocelyne van Houdt-Albert** – Lieve pap en mam, jullie hebben mij altijd geleerd dat je alles kunt worden in het leven als je maar graag genoeg wilt en je best hiervoor doet. Hieruit put ik mijn volhardendheid en daar ben ik trots op. Soms voelde het alsof het niet ging lukken, maar door jullie liefde en steun heb ik nu steeds kunnen bereiken wat ik beoogde. Ik blijf julli eeuwig dankbaar! Nu jullie rol verder is gegroeid tot papi en mami zie ik weer waarom het leve

David van Houdt – mijn grote, kleine broer, zoals ik het boekje heb zien groeien in een paar jaar, heb ik ook jou ook zien groeien. Hopelijk heb ik jou, als een van je grote zussen, kunnen inspireren. Inmiddels kan ik ook veel van jou leren (zie mijn stellingen) en hopelijk gaan daar nog veel wijze lessen bij komen.

Izak Mauritz en **Inge Mauritz-Assendelft** – lieve schoonouders, ik had geen betere kunnen wensen. Vanaf de eerste keer dat wij elkaar leerde kennen voelde het als een warm welkom in de nieuwe familie en sindsdien is dat alleen maar gegroeid. Ook jullie zijn er voor mij en ons gezin onvoorwaardelijk. De gezellige gesprekken van Izak en heerlijke kookkunsten van Inge maakt dat ik altijd graag bij jullie kom en dat doe ik dan ook regelmatig. Heel handig nu ook zo dicht in de buurt.

Schoonbroers – **Marvin Renardus** en **Renz van de Peppel**, wat ben ik blij dat mijn lieve zus en schoonzus zulke geweldige mannen hebben gevonden. Nu we ook allemaal ongeveer tegelijk een gezin zijn gestart voelt de band nog hechter. Bedankt voor het groter en leuker maken van deze familie.

Tobin Mauritz – mijn schatje, wat maak jij me gelukkig. Jou zien opgroeien is het mooiste wat er is. We gaan nog veel prachtige avonturen beleven, straks ook samen met je broertje.

Harm Mauritz – Loof, wat ben ik blij dat we samen het leven trotseren. Want hoewel we allebei altijd druk zijn met onze carriere ambities en daarbij nog ons uitbreidend gezin, heb je toch ook nog geduld om mij te steunen zoals bij het voltooien van dit proefschrift. Gelukkig was het de afgelopen jaren niet alleen maar hard werken, maar kunnen we samen ook erg genieten van het leven en het samen zijn. Nu mijn proefschrift klaar is kan ik hopelijk nog meer samen met jou en onze beide mannetjes het leven vieren.

Curriculum Vitae

Claire van Houdt werd geboren op 10 oktober 1984 te Soest. Na het behalen van haar VWO diploma in 2003 aan het Baarnsch Lyceum startte zij met haar studie Geneeskunde aan de Universiteit van Utrecht. Tijdens haar studie is zij voor haar co-schap Tropengeneeskunde naar Haydom, Tanzania, gegaan en heeft zij haar keuze co-schap KNO in Marseille, Frankrijk, verricht bij prof. dr. J.P.Y. Magnan. In haar laatste jaar heeft zij op de afdeling plastische chirurgie in het UMC Utrecht, onder begeleiding van prof. dr. M. Kon en dr. A.H. Schuurman, co-schappen gelopen en heeft zij onderzoeksstage naar pijn bij hand en pols chirurgie gedaan. Hier werd haar voorkeur voor de plastische chirurgie bevestigd en werd de basis voor de wens om aanvullend wetenschappelijk onderzoek te doen gelegd. Na het afronden van haar studie in 2010 kon zij direct starten als arts-assistent bij de chirurgie in de Gelderse Vallei in Ede. In 2011 kwam de kans om als arts-assistent te werken in het Radboudumc. Toen prof. dr. D.J.O. Ulrich in 2012 als opleider en hoofd van de afdeling Plastische chirurgie in het Radboudumc kwam werd al snel gesproken over het verrichten van een promotietraject. In 2013 kon zij in samenwerking met de vakgroep Biomaterialen van de afdeling Tandheelkunde in het Radboudumc starten met haar onderzoek naar “botvervangende materialen in gecompromitteerde condities”, onder begeleiding van prof. dr. J.A. Jansen en dr. ing. J.J.J.P. van den Beucken. Na 2 jaar fulltime onderzoek doen en data verzamelen is zij eerst terug gegaan naar de afdeling plastische chirurgie alvorens zij in 2016 met haar opleiding als plastisch chirurg startte. De opleiding startte zij bij de afdeling Chirurgie in het ziekenhuis Gelderse Vallei in Ede, met als opleiders dr. R.M.H.G. Mollen en dr. A.M. Bosch. Het onderzoek verricht binnen de vakgroep Biomaterialen is in de jaren erna verder afgerond en heeft uiteindelijk geresulteerd in dit proefschrift. In 2020 heeft Claire een jaar perifere ervaring opgedaan in het Jeroen Bosch ziekenhuis onder begeleiding van dr. R.J.P.M. Franken en dr. E.P.A. van der Heijden. Momenteel is zij bezig haar laatste jaar van de opleiding plastische chirurgie af te ronden.

Claire woont samen met Harm Mauritz en hun zoon Tobin in Wageningen en in juni verwachten zij de komst van hun tweede zoon.

List of publications

Related to this thesis

1. **Bone regeneration and gene expression in bone defects under healthy and osteoporotic bone conditions using two commercially available bone graft substitutes.**
   van Houdt CI, Tim CR, Crovace MC, Zanotto ED, Peitl O, Ulrich DJ, Jansen JA, Parizotto NA, Renno AC, van den Beucken JJ. Biomed Mater. 2015 May 8;10(3):035003. doi: 10.1088/1748-6041/10/3/035003.Biomed Mater. 2015. PMID: 25953955

2. **Toward accelerated bone regeneration by altering poly(D,L-lactic-co-glycolic) acid porogen content in calcium phosphate cement.**
   van Houdt CI, Preethanath RS, van Oirschot BA, Zwarts PH, Ulrich DJ, Anil S, Jansen JA, van den Beucken JJ. J Biomed Mater Res A. 2016 Feb;104(2):483-92. doi: 10.1002/jbm.a.35584. Epub 2015 Oct 29.J Biomed Mater Res A. 2016. PMID: 26454146

3. **Porous titanium scaffolds with injectable hyaluronic acid-DBM gel for bone substitution in a rat critical-sized calvarial defect model.**
   van Houdt CI, Cardoso DA, van Oirschot BA, Ulrich DJ, Jansen JA, Leeuwenburgh SC, van den Beucken JJ. Tissue Eng Regen Med. 2017 Sep;11(9):2537-2548. doi: 10.1002/term.2151. Epub 2016 Mar 28.J Tissue Eng Regen Med. 2017. PMID: 27017921

4. **The performance of CPC/PLGA and Bio-Oss® for bone regeneration in healthy and osteoporotic rats.**
   van Houdt CI, Ulrich DJ, Jansen JA, van den Beucken JJ. J Biomed Mater Res B Appl Biomater. 2018 Jan;106(1):131-142. doi: 10.1002/jbm.b.33801. Epub 2016 Nov 27.J Biomed Mater Res B Appl Biomater. 2018. PMID: 27889939

5. **Alendronate release from calcium phosphate cement for bone regeneration in osteoporotic conditions.**
   van Houdt CIA, Gabbai-Armelin PR, Lopez-Perez PM, Ulrich DJO, Jansen JA, Renno ACM, van den Beuken JJJP. Sci Rep. 2018 Oct 18;8(1):15398. doi: 10.1038/s41598-018-33692-5.Sci Rep. 2018. PMID: 30337567

6. **Overcoming critical-sized segmental bone defects in osteoporotic condition using a hyaluronan with bisphosphonate and calcium phosphate based hydrogel enhanced with BMP-2**
   van Houdt CIA, Koolen MKE, Lopez-Perez PM, Ulrich DJO, Jansen JA, Weinans HH, van den Beuken JJJP. Macromolecular Bioscience 2021 submitted

Other

7. **Comparison of three different incision techniques in A1 pulley release on scar tissue formation and postoperative rehabilitation.**
   Kloeters O, Ulrich DJ, Bloemsma G, van Houdt CI. Arch Orthop Trauma Surg. 2016 May;136(5):731-7. doi: 10.1007/s00402-016-2430-z. PMID: 26926477

Datamanagement plan

The data obtained during this PhD at the Radboud university medical center (Radboudumc) have been captured and stored on paper in traditional laboratory note books as well as on the local archive of the department of Biomaterials at the Radboudumc. All data was stored in widely used file formats to ensure interoperability when re-use of data is needed. Data remains accessible by the PhD candidate, (co-)promotors and assigned laboratory members of the department of Biomaterials for 15 years after publication of each study.

All animal experiments were conducted in accordance with institutional, national and international guidelines for animal care and the Dutch law concerning animal welfare. The studies were reviewed and approved by the Experimental Animal Committee of the Radboud University.

For reusability of the data provided in the Materials and Method section of each chapter has been written as detailed as possible. Published data is accessible via PubMed as well as all data files can be requested to the corresponding author of the articles or author of this thesis.

PhD PORTFOLIO

Institute for Molecular Life Sciences
Radboudumc

Name PhD student: ***C.I.A. van Houdt***	**PhD period:** ***01-02-2013 – 01-02-2015***
Department: ***Biomaterials***	**Promotor(s):** ***Prof. J.A. Jansen, Prof. D.J.O. Ulrich***
Research School: ***Radboud Institute for Molecular Life Sciences***	**Co-promotor(s):** ***Dr. Ing. J.J.J.P. van den Beucken***

	Year(s)	ECTS
TRAINING ACTIVITIES		
a) Courses & Workshops		
- **Laboratory Animal Science**	21-01-2013	3
- **Brandwonden cursus**	19-03-2013	¼
- **Management voor promovendi**	03-10-2013	3
- **NCMLS Graduate course**	10/14-02-2014	2
b) Seminars & lectures^		
- **"Around the nose" international course**	12-06-2013	¼
- **Radboud Grand Rounds** (2x)	15-04-2013 + 05-06-2014	½
c) (Inter)national Symposia & congresses^		
- **Wetenschappelijke vergadering** (NVPC, apr 2013)	05-04-2013	¼
- **24th meeting EURAPS** (Antalya, Turkey)	23/25-06-2013	¾
- **"Towards a new center for the treatment of complex osseous defects"** (CTRM, Vu A'dam)	28-06-2013	¼
- **Scholingsdag & Wetenschappelijke vergadering** (NVPC, okt 2013)	4/5-10-2013	½
- **Scholingsdag & Wetenschappelijke vergadering** (NVPC, apr 2014)	3/4-04-2014	½
- **Conference for Society for Biomaterials*** (SFB Denver USA, apr 2014)	16/19-04-2014	2 ½
- **Two-Day PhD retreat#** (RIMLS, mei 2014)	8/9-05-2014	1 ¼
- **Scholingsdag & Wetenschappelijke vergadering*** (NVPC, okt 2014)	3/4-10-2014	¾
- **New Frontiers Symposium 2014** (RIMLS, okt 2014)	16/17-10-2014	1
d) Other		
- **Stagemarkt BMW 2013#**	18-09-2013	¼
- **Stagemarkt BMW 2014#**	16-09-2014	¼
TEACHING ACTIVITIES		
e) Lecturing		
- **PhD meeting Biomaterials***	20-05-2014	2
f) Other		
- **Wetenschapsdag Tandheelkunde***	05-06-2014	½
- **Research seminar Biomaterials* (presented 3x)**	2012-2014	¾
TOTAL		**20 ½**

^Indicate oral and poster presentations with a * and # after the name of the activity, respectively.

Addition: Since the PhD period was over 2 year's time in stead of 4 years the total of 20 points (in stead of 40) was considered sufficient by Mentor, Promotors and Co-promotor.